**République Algérienne Démocratique et Populaire**

**Ministère de l'Enseignement Supérieur et de la Recherche Scientifique**

**Université d'El Oued**

**Faculté des Sciences Exactes**

**Laboratoire de Biodiversité et Application de Biotechnologie en Milieu Agricole**

**(BABDA)**

**Thèse de Doctorat**

**Présentée en vue de l'obtention du diplôme de Doctorat en troisième cycle (LMD)**

**Filière: Chimie**

**Spécialité: Chimie Analytique**

# Synthèse et Activité de Quelques Hétérocycles Azotés

**Présenté par: Halla ABDELBAKI**

**Supervisé par: Amar DJEMOUI**

**Soutenue le 05/11/2025, en présence du comité d'examen:**

| Nom | Rang | Affiliation | Rôle |
|---|---|---|---|
| Mohamed DEHAMCHIA | Professeur | U. El Oued | Président |
| Amar DJEMOUI | Professeur | U. Djelfa | Directeur de thèse |
| Mohamed Ridha OUAHRANI | Professeur | U. El Oued | Co-directeur de thèse |
| Nacer Salah NEGHMOUCHE | MCA | U. El Oued | Examinateur |
| Saad ZEGHDI | Professeur | U. Ouargla | Examinateur |
| Nadji BELKHEIRI | Professeur | U. Djelfa | Examinateur |

**Année académique: 1446-1447 AH / 2024-2025**

People's Democratic Republic of Algeria

Ministry of Higher Education and Scientific Research

University of El Oued

Faculty of Exact Sciences

Laboratory of Biodiversity and Application of Biotechnology in Agricultural Field

(BABDA)

A Doctoral Thesis

Submitted in fulfillment of the requirements for the Doctorate degree in the third cycle (LMD)

Field: Chemistry

Specialization: Analytical Chemistry

# Synthesis and Activity of Some Nitrogen-Containing Heterocycles

Presented by: Halla ABDELBAKI

Supervised by: Amar DJEMOUI

Defended on 05/11/2025, in the presence of the Examination Committee:

| Name | Rank | Affiliation | Role |
|---|---|---|---|
| Mohamed DEHAMCHIA | Professor | U. El Oued | Chair |
| Amar DJEMOUI | Professor | U. Djelfa | Supervisor |
| Mohamed Ridha OUAHRANI | Professor | U. El Oued | Co-supervisor |
| Nacer Salah NEGHMOUCHE | MCA | U. El Oued | Examiner |
| Saad ZEGHDI | Professor | U. Ouargla | Examiner |
| Nadji BELKHEIRI | Professor | U. Djelfa | Examiner |

Academic Year: 1446-1447 AH / 2024-2025

# *Dédications…*

*To my dear father, the one who encouraged me to succeed throughout my life.*

*To my dear mother, my support, my foundation, and the love of my heart, to whom I owe my presence here now.*

*To Iman my beloved sister, my companion on this journey.*

*To Adel and Ihab my brothers, my support in life.*

*To everyone who taught me a letter over all these years.*

*To everyone who loves me and wishes to see me succeed.*

*To everyone who helped me.*

*To everyone who believed in me.*

*To all those, I dedicate this humble work*

*Halla*

# Acknowledgments

After all these years of dreaming, hoping, working, and striving, I thank Allah for the blessing of reaching my goal. The dream that once began with a visit to the beautiful city of El Oued has culminated in my graduating as a doctor.

I cannot help but express my profound gratitude to:

My professors DJEMOUI Amar and OUAHRANI Mohamed Ridha for their supervision of this work and their continuous academic and moral support, encouraging me to complete this project.

Professor DEHAMCHIA Mohamed for accepting the chairmanship of the committee, for his support, encouragement, and unwavering assistance over these years.

Professor ZEGHDI Saad and Professor BELKHEIRI Nadji for agreeing to discuss this thesis and for their willingness to travel. Special thanks also to Professor NEGHMOUCHE Nacer Salah for his acceptance to review this work

Thanks are also extended to the technicians and engineers in laboratories who contributed to this work : Chemistry Laboratory and Physics Laboratory at the Faculty of Exact Sciences and Computer Science as well as the biology laboratory at the biology department in the university of Djelfa; Chemistry laboratory of the Faculty of exact sciences at the University of El Oued as well as the VTRS laboratory .

My dear friend Siham TEI for her kindness and great help.

Dr. Ilham BEN OMAR and Ichrak BOUGUESSA for their assistance, valuable advice, and significant help in completing this thesis.

To those who I have had the opportunity to get to know during these years.

A special thanks to Ms BOUAKAZ. S, Dr BELKACEM. Z, Dr KHERKHACHE.H, Dr Djoumaa and Dr KACIMI from the university of Djelfa for their support and advice.

## ABREVIATIONS AND SYMBOLS

| Symbol | Meaning |
|---|---|
| **Å** | Angstrom |
| **ABTS** | 2,2-azinobis-(3-éthyle-benzothiazoline-6-sulphonate) |
| **AcOH** | acetic acid |
| **AFM** | Atomic force microscopy |
| **AA** | Ascorbic acid |
| **AAC** | Azide-Alkyne Cycloaddition |
| **Ag** | silver |
| **AgOAc** | Silver acetate |
| **AH** | antioxidant |
| **AscNa** | Sodium Ascorbate |
| **Au** | gold |
| **A549** | lung cancer cell line |
| **Boc** | tert-butyloxycarbonyl |
| **Br** | Brome |
| **CA** | cyclo addition |
| **Cat** | Catalyst |
| **CAT** | Catalase |
| **°C** | Degré Celsius |
| **$CDCl_3$** | Deuterated chloroform |
| **$CH_3CN$** | Acetonitrile |
| **$CH_3COOH$** | Acetic Acid |
| **Conc** | Concentrated |
| **Cl** | Chloride |
| **Cm** | centimeter |
| **Cu** | copper |
| **CuAAC** | Copper(I)-catalysed azide-alkyne cycloaddition |
| **$CuCl_2$** | cupric chloride |
| **CuO** | cupric oxide |
| **$Cu_2O$** | cuprous oxide |
| **$Cu(OAc)_2$** | copper acetate |
| **$CuSO_4$** | Copper sulfate |

| | |
|---|---|
| **CuI** | copper iodide |
| **[Cp*RuCl]** | penta-methylcyclopentadienyl ruthenium chloride |
| **CVD** | chemical vapor deposition |
| **1D** | one dimension |
| **2D** | second dimension |
| **3D** | third dimension |
| **d** | Doublet |
| **DCE** | Dichloroethane |
| **dd** | Split doublet |
| **ddd** | split doublet split |
| **dt** | Doublet of triplet |
| **DIPEA** | Diisopropylethylamine |
| **DMF** | N,N-diméthylformamide |
| **DMSO** | Diméthyl sulfoxyde |
| **DMSO-d6** | deuterated Diméthyl sulfoxyde |
| **DNA** | Deoxyribonucleic acid |
| **DIC** | N,N′-Diisopropylcarbodiimide |
| **DP RT-associated HIV-1** | DNA Polymerase activity associated with HIV-1 Reverse Transcriptase |
| **DPPH** | 2,2-diphényl-1-picrylhydrazyle |
| **DRO** | Radicals derived from oxygen |
| **EDX** | X-ray elemental analysis |
| **Éq** | Équivalent |
| **EtOH** | ethanol |
| **eV** | electron volt |
| **$FeCl_3$** | Ferric Chloride |
| **$Fe_3O_4$** | Iron (II, III) oxide |
| **FGFG** | Phenyl-Glycine-Phenyl-Glycine |
| **FRAP** | Ferric reducing capacities of antioxidants |
| **FT-IR** | Fourier transform infrared |
| **g** | gram |
| **GPX** | glutathione peroxidase |
| **GSH** | glutathione |

| | |
|---|---|
| **h** | Hour |
| **H** | Hydrogen |
| **HCl** | Hydrochloric acid |
| **HepG2** | hepatoblastoma cell line |
| **HIV-1** | Human immunodeficiency virus type 1 |
| **HIV-1 RT** | HIV reverse transcriptase |
| **Hz** | Hertz’ |
| **$H_2O$** | water |
| **$H_2SO_4$** | Sulfuric Acid |
| **HMBA** | 4-Hydroxymethylbenzoic acid |
| **I %** | Inhibition pourcentage |
| **$IC_{50}$** | Median inhibitory concentration |
| **INT** | intermediate |
| **IUPAC** | International Union of Pure and Applied Chemistry |
| **J** | Coupling constant expressed in Hz |
| **$K_2CO_3$** | Potassium Carbonate |
| **L** | ligand |
| **LED** | light-emitting diode |
| **m** | Multiplet |
| **mm** | Millimeter |
| **M** | 1 mol /litre |
| **MCF-7** | breast cancer cell line |
| **MCRs** | Multi-Componant Réaction |
| **Me** | methyl |
| **MeOH** | methanol |
| **min** | minutes |
| **Mg** | Magnesium |
| **mL** | Milliliter |
| **mol** | Mole |
| **M-NPs** | Metal nanoparticles |
| **MONPs** | Metal oxide nanoparticles |
| **MAAC** | Metal azide–alkyne cycloaddition |
| **MW** | Microwave |

| | |
|---|---|
| **$NaN_3$** | Sodium azide |
| **N** | Nitrogen |
| **NaAsc** | Sodium ascorbate |
| **NaH** | Sodium hydride |
| **NaOH** | sodium hydroxide |
| **nm** | nanometers |
| **NMR** | Nuclear magnetic resonance |
| **1H NMR** | Nuclear magnetic resonance of the proton |
| **13C NMR** | Nuclear magnetic resonance of carbon 13 |
| **Ni** | Nickel |
| **NPs** | nanoparticles |
| **O** | Oxygen |
| **Pd** | Palladium |
| **PEGA800** | Resin |
| **Prod** | product |
| **Ph** | Phenyl |
| **PH** | Hydrogen potential (measurement of acidity) |
| **ppm** | Parts per million |
| **q** | Quartet |
| **R** | radical |
| **Ref** | reference |
| **RNase H** | Ribonuclease H |
| **ROS** | reactive oxygen species |
| **Ru** | ruthenium |
| **RuAAC** | Alkyne-Azide Cycloaddition catalyzed by ruthenium |
| **rt** | room temperature |
| **s** | Singlet |
| **S** | sulfur |
| **SEM** | Scanning electron microscopy<br>superoxide dismutase |
| **SPAAC** | Strain-promoted azide–alkyne cycloaddition reaction |
| **t** | Triplet |
| **TBAB** | Tetrabutylammonium bromide |

| | |
|---|---|
| **TBTA** | Tris((1-benzyl-4-triazolyl)methyl)amine |
| **TEM** | Transmission electron microscopy |
| **$TiO_2$** | Titanium dioxide |
| **TLC** | Thin layer chromatography |
| **TMS** | Tétraméthylsilane ($Me_4Si$) |
| **TSCs** | Thiosemicarbazones |
| **TZ** | thiazole |
| **µg** | microgram |
| **UV-vis** | Ultraviolet-visible |
| **W/v** | weight by volume |
| **Zn** | zinc |
| **µm** | micro-meter |
| **R&D** | Research and development |
| **X** | halogen |
| **XRD** | X-Ray diffraction analysis |
| **σ** | chemical shift |
| Δ | heat |
| **%** | percent |
| ° | degree |
| **λ** | wavelength |
| **β** | full width half maximum |
| **θ** | diffraction angle |
| > | bigger than |
| **π** | pi |
| **υ** | vibrational frequency |

## LIST OF FIGURES

**LIST OF TABLES**

**TABLE OF CONTENTS**

# GENERAL INTRODUCTION

Modern organic chemistry is based on natural products, which are essential for the production of agricultural chemicals, pharmaceuticals, and other useful products [1]. The progress of scientific research and technological innovation depends on the production of complex organic molecules selectively and effectively [2]. Researchers are looking at innovative ways to improve raw materials and significantly reduce environmental impact as the demand for new compounds with specialized biological activity increases [3].

Because they are found in many biological processes and are important in medicine, heterocycles are important in organic chemistry [4]. Common heteroatoms are nitrogen, oxygen, and sulfur. Heterocycles are cyclic compounds with atoms of at least two different elements in their rings [5]. 1,2,3-triazoles and thiazoles stand out among these compounds because of their wide range of biological activities. The potential of the 1,2,3-triazole moiety as an antimicrobial, anti-inflammatory, and carcinogenic agent has attracted interest [6]. They are useful in chemistry due to their unique electrical properties and ability to form hydrogen bonds [7]. Similarly, thiazole derivatives are useful targets for drug discovery as they are associated with many therapies such as cancer treatment and antibiotics [8].

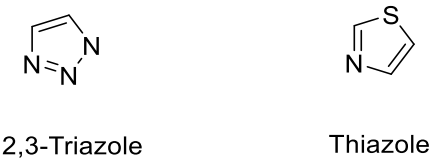


1,2,3-Triazole Thiazole

**Figure 1.** Triazole and thiazole structures

Especially with the introduction and application of nanotechnology in catalysis, tremendous progress has been made in organic synthesis in recent years [9]. Due to their dramatic increase in reaction rate and selectivity, catalysts are important for organic synthesis [10]. Materials efficiency, recycling, and environmental sustainability are three areas commonly consumed by conventional catalyst methods failure. For these problems, microbeads have become an alternative in recent years [11]. Microbeads are spherical particles that generally range in size from 1 to 1000 μm [12] and can be made of various materials such as silica, polymers [13]. leading to their large surface areas leading to enhanced catalytic activity, and enables better contact with reagents [14]. ease of handling [15] and derived from the synthesis of mixed materials, which simplifies cleaning procedures and reduces waste [16]. In addition, microbeads may have special characteristics for certain reactions or applications for more suitable tools in the chemical industry. These characteristics include high response rates, selectivity, and easy recovery and recyclability [17].

This work focuses on the synthesis of thiazoles and 1,2,3-triazoles using $Cu_2O$ microbeads as catalysts. By applying these advanced features to condensation reactions with thiosemicarbazide and aldehyde derivatives, we aim to reduce reaction time and byproduct formation and achieve high yields of new compounds. The use of microbeads increases the efficiency of the reactions and also aligns with the principles of green chemistry by reducing waste and energy consumption[18].

This study focuses on the biological investigation of the synthesis of heterocyclic compounds in addition to the synthetic material. An understanding of structure-activity relationships (SAR) is essential to predict the biological behavior of new drugs [19]. By finding a way to investigate how differences in molecular structure affect biological function, we can find candidates for new developments as therapeutic agents. Our findings are further significant by the potential use of these compounds to combat oxidative stress-related diseases.

Furthermore, this work aims to contribute to the heterocycle of the role of microbeads in organic synthesis. As new methods and applications for these materials continue to evolve, it is important to recognize their potential in expanding synthetic chemistry to improve reaction efficiency. This study is not if microbeads can produce heterocyclic compounds but also emphasizes their medicinal applications.

In summary, this will create a global perspective on the application of microbead technology in synthetic biology in all relevant biomedical challenges simultaneously. In addition to synthesizing and testing the prepared 1,2,3-triazoles and thiazoles, we will also report important information on the mechanism and pharmacokinetics.

We divided this thesis into four chapters:

We will present a review on the literature of the synthesis of 1,2,3-triazole in the first chapter, by focusing on the use of metal-based nanoparticles in the green synthesis of 1,2,3-triazole. We will consider a section to the synthesis and applications of $Cu_2O$ microbeads as a catalyst for the synthesis of 1,2,3-triazole.

The second chapter will focus on the synthesis, structural characterization, and physicochemical properties of the synthesized thiosemicarbazone and thiazole derivatives. After providing an overview of the various existing synthetic pathways, we will present all obtained results and ensuing discussions, along with the strategies we adopted.

In the third chapter, we will present the results of studies on the antioxidant activity of our synthesized heterocycles.

Finally, the fourth chapter will compile the experimental protocols and structural characteristics ($^{13}C$ NMR, $^{1}H$ NMR and IR) of the obtained products.

**References:**


[1] S. Alvi, V. Jayant, and R. Ali, "Applications of oxone® in organic synthesis: an emerging green reagent of modern era," *ChemistrySelect,* vol. 7, no. 23, p. e202200704, 2022.

[2] K. R. Campos *et al.*, "The importance of synthetic chemistry in the pharmaceutical industry," *Science,* vol. 363, no. 6424, p. eaat0805, 2019.

[3] A. Fryszkowska and P. N. Devine, "Biocatalysis in drug discovery and development," *Current Opinion in Chemical Biology,* vol. 55, pp. 151-160, 2020.

[4] N. Kumar and N. Goel, "Heterocyclic Compounds: Importance in Anticancer Drug Discovery," *Anti-Cancer Agents in Medicinal Chemistry (Formerly Current Medicinal Chemistry-Anti-Cancer Agents),* vol. 22, no. 19, pp. 3196-3207, 2022.

[5] A. Omar, "Review article; anticancer activities of some fused heterocyclic moieties containing nitrogen and/or sulfur heteroatoms," *Al-Azhar Journal of Pharmaceutical Sciences,* vol. 62, no. 2, pp. 39-54, 2020.

[6] M. J. Vaishnani *et al.*, "Biological importance and synthesis of 1, 2, 3-triazole derivatives: a review," *Green Chemistry Letters and Reviews,* vol. 17, no. 1, p. 2307989, 2024.

[7] D. P. Rotella, "Heterocycles in drug discovery: Properties and preparation," in *Advances in Heterocyclic Chemistry*, vol. 134: Elsevier, 2021, pp. 149-183.

[8] L. R. P. de Siqueira, P. A. T. de Moraes Gomes, L. P. de Lima Ferreira, M. J. B. de Melo Rêgo, and A. C. L. Leite, "Multi-target compounds acting in cancer progression: Focus on thiosemicarbazone, thiazole and thiazolidinone analogues," *European Journal of Medicinal Chemistry,* vol. 170, pp. 237-260, 2019.

[9] P. Rai and D. Gupta, "Magnetic nanoparticles as green catalysts in organic synthesis-a review," *Synthetic Communications,* vol. 51, no. 20, pp. 3059-3083, 2021.

[10] W.-M. Cheng and R. Shang, "Transition metal-catalyzed organic reactions under visible light: recent developments and future perspectives," *ACS Catalysis,* vol. 10, no. 16, pp. 9170-9196, 2020.

[11] M. T. Khan, Y. L. Cheng, S. Hafeez, Y. F. Tsang, J. Yang, and A. Nawab, "Microplastics in wastewater: Environmental and health impacts, detection, and remediation strategies," *Handbook of Microplastics in the Environment,* pp. 1-33, 2020.

[12] N. T. T. Uyen, Z. A. A. Hamid, N. X. T. Tram, and N. Ahmad, "Fabrication of alginate microspheres for drug delivery: A review," *International journal of biological macromolecules,* vol. 153, pp. 1035-1046, 2020.

[13] M. F. Hamza, M. S. Khalafalla, Y. Wei, and N. A. Hamad, "Effect of bi-functionalization silica micro beads on uranium adsorption from synthetic and washing pregnant uranyl solutions," *Journal of Radioanalytical and Nuclear Chemistry,* vol. 330, no. 1, pp. 191-206, 2021.

[14] A. Leemsuthep *et al.*, "Development of Porous Epoxy Micro-Beads Using Ammonium Bicarbonate through a Single Epoxy Droplet in Corn Oil," *Materials,* vol. 14, no. 9, p. 2282, 2021.

[15] T. O. Ajala and B. O. Silva, "The design of ibuprofen-loaded microbeads using polymers obtained from Xanthosoma sagittifoliumand Dillenia indica," *Polim Med,* vol. 50, no. 1, pp. 21-31, 2020.

[16] Z. Khan, M. A. Abourehab, N. Parveen, K. Kohli, and P. Kesharwani, "Recent advances in microbeads-based drug delivery system for achieving controlled drug release," *Journal of Biomaterials Science, Polymer Edition,* vol. 34, no. 4, pp. 541-564, 2023.

[17] Á. D. González-Delgado, G. Cogollo-Cárcamo, and F. Bertel-Pérez, "Mass-Integration and Environmental Evaluation of Chitosan Microbeads Production Modified with of Thiourea and Magnetite Nanoparticles," *Processes,* vol. 11, no. 7, p. 2208, 2023.

[18] L. Soltys, O. Olkhovyy, T. Tatarchuk, and M. Naushad, "Green synthesis of metal and metal oxide nanoparticles: Principles of green chemistry and raw materials," *Magnetochemistry,* vol. 7, no. 11, p. 145, 2021.

[19] E. López-López, E. Fernández-de Gortari, and J. L. Medina-Franco, "Yes SIR! On the structure–inactivity relationships in drug discovery," *Drug Discovery Today,* vol. 27, no. 8, pp. 2353-2362, 2022.

# Chapter I

# Synthesis of 1,2,3-Triazole derivatives Using Metal-Based Nanoparticles

# Part I

# Literature Review

## Introduction

1,2,3-triazoles and their derivatives stands out as an important group of bioactive heterocyclic compounds in the field of organic synthesis, demonstrating diverse pharmacological activities [1]. 1,4-disubstituted derivatives have become particularly notable because of their applications across synthetic organic chemistry [2], medicinal chemistry [3], pesticides [4], supramolecular chemistry [5], polymers [6], and material sciences [7, 8].

copper-based compounds have traditionally functioned as predominant catalysts for the 1,4-disubstituted 1,2,3-triazoles synthesis due to their affordability and reduced toxicity [9]; nevertheless, the process of removing these catalysts from the end product presents difficulties from an economic and environmental standpoint [10].

Considering this, the current focus lies in developing novel techniques that are more cost-effective, and environmentally friendly for synthesizing these compounds, with an emphasis on efficient reaction conditions.

Notably, to overcome the drawbacks associated with traditional homogeneous catalysts the integration of metal-based micro/nanoparticles as heterogeneous catalysts provides a promising way, representing a significant development in sustainable and efficient organic synthesis [11, 12].

### I.1. Triazole

Triazole, or pyrrodiazole, and its derivatives represents a significant class of heterocyclic compounds [13]. First synthesized by Fischer in 1878 [14], this compound, initially referred to as dicyanophenylhydrazine, was later termed 'triazole' by Bladin in 1885 to describe carbon-nitrogen ring systems with the formula $C_2N_3H_3$ [15]. The diverse properties of triazoles have attracted considerable attention in the chemical industry [16], making them a focal point for researchers due to their various applications in the pharmaceutical [17], agrochemical [18], and materials industries [19] .Triazoles valued for their biological importance because of their diverse applications, particularly as herbicides [20], fungicides[21], antimicrobial agents [22], and in the medical field [23]. Its incorporation into medicinal chemistry became increasingly recognized following the success of imidazoles [24]. Triazoles, being isosteres of imidazoles, involve the isosteric replacement of a carbon atom with nitrogen [25] .

### I.1.1. Chemical Structure and Nomenclature

Triazoles are heterocyclic chemical compounds with two carbon atoms and three nitrogen atoms arranged in a five-membered ring [26]. Their solubility and interaction with biomolecular targets are improved by their ability to generate hydrogen bonds. Triazoles are widely used in various fields, due to their aromaticity and electron-rich properties, binding with enzymes and receptors through interactions like hydrogen bonds, coordination bonds, ion-dipole, cation-p, hydrophobic effect, and Van Der Waals force [27].

The triazole exists in two isomeric forms, determined by the position of the nitrogen atom in the heterocycle (figure I.1), both of synthetic origin and not occurring naturally [28]. These are: 1,2,3-triazoles (υ-triazoles ), 1,2,4-triazoles (s-triazoles)


**Figure I.1.** Isomeric forms of triazoles

1,2,3-triazoles or υ-triazoles are synthetic penta-atomic heterocycles that possess a pseudo-aromatic structure, characterized by interactions between π bonds, a substantial dipole moment (4.8–5.6 Debye), and a high propensity for hydrogen bonds formation [29].

These compounds exhibit tautomerism, presenting two structural isomers with two tautomeric forms each [28]. For example, in terms of their molecular forms, 1,2,3-triazoles exist as 2H-1,2,3-triazole in the gas phase and as 1H-1,2,3-triazole in the solid and liquid phases, depending on the location of the substituent typically attached to a nitrogen atom [30]. The rings of 1,2,3-triazoles are planar and contain six π electrons [31].

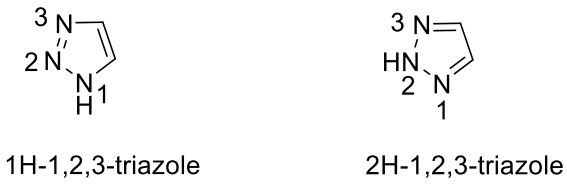


**Figure I.2.** Tautomeric forms of 1,2,3-triazole

Various regioisomers can be generated when substituents are introduced to the nitrogen and carbon atoms of the 1,2,3-triazole framework as illustrated in Figure I.3 [32].

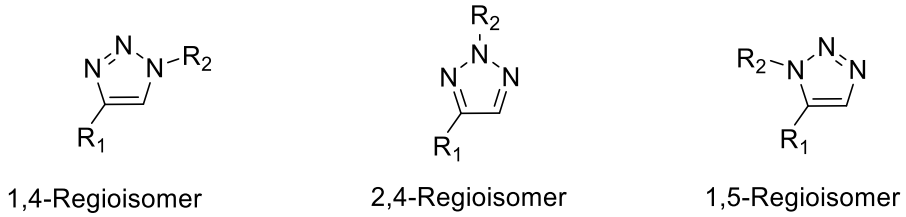


**Figure I.3.** Various regioisomers of 1,2,3-triazoles

### I.1.2. Synthetic Reactivity of 1,2,3-Triazoles

1,2,3-triazoles are broadly categorized into: monocyclic 1,2,3-triazoles, benzotriazoles, and 1,2,3-triazolium salts, regarding their synthetic reactivity [33]. Benzotriazoles and monocyclic 1,2,3-triazoles are remarkably stable under a variety of circumstances, including enzymatic breakdown, oxidative/reductive environments, and hydrolysis. In spite of this stability, reductive cleavage occurs under harsh conditions, producing triazolium salts. Despite being stable, these compounds can undergo a variety of synthetic processes, including complexation, ring-opening, arylation, and alkylation [33].

### I.1.3. Synthetic approaches of 1,2,3-triazole

Initially, the 1,3-dipolar cycloaddition process of azides and alkynes, known as the Huisgen cycloaddition reaction, it is a process that produced 1,2,3-triazoles at high temperatures and lacking selectivity [34]. However, this method found limited application in organic synthesis due to its drawbacks such as high temperature requirements, poor regioselectivity, and low yields. Subsequently, Sharpless and Meldal in 2001 individually described a regioselective approach for synthesizing 1,4-disubstituted 1,2,3-triazoles using azide-alkyne cycloaddition catalyzed by copper(I), widely recognized as the "click reaction" [34].

Another complementary development after the click reaction breakthrough was the ruthenium-catalyzed cycloaddition of alkynes and azides, however it produced 1,5-disubstituted 1,2,3-triazoles only [34]. However, this method is limited by the use of costly metal catalysts, high reaction temperatures, and low yields.

The use of metal catalysts in synthesizing 1,2,3-triazoles is further limited by the toxicity associated with these catalysts, thereby limiting their investigation in biological systems. Consequently, another approach was used in order to avoid the use of metal catalysts. For example Bertozzi and colleagues designed the strain-promoted azide-alkyne cycloaddition (SPAAC) reaction [35]. It envolves the azides and cyclooctynes cycloaddition, which lead to the

production of 1,2,3-triazoles without the use of harmful metal catalysts. Notably, the reaction easier to various modify different biomolecules *in vitro*.

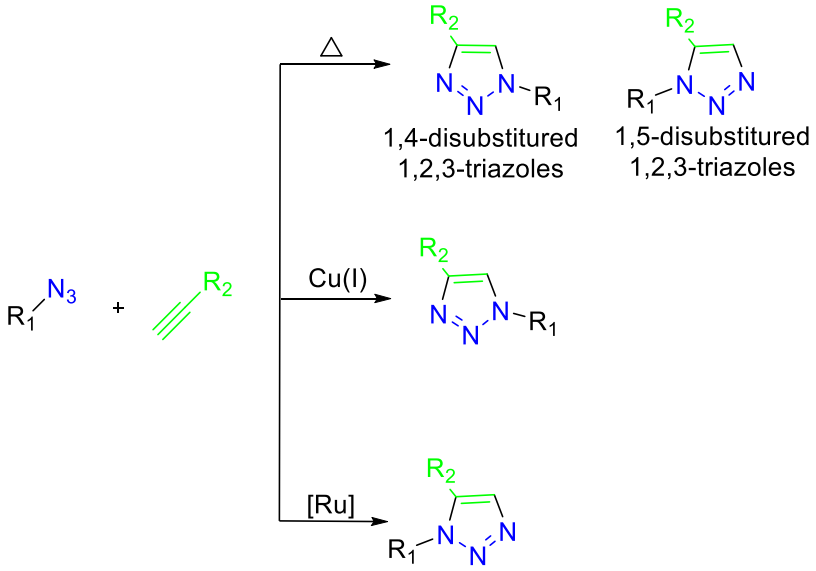


**Figure I.4.** 1,2,3-triazoles production through metal-catalyzed cycloaddition and Huisgen's reactions [34]

### I.1.3.1. "One-pot" synthesis of 1,2,3-triazoles

Purification procedures for chemical synthesis when done on a larger scale are often time-consuming. Repetition of procedures such as phase separation, solvent evaporation, crystallization, filtration, and reaction quenching after each causes longer purification times. For example, even though the reaction can take only a few hours but finishing the required purification procedures can take days [36].

To accelerate synthesis procedures it is important to minimize the amount of post-processing steps needed for each reaction. One efficient strategy is to use one-pot reactions, such as tandem and cascade reactions. A domino (cascade, tandem) reaction involve executing multiple sequential reactions within a single reaction step and requires adding all of the reagents at the beginning, allowing several reactions to proceed in expected order. Notably, in the desired end product is produced without the need to purify intermediates because each reaction can only begin after the previews one is finished. This method results in short synthesis time, higher yields and less chemical waste. Therefore, it is recommended to highlight the importance of pot efficiency is also advocated [37].

In order to be successful one-pot reaction must have high yield and reduce the formation of byproducts and side products in each step. It is also important to use equimolar concentra-

tions of chemicals whenever available. the solvent selection is another important factor in the process [38].

The one-pot reactions must be used to reduce purifying procedures, to achieve quick synthesis and increase resource utilization in chemical production [36] .

In the literature, the "one-pot" synthesis of triazoles has been deeply studied. Interestingly, S. Bahadorikhalili, A. Ghaempanah, Mohammad Sadegh Asgari, et *al*. have proposed a method to synthesize 1,4-disubstituted 1,2,3-triazoles using alkynes and derivatives of aromatic halide [39]. This process involves the catalysis of copper and allows for the formation of the corresponding triazoles in a single reaction vessel with satisfactory yields (Figure I.5).

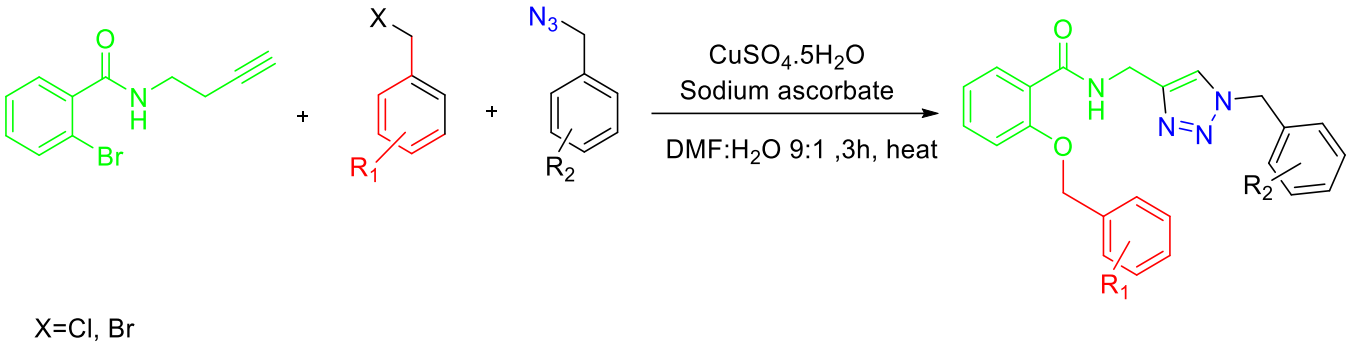


**Figure I.5.** 1,2,3-triazoles “One-pot” synthesis [39]

### I. 1.3.2. Click chemistry

Click chemistry, which is distinguished by quick reactions and high yields, can be effectively used to manufacture heterocyclic compounds containing the 1,2,3-triazole component [40]. this approach enables the synthesis of a variety of derivatives with advantageous yields through an affordable and accessible synthetic pathway. Notably, it does not need any additional purification of intermediates or final products [41].

Sharpless in 2001 gave the concept of click chemistry [42], centers around promoting facile, low-energy reactions that unite two distinct units in a simple and rapid manner. Sharpless outlined specific criteria for a reaction to be classified as "click chemistry" [43], including : modularity, High yields, stereoselectivity, tolerance to water, oxygen, and other functional groups, absence of the need for protective groups and thermodynamic favorability.

Additionally, click chemistry reactions are recommended to:

- Avoid or use non-toxic and easily removable solvents

Occur under straightforward reaction conditions, either employing commercial reagents or being easy to prepare.

Sharpless categorizes click chemistry into various types of chemical transformations[44], including ( Figure I.6):

1. **Cycloadditions:** involving azides and terminal alkynes catalyzed by transition metal complexes This includes 1,3-dipolar cycloaddition reactions, as well as reactions of the Diels-Alder type.

2. **Nucleophilic ring opening reactions:** This involves stretched heterocycles such as epoxides, aziridines, cyclic sulfates, cyclic sulfonamides, episulfonium ions, and aziridium ions .

3. **carbonyls chemistry :** Specifically, the "non-aldol" variety, which includes the creation of ureas, aromatic heterocycles, thioureas, hydrazones, oxime ethers, and amides

4. **Multiple carbon-carbon bonds addition reactions :** This category includes oxidation reactions like epoxidation, dihydroxylation, aziridination, and certain Michael addition reactions.

These categories includes a wide range of reactions demonstrating the versatility and the applicability of click chemistry [44].

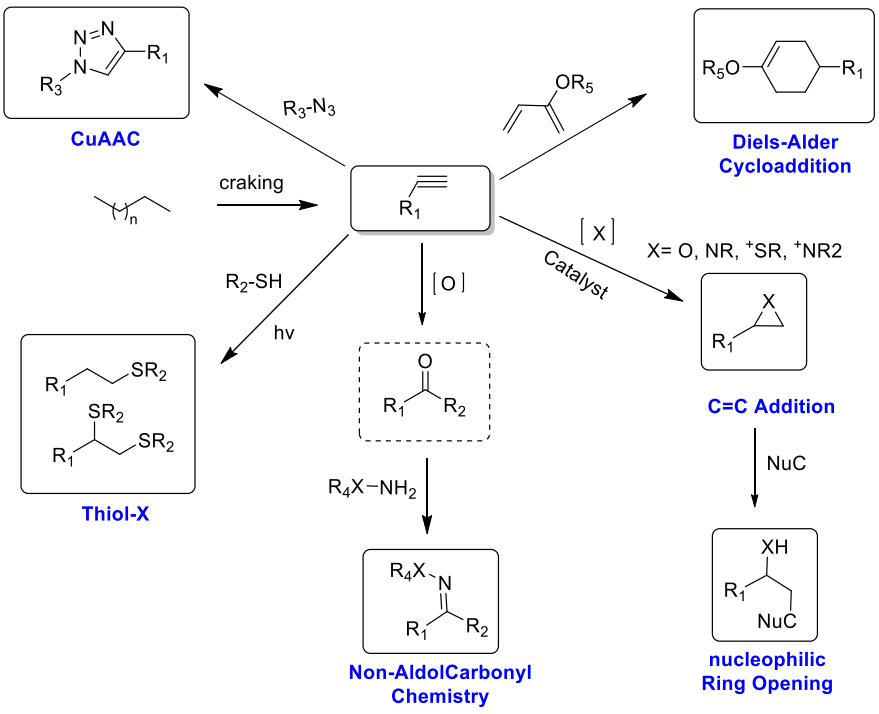


**Figure I.6.** A selection of reactions conforming to the criteria of "click" chemistry [45]

The Huisgen cycloaddition is the most used click chemistry reaction , specifically a 1,3-dipolar cycloaddition between azides and alkynes to form triazole ring. Copper catalysis ensures selective formation of the 1,4 regioisomer, providing numerous advantages such as pure product generation, straightforward reaction conditions, high yields, and the absence of secondary product generation[46].

The requirements for a "click" chemistry reaction are shown in Figure I.7, emphasizing the significance of modularity, high yields, stereoselectivity, tolerance to different circumstances, lack of protecting groups, and thermodynamic favorability.

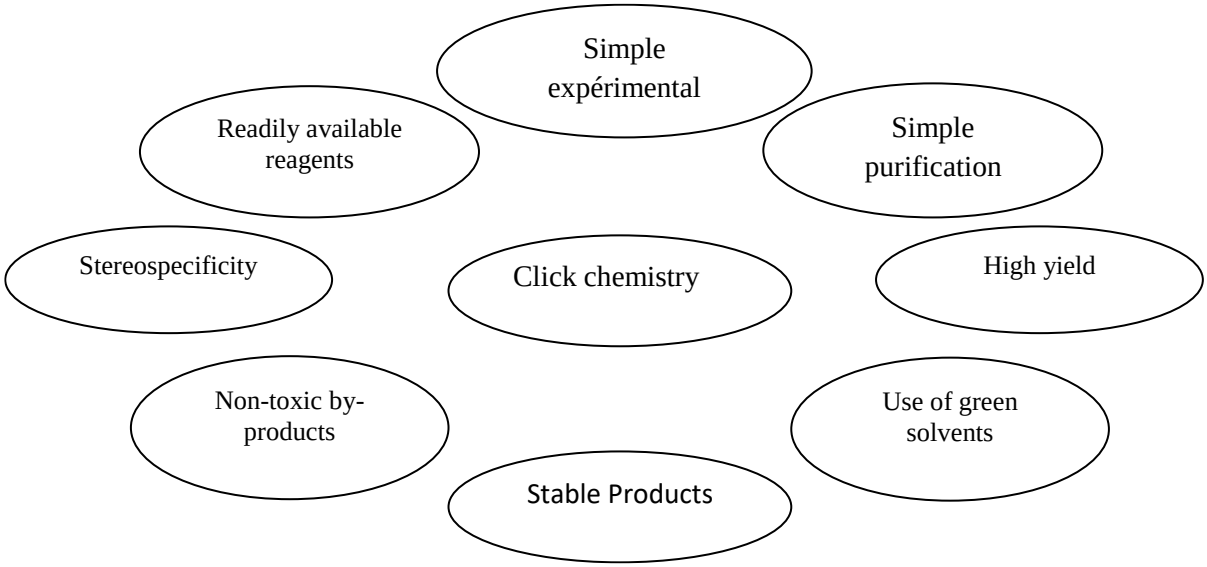


**Figure I.7.** Criteria defining a “click” chemistry reaction

### I. 1.3.2.1. 1,3-Dipolar Cycloaddition Reactions

The 1,2,3-triazole ring is formed by the 1,3-dipolar cycloaddition between azides and alkynes. This cycloaddition method allows the preparation of various five-membered heterocycles via hetero-atomic bonds efficiently and reproducibly [47]. The 1,3-dipolar cycloaddition has been recognized for over a century, it was first discovered by Michael in 1893 and later studied by Huisgen [48]. Additionally, these reactions are used to prepare various natural products [49], such as derivatives of sugars [50], amino acids [51], β-lactams [52] , compounds with pharmacological importance [53], and alkaloids[54]. For example, products like pyrazolines derived from these reactions demonstrate diverse biological activities, such as analgesic, anti-inflammatory, and herbicidal properties [55, 56].

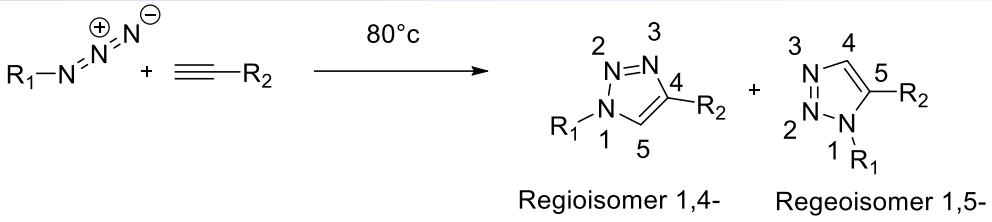


**Figure I.8.** 1,3-dipolar cycloaddition classic Huisgen reaction [57]

Cycloaddition reaction is a reaction that involves the formation of a cyclic structure when two reactants bonds [58]. Dipoles with dispersed four π electrons across three adjacent atoms are important in these reactions. At least one resonance structure is displayed by each dipole, in which opposite charges are positioned in a 1,3 arrangement [59]. Because of this structural features the expression of "1,3-dipolar cycloaddition reaction" is created. This reaction is the most favored method for the synthesis of both five-membered cyclic and heterocyclic compounds [60].

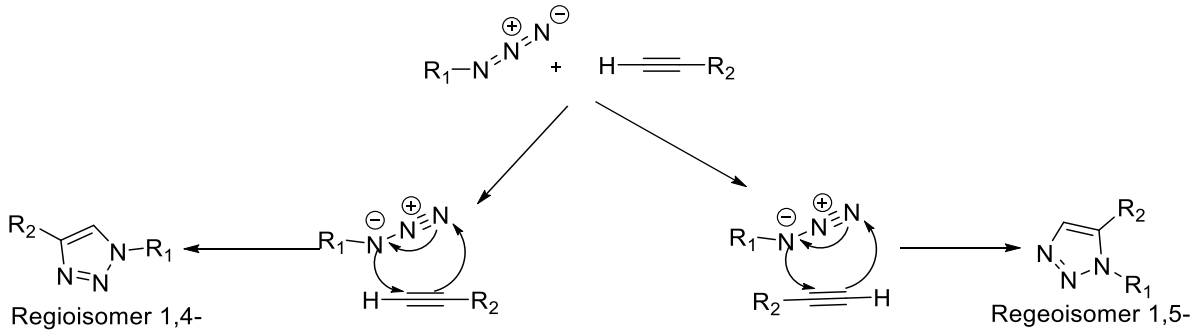


**Figure I.9.** Classic 1,3-dipolar cycloaddition mechanism (thermal) [61]

### I. 1.3.2.2. Copper(I)-catalysed azide-alkyne cycloaddition (CuAAC)

A review of the literature shows that the 1,3-dipolar cycloaddition reaction is important in click chemistry. This reaction involves genuine azides and alkynes. It is used to produce 1,2,3-triazoles [62]. Initially, the 1,3-dipolar azide-alkyne cycloaddition (AAC) synthesis required high temperatures, resulting in a mixture of regioisomers-1,2,3-triazole 1,4-disubstituted and 1,5-disubstituted after several days of reaction [63, 64]. However, not many people were interested in the AAC reaction until the 2000s, when it was finally realised that it could be much more useful.In 2002, Sharpless and Meldal independently invented a new version of the Huisgen reaction, using copper(I) as a catalyst. This meant that they could do the reaction at lower temperatures, and make the 1,4-regioisomer more quickly and selectively [65].

The discovery of Cu(I) catalysis in 2002 was a big step forward in the world of organic synthesis. This discovery caused a big change in the way scientists thought about chemistry, and made

people want to write a lot of new scientific papers on the topic [65]. This is because it makes reactions faster and more selective, which is especially clear when making 1,4-disubstituted triazoles using real alkynes.[48].

There are several ways exist to synthesize 1,2,3-triazoles without using metals[66]. However, the copper(I)-catalysed azide-alkyne cycloaddition (CuAAC) reaction, first developed by Sharpless et *al*., is the most frequently documented approach for achieving high yields

Recently, it has attracted a lot of attention as a very effective way to make important medical structures that we can use to find new medicines[67]. Most of the time, the reaction happens when there are catalytically active copper(I) compounds present, showing how important it is to keep copper(I) stable against oxidation during the CuAAC process using different ligands and reducing agents [68].

The cycloaddition can now happen at room temperature or with a bit of heating because of the amazing Cu(I)-catalyzed alteration, which only makes 1,4-disubstituted 1,2,3-triazoles with simpler processing and purification steps [69]. Cu(I)-catalysed azide-alkyne cycloaddition (CuAAC) is a highly efficient method for the selective production of 1,4-disubstituted 1,2,3-triazoles. The terminal alkyne's role as an improved 1,3-dipolarophile in the reaction with the azide is made stronger by the interaction between Cu(I) and the alkyne [69].

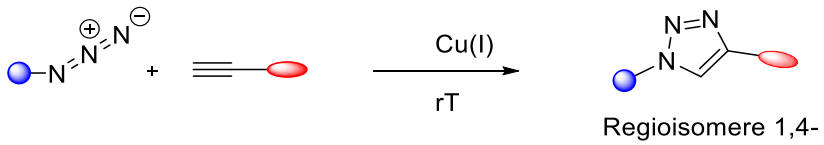


**Figure I.10.** Copper(I)-catalyzed azide-alkyne cycloaddition (CuAAC)

### I. 1.3.2.2.1. Reaction Mechanism of CuAAC

The Huisgen 1,3-dipolar cycloaddition is a simple one-step process that uses organic azides and dipolarophiles [70]. The copper(I)-catalyzed version, which involves copper at various intermediate steps, is known as a multi-stage process [71] .

Kolb et *al*. proposed using a copper(I) catalyst to achieve regioselectivity that favours the 1,4-disubstituted isomer in the copper(I)-catalyzed azide-alkyne cycloaddition (CuAAC). This is a reaction between an azide and a genuine alkyne [72]. This catalyst exclusively yielded the 1,4-

disubstituted triazole, removing the necessity for heating the reaction [72]. his catalyst only produced the 1,4-disubstituted triazole, meaning that heating the reaction was not needed. The image shows the process suggested by Himo et *al*. for this Cu(I)-catalysed joining of alkynes and azides, suggesting that Cu acetylenides play a role in the process [73].

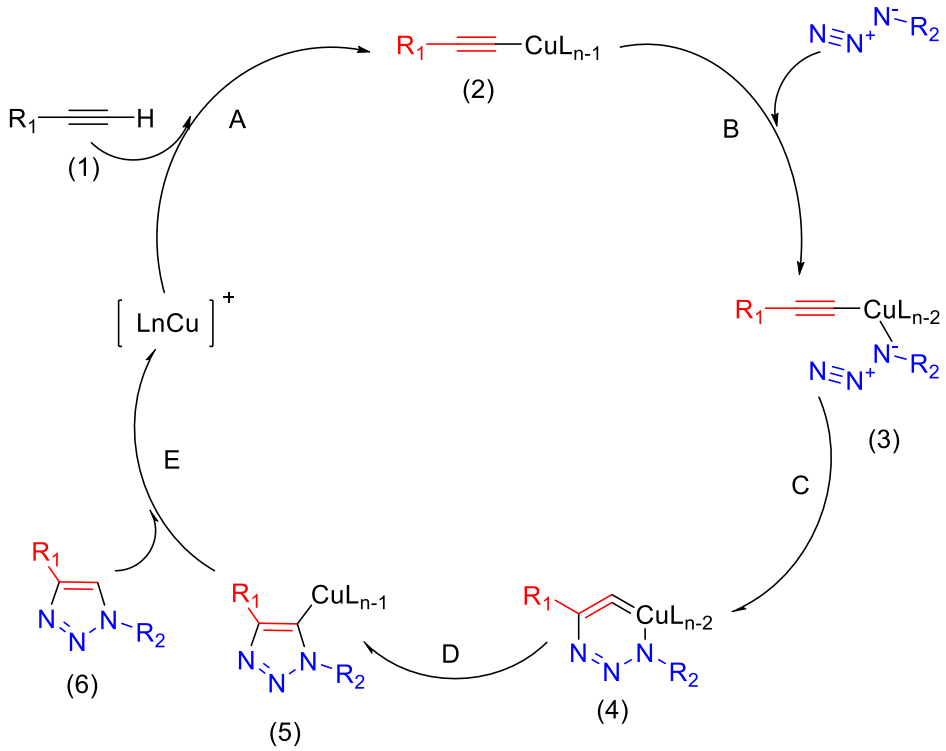


**Figure I.11.** Mechanism of 1,3-cycloaddition catalyzed by Cu(I), according to Himo et *al.* [73]

**Step A:** Alkyne (1) reacts with copper to form a complex known as "Cu-acetylide" (2).

**Step B:** The copper atom activates the azide function, displacing a ligand to generate the intermediate (3).

**Step C:** Next, the two reactive parts come together, allowing the carbon-2 of the acetylide to attach to the nitrogen-3 of the azide. This results the 6-membered metallacycle (4), with copper in oxidation state III.

**Step D:** When the metallacycle (4) contracts, it leads to the copper-triazole derivative (5).

**Step E:** Finally, the addition of a proton to the copper-triazole derivative helps to separate the desired 1,4-disubstituted triazole compound (6) and regenerate the copper catalyst.

Another way to do this is to use more soluble and manageable Cu(II) salts together with reducing agents. This makes catalytic amounts of Cu(I) in the reaction mixtures [74].

### I.1.3.2.2.2. Copper catalysis in the context of the CuAAC

There are many different copper catalysts that can make the CuAAC reaction easier, depending on how the particular Cu(I) entities are made.

#### I. 1.3.2.2.2.1. CuAAC reaction catalyzed by copper iodide (CuI)

A very practical application of copper iodide-catalysed azide-alkyne cycloaddition in the coupling of peptides through side chains or solid phase backbones was demonstrated by Meldal and colleagues. Both reactions showed selectivity towards the formation of 1,2,3-triazoles 1,4-disubstituted and changed the understanding of click reactions [75].

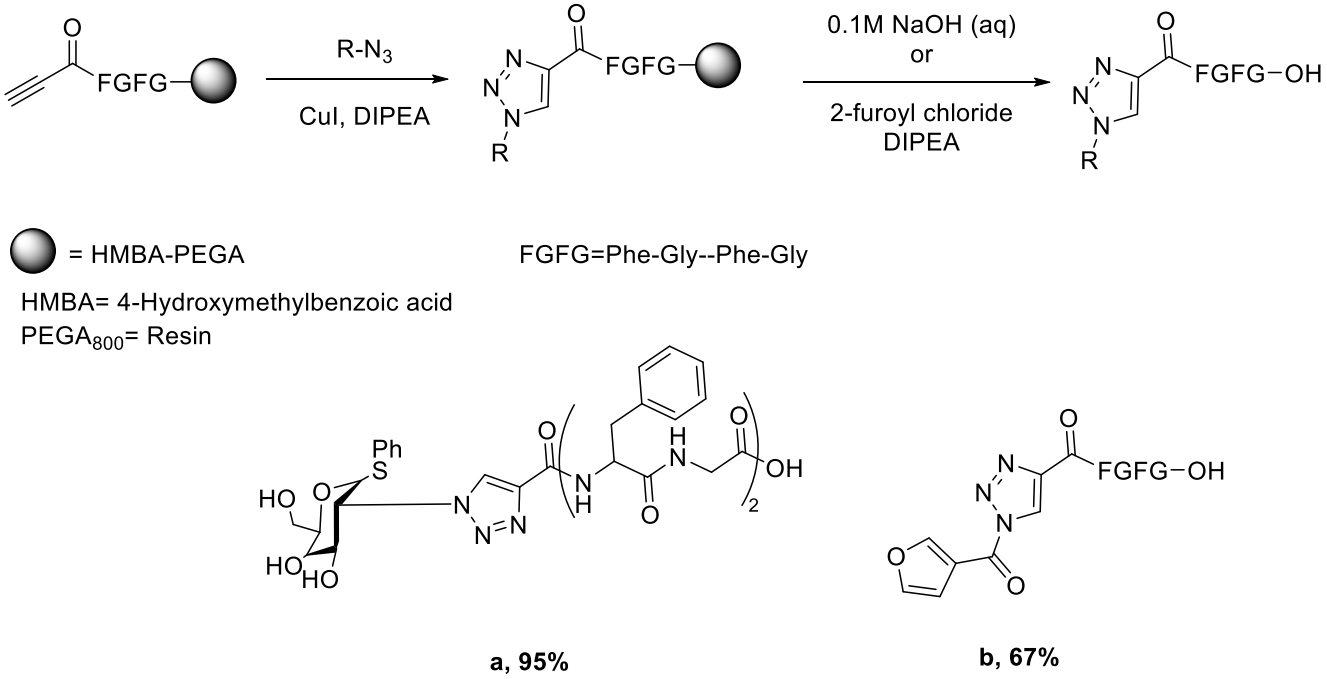


**Figure I.12.** Regiospecific synthesis of peptidotriazoles

#### I. 1.3.2.2.2.2. The CuAAC reaction catalyzed by copper sulfate pentahydrate ($CuSO_4 \cdot 5H_2O$)

Sharpless proposed the potential use of in situ generated copper(I) as an efficient catalyst for carrying out azide-alkyne cycloaddition reactions. This copper(I) is produced by reducing copper sulfate pentahydrate ($CuSO_4 \cdot 5H_2O$) with ascorbic acid. Sharpless and his colleagues demonstrated a typical example of a $CuSO_4$-catalysed click reaction in the presence of sodium ascorbate in a 2:1 mixture of water and tert-butanol at room temperature [75].

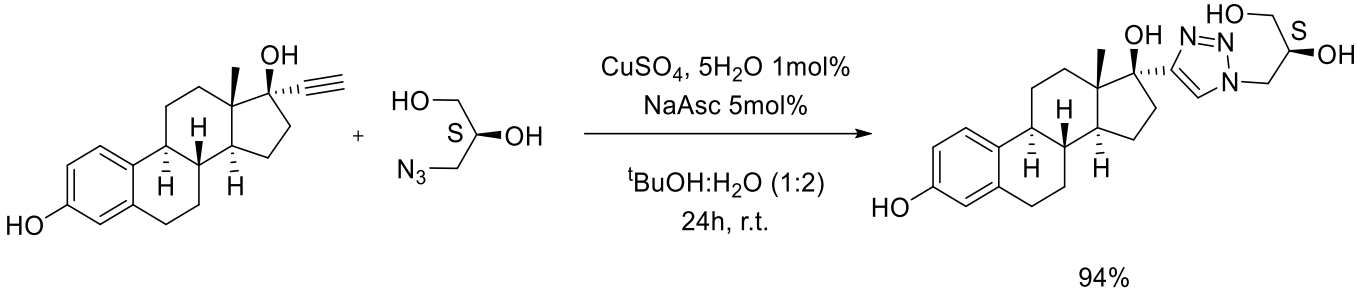


**Figure I.13** Sharpless method for the synthesis of 1,2,3-triazole [75]

The widespread acceptance of Cu(I)-catalysed azide-alkyne cycloaddition (CuAAC) in the chemical community has been attributed to several advantages [76]. Firstly, the use of copper considerably accelerates the cycloaddition process, allowing for an efficient synthesis. Secondly, the reaction can be carried out over a wide temperature range, increasing its versatility. In addition, CuAAC is water resistant, which simplifies reaction conditions and facilitates handling. It also has broad compatibility with different functional groups, making it suitable for a wide range of substrates. In addition, purification of the compounds can often be achieved by extraction or filtration without the need for column chromatography, thus optimising the synthetic process. Finally, the reaction shows tolerance to a pH range of 4 to 12, further highlighting its versatility. In addition, CuAAC enhances tolerance to different functional groups and pH fluctuations, along with its simple reaction conditions and compatibility with a wide range of solvents, including water [77].

### I. 1.3.2.2.3. Azide-Alkyne dipolar cycloaddition catalyzed by Ru(II)

In 2005, Jia and Fokin, together with their respective research groups, developed the ruthenium-catalysed alkyne-azide cycloaddition (RuAAC) reaction. This method enabled the production of 1,5-disubstituted 1,2,3-triazoles with high selectivity at the 1,5-position using terminal alkynes and azides. The usability of RuAAC extends to symmetric internal alkynes and

certain unsymmetric alkynes, providing good regioselectivity [78]. However, establishing regioselective synthesis of fully substituted 1,2,3-triazoles remains a significant challenge.

#### .I. 1.3.2.2.3.1. RuAAC reaction mechanism

In contrast to CuAAC reactions, RuAAC reactions use penta-methylcyclopentadienyl ruthenium chloride [Cp*RuCl] complex to produce high yields of 1,5-disubstituted 1,2,3-triazoles, showing an inverse regioselective behaviour [79]. Experimental and computational studies of the mechanistic aspects of RuAAC reactions, serving as a prototype click process, have shown

that RuAAC reactions occur via oxidative coupling of alkynes and azides to form a six-membered ruthenium-containing cyclic intermediate. In contrast to the copper-catalysed reaction, no ruthenium acetylide intermediate is formed. Consequently, regioisomers of 1,5-disubstituted 1,2,3-triazole are formed as the ruthenacycle undergoes reductive elimination. Interestingly, in contrast to Cu(I)-catalysed reactions, it was found that the ligand environment surrounding the Ru centre determines the catalytic efficiency and regioselectivity of this process [80].

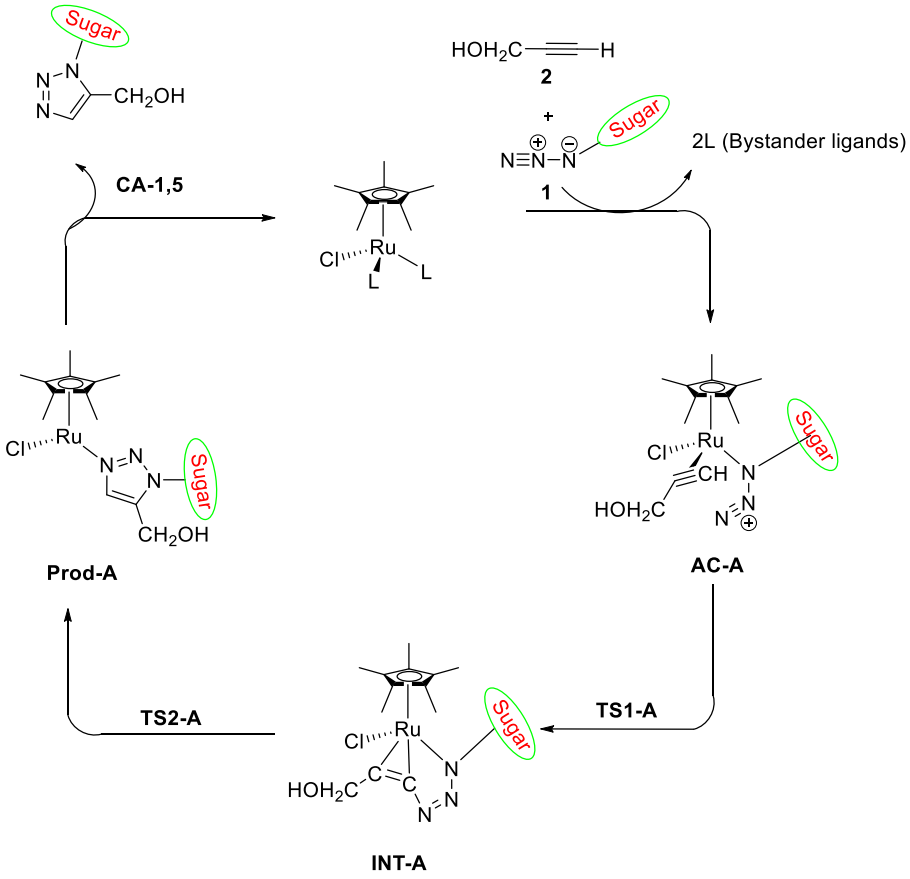


**Figure I.14.** RuAAC reaction mechanism suggested by Fokin [81]

### I. 1.3.2.2.3.2. Advantages of RuAAC

RuAAC presents several advantages, often showing faster reaction rates, higher yields and better regioselectivity. In addition, RuAAC can tolerate a wider range of functional groups, making it more versatile for various synthetic applications [82].

The development of RuAAC has created new opportunities in organic synthesis, bioconjugation, materials science and drug discovery [78]. Researchers continue to investigate and optimize RuAAC reactions to further increase their utility and efficiency.

As an example of this method, Kracker et *al*. used triazole derivatives that were previously prepared from a propargylamine and an a-azido-carboxylic acid to produce peptidotriazolamers

using a building block approach. An alternative strategy would be to use a sub-monomer technique that consists forming an amide bond with an a-azidocarboxylic acid with RuAAC and protected propargylamine [83].

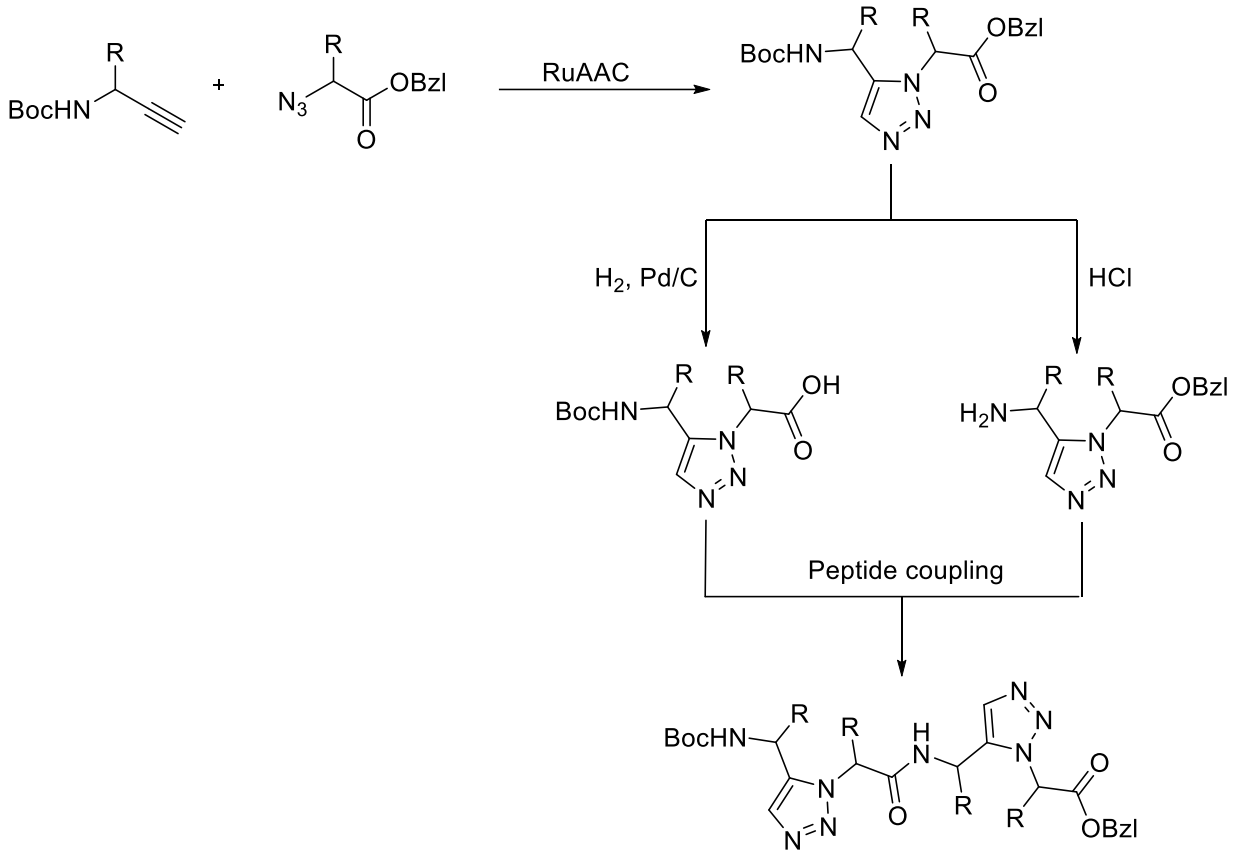


**Figure I.15.** Designed approach for peptidotriazolamer solution synthesis utilizing 1,5-disubstituted triazole building blocks produced by RuAAC.

### I. 1.3.2.2.4.Metal azide–alkyne cycloaddition MAAC

Triazoles are of considerable biological importance and have applications in a wide range of scientific fields, prompting the search for robust synthetic methods. The strategy of azide-alkyne cycloadditions is a powerful method for the preparation of these heterocyclic compounds. In contrast to traditional azide-alkyne cycloadditions (CuAAC), the use of different metals offers a promising approach to triazole synthesis. Besides copper, alternative metals such as zinc (ZnAAC), silver (AgAAC), gold (AuAAC), gold nanoparticles supported on titania (Au/TiO2AAC) and Raney nickel (RaneyNiAAC) can be used for AAC reactions [84].

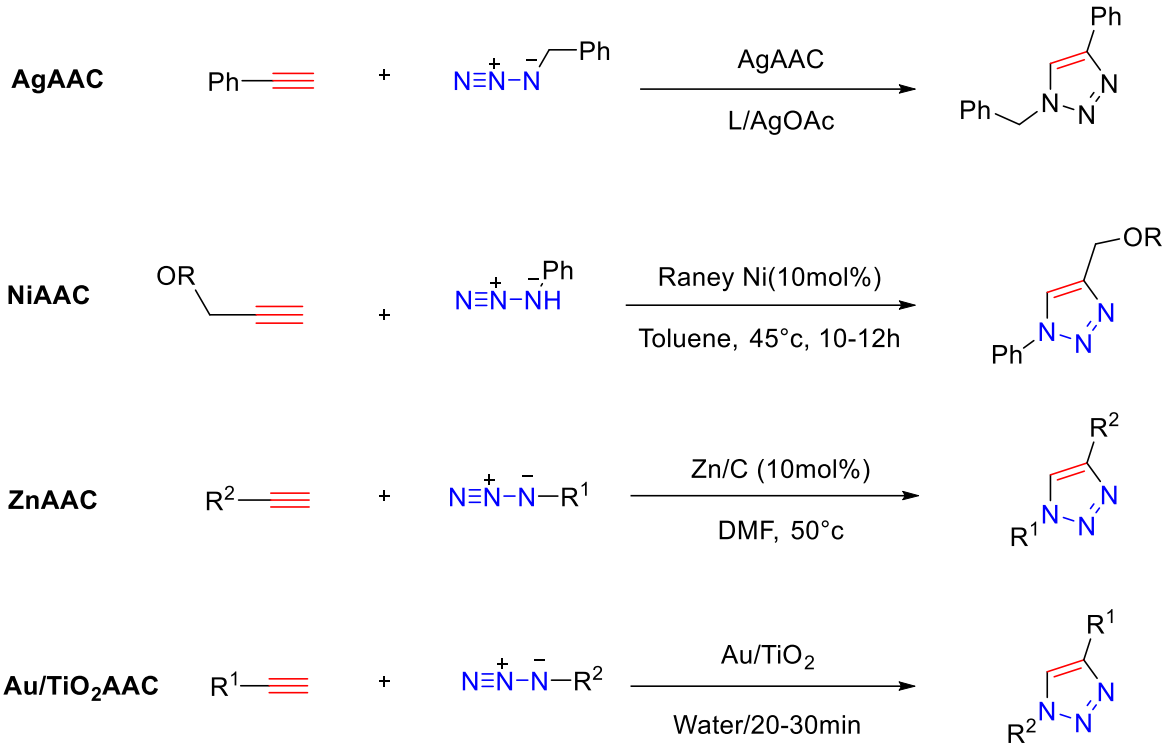


**Figure I.16.** Examples of some metals used in the MAAC for 1,4-disubstituted 1,2,3-triazole synthesis [84]

Regardless of its drawbacks, CuAAC has become a highly efficient and advanced toolkit for the synthesis of novel biomolecules and drugs in medicinal chemistry.

### I. 1.3.2.2.5. Strain-promoted azide–alkyne cycloaddition reaction (SPAAC)

The use of metal catalysts in the synthesis of 1,2,3-triazoles is further limited by the toxicity associated with these catalysts, which restricts their exploration in biological systems. As an alternative approach to the preparation of 1,2,3-triazoles, classified as click reactions, Bertozzi and colleagues investigated reactions involving azides with strained alkenes in the absence of copper [76]. Because of its interesting applications in materials science and chemical biology, strain-promoted azide-alkyne cycloaddition (SPAAC) has attracted considerable interest in recent years [85]. Thus, this approach offers considerable advantages over other established methods [86].

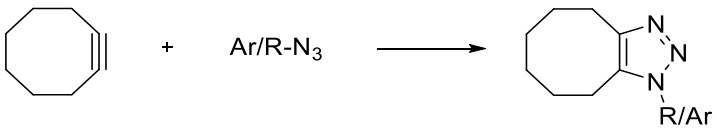


**Figure I.17.** strain promoted azide alkyne cycloaddition (SPAAC) reaction [76]

In 2003, the Bertozzi group developed a solution to this challenge using a different approach [87]. Instead of employing catalysis to reduce the barrier to cycloaddition, they used molecular strains in which the alkyne deviates from its typical linear geometry and has higher energy levels, allowing it to reach the transition state more easily and thus proceed more rapidly [88]. In what they termed 'strain-promoted azide-alkyne cycloadditions', they used cycloalkynes with eight-membered rings [89]. These reactions can be much faster than the Staudinger ligation and can be easily carried out under physiological conditions. By modifying the reactivity of the alkyne component, the efficiency and selectivity of the reaction can be improved [90].

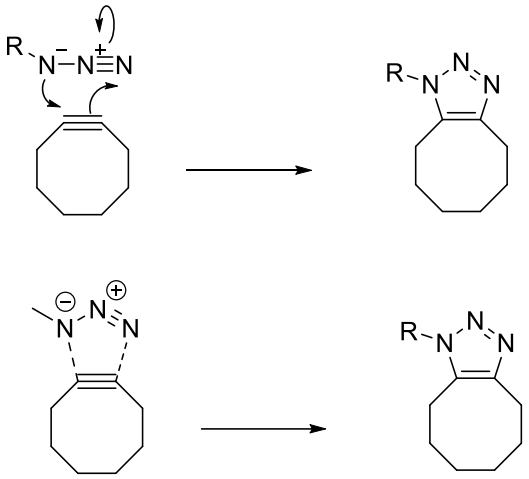

**Figure I.18.** SPAAC mechanism [91]

The SPAAC, in which various cyclooctyne derivatives react with azide-containing molecules, has attracted interest in biorthogonal chemistry. This method allows rapid and selective chemical coupling under aqueous conditions, eliminating the need for harmful substances [92].

Different reactivities during their cleavage reactions. The impressive study used sequential and fully controlled CuAAC click conjugation of three different glycans to an alkyne-modified peptide. Real peptide mimetics with successive triazoles linked to a single substituted carbon were outlined. In α-hydroxy-β-azidotetrazoles, the hydroxytetrazole acts as an alkyne protecting group which is released by hydroxyl activation. Following the formation of triazoles with the azide, a new terminal alkyne for CuAAC is released, allowing the synthesis of molecular libraries containing up to three consecutive triazoles (Figure I.19) [93].

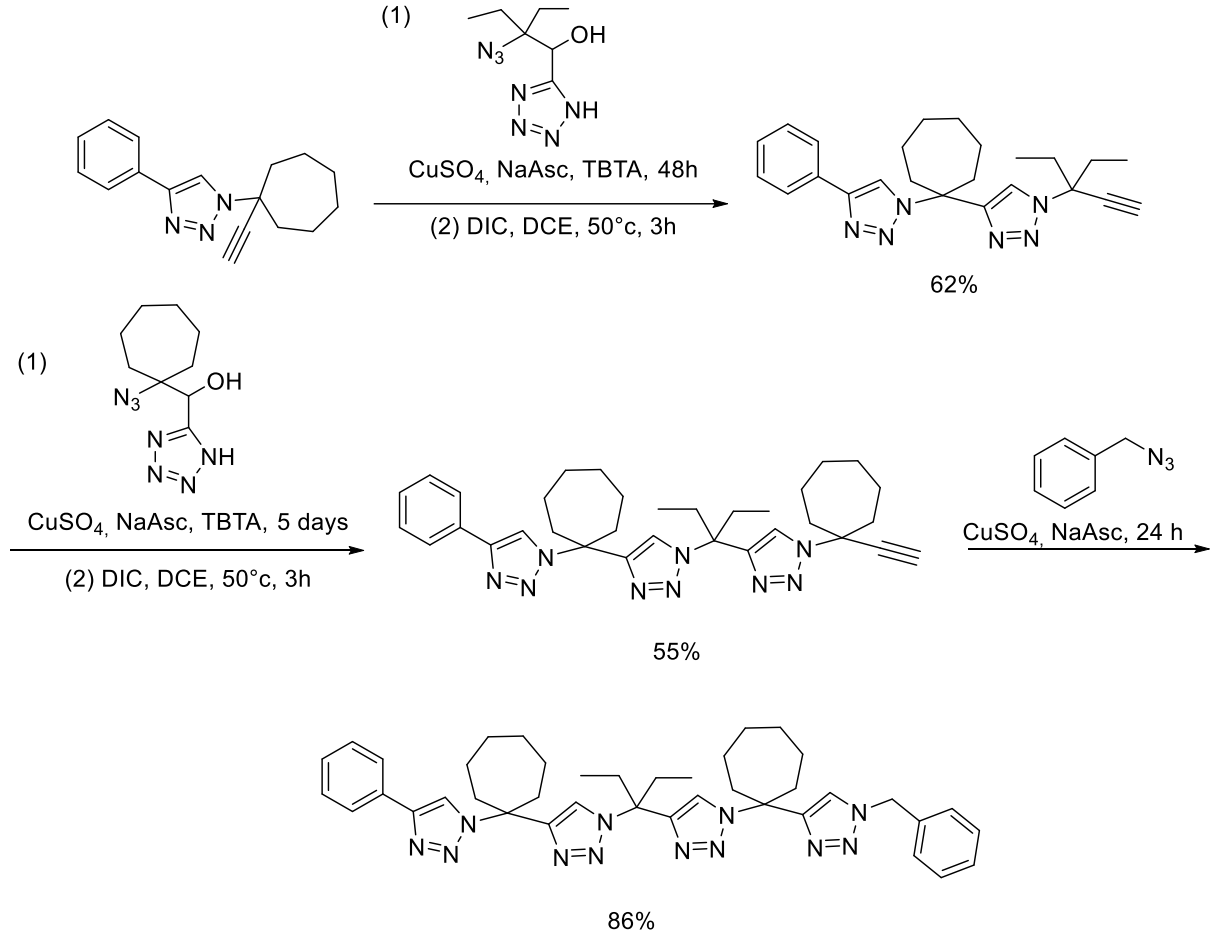


**Figure I.19.** a recent click assembly that uses a triazole substitute to create longer oligomeric α-amino acid peptide mimetics [93].

It is possible to apply SPAAC approach without the need for a Cu(I) catalyst. These reactions work particularly well in bioconjugation applications where the presence of additional metals is undesirable [94].

Advances in biomedical research has been supported by Click chemistry, wich includes methods such as SPAAC (strain-promoted azide-alkyne cycloaddition).

This reaction is an excellent illustration of how click chemistry has strengthened and enhanced biomedical investigations [95].

### I. 1.3.2.2.6. Microwave Activation

Microwave chemistry is a technique that's used more and more in the field of "click" chemistry. It is easy to use, fast, and selective, and compared to traditional methods it has several advantages due to its ability to reduce reaction times and improve yields making it recognized for its environmental friendliness. Dharavath et *al.* [96] report that microwave activation can be coupled with 1,3-cycloaddition reactions via "click" chemistry.

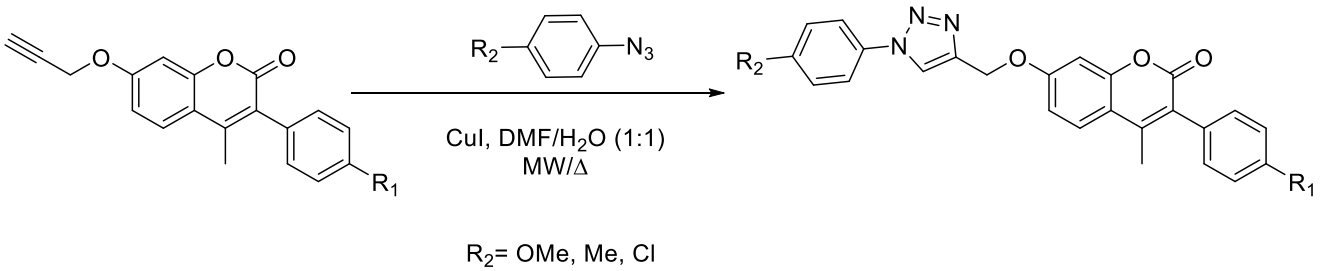


$R_2$= OMe, Me, Cl

**Figure I.20.** 1,4-disubstituted 1,2,3-triazole synthesis using a microwave-assisted method [96]

### I.1.3.3. Multicomponent reactions (MCRs)

Processes that involve combining three or more initial elements in a "one-pot" fashion are known as multicomponent reactions (MCRs). This approach results in a single product that incorporates significant portions of all components when follow successive reactions of participating reagents, Importantly, these reactions utilize the in situ formation of reaction intermediates [97].

the first MCR was discovered by Strecker in 1850 and it marked a turning point moment in the evolution of these reactions over history [98].

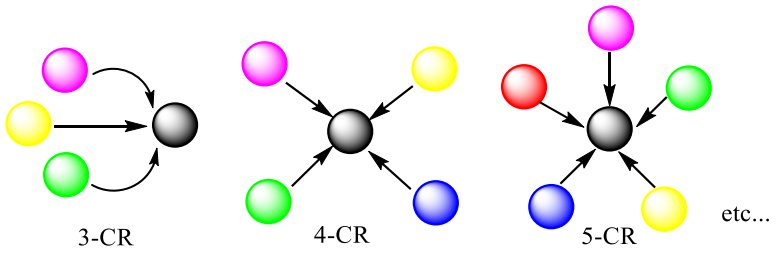


**Figure I.21.** Principle of multicomponent reactions

These "one-pot" transformations, characterized as multicompound reactions, allow for the rapid and selective synthesis of complex structures, such as imines [99], amino acids [100], β-amino ketones [101], amides [102], amidines [103], natural products [104], and various structural heterocycles [105]. Is no longer necessary to isolate intermediate compounds when is multiple bonds are simultaneously formed in a single sequence [106].

the efficiency and practicality of these synthetic approaches is enhanced by the fact that the starting materials for MCRs are often simple, commercially available, or easily accessible [107]. The chronological presentation of important MCRs demonstrates their historical development, showcasing their utility in synthesizing diverse compounds.

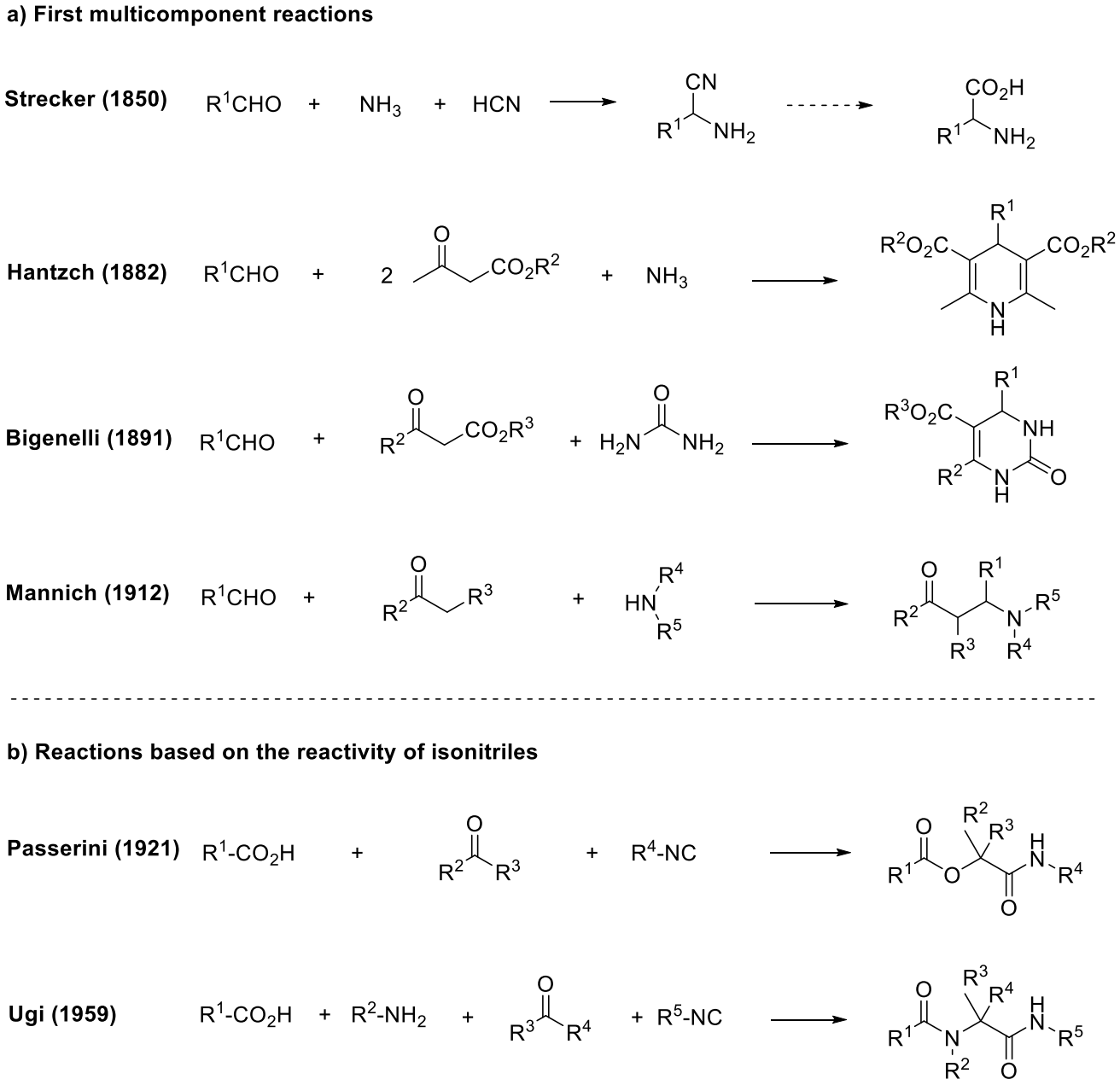


**Figure I.22.** Multicomponent reactions history [108]

The broad scope and historical evolution of MCRs is demonstrated by these reactions, highlighting their importance in synthesizing compounds with different structures.

Due to their active nature 1,2,3-triazole heterocycles hold significant importance in organic synthesis, displaying numerous and outstanding biological and pharmaceutical properties [109].

1,2,3-triazole synthesis is generally accomplished by MCRs. The following examples present the synthesis of triazole derivatives, categorized according to the type of coupling (Figure I.23) .

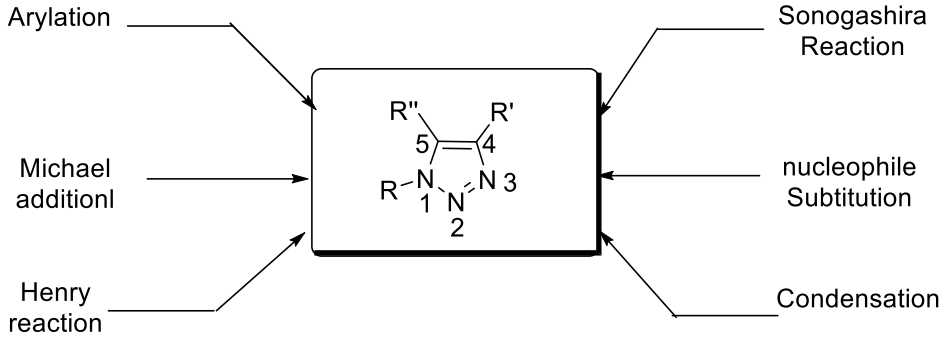


**Figure I.23.** Various routes to access triazoles via MCRs

1,3-dipolar cycloaddition, which involves terminal alkyne, benzyl halides, and sodium azide, is an example of MCR, the azide-alkyne, yielding 1,2,3-triazoles (FigureI.24). Presently, The most commonly used method for synthesizing 1,4-disubstituted 1,2,3-triazoles from various organic azides and terminal alkynes through [3+2] cycloaddition is the copper(I)-catalyzed azide-alkyne cycloaddition, also referred to as the Click or Huisgen-Meldal-Sharpless reaction [110].

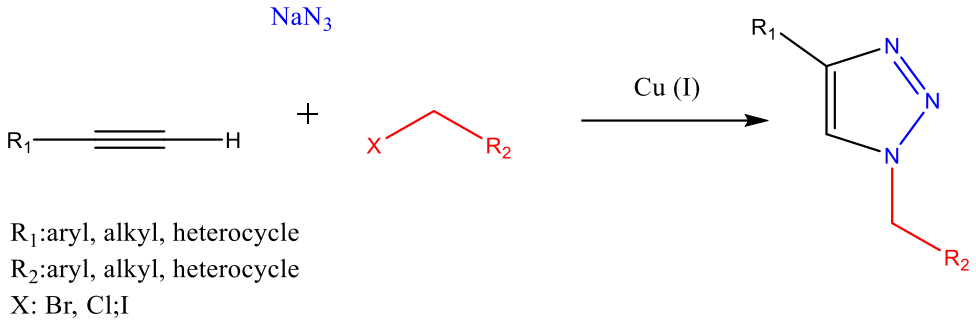


**Figure I.24.** synthesis of 1,4-disubstituted 1,2,3-triazole using multicomponent click reaction [111]

MCR processes hold considerable significance [112], owing to their alignment with economic and ecological criteria [113], in organic and medicinal chemistry due to various advantageous characteristics such as selectivity [114], atom efficiency [115], convergence [116], adaptability [117], and molecular intricacy [118].

### II. Metal-Based Nanoparticles: Innovative Catalysts for synthesis of 1,2,3-Triazole

The CuAAC is capable of generating organic azides in situ from appropriate precursors, would offer significant advantages in terms of safety and efficiency. Nonetheless, the homogenous nature of the catalysts is frequently the main cause of CuAAC procedures' disadvantages, leading to challenges in separating the catalyst and products and necessitating the use of stabilizing ligands and reducing agents like sodium ascorbate. Sodium ascorbate, a crucial component in CuAAC conditions, is prone to oxidation in the presence of air, resulting in the generation of

ascorbate by-products such as dehydroascorbate. Additionally, it can chelate copper ions during the reaction. Therefore, developing efficient heterogeneous systems is highly preferable to mitigate these issues. These difficulties are successfully avoided by using a one-pot method in heterogeneous settings to synthesize 1,2,3-triazoles from in-situ-formed organic azides, addressing safety concerns associated with handling potentially explosive azides as well. Recently, many studies have emphasized heterogeneous catalyst conditions to overcome these problems, offering advantages such as easy separation of catalyst and products by filtration from the reaction mixture, increased diffusion with an increased number of catalyst active sites, and provides a reusable catalyst [119].

Recently, nanomaterials have become the focus of attention due to their unique properties, which set them apart from their bulk counterparts. Metal nanoparticles in particular have emerged as multifunctional catalysts for a wide range of organic transformations. Among these, copper nanoparticles have gained popularity due to their low cost, and have been shown to be effective, especially in catalytic and biological applications. Moreover, there is an increasing interest in leveraging environmentally friendly, economically feasible, readily accessible, and sturdy stabilizer or support elements must be used in the synthesis of metal nanoparticles [120].

## II.1. Introduction to metal nanoparticles and their unique properties as catalysts

Nanotechnology focuses on creating and utilizing systems and structures through the nanoscale manipulation of molecules and atoms. Richard Feynman originally presented the idea in his 1959 talk at the American Physical Society, where he discussed the assembly of the molecular construction of atomic blocks. Nevertheless, years later in 1974 Norio Taniguchi , a Japanese scientist, coined the notion "nanotechnology", he dreamed about nanoscale precision manufacturing. The nanotechnology discipline was further developed by contributions from Eric Drexler, Chad Mirkin, and Richard Smalley. Additionally, there exist a branch called green nanotechnology, which focuses on the use and sustainable production of nanomaterials to benefit society [121].

## II.2. Definitions

### II.2.1. Nanoscience and Nanotechnology

Nanoscience and nanotechnology are words derived from the prefix "nano", which goes back to the Greek word meaning "dwarf" or very small, referring to the scale of one billion meters ($10^{-9}$ m). It is important to distinguish between nanotechnology and nanoscience. Nanoscience investigates the structure and properties of molecules at very small scales, typically between 1

and 100 nm. Nanotechnology, on the other hand, refers to the application of this knowledge in machines and technologies [122].

### II.2.2. Nanoparticles

Nanoparticles are materials characterized by those nanoscale dimensions, which typically fall in the range of 1 to 100 nanometers, providing a interface between individual molecules and bulk materials.

Nanoparticles exhibit unique physicochemical properties due to their size such as quantum confinement effects, large specific surface area, high energy etc. They range from metallic materials such as silver, gold, copper, zinc to metal oxides, silicate polymers organic -carbon-based material chemical compounds can exhibit a wide range of chemical structures [123].

Furthermore, nanoparticles can assume various shapes such as spherical, spherical, paper-like, or tubular. The solution treatment and the presence of bioactive substances in that solution have an impact on these striking alterations in the nanoparticles' shape and chemical composition [123].

## II.3. Classification of nanoparticles

When compared to their counterparts, nanoparticles which can be made of metal, metal oxides, organic matter, or carbon display distinct chemical, biological, and physical characteristics at the nanoscale level. These properties include increased mechanical flexibility, better reactivity or stability of chemical compounds and their tests, and much higher compared to volume. Numerous items have been created using nanoparticles, which differ in size, shape, and composition in addition to their substance [124].

Nanoparticles vary not only in material but also in dimensions, shapes, and sizes. They can exist in different dimensional forms: zero-dimensional structures, where all three dimensions converge to a single point, encompass nanoparticles and quantum dots (e.g., nano dots); one-dimensional (1D) structures, where only one parameter varies, include nanofibers, nanotubes, and nanowires (such as graphene); 2D structures that have length and width (for example carbon nanotubes); and 3D structures, often referred to as bulk nanomaterials, are characterized by equi-axed nanometer-sized grains and are defined by three arbitrary dimensions that are not confined to the nanoscale (e.g., gold nanoparticles) [125]. In summary, nanoparticles come in diverse shapes, sizes, and structures, making them versatile for various applications [126].

Essentially, nanoparticle synthesis involves two main methods : the 'bottom-up' and 'top-down' approaches. In the 'top-down' approach, nanoparticles are produced by reducing the size of bulk materials, often through physical or chemical means such as photoreduction methods, thermal evaporation, chemical etching, sputtering, lithography, and mechanical operations like milling and grinding. However, this approach is hindered by surface structure imperfections. Conversely, the 'bottom-up' strategy depends on wet chemical techniques like metal ion oxidation or chemical reduction, as well as techniques such as hydrothermal, solvothermal, radiation-induced, co-precipitation, microemulsion, pyrolysis, sol-gel chemistry, chemical vapor deposition (CVD), and electrodeposition. This approach, alternatively referred to as the self-assembly technique, this method involves creating nanoparticles from smaller components, including small particles, atoms and molecules [127].

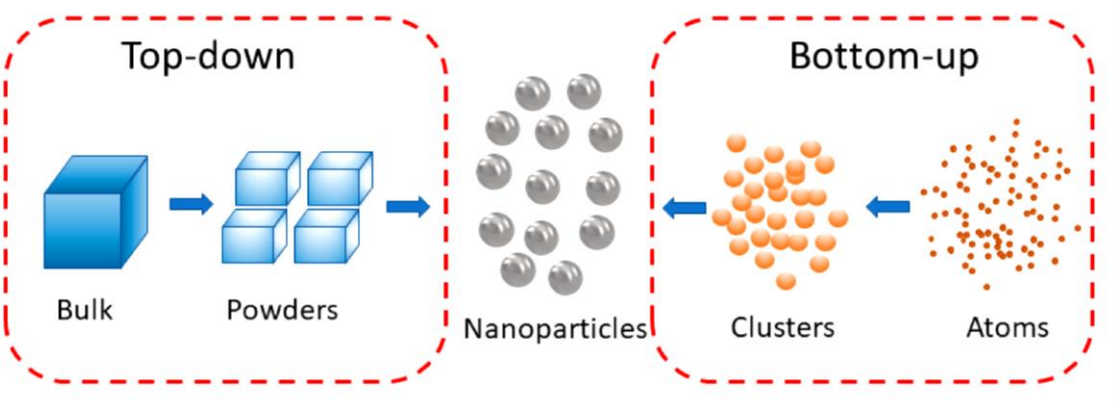


**Figure I.25.** Methods for synthesis of nanoparticles 'top-down' and 'bottom-up' [128]

The use of characterization methods is crucial for verifying these particles are indeed at the nanoscale and for ascertaining the composition and structure of materials, as well as evaluating the success of the preparation method. This essential step is vital for gaining a thorough comprehension of the material's properties. Over time, newer and more sophisticated methods have emerged alongside traditional characterization techniques (such as: XRD, SEM, TEM, AFM, UV-spectroscopy, and FTIR), contributing to a deeper understanding of materials [129].

Metal oxide nanoparticles (MONPs) in particular have garnered significant attention due to their remarkable characteristics. By means of the creation and design of engineered MONPs, researchers have been able To surpass constraints imposed by their larger counterparts, facilitating groundbreaking advancements in biomolecule sensing, targeted drug delivery and biological imaging other applications. Furthermore, MONPs exhibit enhanced cellular penetration capabilities and improved biocompatibility, enabling deeper interaction with cellular structures without causing systemic toxicity. As a result, MONPs are increasingly utilized in clinical practice

as biosensors, wound dressings for promoting healing, antibacterial agents, and agents for both enhancing image contrast and anticancer treatment [130].

Nanoparticles exhibit applications in several scientific fields (such as agriculture, medicine, textile, food industry and environment). One notable use of NPs and MONPs is in producing nanocatalysts. The efficacy of catalysts is heavily influenced by their particle size and distribution. Nanoparticles (NPs) exhibit advantageous chemical properties as catalysts due to factors such as their substantial surface area relative to volume, surface structure, and electronic characteristics, all of which are closely associated with particle size [131].

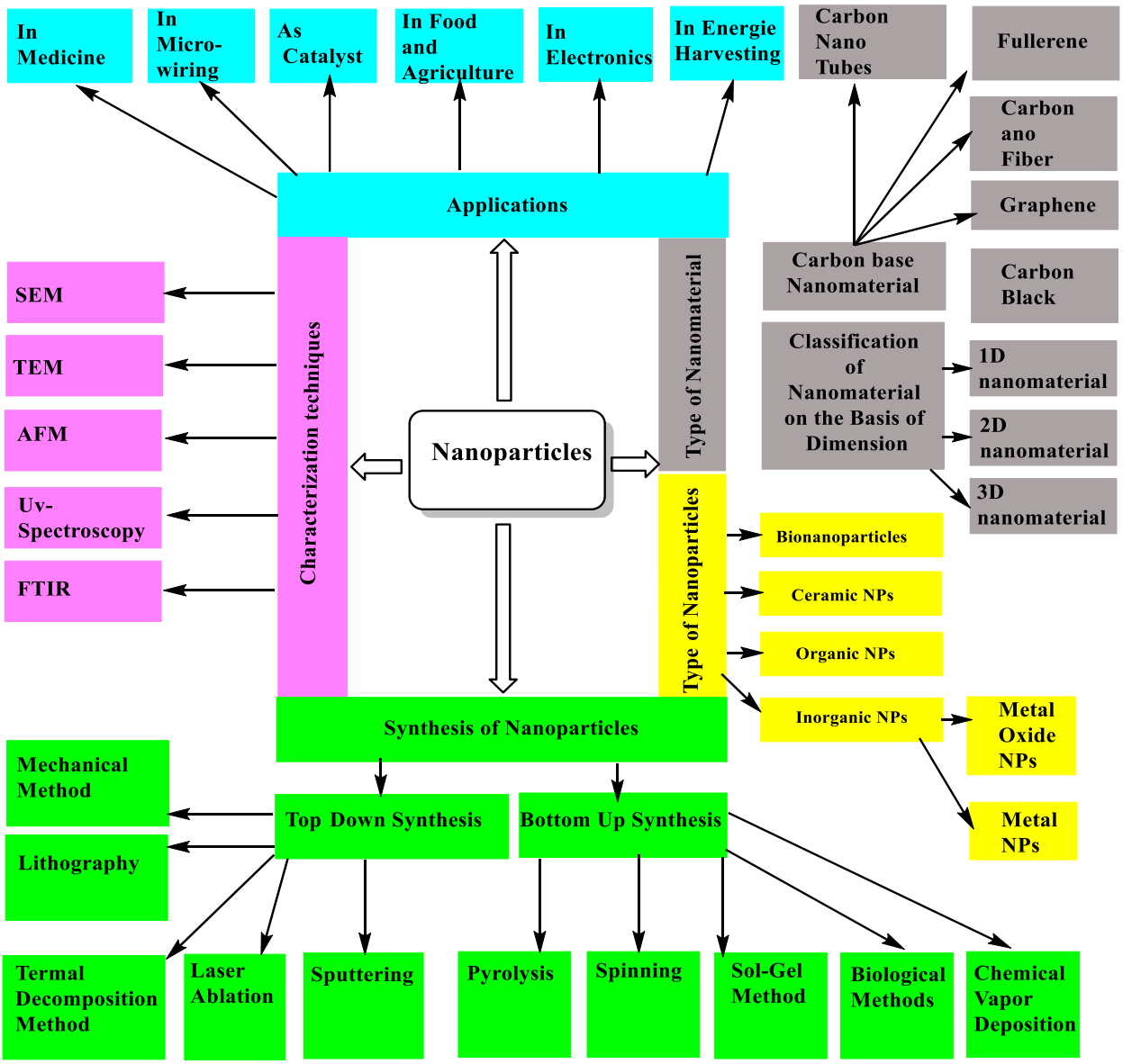


**Figure I.26.** synthesis, classification, characterizations and applications of nanoparticles [132]

### II.3.1. Metal and metal oxide nanoparticles in catalysis

Catalysts are commonly classified into three primary categories: bio, heterogeneous and homogeneous catalysts. Recovering catalysts that are homogeneous can be challenging, which often makes the process less cost-effective. While homogeneous catalysts typically exhibit good to excellent selectivity, they often lack thermal stability. Despite this limitation, homogeneous catalysis may be preferred in certain situations due to its high selectivity. However, heterogeneous catalysis is generally more favored. Therefore, addressing environmental concerns necessitates the development of new strategies that offer high yields, selectivity, operate under mild reaction conditions, tolerate a wide range of pressure and temperature, enable recoverability and reusability of catalytic systems, and minimize waste generation. In this context, heterogeneous catalysis frequently emerges as an effective alternative to homogeneous catalysts [133]. Metal nanoparticles (M-NPs) and metal oxide nanoparticles (MONPs) with precise size distributions attraced considerable attention in both industrial applications and scientific research because of their remarkable characteristics stemming from their substantial surface-to-volume ratios . These nanoparticles exhibit characteristics advantageous for efficient catalysis. Heterogeneous catalysis allows for operation at elevated temperatures and facile catalyst recovery but suffers from issues like low selectivity and a lack of clear understanding regarding mechanistic aspects necessary for parameter enhancement. Nevertheless, transition metal nanoparticles play a fundamental role in catalysis by imitating catalytic processes and metal surface activation at the nanoscale, thereby improving the heterogeneous catalysis's selectivity and efficiency [134].

## II.4. Copper and copper oxide nanoparticles

Copper is a heavy metal that is ductile and malleable, possessing a density exceeding 5 $g/cm^{-3}$, and showing a lack of reactivity to chemicals. Furthermore, it serves as an indispensable trace micronutrient, crucial for vital enzyme processes essential for the survival of both humans and animals. Apart from its diverse range of applications, copper is intricately involved in enzymatic processes, including those facilitated by tyrosinase, dopamine hydroxylase and lysyl oxidase. Its metabolic functions are closely linked to the creation of copper protein complexes and chelates. In the realm of biology, copper plays a pivotal role in oxygen transport through its involvement in hemocyanin, a counterpart to hemoglobin found in mollusks and crustaceans [135].

Stable copper oxide is extensively employed as a semiconductor among transition metal oxides, with its composition comprising various crystalline phases influenced by the environ-

ment and copper's coordination states. Within these phases exist: cuprous oxide (cuprite, $Cu_2O$) and cupric oxide (tenorite, CuO), two forms that are thermodynamically stable [136].

Cuprous oxide ($Cu_2O$) belongs to the class of p-type semiconducting compounds and exhibits favorable manufacturing and electrical characteristics, making it an attractive prospect for electronic and energy devices. Cuprous oxide possesses a cubic crystalline structure with 4.2696 Å lattice parameter. This crystal structure aligns with the space group $Pn\bar{3}m$, Distinguished by a full octahedral symmetry [137].

Copper oxide ($Cu_2O$) nanoparticles hold significant appeal due to their various industrial applications like enhancing ink permeability, serving as sensors, and acting as carriers in solar cells. Additionally, they are relevant in biological contexts and exhibit antibacterial and antiviral properties [138]

### .II.4.1. Copper nanoparticles as catalysts

Copper nanoparticles (Cu-NPs) exhibit significant catalytic activity across diverse applications, including materials and medicine, owing to their nanometer-scale dimensions. Their easy availability, low cost, and environmentally friendly nature have led to increased attention in organic synthesis. In recent years, numerous catalytic systems have emerged, showcasing excellent selectivity in various organic reactions catalyzed by copper, such as the Suzuki, Heck, Click, and oxygen arylation reactions, among others. However, despite the many advantages and potential of Cu nanoparticles as effective catalysts, their catalytic properties remain relatively underexplored in comparison to other metals like Mg, Pd, Ni and Zn [134].

## II.5. Advantages of using metal nanoparticles for synthesizing 1,4-disubstituted 1,2,3-triazoles

The Huisgen 1,3-dipolar cycloaddition reaction, often catalyzed by Cu and Cu-based nanoparticles (NPs), is celebrated as one of the most renowned click reactions. This reaction, which involves azides and terminal alkynes, finds extensive applications across various industries, synthetic chemistry, and biology. Its uses range from anti-HIV and anti-viral activities to anti-cancer properties, anti-tumor properties, anti-tumor properties, and beyond Although synthetic properties can be used with variants have developed this reaction though, but generally different metabolites are preferred [139]. This preference stems from their strong catalytic efficiency [140], easy adjustability [141], improved selectivity [142], mild reaction conditions [143], heterogeneous nature [144], versatility [145], green chemistry [146].

## II.6. Examples of specific metal nanoparticles employed in triazole synthesis

In the field of heterogeneous catalysis, nanoparticles have become a focal point for chemists because of their substantial active surface areas compared to homogeneous catalysts, enabling them to efficiently catalyze a range of organic transformations. Among these, copper-based nanoparticles have gained prominence as catalysts for numerous organic reactions. Their popularity stems from their easy accessibility and abundance, making them highly versatile for diverse catalytic applications [147].

In 2015, Jalal Albadi et *al*. reported the efficient and recyclable nature of CuO/ZnO nanocatalysts, prepared via a co-precipitation technique and demonstrated good performance in click reactions, for the selective preparation of 1,2,3-triazoles from terminal alkynes and benzyl halides in water [148].

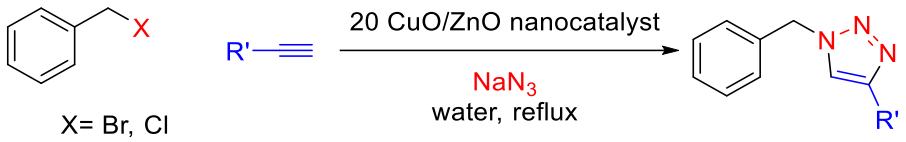


**Figure I.27.** Synthesis of 1,2,3-triazoles catalyzed by CuO/ZnO nanocatalyst [148].

In 2017, Fatemeh Ebrahimpour Malamir et *al*. designed a novel heterogeneous catalyst comprising 4-amino-2-methyl-10H-thien [2,3-b][1,5]-benzodiazepine (ATD) hydrochloride with modified poly(styrene-co-maleic anhydride) (SMA) to anchor Cu(I) ions. This catalyst efficiently mediated the selective 1,4-disubstituted-1,2,3 triazoles synthesis via click reaction copper-catalyzed, exhibiting excellent reusability and regioselectivity [149].

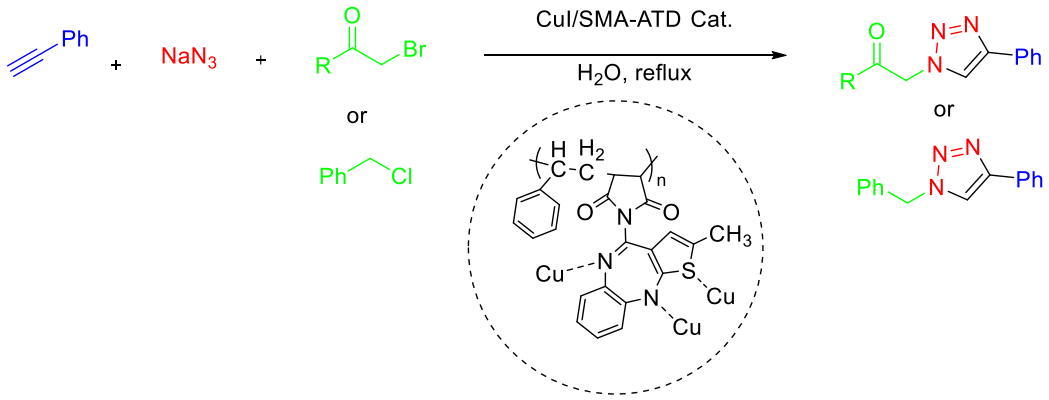


**Figure I.28.** Synthesis of 1,4-disubstitued 1,2,3-triazoles via click reaction [149]

Ahmad Shaabani designed a bio-nanoreactor catalyst, linked to magnetic multiwall carbon nanotubes anchored with chitosan nanoparticles (CS NPs/MWCNT@$Fe_3O_4$), for the 1,2,3-

triazoles preparation via click-based reactions with several constituents in a green medium. The catalyst exhibited excellent potential for reusable catalysis due to its easy recovery and recycling properties [150].

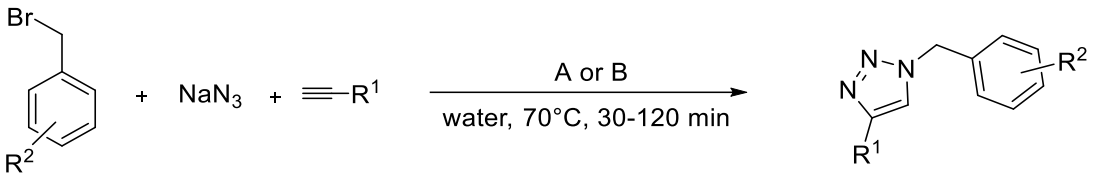


**Figure I.29.** 1,4-disubstituted 1,2,3-triazoles preparation with CS NPs/MWCNT@$Fe_3O_4$ **(A)** and Cu-CS NPs/MWCNT@$Fe_3O_4$ **(B)** as catalysts **[150]**

In 2018, Onkar S. Nayal developed a highly effective, environmentally friendly, and economically viable method employing heterogeneous copper(I) iodide nanoparticles (CuI NPs) as catalysts for synthesizing tertiary-3-aminopropenoates from alkynes and secondary amines This strategy demonstrated broad utility in synthesizing a diverse range of tertiary-3-aminopropenoates by utilizing alkynes and amines as cross-coupling partners. The gram-scale synthesis of physiologically active ciprofloxacin and its derivatives highlighted the significance of this transition. Furthermore, this technique was successfully employed in the 1,4-disubstituted-1,2,3-triazoles preparation, highlighting its versatility in accessing valuable chemical motifs with potential pharmaceutical applications[147].

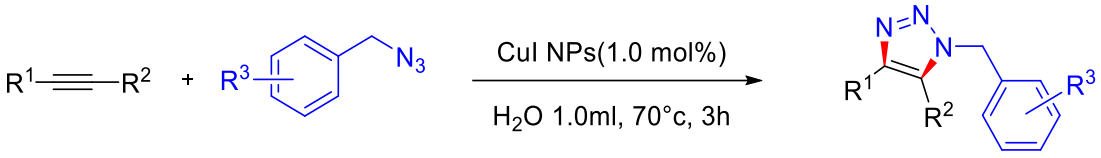


**Figure I.30.** 1,4-disubstituted-1,2,3-triazoles synthesis using CuI NPs [147]

In their 2018 study, F. Fu and R. Ciganda synthesized a water-soluble copper nanoparticles supported by a cobalticinium network (CuNPs–$CoCp_2$ ). These nanoparticles catalyzed the alkyne–azide cycloaddition reaction in water, resulting in 1,2,3-triazoles with yields of ≤99% at 35 °C [151].

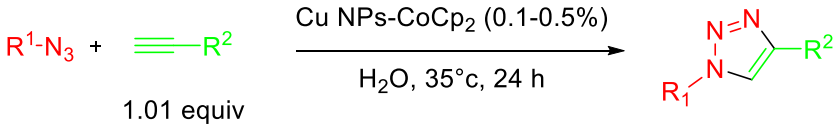


**Figure I.31.** AAC in water in presence of CuNPs–$CoCp_2$

In their 2019 study, Ali Maleki developed a copper (I) oxide nanoparticle-supported heterogeneous nanocatalyst ($Cu_2O$/Agar@$Fe_3O_4$)that has the benefit of being simultaneously economical and environmentally friendly. This catalyst facilitated the preparation of 1,4-disubstituted 1,2,3-triazoles in excellent yields in a one-pot three-component reaction under environmentally friendly conditions, with easy catalyst recovery and reuse for multiple runs [139].

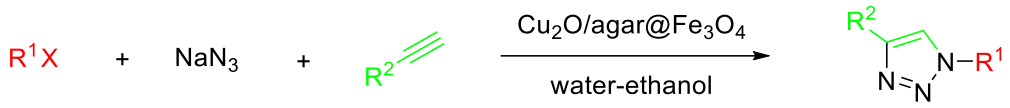


**Figure I.32.** $Cu_2O$/agar@$Fe_3O_4$ nanocatalyst for the 1,2,3-triazoles synthesis [139].

In 2019, G. Sandhya Rani developed a new type of carbon-based catalyst containing copper and sulfonate groups ($SO_3$Cu-carbon) has been developed for selectively producing β-hydroxy 1,2,3-triazoles through the reaction of azides and alkynes in water. The catalyst exhibited excellent stability, reusability, and catalytic efficiency [152].

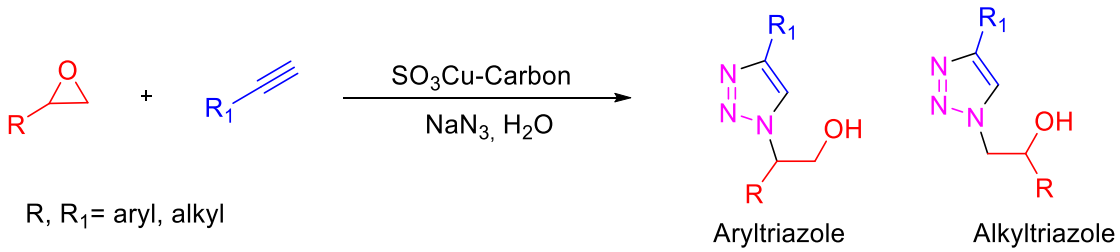


**Figure I.33**. Multicomponent synthesis of β-hydroxy 1,2,3-triazoles Catalysed by $SO_3$Cu-Carbon[152]

In a 2020 study, Razieh Deilam stabilized Cu(II) nanoparticles using $NiFe_2O_4$ nanoparticles modified by graphene quantum dots (Cu(II)/GQDs/$NiFe_2O_4$). The green synthesis of 1,4-disubstituted 1,2,3-triazoles via alkyne–aryl azide cycloaddition was made easier by this magnetically retrievable catalytic system, with reusability demonstrated over five cycles and efficient catalyst recovery [153].

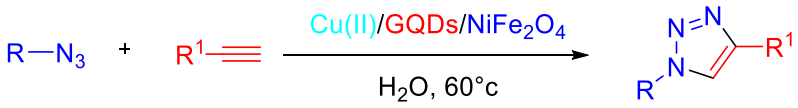


**Figure I.34.** The green synthesis of 1,4-disubstituted 1,2,3-triazoles by a magnetically retrievable catalytic system

In 2021, Kumar et *al.* synthesized a very effective catalyst, a graphene oxide (GO) supported Cu(II) Schiff base complex (GO-SB-Cu), for synthesizing 2H-indazoles and 1,4-disubstituted1,2,3-triazoles. This catalyst under mild reaction conditions demonstrated excellent recyclability and stability [154].

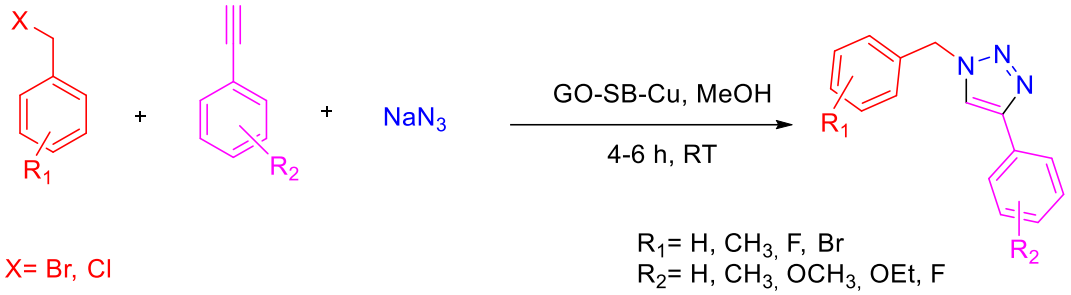


**Figure I.35.** Synthesis of 1,4-disubstituted 1,2,3-triazole derivatives [154]

In their 2023 study, Soo-Jung Kwak et *al*. the Cu@PCT@CNT catalytic platform was synthesized by anchoring it onto multi-walled carbon nanotubes modified with poly[3-(carboxypropyl)thiophene-2,5-diyl]. This platform effectively mediated the CuAAC, yielding 1,4-disubstituted 1,2,3-triazoles in a heterogeneous environment with satisfactory results [155].

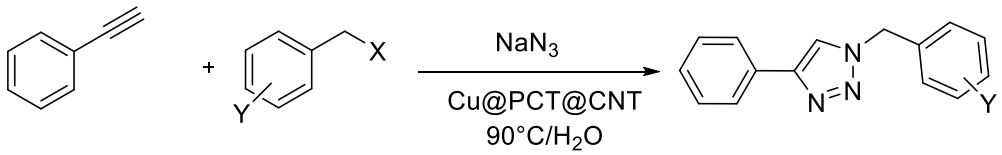


**Figure I.36.** Scope of benzyl derivatives [155]

## II.7. Green synthesis of nanoparticles using plants extracts

Utilizing plants for nanoparticle synthesis offers an eco-friendly approach, particularly valuable for detoxification purposes. This method harnesses the inherent properties of plants to reduce metallic ions and stabilize them, facilitating nanoparticle synthesis on the nano-scale. this procedure involves the combination of plant extract with a metal salt solution a room temperature, resulting in a noticeable change in solution color indicative of nanoparticle formation. This eco-friendly approach has garnered significant research attention recently due to its reduced environmental impact and lower toxicity compared to conventional synthesis methods [156].

Recently, there has been a significant research focus on synthesizing nanoparticles (NPs) using plant extracts, primarily due to their reduced environmental impact and lower toxicity to human health. NPs synthesized from plants not only exhibit enhanced stability in terms of size

and shape but also offer higher yields compared to other synthesis methods. Plant extracts serve as both reducing agents and stabilizers for NPs, enabling the reduction of toxicity in both the environment and the human body by eliminating the need for chemical agents [157].

The majority of phytochemicals, including terpenes, alkaloids, saponins, phenols, and alcohols, which are present in various plant materials, are involved in the reduction processes of metal salts . These phytochemicals are commonly found in different plant parts, including roots, stems, leaves, fruits and flowers [158]. These compounds facilitate the production of nanoparticles acting as reducing agents, while also acting as capping agents and stabilizers for them. The applications of these metal nanoparticles span across medicine, agriculture, and numerous other technologies. Researchers are particularly interested in plant species that display color or fragrance in their roots, leaves or flowers, as they contain the necessary chemicals capable of producing metal nanoparticles by reducing metal ions. The specific biogenic-synthetic route employed, incubation time, temperature, solution concentration and pH are factors that influence the size and morphology of metal nanoparticles [159].

### II.7.1. Mechanisms involved in nanoparticles green synthesis utilizing plant extracts

The green biosynthesis mechanism of nanoparticles involves three primary phases: termination, growth, and activation. Plant metabolites function as green reducing agents to extract metal ions from their salt precursors during the activation phase, leading to their reduction resulting in the reduction of these particles to nanoscale zero-valent metallic particles from mono or divalent oxidation states. After reduced metal atoms are nucleated, separated metal atoms join to produce nanoparticles with a variety of morphologies during the growth phase. Additional biological reduction of metal ions occurs during this phase, resulting in improved thermodynamic stability of the nanoparticles. Finally, in the termination phase, nanoparticles attain its most stable forms involve plant metabolites serving as a cap. The first sign of nanoparticle creation is a change in the color of the culture media, caused by a reduction in metal ion oxidation states [160].

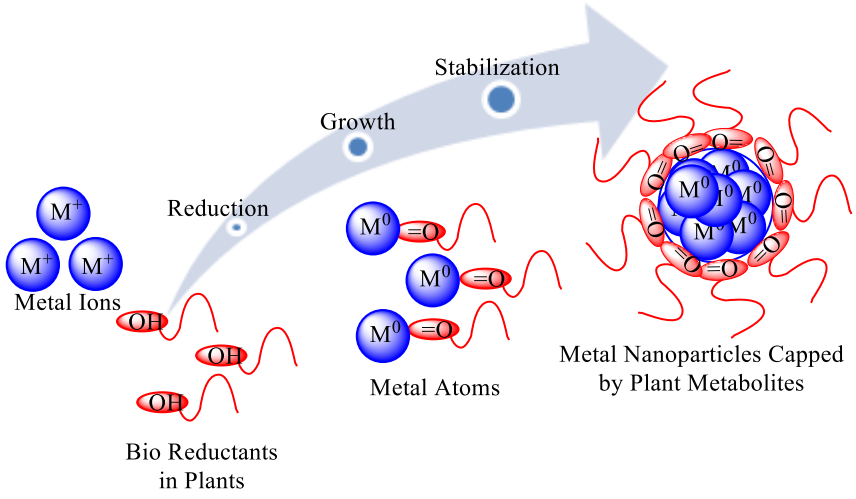


**Figure I.37.** A possible mechanism for the synthesis of MNP [160]

### II.7.2. Secondary metabolites and the synthesis of nanoparticles:

Various plant species have been documented to be used in the green synthesis of nanoparticles by utilizing their extracts, such as *Artemisia Campestris L.* . A diverse array of molecules, including proteins and a spectrum of substances with low molecular weights have been found to be involved in this process, including quinones, glutathiones, polysaccharides, antioxidants, alkaloids, amino acids, alcohol compounds, terpenoids, polyphenols and organic acids. It has also been proposed that proteins, sugars, terpenoids, polyphenols, alkaloids, and phenolic acids resulting from the reduction of metal ions contribute to the stability of the nanoparticles [161].

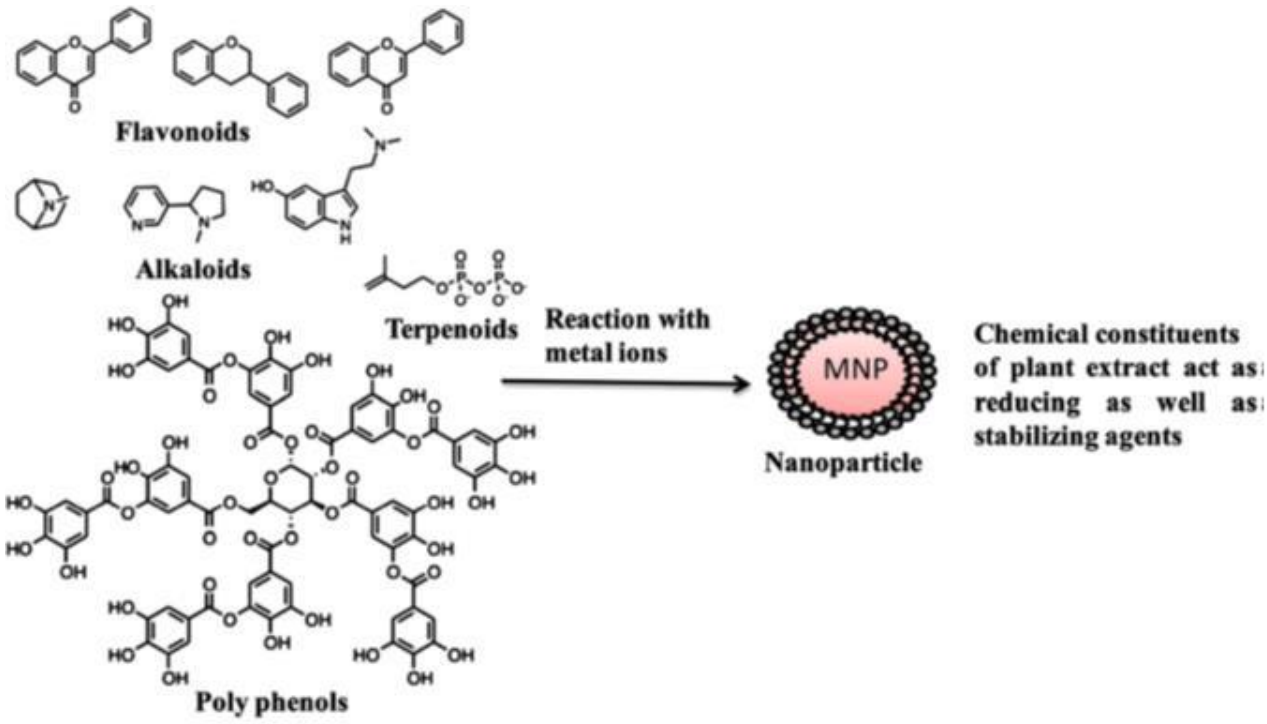


**Figure I.38.** Probable biomolecules involved in the synthesis of nanoparticles [162]

**Conclusion:**

In conclusion, the 1,4-disubstituted 1,2,3-triazoles synthesis holds immense promise in various scientific disciplines. Overcoming the challenges associated with copper-based catalysts through the adoption of environmentally friendly methodologies, particularly those utilizing metal-based micro/nanoparticles, represents a significant stride towards sustainable and efficient organic synthesis.

# Part II

# Findings and Discussion

## Introduction

In this chapter section, We'll outline the synthesis pathway for derivatives of 1,2,3-triazole 1,4-disubstituted. Three synthetic strategies are considered to achieve these heterocyclic motifs:

1. **First Strategy**: This strategy involves the preparation of alkyne derivatives through the condensation of an aromatic aldehyde with propargyl bromide.
2. **Second Strategy**: This strategy focuses on synthesizing $Cu_2O$ nanoparticles (NPs) using extracts of *Artemisia campestris L*.
3. **Third Strategy**: This strategy involves reacting the obtained products with benzyl chloride derivatives and sodium azide in the presence of $Cu_2O$ NPs, synthesized under the conditions of a one-pot multi-component reaction.

## I. Alkyne derivatives preparation

### I.1. Synthesis

Alkynes (**3a-c**) were initially created from 4- hydroxybenzaldehyde **1a**, vanilin **1b** and salicylaldehide **1c** and propargyl bromide in DMF with stirring conditions at 80°C while $K_2CO_3$ was present [163]. The reaction were monitored with TLC. This process allowed for the synthesis of the desired alkynes in the form of light hazel and light beige crystals in excellent yields. The target compounds **3a-c**, upon workup and purification by crystallization in EtOH, giving yields from 67.8- 87.7% after two hours. Results and physicochemical characteristics are described in table I.1.

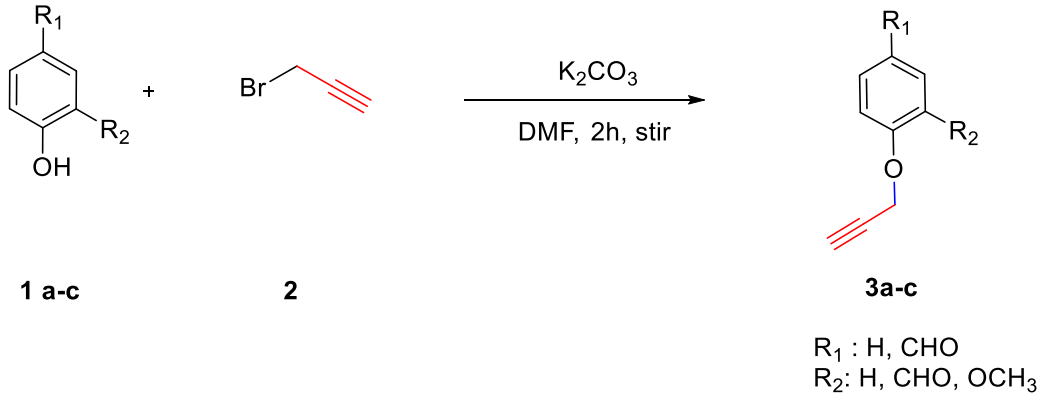


**Figure I.39** Preparation of alkyne derivatives (**3a-c**) using aromatic aldehyde (**1a-c**)

**Table I.1.** Physicochemical and structural characteristics of alkyne derivatives **3a-c**

| **Ref** | **Aldehyde** | **Yield %*** | **Melting point (°C)** | **IR ($cm^{-1}$)** | |
|---|---|---|---|---|---|
| | | | | **C≡C-H** | **C-O-C** |
| **3a** | 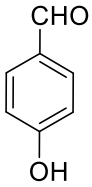 4-hydroxy benzaldehyde **1a** | 83 | 81-83 | 2110 (C≡C) 3200 (C-H) | 1160 |
| **3b** | 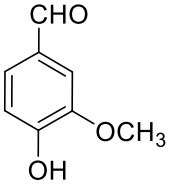 Vaniline **1b** | 75 | 84-86 | 2110 (C≡C) 3220 (C-H) | 1154 |
| **3c** | 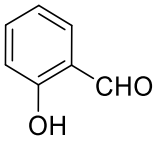 Salicylaldehyde **1c** | 74 | 66-68 | 2110 (C≡C) 3280 (C-H) | 1187 |

***:** yield of pur products **Reaction condition:** 2h, stir,80 °C

## I.2. Characterization

The structures of the alkyne derivatives **3a-c** obtained were established by the usual IR spectroscopic method. The FT-IR spectra of the alkyne derivatives **3a-c** show the presence of an absorption band at 1187 $cm^{-1}$ corresponding to the ether function (C-O) stretching vibration and the presence of two absorption bands corresponding to the alkyne function stretching vibration at 2110 $cm^{-1}$ (C≡C) and 3280 $cm^{-1}$(C-H). Thus, the FT-IR spectra are characterized by the existence of absorption bands around 1685 $cm^{-1}$, characteristic of the aldehyde (C=O) groups. The presence of the aromatic ring in the obtained products (aromatic aldehydes) is clearly evidenced by the appearance of characteristic bands of the aromatic ring around 700 and 800 $cm^{-1}$. Furthermore, the compound **3b**'s IR spectra reveals the existence of two characteristic bands of the $CH_3$ group around 3000 and 1403 $cm^{-1}$.

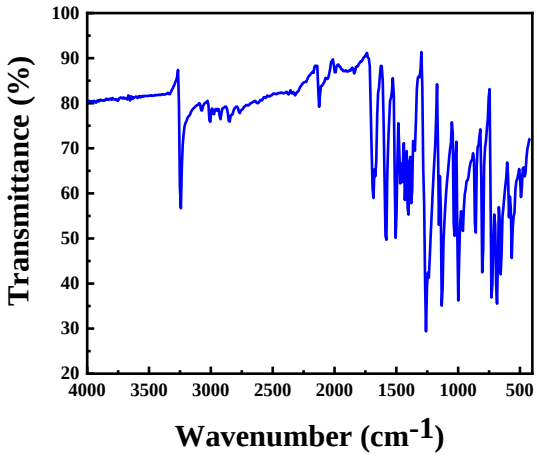


**Figure I.40.** compound's **3b** FTIR Spectrum

## II. $Cu_2O$ microbeads Preparation

### II.1. Plant extraction

Fresh *Artimisia Campestris L.* leaves were allowed to dry for 15 days at room temperature , after being carefully washed with tap water. The desiccated leaves were then processed to a superfine dust. To complete the procedure of extraction the maceration method was used. In an Erlenmeyer flask, powdered leaves (10 g) were mixed with hot deionized water (100 mL) at 100℃ for one hour. After extracting the product, it was filtered and kept in storage at 4℃ until needed.

### II.2. Synthesis of $Cu_2O$ microbeads

A 10 mL of a 1M $CuSO_4.5H_2O$ solution was prepared, then combined, in an appropriate ratio, with 10 mL of aqueous plant extract already prepared. For 30 minutes, this mixture was agitated magnetically at 70 ℃. $Cu_2O$ microbeads developed and distributed throughout the phase, causing the blue color that was initially linked with the $Cu^{2+}$ ions presence to change into a solution with reddish-brown color during the process. The centrifugation process was used to collect the $Cu_2O$ microbeads to obtain the $Cu_2O$ powder sample that had been dried for two hours at 80 ℃.

### II.3. Characterization

The utilization of UV-Vis spectroscopy, FTIR and XRD is essential in differentiating between various copper oxide compounds, including $Cu_2O$ and CuO, as these techniques reveal unique patterns linked to their crystal structures and functional groups.

Figure I.41 (b) displays the $Cu_2O$ microbeads sample's XRD pattern. The presence of the $Cu_2O$ phase is shown by the results of the XRD analysis, which show strong and intense peaks at 51.40°, 43.28°, 36.50°, and 34.21°, respectively, that corresponds to the planes (211), (200), (111), and (111). These peaks align with the $Cu_2O$ close-packed cubic structure (ccp) (JCPDS, card no:05.0667); the absence of CuO phase, suggests that the manufactured particles are pure. the $Cu_2O$ microbeads crystallite average size was determined utilising the Debye-Scherer formula ($D = K \lambda/\beta \cos \theta$), and seem to be 22.81 nm. where $\theta$ is the diffraction angle, $\beta$ is the full width half maximum (in radians), and $\lambda$ (0.1541) is the X-ray wavelength.

The FTIR spectrum displayed in the Figure I.41 (a) shows distinct peaks representing the extract's components (both the phytochemicals and the inorganic (Cu-O) components). It implies that phytochemicals are incorporated into the $Cu_2O$ microbeads, indicating interactions between copper ions and the organic extract during synthesis. Cu-O stretching vibrations absorption peak appears at 610 $cm^{-1}$ corresponds to the $Cu_2O$ microbeads [164], while O-H stretching vibrations peak appears at 3,100 $cm^{-1}$. The O-H peak has a reduced intensity as a result certain O-H groups being oxidized during the reduction of Copper ions to Cu(I) [165]. The O-H peak's broader shape could be the result of C-H bonds stretching vibrations at 2,656 and 2,890 $cm^{-1}$ overlapping with one another, contributing to the C-H group's decreased intensity. Interactions between $Cu^+$ ions and O-H groups in the extract's organic components may also be the cause of this widening, which would affect the vibrational pattern [166]. There was atmospheric carbon dioxide present during the measurement, as indicated by the peak at 2,120 $cm^{-1}$ linked to $CO_2$ stretching vibrations [167]. Additionally, the C=O and C=C bonds stretching vibrations in the group of ketone (C=O) show up at 1,512 $cm^{-1}$ and 1,608 $cm^{-1}$, respectively [166]. The stretching vibrations of C-O is attributed to the peak at 1,034 $cm^{-1}$ [168], while the peak at 685 $cm^{-1}$ indicated the C-H bonds bending modes of vibration.

A notable absorption peak at 220 nm is revealed in the UV-Vis spectra depicted in the Figure I.42 (a), serving as compelling evidence that $Cu_2O$ was successful formed and not CuO. As a result of differences corroborated by earlier research, distinctive absorption UV-Vis spectrum patterns are manifested as a result of variances in CuO and $Cu_2O$ phases electronic structures and bandgap energies. In particular, a conspicuous peak of absorption at approximately 640 nm distinguishes CuO, despite $Cu_2O$ exhibits between the 200–270 nm range a principal absorption peak, the visible spectrum indicated a red shift [169]. Typically the $Cu_2O$ microbeads' bandgap hovers around 2.7 eV (Figure I.42 (b)), classifying it as a direct bandgap semiconductor[170], thus reinforcing the notion that microbeads of $Cu_2O$ are fabricated rather than CuO. CuO's bandgap is comparatively smaller, typically ranging between 1.3–1.7 eV [171]. However, it's worth

noting that absorption and bandgap energy values may exhibit slight variations influenced by factors such as specific experimental conditions, crystal structure and particle size [172].

Numerous factors are crucial in determining the $Cu_2O$ microbeads size and morphology, encompassing temperature solution, the employed plant extract quantity, pH, and the $CuSO_4.5H_2O$ solution concentration utilized [173, 174].

SEM images depicted in Figure I.43 (a,b) distinctly exhibit spherical flower-like structures as the predominant morphology of $Cu_2O$ microbeads. The histogram displayed in Figure I.43 (c) depicts a consistent distribution of particle sizes, demonstrating that the created $Cu_2O$ microbeads are between 6 and 3 µm in size. To delve deeper into the elemental composition we used EDX (spectroscopy of X-ray energy dispersive). The EDX-SEM analysis presented in the Figure I.43 (d) elucidates that it is primarily constituted of oxygen (O) at 23.73% and copper (Cu) at 54.91%, in accordance with $Cu_2O$ phase anticipated elemental composition. Noteworthy is the content of carbon (C) at 21.72% suggests that phytochemicals from the extract were adsorbed throughout the $Cu_2O$ microbead production process [175]. These observations corroborate the findings derived from FTIR analysis.

A three-stage growing process is required to generate flower-like $Cu_2O$ microbeads (Figure I.43(a,b)). The following stages are involved in this process:

The first stage of the procedure involves the chemical reaction of $CuSO_4.5H_2O$ with an extract derived from the leaves of *Artemisia campestris L.* to produce $Cu(OH)_4^{2-}$.

In the intermediate stage, the bioactive compounds in the leaf extract of *Artemisia campestris L.* enable a quick reduction to occur once $Cu(OH)_4^{2-}$ is produced. The formation and development of tiny $Cu_2O$ nanoparticles occur as a result of this reduction process, facilitated with constant stirring.

In the second stage, larger $Cu_2O$ microbeads are formed by the self-assembly or aggregation of the small $Cu_2O$ nanoparticles produced in the first stage. This is the second stage of growth, where the particles become microbeads.

In the last Stage, the tiny building block nanoparticles inside the $Cu_2O$ microbeads become larger over time and go through a process called Ostwald ripening. Structure-directing agents are the biomolecules from the leaf extract of *Artemisia campestris L.* that are absorbed on the surfaces of the nanoparticles, are essential for regulating the nanoparticles' surface condition, which leads to the creation of $Cu_2O$ microbeads in a flowers shape.

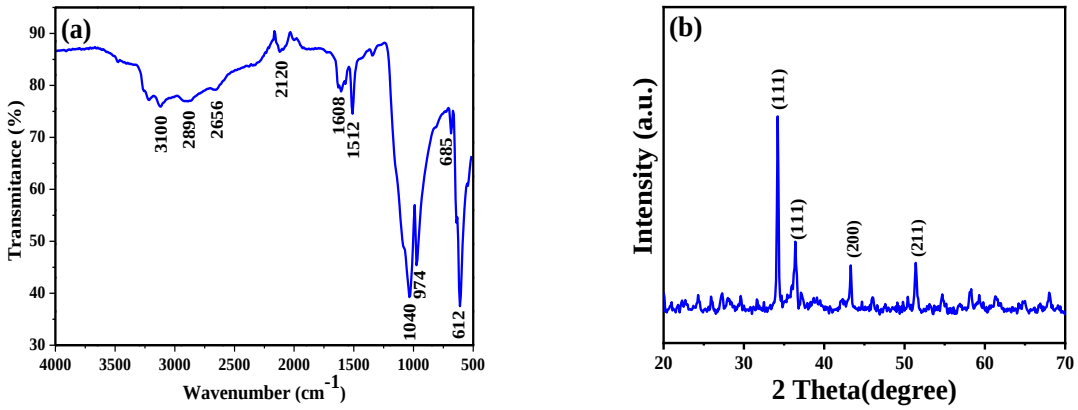


**Figure I.41.** the synthesized flower-like $Cu_2O$ microbeads analysis: **(a)** FTIR spectrum **(b)** XRD diffraction pattern

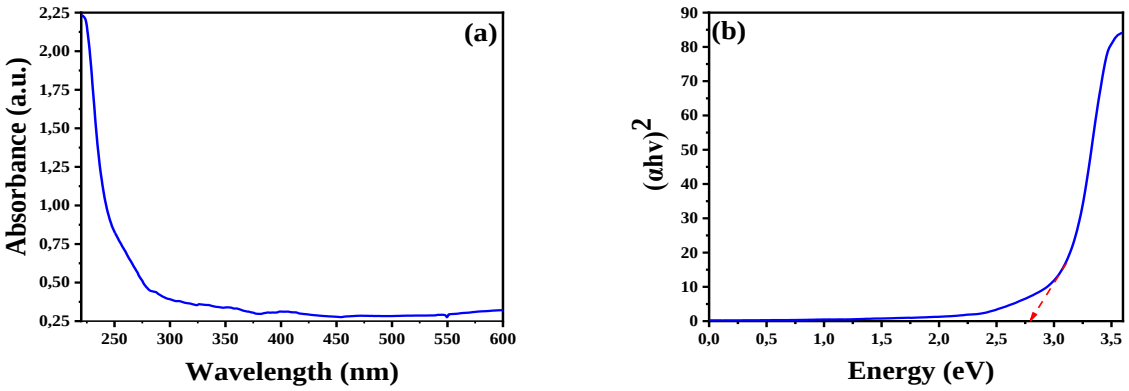


**Figure I.42.** The optical properties of $Cu_2O$ microbeads prepared using the extract of *Artimisia Campestris L.* **(a)** optical energie bandgap, and **(b)** UV-Vis Spectrum

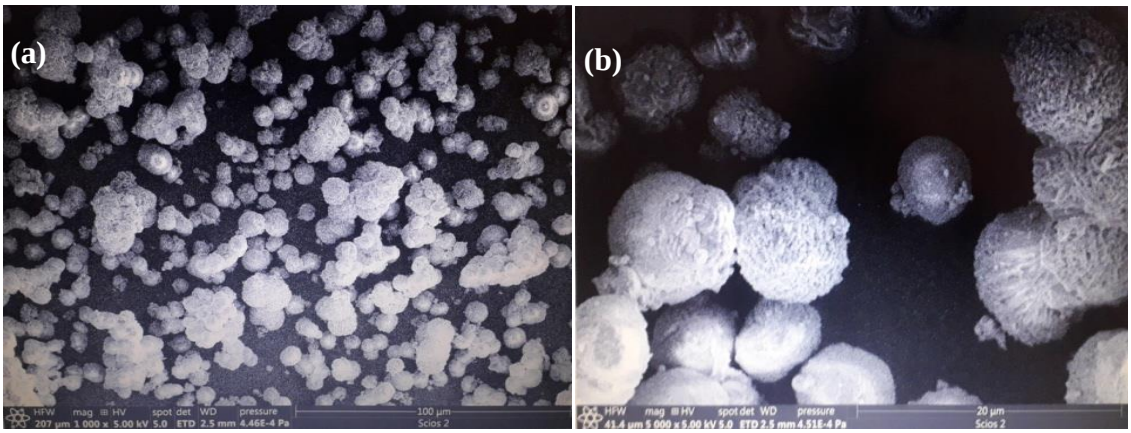

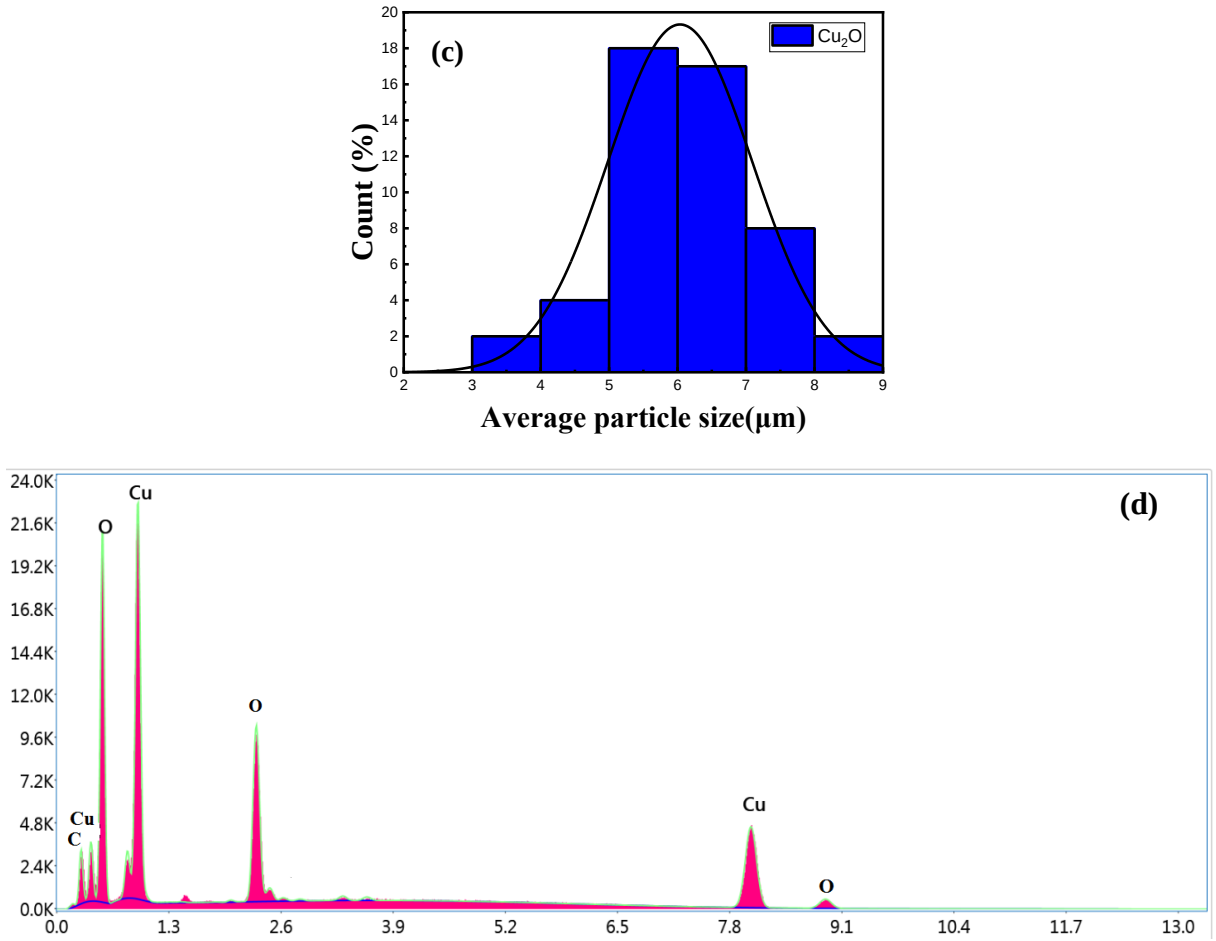


**Figure I.43.** $Cu_2O$ microbeads prepared with the extract of *Artimisia Campestris L* were subjected to SEM analysis.: **(a, b)** SEM pictures utilizing different magnification, **(c)** the distribution of particle size, and **(d)** elemental analysis of EDX

## III. 1,2,3-triazole preparation

### III.1. Synthesis

Using the previously reported procedures [11] as a guide, we performed the one-pot, three-component CuAAC reaction between alkynes (**3a-c**), sodium azide **4**, and benzyl chloride **5** in DMF:$H_2O$ (2:1, v/v) under reflux conditions at 90°c for 3-4 hours. The $Cu_2O$ microbeads was used as the catalyst system. producing the relevant 1,2,3-triazole 1,4-disubstituted compounds in moderate to exceptional yields (**6a-f**).

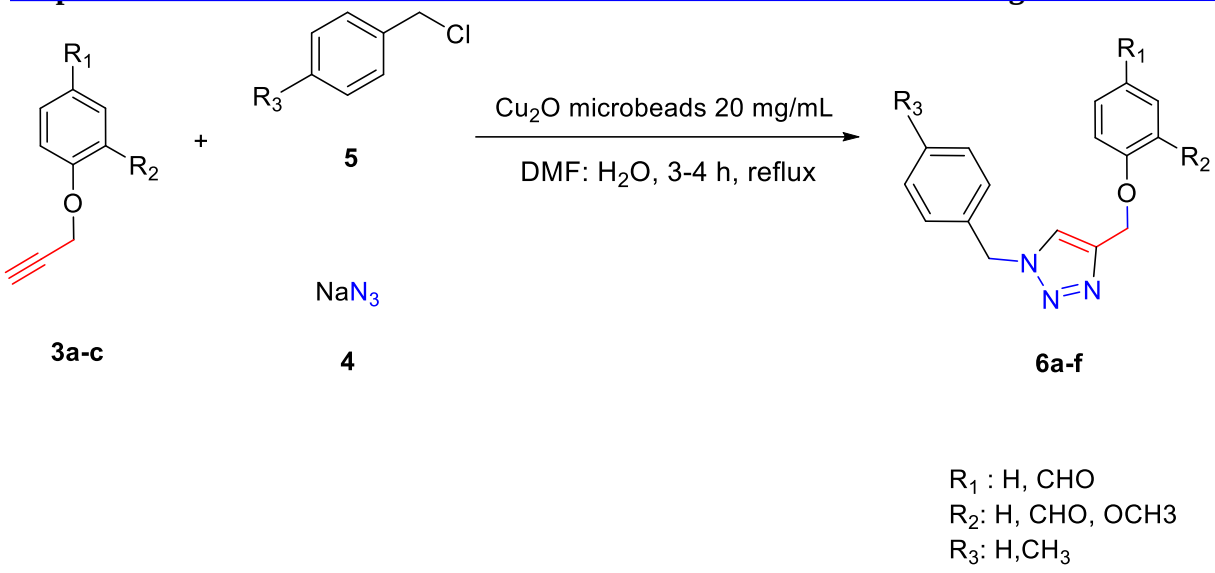


**Figure I.44.** using $Cu_2O$-microbeads as catalyst to Synthesize the 1,2,3-triazole derivatives

**Table I.2:** Structural and physicochemical characteristics of 1,2,3-trizole derivatives **6a-f**

| Ref | Alkyne | Benzyle chloride derivative | Yield % | Melting points (°C) | FTIR ($cm^{-1}$) | | | $^1$H NMR (δ:ppm) | | |
|---|---|---|---|---|---|---|---|---|---|---|
| | | | | | C=O | C-O-R | C-N | CHO | $CH_2O$ | $CH_2Ar$ |
| **6a** | 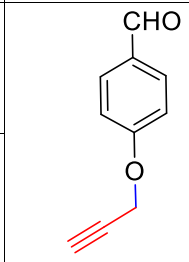 **3a** | Benzyle chloride | 70 | 140-143 | 1675 | 1163 | 835 | 9.57 | 4. 96 | 5.24 |
| **6b** | | 4-methyl benzyle chloride | 50 | 134-136 | 1680 | 1163 | 830 | 9.61 | 4.98 | 5.22 |
| **6c** | 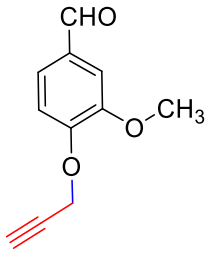 **3b** | Benzyle chloride | 85 | 124-126 | 1670 | 1130 | 867 | 9.90 | 5.41 | 5.58 |
| **6d** | | 4-methylbenzyle chloride | 33 | 109-111 | 1670 | 1140 | 821 | 9.84 | 5.34 | 5.47 |
| **6e** | 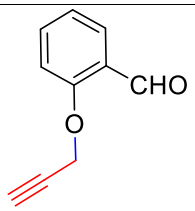 **3c** | Benzyle chloride | 70 | 138-140 | 1675 | 1154 | 848 | 10.31 | 5.20 | 5.44 |
| **6f** | | 4-methyle benzyle chloride | 68 | 141-143 | 1680 | 1154 | 844 | 10.41 | 5.29 | 5.49 |

## III.2. Characterization

Using standard spectroscopic techniques (IR, $^{13}$C NMR and$^{1}$H NMR), structures of the triazole derivatives **6a–f** were determined. In the FT-IR spectra of the triazoles, two absorption bands corresponding to the triazole nucleus's **C-N** stretching vibrations are seen at approximately 3107 and 3263 $cm^{-1}$. The presence of absorption bands around 1670 $cm^{-1}$, indicative of (**C=O**) groups (referring to ether group), is characteristic of the FT-IR spectra. The typical bands of the aromatic nucleus, observed at around 700 and 800 $cm^{-1}$ (**C-H** bending out-of-plane) and 1550-1600 $cm^{-1}$ (aromatic stretching of **C=C**), clearly indicate the presence of aromatic rings in the obtained products (aromatic aldehydes)

As a result, $^{1}$H NMR was used to characterize the structures of products **6a–f**; in fact, the spectrum of the product **6d**, which is shown in Figure I.45 (a), demonstrates:

1.The aldehyde proton is represented by the singlet at 9.84 ppm in the NMR spectrum (**CHO**). Because of the carbonyl group's deshielding effect, aldehyde protons usually resonate downfield and appear at 9–10 ppm.

2.The triazole ring (**CH**) proton resonates as a singlet at 7.55 ppm. Because of the aromatic character of the ring and the neighboring nitrogen atoms' ability to withhold electrons, the **CH** proton on the triazole ring experiences this usual chemical shift, which manifests downfield.

3. With a 7H integration, the aromatic protons resonate as a multiplet between 7.17 and 7.45 ppm.

4. The **$CH_2$Ar** signal is also distinctive. The methylene protons (**$CH_2$**) resonate as a singlet at 5.47 ppm with an integration of two protons (2H). This chemical shift, which is indicative of a benzylic **$CH_2$** group, results from the nearby aromatic ring's deshielding action and appears somewhat downfield.

5. It is also possible to detect the signals of the ether group's protons (**O-$CH_2$**). The singlet corresponding to the methylene group (**O-$CH_2$**) with an integration of two protons (2H) appears at 5.34 ppm. The electron-withdrawing action of the oxygen atom usually causes the protons of a methylene group (**$CH_2$**) connected to an oxygen (ether group) to become deshielded, causing a downfield chemical shift.

6. The protons of the methoxy group (**O-$CH_3$**) and the methyl group attached to a phenyl ring (**$CH_3$Ph**) appear as singlets at 3.89 ppm and 2.35 ppm, respectively. Regarding the methoxy

group. The deshielding action of the electronegative oxygen atom, which normally causes methoxy protons to resonate about 3.5–4.0 ppm, is what causes the chemical shift to be downfield. The three protons of the methyl group that are immediately linked to a phenyl ring are represented by the singlet at 2.35 ppm (because of the aromatic ring's minor deshielding impact).

The $^{13}C$ NMR data of the compound **6d** indicates that the compound has the following carbon environments, supporting the structure of the molecule:

- The shift at 190.89 ppm corresponds to the carbon of the aldehyde group (**CHO**).
- Shifts at 153.09, 149.99,130.66, 126.69, 112.73, and 109.30 ppm likely correspond to aromatic carbons with different substitution patterns. This range suggests multiple aromatic carbons in different environments, possibly affected by electron-withdrawing or electron-donating groups.
- Shift at 138.88 corresponds to a quaternary carbon in a aromatic ring.
- Shift at 129.83 corresponds to two equivalent carbons in aromatic ring.
- Shift at 128.24 corresponds to two equivalent carbons in aromatic ring.
- A shift at 122.97 ppm may correspond to the carbon (**CH**) in the triazole ring.
- A shift at 143.56 ppm likely corresponds to another carbon in the triazole ring (**C-N**). This characteristic shift is typical for a quaternary carbons in nitrogen-containing heterocycles like triazole, influenced by the nitrogen atoms.
- A shift at 63.02 ppm is attributed to a methylene group (**O-$CH_2$**) attached to an oxygen atom, consistent with an ether linkage.
- The shift at 56.01 ppm corresponds to the methylene carbon (**$CH_2$Ar**) in the benzylic position.
- The methoxy carbon (**O-$CH_3$**) is represented by a shift at 54.13 ppm.
- A shift at 21.14 ppm corresponds to the methyl carbon (**$CH_3$Ar**) attached to an aromatic ring.

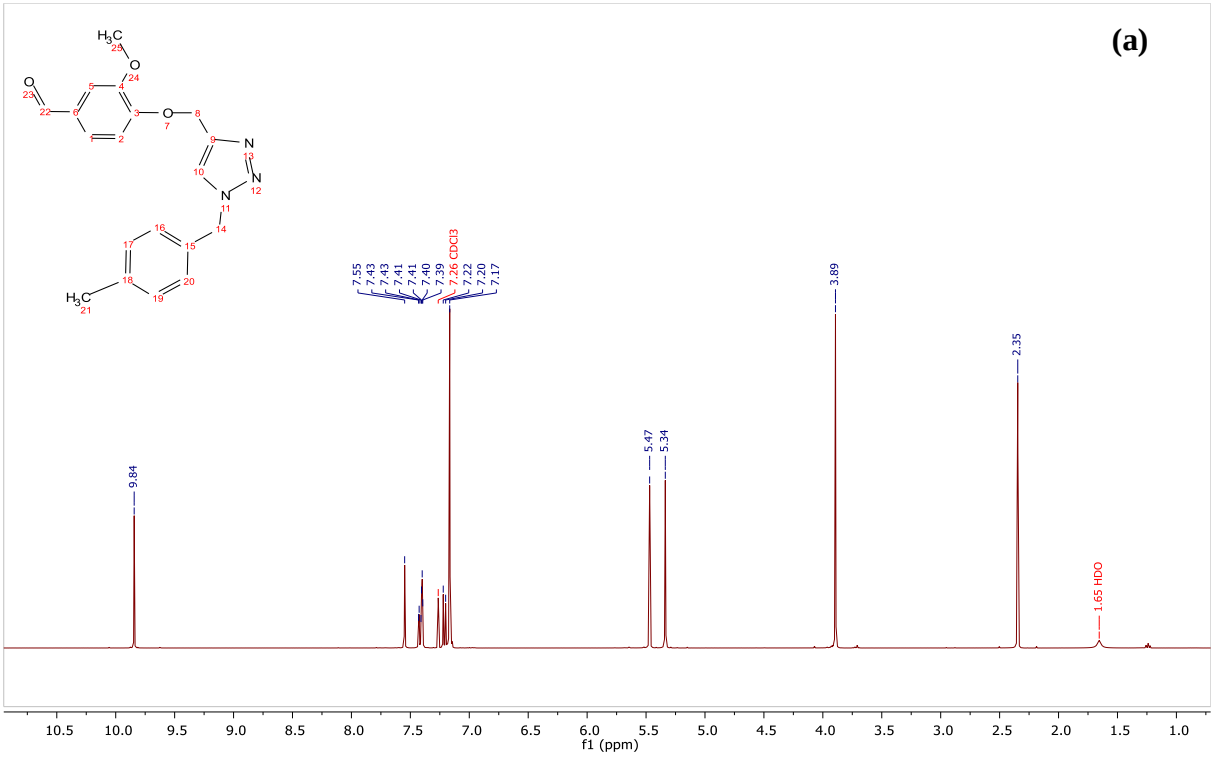


**1H NMR (400 MHz, Chloroform-*d*) δ** 9.84 (s, 1H), 7.55 (s, 1H), 7.45 – 7.37 (m, 2H), 7.21 (d, 1H), 7.17 (s, 4H), 5.47 (s, 2H), 5.34 (s, 2H), 3.89 (s, 3H), 2.35 (s, 3H).

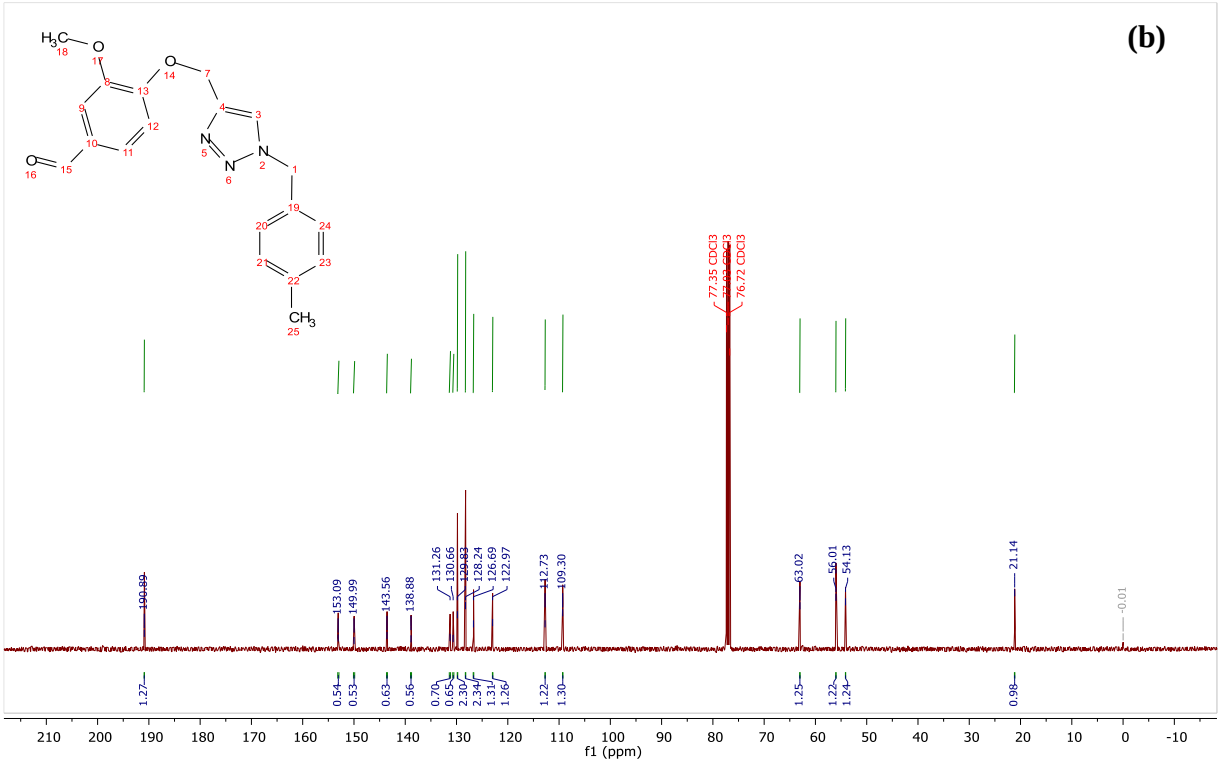


**13C NMR (101 MHz, $CDCl_3$) δ** 190.89, 153.09, 149.99, 143.56, 138.88, 131.26, 130.66, 129.83, 128.24, 126.69, 122.97, 112.73, 109.30, 63 56.01, 54.13, 21.14.

**Figure I.45.** Analysis of compound **6d**: **(a)** $^{1}$H NMR spectra; **(b)** $^{13}$C NMR Spectra .

The predicted mechanism for the formation of 1,2,3-trizole 1,4-disubstituted derivative **6d**, is illustrated in Figure I.46.

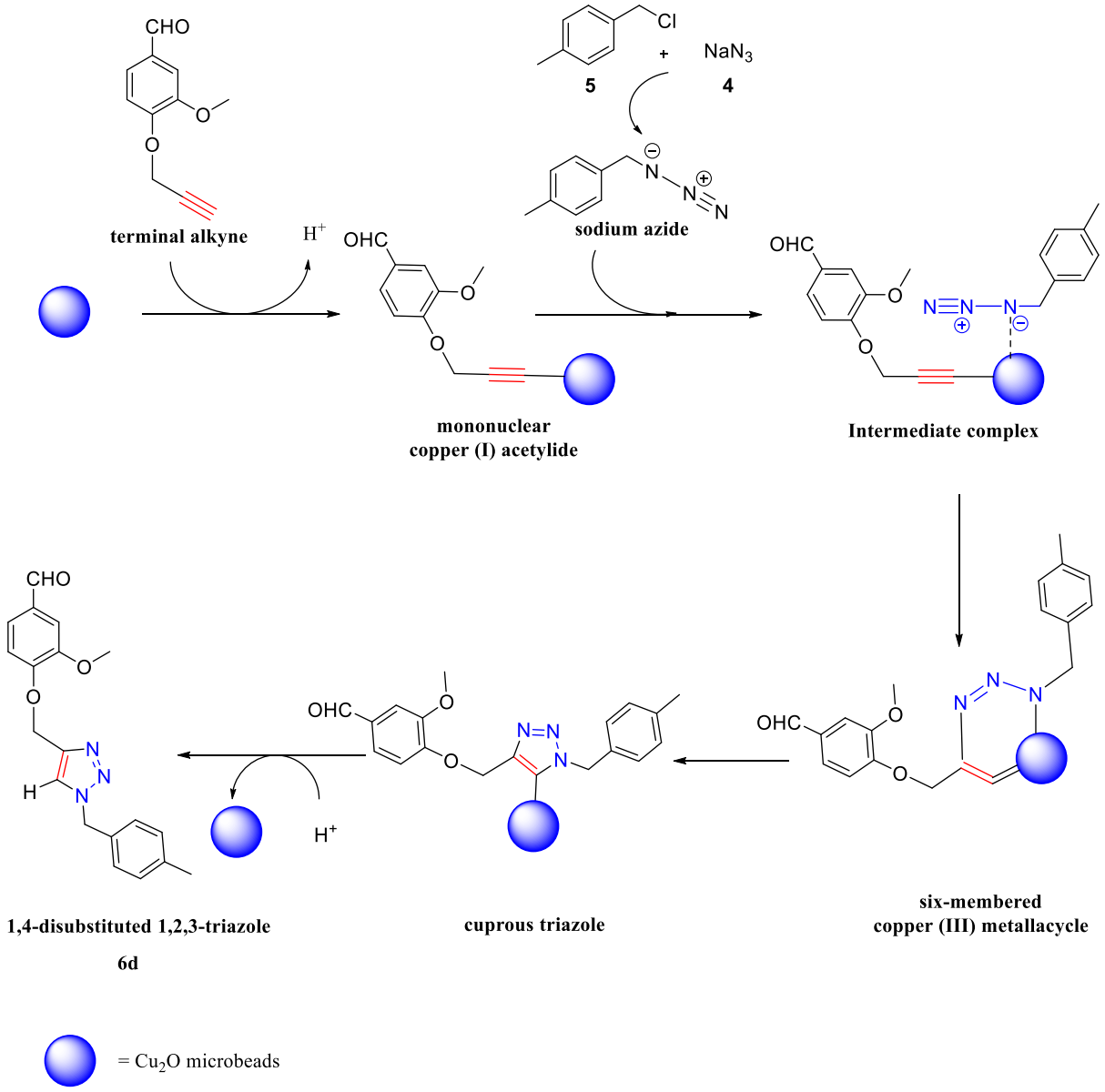


**Figure I.46.** The catalytic mechanism for the CuAAC to form the compound **6d**

### III.3. Enhancing the organic synthesis reaction parameters

The amount of each reactant $NaN_3$, benzyl chloride, 3-Methoxy-4-(Prop-2- yn-1-yloxy)benzaldehyde affects how 4-((1-benzyl-1H-1,2,3-triazol-4-yl)oxy)-3-methoxybenzalde -hyde **6c** is synthesized. These reagents are very important in determining the kind and yield of the finished product. Changes in the types or amounts of reactants can affect the kinetics of the reaction and affect the production of the intended result. Three main aspects of this study were examined: first, the amount of tuning catalyst utilized; second, the choice of solvent; and third, and the reusability of catalyst evaluation. The ideal conditions for the synthesis of **6c** (shown in Figure I.44) are examined in Table I.3 and I.4. Melting points and TLC were used to verify the synthetic compounds in all of these tests.

### III.3.1. Impact of catalyst dose

Catalyst concentration is a crucial factor in the synthesis of the product 4-((1-benzyl-1H-1,2,3-triazol-4-yl)oxy)-3-methoxybenzaldehyde **6c**, which is expressed in mg/mL. The information in Table I.3 clearly shows how much the $Cu_2O$ catalyst amount affects the finished product's yield. The DMF: $H_2O$ solvent system yielded higher product yields (5, 15, 52, 56%) and up to 85% at (20 mg/mL) as a maximum yield. when the catalyst dose was increased from 1 to 20 mg/mL. However, the yield somewhat decreased to 75 and 70 %, respectively, when dosage of the catalyst increases to 25 and 30 mg/mL. This suggests a strong relationship between the yield of the product and the amount of the catalyst**.**

**Table I.3.** Impact of catalyst dose on the synthesis of the compound **6c**

| **Reagents** | **Solvent** | **Dose of the catalyst (mg/mL)** | **Products** | **Yield (%)*** |
|---|---|---|---|---|
| 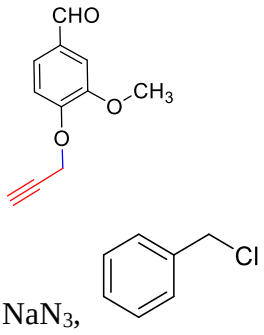  $NaN_3$, | DMF: $H_2O$ (8:2) | 1 | 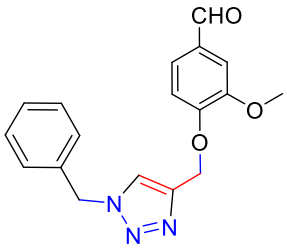  | 5 |
| | | 5 | | 15 |
| | | 10 | | 52 |
| | | 15 | | 56 |
| | | 20 | | 85 |
| | | 25 | | 75 |
| | | 30 | | 70 |

***Yield of pure product**

**Reaction conditions:** 3 h , 90 °C.

### III.3.2. Impact of the type of solvent

The production of **6c** is largely dependent on the solvent selection. Table I.4 presents data indicating varying yields for various solvents, highlighting the crucial significance in this chemical process in terms of solvent selection. The amount of catalyst ($Cu_2O$ microbeads) and product yield in the DMF: $H_2O$ system showed a direct link, the $Cu_2O$ microbeads peaks at 85% with 20mg/mL. Out of all the solvents tested, this combination proved to be the most effective. In contrast, yields from various solvents, including acetone, DMSO, $CHCl_3$, EtOH:$H_2O$, and $CH_2Cl_2$:$H_2O$, ranged from 20 to 56% at the same dose of $Cu_2O$ microbeads (20 mg/mL). The variation in yields highlights how various solvents have a substantial influence on the efficiency of the reaction, influencing things like catalyst and reagents' stability, reactivity and solubility.

High yields are made possible by the DMF:$H_2O$ combination, which emphasizes how important solvent choice is to maximizing the results of this work.

**Table I.4 .** Type of solvent's effect of the on the **6c** synthesis

| **Reagents** | **Solvent** | **catalyst Dose** (mg/mL) | **Products** | **Yield (%)*** |
|---|---|---|---|---|
| 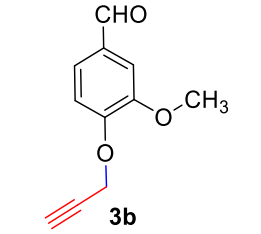  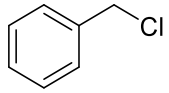  $NaN_3$ , | EtOH : $H_2O$ | 20 | 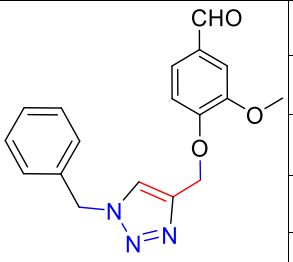  | 20 |
| | DMSO | | | 56 |
| | $CH_2Cl_2$: $H_2O$ | | | 30 |
| | Acetone | | | 50 |
| | $CHCl_3$ | | | No reaction occurred |
| | DMF: $H_2O$ | | | 85 |

***Yield of pure product

**Reaction conditions:** 3 h, 90 °C

### III.3.3. Impact of the $Cu_2O$ Microbeads' reusability

The impact of the $Cu_2O$ microbeads' reusability (at first at 20 mg/mL) on the organic product's yield across several cycles is depicted in Figure I.47, 85% is the initial yield in the first cycle. But the yield noticeably decreases as the catalyst is employed again in later cycles. Even with the catalyst being reused, the yield decreases from the first cycle to 75% in the second cycle. The ensuing cycles exhibit a similar declining trend, with yields reaching in the third cycle 50% and a further decline in the fourth to 25%. Over the course of four cycles, the product yield decreased, which suggests that the efficiency of the catalyst is decreasing, most likely as a result of the catalyst being lost during the centrifuging recovery process and possible surface modification or deactivation of the $Cu_2O$ microbeads from frequent use. This suggests that in order to maintain stable or increased yields over repeated usage, catalyst recovery or regeneration measures must be put into place.

The creation of flower-like $Cu_2O$ microbeads with a distinct form that has never been documented before is the work's main innovation. This emphasizes how unique and potentially innovative this discovery is in the field of plant-mediated catalyst production.

$Cu_2O$ microbeads offer a sustainable, eco-friendly substitute that is highly recyclable. $Cu_2O$ microbeads retain even after several cycles a high yield (70%). This highlights their effective-

ness and consistency, rendering them a financially feasible and ecologically sustainable choice. $Cu_2O$ microbeads' recyclability improves the efficiency of organic synthesis, which is in line with the green chemistry's principles since it minimizes environmental impact and waste. These features highlight the value of $Cu_2O$ microbeads as an environmentally friendly catalyst for chemical synthesis.

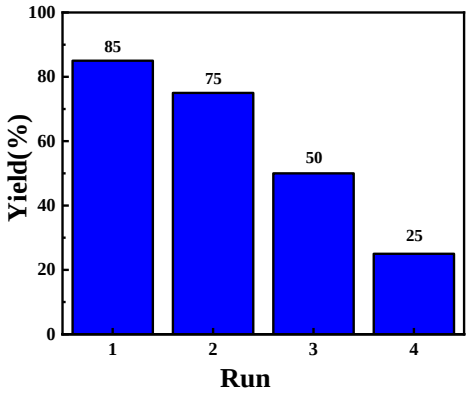


**Figure I.47.** Impact of the reusability of the catalyst on the preparation of **6c**. (**Reaction conditions:** reflux at 90 °C, 3h, DMF:$H_2O$,$Cu_2O$ microbeads 20 mg/mL)

**Conclusion**

In this chapter by using $Cu_2O$ microbeads as a catalyst, we were able to successfully manufacture 1,2,3-triazoles 1,4-disubstituted. The outcomes showed how effective and adaptable $Cu_2O$ microbeads are at promoting the click reaction between alkynes and azides, the intended triazole derivatives were produced in moderate circumstances. This catalytic method delivers good yields and great regioselectivity while also providing a more environmentally friendly and sustainable way for triazole synthesis.

## References


[1] R. Narigara, D. Joshi, Y. Bhola, and G. Jani, "Synthesis and biological activity of some various aldehyde and 1, 2, 3-triazole containing heterocyclic compounds," *World Scientific News,* no. 123, pp. 246-257, 2019.

[2] E. O. Shestakova *et al.*, "Investigation of 1, 4-Substituted 1, 2, 3-Triazole Derivatives as Antiarrhythmics: Synthesis, Structure, and Properties," *Pharmaceuticals,* vol. 15, no. 12, p. 1443, 2022.

[3] V. D. da Silva *et al.*, "Design, synthesis, structural characterization and in vitro evaluation of new 1, 4-disubstituted-1, 2, 3-triazole derivatives against glioblastoma cells," *Bioorganic chemistry,* vol. 83, pp. 87-97, 2019.

[4] A. V. Costa *et al.*, "Synthesis of glycerol-derived 4-alkyl-substituted 1, 2, 3-triazoles and evaluation of their fungicidal, phytotoxic, and antiproliferative activities," *Journal of the Brazilian Chemical Society,* vol. 31, pp. 821-832, 2020.

[5] M. S. Shad, P. V. Santhini, and W. Dehaen, "1, 2, 3-Triazolium macrocycles in supramolecular chemistry," *Beilstein Journal of Organic Chemistry,* vol. 15, no. 1, pp. 2142-2155, 2019.

[6] S. Yamasaki, Y. Kamon, L. Xu, and A. Hashidzume, "Synthesis of dense 1, 2, 3-triazole polymers soluble in common organic solvents," *Polymers,* vol. 13, no. 10, p. 1627, 2021.

[7] S. Noriega, E. Leyva, E. Moctezuma, L. Flores, and S. Loredo-Carrillo, "Recent catalysts used in the synthesis of 1, 4-disubstituted 1, 2, 3-triazoles by heterogeneous and homogeneous methods," *Current Organic Chemistry,* vol. 24, no. 5, pp. 536-549, 2020.

[8] L.-M. Rečnik, W. Kandioller, and T. L. Mindt, "1, 4-Disubstituted 1, 2, 3-triazoles as amide bond surrogates for the stabilisation of linear peptides with biological activity," *Molecules,* vol. 25, no. 16, p. 3576, 2020.

[9] J. Dai, S. Tian, X. Yang, and Z. Liu, "Synthesis methods of 1, 2, 3-/1, 2, 4-triazoles: A review," *Frontiers in Chemistry,* vol. 10, p. 891484, 2022.

[10] S. Shaabani, A. Tavousi Tabatabaei, and A. Shaabani, "Copper (I) oxide nanoparticles supported on magnetic casein as a bio-supported and magnetically recoverable catalyst for aqueous click chemistry synthesis of 1, 4-disubstituted 1, 2, 3-triazoles," *Applied Organometallic Chemistry,* vol. 31, no. 2, p. e3559, 2017.

[11] H. Abdelbaki *et al.*, "Plant mediated synthesis of Flower-Like Cu2O Microbeads from Artimisia Campestris L. Extract for the Catalyzed Synthesis of 1, 4-Disubstituted 1, 2, 3-Triazole Derivatives," *Frontiers in Chemistry,* vol. 11, p. 1342988, 2024.

[12] K. T. Jha and P. A. Chawla, "Nanometals: As click catalysts for 1, 4-triazole cycloaddition (2020-till date)," *Sustainable Chemistry and Pharmacy*, vol. 35, p. 101195, 2023.

[13] M. A. Dar, S. Shrivastava, and P. F. Iqbal, "Click chemistry and anticancer properties of 1, 2, 3-triazoles," *World J. Pharm. Res*, vol. 4, pp. 1949-1975, 2015.

[14] A. Kudelko and M. Olesiejuk, "Efficient Synthesis of Conjugated 1, 2, 4-Triazole Derivatives under Suzuki Cross-Coupling Reactions in the Presence of Ionic Liquids."

[15] A. H. MALANI, A. H. Makwana, and H. R. Makwana, "A brief review article: Various synthesis and therapeutic importance of 1, 2, 4-triazole and its derivatives," *Moroccan Journal of Chemistry*, vol. 5, no. 1, pp. 5-1 (2017) 41-58, 2017.

[16] A. Kawka, G. Hajdaś, D. Kułaga, H. Koenig, I. Kowalczyk, and T. Pospieszny, "Molecular structure, spectral and theoretical study of new type bile acid–sterol conjugates linked via 1, 2, 3-triazole ring," *Journal of Molecular Structure*, vol. 1273, p. 134313, 2023.

[17] S. Kumar, S. L. Khokra, and A. Yadav, "Triazole analogues as potential pharmacological agents: A brief review," *Future Journal of Pharmaceutical Sciences*, vol. 7, no. 1, p. 106, 2021.

[18] M. Ding, S. Wan, N. Wu, Y. Yan, J. Li, and X. Bao, "Synthesis, structural characterization, and antibacterial and antifungal activities of novel 1, 2, 4-triazole thioether and thiazolo [3, 2-b]-1, 2, 4-triazole derivatives bearing the 6-fluoroquinazolinyl moiety," *Journal of Agricultural and Food Chemistry*, vol. 69, no. 50, pp. 15084-15096, 2021.

[19] M. Hrimla, L. Bahsis, M. R. Laamari, M. Julve, and S.-E. Stiriba, "An overview on the performance of 1, 2, 3-triazole derivatives as corrosion inhibitors for metal surfaces," *International Journal of Molecular Sciences*, vol. 23, no. 1, p. 16, 2021.

[20] Y.-E. Wang *et al.*, "Design, synthesis, and herbicidal activity of thioether containing 1, 2, 4-triazole schiff bases as transketolase inhibitors," *Journal of Agricultural and Food Chemistry*, vol. 69, no. 40, pp. 11773-11780, 2021.

[21] D. L. Roman, D. I. Voiculescu, M. Filip, V. Ostafe, and A. Isvoran, "Effects of triazole fungicides on soil microbiota and on the activities of enzymes found in soil: A review," *Agriculture*, vol. 11, no. 9, p. 893, 2021.

[22] T. El Malah, H. F. Nour, A. A. Satti, B. A. Hemdan, and W. A. El-Sayed, "Design, synthesis, and antimicrobial activities of 1, 2, 3-triazole glycoside clickamers," *Molecules*, vol. 25, no. 4, p. 790, 2020.

[23] K. I. Slavova, L. T. Todorov, N. P. Belskaya, M. A. Palafox, and I. P. Kostova, "Developments in the application of 1, 2, 3-triazoles in cancer treatment," *Recent Patents on Anti-Cancer Drug Discovery,* vol. 15, no. 2, pp. 92-112, 2020.

[24] B. P. Swain, *Nanostructured Biomaterials: Basic Structures and Applications*. Springer Nature, 2022.

[25] M. P. Evangelin *et al.*, "An updated review on 1, 2, 4 Triazoles," *Journal of Pharmacognosy and Phytochemistry,* vol. 8, no. 4, pp. 292-299, 2019.

[26] G. Varvounis, I. E. Gerontitis, and V. Gkalpinos, "Metal-catalyzed synthesis of five-membered ring N-heterocycles. A recent update," *Chemistry of Heterocyclic Compounds,* vol. 54, pp. 249-268, 2018.

[27] M.-X. Song and X.-Q. Deng, "Recent developments on triazole nucleus in anticonvulsant compounds: a review," *Journal of enzyme inhibition and medicinal chemistry,* vol. 33, no. 1, pp. 453-478, 2018.

[28] B. M. Shah, P. Modi, and P. Trivedi, "Recent Investigation on Synthetic 'Triazoles' Scaffold as Potential Pharmacological Agents: A Comprehensive Survey," *Chemistry Africa,* pp. 1-19, 2023.

[29] E. E. Cogollo *et al.*, "Hydrogen bonding interactions in fluorinated 1, 2, 3-triazole derivatives," *New Journal of Chemistry,* vol. 44, no. 37, pp. 16006-16019, 2020.

[30] L. A. Wallace, "Studying the Effects of Hydrogen Bonding in 1H-1, 2, 3-Triazole and Its Derivatives," 2018.

[31] K. B. H. Salah *et al.*, "How are 1, 2, 3-triazoles accommodated in helical secondary structures?," *Organic & Biomolecular Chemistry,* vol. 16, no. 19, pp. 3576-3583, 2018.

[32] R. O. SOUZA, L. S. Miranda, and E. MARIZ, "Strategies towards the synthesis of N 2-substituted 1, 2, 3-triazoles," *Anais da Academia Brasileira de Ciências,* vol. 91, 2019.

[33] C. S. Santos, R. J. de Oliveira, R. N. de Oliveira, and J. C. R. Freitas, "1, 2, 3-Triazoles: general and key synthetic strategies," *Organic Chemistry,* no. part i, pp. 0-0, 2020.

[34] E. Wojaczyńska and J. Wojaczyński, "Synthesis and Applications of 1, 2, 3-Triazoles," in *Advances in Organic Synthesis*: Bentham Science Publications Sharjah, UAE, 2018, pp. 156-232.

[35] M. P. Jedináková, "Study of New Systems for Non-catalyzed Conjugation Reaction with Azides," 2017.

[36] Y. Hayashi, "Time economy in total synthesis," *The Journal of Organic Chemistry,* vol. 86, no. 1, pp. 1-23, 2020.

[37] G. Facchetti, G. Coffetti, R. Gandolfi, and I. Rimoldi, "One-pot reactions in catalysis: a valuable tool for the synthesis of enantiopure intermediates for pharmaceutical applications," 2022.

[38] Y. Hayashi, "Time and pot economy in total synthesis," *Accounts of Chemical Research,* vol. 54, no. 6, pp. 1385-1398, 2021.

[39] M. S. Asgari *et al.*, "Copper-catalyzed one-pot synthesis of amide linked 1, 2, 3-triazoles bearing aryloxy skeletons," *Tetrahedron Letters,* vol. 65, p. 152765, 2021.

[40] S. G. Agalave, S. R. Maujan, and V. S. Pore, "Click chemistry: 1, 2, 3-triazoles as pharmacophores," *Chemistry–An Asian Journal,* vol. 6, no. 10, pp. 2696-2718, 2011.

[41] G. O. Resende *et al.*, "Synthesis of 1, 2, 3-triazole derivatives and its evaluation as corrosion inhibitors for carbon steel," *International Journal of Electrochemistry,* vol. 2019, 2019.

[42] L. L. Kiessling, "Profile of Carolyn R. Bertozzi, Morten Meldal, and K. Barry Sharpless: 2022 Nobel laureates in Chemistry," *Proceedings of the National Academy of Sciences,* vol. 120, no. 35, p. e2308367120, 2023.

[43] G. S. Kumar and Q. Lin, "Light-triggered click chemistry," *Chemical reviews,* vol. 121, no. 12, pp. 6991-7031, 2020.

[44] J. Kaur, M. Saxena, and N. Rishi, "An overview of recent advances in biomedical applications of click chemistry," *Bioconjugate Chemistry,* vol. 32, no. 8, pp. 1455-1471, 2021.

[45] A. Mirjafari, "Ionic liquid syntheses via click chemistry: expeditious routes toward versatile functional materials," *Chemical Communications,* vol. 54, no. 24, pp. 2944-2961, 2018.

[46] M. Breugst and H. U. Reissig, "The huisgen reaction: Milestones of the 1, 3-dipolar cycloaddition," *Angewandte Chemie International Edition,* vol. 59, no. 30, pp. 12293-12307, 2020.

[47] Z. Tribak, M. K. Skalli, O. Senhaji, and Y. K. Rodi, "Synthesis, structural characterization and comparison of experimental and theoretical results by DFT level of molecular structures of 1, 2, 3-triazoles derived from 5-chloroisatin," *Int. J. Adv. Chem,* vol. 5, pp. 91-5, 2017.

[48] M. Chetia, A. A. Ali, A. Bordoloi, and D. Sarma, "Facile route for the regioselective synthesis of 1, 4-disubstituted 1, 2, 3-triazole using copper nanoparticles supported on nanocellulose as recyclable heterogeneous catalyst," *Journal of Chemical Sciences,* vol. 129, pp. 1211-1217, 2017.

[49] R. Huisgen *et al.*, "Current trends towards the synthesis of bioactive heterocycles and natural products using 1, 3-dipolar cycloadditions (1, 3-DC) with azomethine ylides," *Synthesis*, vol. 49, no. 13, pp. 2819-2851, 2017.

[50] A. A. Adhreai, M. ALSaeedy, M. Farooqui, A. Alrabie, I. Al-Qadsy, and U. Al-Timari, "Stereoselective synthesis of novel chiral open-chain d-ribose and d-glucose-derived nitrones through 1, 3-dipolar cycloaddition of maleimide and maleic acid and investigation of their antimicrobial activity via molecular docking and ADMET studies," *Journal of Molecular Structure*, vol. 1256, p. 132481, 2022.

[51] A. S. Filatov *et al.*, "Concise synthesis of tryptanthrin spiro analogues with in vitro antitumor activity based on one-pot, three-component 1, 3-dipolar cycloaddition of azomethine ylides to cyclopropenes," *Synthesis*, vol. 51, no. 03, pp. 713-729, 2019.

[52] A. J. Alves and T. M. Pinho e Melo, "Synthesis of novel chiral spiroisoxazolidine-β-lactams from 6-alkylidenepenicillanates: A 1, 3-dipolar cycloaddition approach," *European Journal of Organic Chemistry*, vol. 2020, no. 39, pp. 6259-6269, 2020.

[53] G. Lotfy *et al.*, "Regio-and stereoselective synthesis of new spirooxindoles via 1, 3-dipolar cycloaddition reaction: Anticancer and molecular docking studies," *Journal of Photochemistry and Photobiology B: Biology*, vol. 180, pp. 98-108, 2018.

[54] J. Zhong, H. He, and S. Gao, "Exploration of 1, 3-dipolar cycloaddition reactions to construct the core skeleton of Calyciphylline A-type alkaloids," *Organic Chemistry Frontiers*, vol. 6, no. 22, pp. 3781-3785, 2019.

[55] K. Karrouchi *et al.*, "Synthesis and pharmacological activities of pyrazole derivatives: A review," *Molecules*, vol. 23, no. 1, p. 134, 2018.

[56] A. Sapkal and S. Kamble, "Greener and environmentally benign methodology for the synthesis of pyrazole derivatives," *ChemistrySelect*, vol. 5, no. 42, pp. 12971-13026, 2020.

[57] N. Agouram, E. M. El Hadrami, and A. Bentama, "1, 2, 3-Triazoles as biomimetics in peptide science," *Molecules*, vol. 26, no. 10, p. 2937, 2021.

[58] B. M. Trost and G. Mata, "Forging odd-membered rings: palladium-catalyzed asymmetric cycloadditions of trimethylenemethane," *Accounts of Chemical Research*, vol. 53, no. 7, pp. 1293-1305, 2020.

[59] T. Deb, J. Tu, and R. M. Franzini, "Mechanisms and substituent effects of metal-free bioorthogonal reactions," *Chemical reviews*, vol. 121, no. 12, pp. 6850-6914, 2021.

[60] H. Zhao and Y. Zhao, "Engaging Isatins and Amino Acids in Multicomponent One-Pot 1, 3-Dipolar Cycloaddition Reactions—Easy Access to Structural Diversity," *Molecules,* vol. 28, no. 18, p. 6488, 2023.

[61] A. Djemoui, "Synthèse de nouveaux dérivés chalcones benzimidazoliques contenant du 1, 2, 3-triazoles via la Réaction de Click et étude de leurs activités biologiques," Universty of Eloued, 2019.

[62] N. Nebra and J. García-Álvarez, "Recent progress of Cu-catalyzed azide-alkyne cycloaddition reactions (CuAAC) in sustainable solvents: Glycerol, deep eutectic solvents, and aqueous media," *Molecules,* vol. 25, no. 9, p. 2015, 2020.

[63] J. Das, S. Dey, and T. Pathak, "Metal-free route to carboxylated 1, 4-disubstituted 1, 2, 3-triazoles from methoxycarbonyl-modified vinyl sulfone," *The Journal of Organic Chemistry,* vol. 84, no. 23, pp. 15437-15447, 2019.

[64] S. P. Amaral, J. Correa, and E. Fernandez-Megia, "Accelerated synthesis of dendrimers by thermal azide–alkyne cycloaddition with internal alkynes," *Green Chemistry,* vol. 24, no. 12, pp. 4897-4901, 2022.

[65] P. Kalra *et al.*, "Metals as “Click” catalysts for alkyne-azide cycloaddition reactions: An overview," *Journal of Organometallic Chemistry,* vol. 944, p. 121846, 2021.

[66] H. B. Jalani, A. Ç. Karagöz, and S. B. Tsogoeva, "Synthesis of substituted 1, 2, 3-triazoles via metal-free click cycloaddition reactions and alternative cyclization methods," *Synthesis,* vol. 49, no. 01, pp. 29-41, 2017.

[67] M. Contin, C. Garcia, C. Dobrecky, S. Lucangioli, and N. D’Accorso, "Advances in drug delivery, gene delivery and therapeutic agents based on dendritic materials," *Future Medicinal Chemistry,* vol. 11, no. 14, pp. 1791-1810, 2019.

[68] P. Saini, G. Singh, G. Kaur, J. Singh, and H. Singh, "Robust and Versatile Cu (I) metal frameworks as potential catalysts for azide-alkyne cycloaddition reactions," *Molecular Catalysis,* vol. 504, p. 111432, 2021.

[69] A. A. Saikia *et al.*, "Sequencing [3+ 2]-cycloaddition and multicomponent reactions: A regioselective microwave-assisted synthesis of 1, 4-disubstituted 1, 2, 3-triazoles using ionic liquid supported Cu (II) precatalysts in methanol," *Tetrahedron Letters,* vol. 61, no. 36, p. 152273, 2020.

[70] K. A. Kumar, "Comprehensive review on Huisgen’s cycloaddition reactions," *Int. J. ChemTech Res,* vol. 5, p. 3032, 2013.

[71] D. Sarma, J. Sultana, R. Hazarika, and B. Dutta, "Basic Ionic Liquid Catalyzed Cycloaddition Reactions for the Synthesis of 1, 2, 3-Triazoles," *Advances in Organic Synthesis: Volume 15,* vol. 5, p. 379, 2021.

[72] S. Röper and H. C. Kolb, "Click chemistry for drug discovery," *Fragment-based Approaches in Drug Discovery*, pp. 311-339, 2006.

[73] F. Himo *et al.*, "Copper (I)-catalyzed synthesis of azoles. DFT study predicts unprecedented reactivity and intermediates," *Journal of the American Chemical Society*, vol. 127, no. 1, pp. 210-216, 2005.

[74] M. Emami, R. Bikas, N. Noshiranzadeh, A. Kozakiewicz, and T. Lis, "Cu (II)-hydrazide coordination compound supported on silica gel as an efficient and recyclable heterogeneous catalyst for green click synthesis of β-hydroxy-1, 2, 3-triazoles in water," *ACS omega*, vol. 5, no. 22, pp. 13344-13357, 2020.

[75] R. Ramkumar and P. Anbarasan, "Cu-Catalyzed Click Reactions," *Copper Catalysis in Organic Synthesis*, pp. 177-207, 2020.

[76] S. Jana, "Synthesis of 1, 2, 3-triazoles and biological evaluation," 2017.

[77] A. K. Agrahari *et al.*, "Cu (I)-catalyzed click chemistry in glycoscience and their diverse applications," *Chemical Reviews*, vol. 121, no. 13, pp. 7638-7956, 2021.

[78] A. Biswas, D. Singha, and N. Pal, "Click Chemistry: copper, ruthenium catalyzed and photoinduced azide-alkyne cycloaddition," *Int. J. Exp. Res. Rev*, vol. 26, pp. 45-69, 2021.

[79] R. Taguchi, M. Nakahata, Y. Kamon, and A. Hashidzume, "Synthesis of Dense 1, 2, 3-Triazole Oligomers Consisting Preferentially of 1, 5-Disubstituted Units via Ruthenium (II)-Catalyzed Azide–Alkyne Cycloaddition," *Polymers*, vol. 15, no. 9, p. 2199, 2023.

[80] T. Hosseinnejad and S. Mahdavian, "Quantum chemistry study on regioselectivity in ruthenium catalyzed synthesis of 1, 5-disubstituted 1, 2, 3-triazoles," *Computational and Theoretical Chemistry*, vol. 1143, pp. 29-35, 2018.

[81] Y. Yousfi, W. Benchouk, and S. M. Mekelleche, "Understanding the regioselectivity of the copper (I)-and ruthenium (II)-catalyzed [3+ 2] cycloadditions of azido derivative of ribose with terminal alkyne: A theoretical study," *Theoretical Chemistry Accounts*, vol. 140, no. 1, p. 4, 2021.

[82] W. Song, M. Li, K. Dong, and Y. Zheng, "Ruthenium-Catalyzed Highly Regioselective Azide-Internal Thiocyanatoalkyne Cycloaddition under Mild Conditions: Experimental and Theoretical Studies," *Advanced Synthesis & Catalysis*, vol. 361, no. 22, pp. 5258-5263, 2019.

[83] O. Kracker *et al.*, "1, 5-Disubstituted 1, 2, 3-Triazole-Containing Peptidotriazolamers: Design Principles for a Class of Versatile Peptidomimetics," *Chemistry–A European Journal*, vol. 24, no. 4, pp. 953-961, 2018.

[84] R. S. Gomes, G. A. Jardim, R. L. de Carvalho, M. H. Araujo, and E. N. da Silva Júnior, "Beyond copper-catalyzed azide-alkyne 1, 3-dipolar cycloaddition: Synthesis and mechanism insights," *Tetrahedron*, vol. 75, no. 27, pp. 3697-3712, 2019.

[85] F. C. Pigge, "Strain-Promoted Cycloadditions for Development of Copper-Free Click Reactions," *Current Organic Chemistry*, vol. 20, no. 18, pp. 1902-1922, 2016.

[86] J. Dommerholt, F. P. Rutjes, and F. L. van Delft, "Strain-promoted 1, 3-dipolar cycloaddition of cycloalkynes and organic azides," *Cycloadditions in Bioorthogonal Chemistry*, pp. 57-76, 2016.

[87] S. Li *et al.*, "Comparative analysis of Cu (I)-catalyzed alkyne-azide cycloaddition (CuAAC) and strain-promoted alkyne-azide cycloaddition (SPAAC) in O-GlcNAc proteomics," *Electrophoresis*, vol. 37, no. 11, pp. 1431-1436, 2016.

[88] T. Harris and I. V. Alabugin, "Strain and stereoelectronics in cycloalkyne click chemistry," *Mendeleev Communications*, vol. 29, no. 3, pp. 237-248, 2019.

[89] V. Terzic, G. Pousse, R. Méallet-Renault, P. Grellier, and J. Dubois, "Dibenzocyclooctynes: Effect of Aryl Substitution on Their Reactivity toward Strain-Promoted Alkyne–Azide Cycloaddition," *The Journal of Organic Chemistry*, vol. 84, no. 13, pp. 8542-8551, 2019.

[90] L. Cheng, X. Kang, D. Wang, Y. Gao, L. Yi, and Z. Xi, "The one-pot nonhydrolysis Staudinger reaction and Staudinger or SPAAC ligation," *Organic & Biomolecular Chemistry*, vol. 17, no. 23, pp. 5675-5679, 2019.

[91] S. Markus, M. Herth, and C. BM Poulie, "Chapter Pretargeted Theranostics," 2021.

[92] K. Li, D. Fong, E. Meichsner, and A. Adronov, "A Survey of Strain-Promoted Azide–Alkyne Cycloaddition in Polymer Chemistry," *Chemistry–A European Journal*, vol. 27, no. 16, pp. 5057-5073, 2021.

[93] M. Meldal and F. Diness, "Recent fascinating aspects of the CuAAC click reaction," *Trends in Chemistry*, vol. 2, no. 6, pp. 569-584, 2020.

[94] Z.-J. Zheng, D. Wang, Z. Xu, and L.-W. Xu, "Synthesis of bi-and bis-1, 2, 3-triazoles by copper-catalyzed Huisgen cycloaddition: A family of valuable products by click chemistry," *Beilstein journal of organic chemistry*, vol. 11, no. 1, pp. 2557-2576, 2015.

[95] Q. Zhang, G. Kuang, L. Wang, P. Duan, W. Sun, and F. Ye, "Designing bioorthogonal reactions for biomedical applications," *Research*, vol. 6, p. 0251, 2023.

[96] R. Dharavath *et al.*, "Microwave-assisted synthesis, biological evaluation and molecular docking studies of new coumarin-based 1, 2, 3-triazoles," *RSC advances*, vol. 10, no. 20, pp. 11615-11623, 2020.

[97] S. Zhi, X. Ma, and W. Zhang, "Consecutive multicomponent reactions for the synthesis of complex molecules," *Organic & Biomolecular Chemistry,* vol. 17, no. 33, pp. 7632-7650, 2019.

[98] C. S. Graebin, F. V. Ribeiro, K. R. Rogério, and A. E. Kümmerle, "Multicomponent reactions for the synthesis of bioactive compounds: A review," *Current Organic Synthesis,* vol. 16, no. 6, pp. 855-899, 2019.

[99] R. Innocenti, E. Lenci, and A. Trabocchi, "Recent advances in copper-catalyzed imine-based multicomponent reactions," *Tetrahedron Letters,* vol. 61, no. 29, p. 152083, 2020.

[100] M. Nourisefat, F. Panahi, and A. Khalafi-Nezhad, "Amino acids and peptides as reactants in multicomponent reactions: modification of peptides with heterocycle backbones through combinatorial chemistry," *Molecular Diversity,* vol. 23, pp. 317-331, 2019.

[101] S. Mohurle, S. D. Pasuparthy, D. Talamarla, V. Kali, and B. Maiti, "[BCMIM][Cl] ionic liquid catalyzed diastereoselective synthesis of β-amino ketones via facile, one-pot, multicomponent Mannich reaction under solvent-free condition," *Journal of Heterocyclic Chemistry,* vol. 60, no. 9, pp. 1545-1557, 2023.

[102] S. E. John, S. Gulati, and N. Shankaraiah, "Recent advances in multi-component reactions and their mechanistic insights: A triennium review," *Organic Chemistry Frontiers,* vol. 8, no. 15, pp. 4237-4287, 2021.

[103] K. M. van Vliet, L. H. Polak, M. A. Siegler, J. I. van der Vlugt, C. F. Guerra, and B. de Bruin, "Efficient copper-catalyzed multicomponent synthesis of N-acyl amidines via acyl nitrenes," *Journal of the American Chemical Society,* vol. 141, no. 38, pp. 15240-15249, 2019.

[104] L. Reguera, Y. Méndez, A. R. Humpierre, O. Valdés, and D. G. Rivera, "Multicomponent reactions in ligation and bioconjugation chemistry," *Accounts of Chemical Research,* vol. 51, no. 6, pp. 1475-1486, 2018.

[105] S. Ishwar Bhat, "One-Pot Construction of Bis-Heterocycles through Isocyanide Based Multicomponent Reactions," *ChemistrySelect,* vol. 5, no. 27, pp. 8040-8061, 2020.

[106] M. O. Rodrigues, M. N. Eberlin, and B. A. Neto, "How and why to investigate multicomponent reactions mechanisms? A critical review," *The Chemical Record,* vol. 21, no. 10, pp. 2762-2781, 2021.

[107] P. Brandão, C. S. Marques, E. P. Carreiro, M. Pineiro, and A. J. Burke, "Engaging isatins in multicomponent reactions (MCRs)–easy access to structural diversity," *The Chemical Record,* vol. 21, no. 4, pp. 924-1037, 2021.

[108] N. Monteiro, "Organometallic Multicomponent Reactions," *Multi-component Reactions in Molecular Diversity,* vol. 1, pp. 1-58, 2019.

[109] H. Kumar, M. Dhameja, M. Rizvi, and P. Gupta, "Progress in the Synthesis of Fused 1, 2, 3-Triazoles," *ChemistrySelect,* vol. 6, no. 20, pp. 4889-4947, 2021.

[110] D. P. Vala, R. M. Vala, and H. M. Patel, "Versatile Synthetic Platform for 1, 2, 3-Triazole Chemistry," *Acs Omega,* vol. 7, no. 42, pp. 36945-36987, 2022.

[111] E. Afzali, Z. Mirjafary, A. Akbarzadeh, and H. Saeidian, "vvComplexation of copper ion-containing immobilized ionic liquid in designed hierarchical-functionalized layered double hydroxide nanoreactor for azide–alkyne cycloaddition reaction," *Inorganic Chemistry Communications,* vol. 132, p. 108858, 2021.

[112] S. Saranya, K. Rohit, S. Radhika, and G. Anilkumar, "Palladium-catalyzed multicomponent reactions: an overview," *Organic & Biomolecular Chemistry,* vol. 17, no. 35, pp. 8048-8061, 2019.

[113] S. Saranya, T. Aneeja, M. Neetha, and G. Anilkumar, "Recent advances in the iron-catalysed multicomponent reactions," *Applied Organometallic Chemistry,* vol. 34, no. 12, p. e5991, 2020.

[114] O. Ghashghaei, F. Seghetti, and R. Lavilla, "Selectivity in multiple multicomponent reactions: types and synthetic applications," *Beilstein journal of organic chemistry,* vol. 15, no. 1, pp. 521-534, 2019.

[115] B. Ganem, "Strategies for innovation in multicomponent reaction design," *Accounts of chemical research,* vol. 42, no. 3, pp. 463-472, 2009.

[116] C. G. Neochoritis, T. Zhao, and A. Dömling, "Tetrazoles via multicomponent reactions," *Chemical reviews,* vol. 119, no. 3, pp. 1970-2042, 2019.

[117] L. Reguera and D. G. Rivera, "Multicomponent reaction toolbox for peptide macrocyclization and stapling," *Chemical reviews,* vol. 119, no. 17, pp. 9836-9860, 2019.

[118] V. G. Nenajdenko, "Access to molecular complexity. Multicomponent reactions involving five or more components," *Russian Chemical Reviews,* vol. 89, no. 11, p. 1274, 2020.

[119] A. Talha *et al.*, "One-pot four-component tandem synthesis of novel sulfonamide-1, 2, 3-triazoles catalyzed by reusable copper (II)-adsorbed on mesoporous silica under ultrasound irradiation," *Tetrahedron,* vol. 90, p. 132215, 2021.

[120] K. Lal and P. Rani, "Recent developments in copper nanoparticle-catalyzed synthesis of 1, 4-disubstituted 1, 2, 3-triazoles in water," *ARKIVOC: Online Journal of Organic Chemistry,* 2016.

[121] S. Srivastava, A. Bhargava, S. Srivastava, and A. Bhargava, "Green nanotechnology: an overview," *Green Nanoparticles: The Future of Nanobiotechnology,* pp. 1-13, 2022.

[122] S. Bayda, M. Adeel, T. Tuccinardi, M. Cordani, and F. Rizzolio, "The history of nanoscience and nanotechnology: from chemical–physical applications to nanomedicine," *Molecules*, vol. 25, no. 1, p. 112, 2019.

[123] G. Pal, P. Rai, and A. Pandey, "Green synthesis of nanoparticles: A greener approach for a cleaner future," in *Green synthesis, characterization and applications of nanoparticles*: Elsevier, 2019, pp. 1-26.

[124] S. A. M. Ealia and M. P. Saravanakumar, "A review on the classification, characterisation, synthesis of nanoparticles and their application," in *IOP conference series: materials science and engineering*, 2017, vol. 263, no. 3: IOP Publishing, p. 032019.

[125] D. M. Teleanu, C. Chircov, A. M. Grumezescu, A. Volceanov, and R. I. Teleanu, "Impact of nanoparticles on brain health: an up to date overview," *Journal of clinical medicine*, vol. 7, no. 12, p. 490, 2018.

[126] I. Khan, K. Saeed, and I. Khan, "Nanoparticles: Properties, applications and toxicities," *Arabian journal of chemistry*, vol. 12, no. 7, pp. 908-931, 2019.

[127] N. M. Ishak, S. Kamarudin, and S. Timmiati, "Green synthesis of metal and metal oxide nanoparticles via plant extracts: an overview," *Materials Research Express*, vol. 6, no. 11, p. 112004, 2019.

[128] H. Lu *et al.*, "Modular and integrated systems for nanoparticle and microparticle synthesis—a review," *Biosensors*, vol. 10, no. 11, p. 165, 2020.

[129] D. Titus, E. J. J. Samuel, and S. M. Roopan, "Nanoparticle characterization techniques," in *Green synthesis, characterization and applications of nanoparticles*: Elsevier, 2019, pp. 303-319.

[130] A. M. Negrescu, M. S. Killian, S. N. Raghu, P. Schmuki, A. Mazare, and A. Cimpean, "Metal oxide nanoparticles: review of synthesis, characterization and biological effects," *Journal of Functional Biomaterials*, vol. 13, no. 4, p. 274, 2022.

[131] M. Nasrollahzadeh, S. M. Sajadi, M. Sajjadi, and Z. Issaabadi, "An introduction to nanotechnology," in *Interface science and technology*, vol. 28: Elsevier, 2019, pp. 1-27.

[132] I. Ijaz, E. Gilani, A. Nazir, and A. Bukhari, "Detail review on chemical, physical and green synthesis, classification, characterizations and applications of nanoparticles," *Green Chemistry Letters and Reviews*, vol. 13, no. 3, pp. 223-245, 2020.

[133] Y. Jain, M. Kumari, H. Laddha, and R. Gupta, "Ultrasound Promoted Fabrication of CuO-Graphene Oxide Nanocomposite for Facile Synthesis of Fluorescent Coumarin Based 1, 4-disubsituted 1, 2, 3-triazoles in Aqueous Media," *ChemistrySelect*, vol. 4, no. 23, pp. 7015-7026, 2019.

[134] M. J. Ndolomingo, N. Bingwa, and R. Meijboom, "Review of supported metal nanoparticles: synthesis methodologies, advantages and application as catalysts," *Journal of Materials Science,* vol. 55, no. 15, pp. 6195-6241, 2020.

[135] N. Malhotra, T.-R. Ger, B. Uapipatanakul, J.-C. Huang, K. H.-C. Chen, and C.-D. Hsiao, "Review of copper and copper nanoparticle toxicity in fish," *Nanomaterials,* vol. 10, no. 6, p. 1126, 2020.

[136] M. S. Abdel-wahab and A. H. Hammad, "Role of nickel in the phase change from nanocrystalline Cu2O to CuO sputtered films and the formation of a metastable phase of Cu4O3," *Materials Today Communications,* vol. 28, p. 102605, 2021.

[137] J. A. Resende, "Copper-based p-type semiconducting oxides: From materials to devices," Université Grenoble Alpes; Université de Liège, 2017.

[138] A. Y. Kudhur, E. T. Salim, I. Kara, R. O. Mahdi, and F. H. Alsultany, "Applications of Cu2O nanoparticles prepared via various techniques: a review paper," *Int. J. Nanoelectron. Mater.,* vol. 15, pp. 131-137, 2022.

[139] A. Maleki, M. Panahzadeh, and R. Eivazzadeh-keihan, "Agar: A natural and environmentally-friendly support composed of copper oxide nanoparticles for the green synthesis of 1, 2, 3–triazoles," *Green Chemistry Letters and Reviews,* vol. 12, no. 4, pp. 395-406, 2019.

[140] B. Babaei, M. Mamaghani, and M. Mokhtary, "Sustainable approach to the synthesis of 1, 4-disubstitued triazoles using reusable Cu (II) complex supported on hydroxyapatite-encapsulated α-Fe 2 O 3 as organic–inorganic hybrid nanocatalyst," *Reaction Kinetics, Mechanisms and Catalysis,* vol. 128, pp. 379-394, 2019.

[141] Z. Li *et al.*, "Two-dimensional transition metal carbides as supports for tuning the chemistry of catalytic nanoparticles," *Nature communications,* vol. 9, no. 1, p. 5258, 2018.

[142] T. S. Rodrigues, A. G. da Silva, and P. H. Camargo, "Nanocatalysis by noble metal nanoparticles: controlled synthesis for the optimization and understanding of activities," *Journal of Materials Chemistry A,* vol. 7, no. 11, pp. 5857-5874, 2019.

[143] M. Duan *et al.*, "Bimetallic nanoparticles/metal-organic frameworks: Synthesis, applications and challenges," *Applied Materials Today,* vol. 19, p. 100564, 2020.

[144] M. Miceli, P. Frontera, A. Macario, and A. Malara, "Recovery/reuse of heterogeneous supported spent catalysts," *Catalysts,* vol. 11, no. 5, p. 591, 2021.

[145] R. Saha, B. Mondal, and P. S. Mukherjee, "Molecular cavity for catalysis and formation of metal nanoparticles for use in catalysis," *Chemical Reviews,* vol. 122, no. 14, pp. 12244-12307, 2022.

[146] J. Singh, T. Dutta, K.-H. Kim, M. Rawat, P. Samddar, and P. Kumar, "'Green'synthesis of metals and their oxide nanoparticles: applications for environmental remediation," *Journal of nanobiotechnology,* vol. 16, pp. 1-24, 2018.

[147] O. S. Nayal, M. S. Thakur, M. Kumar, Shaifali, R. Upadhyay, and S. K. Maurya, "Sustainable and Efficient CuI-NPs-Catalyzed Cross-Coupling Approach for the Synthesis of Tertiary 3-Aminopropenoates, Triazoles, and Ciprofloxacin," *Asian Journal of Organic Chemistry,* vol. 7, no. 4, pp. 776-780, 2018.

[148] J. Albadi, A. Alihosseinzadeh, and A. Mansournezhad, "Regioselective synthesis of 1, 2, 3-triazoles catalyzed over ZnO supported copper oxide nanocatalyst as a new and efficient recyclable catalyst in water," *Acta Chimica Slovenica,* vol. 62, no. 3, pp. 617-624, 2015.

[149] F. Ebrahimpour-Malamir, T. Hosseinnejad, R. Mirsafaei, and M. M. Heravi, "Synthesis, characterization and computational study of CuI nanoparticles immobilized on modified poly (styrene-co-maleic anhydride) as a green, efficient and recyclable heterogeneous catalyst in the synthesis of 1, 4-disubstituted 1, 2, 3-triazoles via click reaction," *Applied Organometallic Chemistry,* vol. 32, no. 1, p. e3913, 2018.

[150] A. Shaabani, R. Afshari, and S. E. Hooshmand, "Crosslinked chitosan nanoparticle-anchored magnetic multi-wall carbon nanotubes: A bio-nanoreactor with extremely high activity toward click-multi-component reactions," *New Journal of Chemistry,* vol. 41, no. 16, pp. 8469-8481, 2017.

[151] Y. Uozumi and A. Tazawa, "Alkyne–Azide Cycloaddition on Water-Soluble Copper NP–Cobaltocene Catalyst," *Synfacts,* vol. 14, no. 12, p. 1309, 2018.

[152] G. S. Rani, M. Vijay, and B. L. Prabhavathi Devi, "SO3Cu-Carbon: A Novel Heterogeneous Catalyst for the Synthesis of β-Hydroxy 1, 2, 3-Triazoles by One Pot Cycloaddition Reaction," *ChemistrySelect,* vol. 4, no. 34, pp. 10133-10142, 2019.

[153] R. Deilam, F. Moeinpour, and F. S. Mohseni-Shahri, "Catalytic performance of Cu (II)-supported graphene quantum dots modified NiFe 2 O 4 as a proficient nano-catalyst in the synthesis of 1, 2, 3-triazoles," *Monatshefte Für Chemie-Chemical Monthly,* vol. 151, pp. 1153-1162, 2020.

[154] A. Kumar, S. Verma, and D. D. Pathak, "Synthesis and characterization of a recyclable graphene oxide-surface-engineered copper (II) Schiff base complex: Catalytic application in synthesis of 1, 2, 3-triazoles and 2H-indazoles," *Journal of Environmental Chemical Engineering,* vol. 9, no. 4, p. 105791, 2021.

[155] S.-J. Kwak, U. S. Shin, and S.-H. Kim, "A heterogeneous Cu-catalyst immobilized on poly (3-carboxythiophene)-modified multi-walled carbon nanotubes for click reaction," *Journal of Chemical Sciences,* vol. 135, no. 1, p. 10, 2023.

[156] A. J. Shnoudeh *et al.*, "Synthesis, characterization, and applications of metal nanoparticles," in *Biomaterials and bionanotechnology*: Elsevier, 2019, pp. 527-612.

[157] M. Yadi *et al.*, "Current developments in green synthesis of metallic nanoparticles using plant extracts: a review," *Artificial cells, nanomedicine, and biotechnology,* vol. 46, no. sup3, pp. 336-343, 2018.

[158] J. O. Adeyemi, A. O. Oriola, D. C. Onwudiwe, and A. O. Oyedeji, "Plant extracts mediated metal-based nanoparticles: synthesis and biological applications," *Biomolecules,* vol. 12, no. 5, p. 627, 2022.

[159] K. S. Siddiqi and A. Husen, "Recent advances in plant-mediated engineered gold nanoparticles and their application in biological system," *Journal of Trace Elements in Medicine and Biology,* vol. 40, pp. 10-23, 2017.

[160] A. A. Barzinjy and H. H. Azeez, "Green synthesis and characterization of zinc oxide nanoparticles using Eucalyptus globulus Labill. leaf extract and zinc nitrate hexahydrate salt," *SN Applied Sciences,* vol. 2, no. 5, p. 991, 2020.

[161] G. Marslin *et al.*, "Secondary metabolites in the green synthesis of metallic nanoparticles," *Materials,* vol. 11, no. 6, p. 940, 2018.

[162] L. H. Madkour, "Ecofriendly green biosynthesized of metallic nanoparticles: bio-reduction mechanism, characterization and pharmaceutical applications in biotechnology industry," *Drugs Ther,* vol. 3, pp. 1-11, 2017.

[163] M. B. Tehrani *et al.*, "Phthalimide-1, 2, 3-triazole hybrid compounds as tyrosinase inhibitors; synthesis, biological evaluation and molecular docking analysis," *Journal of Molecular Structure,* vol. 1176, pp. 86-93, 2019.

[164] M. Mannarmannan and K. Biswas, "Phytochemical-Assisted Synthesis of Cuprous Oxide Nanoparticles and Their Antimicrobial Studies," *ChemistrySelect,* vol. 6, no. 14, pp. 3534-3539, 2021.

[165] S. Lermontova, I. Grigoryev, N. Peskova, I. Balalaeva, V. Boyarskii, and L. Klapshina, "Novel Cyanoarylporphyrazines with Triazole Groups at the Macrocycle Periphery as Potential Sensibilizers of Photodynamic Therapy and Optical Probes of Intracellular Viscosity," *Russian Journal of General Chemistry,* vol. 88, pp. 2339-2346, 2018.

[166] I. Maulana, D. Fasya, B. Ginting, and R. Efendi, "Biosynthesis of copper nanoparticles using methanol extract of sugar-apple leaves (Anonnaceae squamosa), and its antioxidant

activity," in *Journal of Physics: Conference Series*, 2022, vol. 2193, no. 1: IOP Publishing, p. 012057.

[167] M. Kumar, R. R. Das, M. Samal, and K. Yun, "Highly stable functionalized cuprous oxide nanoparticles for photocatalytic degradation of methylene blue," *Materials Chemistry and Physics,* vol. 218, pp. 272-278, 2018.

[168] L. Dou, X. Zhang, M. M. Zangeneh, and Y. Zhang, "Efficient biogenesis of Cu2O nanoparticles using extract of Camellia sinensis leaf: Evaluation of catalytic, cytotoxicity, antioxidant, and anti-human ovarian cancer properties," *Bioorganic chemistry,* vol. 106, p. 104468, 2021.

[169] A. K. Bhardwaj, V. Kumar, V. Pandey, R. Naraian, and R. Gopal, "Bacterial killing efficacy of synthesized rod shaped cuprous oxide nanoparticles using laser ablation technique," *SN Applied Sciences,* vol. 1, pp. 1-8, 2019.

[170] S. S. G. Srinivasan, B. Govardhanan, M. Ashok, and M. S. Kumar, "Influence of deposition time on the visible-light-driven photocatalytic activity of Cu2O thin films by reactive sputtering at room temperature," *Materials Letters,* vol. 284, p. 128980, 2021.

[171] D. Jeong *et al.*, "Characterization of Cu 2 O/CuO heterostructure photocathode by tailoring CuO thickness for photoelectrochemical water splitting," *RSC advances,* vol. 12, no. 5, pp. 2632-2640, 2022.

[172] B. Djamila, L. S. Eddine, B. Abderrhmane, A. Nassiba, and A. Barhoum, "In vitro antioxidant activities of copper mixed oxide (CuO/Cu2O) nanoparticles produced from the leaves of Phoenix dactylifera L," *Biomass Conversion and Biorefinery,* pp. 1-14, 2022.

[173] R. Chokkareddy and G. G. Redhi, "Green synthesis of metal nanoparticles and its reaction mechanisms," *Green Metal Nanoparticles: Synthesis, Characterization and Their Applications,* pp. 113-139, 2018.

[174] B. Djamila, L. S. Eddine, B. Abderrhmane, A. Nassiba, and A. Barhoum, "In vitro antioxidant activities of copper mixed oxide (CuO/Cu," 2022.

[175] K. Pakzad, H. Alinezhad, and M. Nasrollahzadeh, "Green synthesis of Ni@ Fe3O4 and CuO nanoparticles using Euphorbia maculata extract as photocatalysts for the degradation of organic pollutants under UV-irradiation," *Ceramics International,* vol. 45, no. 14, pp. 17173-17182, 2019.

# Chapter II

# Thiosemicarbazones as a Suitable Intermediates for Thiazole Synthesis

# Part I

# Literature Review

# I. Overview on thiosemicarbazones

## I.1. Introduction

The class of substances known as Schiff bases encompasses a variety of compounds with diverse biological properties, including anticonvulsive, antipyretic, antitumor, anti-inflammatory, and antibacterial activities[1]. thiosemicarbazones (TSCs) with sulfur and nitrogen as donor atoms are an important class of Schiff-based ligands that are of great interest, because of their structural diversity, ion-sensing capacity, biological implications, and bonding mechanisms [2].

For decades, TSCs have attracted interest because of their potential as medicinal agents and their adaptability as ligands, which allows them to generate a diverse array of coordination conditions [3]. these compounds are beneficial for organic synthesis, especially for the synthesis of thiazoles.

## I.2.Concept of thiosemcarbazones

TSCs, possess the overall structure $R_1R_2CNNR_3CSNR_4R_5$ , a subclass of Schiff bases, have shown a variety of characteristics, such as antibacterial, antifungal and antitumor activities. These compounds are named "thiosemicarbazones" based on their corresponding ketone or aldehyde precursors and can be synthesized through the condensation process involving a ketone or aldehyde with thiosemicarbazide. General structure of the thiosemicarbazone moiety is depicted in Figure II.1 [4] .


**Figure II.1.** Schiff base and Thiosemicarbazones general structures [4]

For an extended period, thiosemicarbazide has been a prominent medicinal product. These compounds have become crucial in chemical synthesis to produce various heterocycles. Biologically active compounds such as triazoles and thiazoles are often generated through their interactions with molecules containing C=O and C=N groups[5].

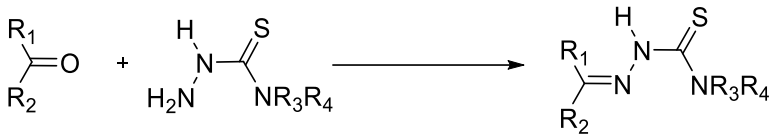

**Figure II.2.** Thiosemicarbazones synthesis [6]

Thiosemicarbazones show thione-thiol tautomerism due to the NH-C=S group. While TSCs exist in the thione form predominantly, and they strongly exhibit equilibrium between the thiol and thione forms in solution [7].

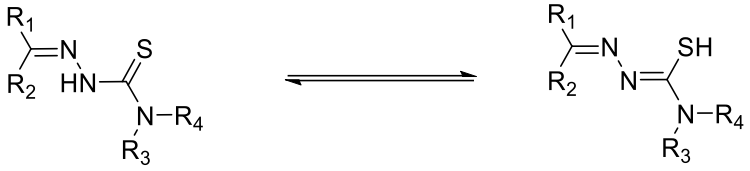

**Figure II.3.** Thiosemicarbazone forms (thione and thiol forms) [7]

Thiosemicarbazones have thiol-thione tautomerism since they can occur in two distinct isomers: Z (cis) and E (trans). Studies in theory and experimentation have demonstrated that the thione form's E-isomer is more stable in the solid state [8].

Typically, TSCs exhibit chelating ligand behavior and form complexes through reactions with metallic cations in order to create metallic complexes demonstrating the flexible coordination chemistry of TSCs. They often coordinate with transition metals through the sulfur and nitrogen donor atoms in their (N, N, S) tridentate or (N, S) bidentate forms[9]. The TSCs are effective chromogenic agents for metal ions because of the potent chelating power of the thioketone sulfur (>C=S) and hydrazine nitrogen atom (>C=N) [10].

### I.3. Synthesis of TSCs

Thiosemicarbazones are a class of chemicals related to semicarbazones that have garnered significant attention because of their diverse biological functions. Thiosemicarbazides serve as the main precursors for accessing thiosemicarbazones, starting from aldehydes or ketones [11]. The literature has reported several methods for synthesizing thiosemicarbazides and their derivatives, thiosemicarbazones. Here, we cite some of these synthesis methods:

Using the natural monoterpene (-)-camphene, Souza and colleages, synthesize 17 new thiosemicarbazones then assessed their cytotoxicity and anti-M. tuberculosis activity in VERO cells [12].

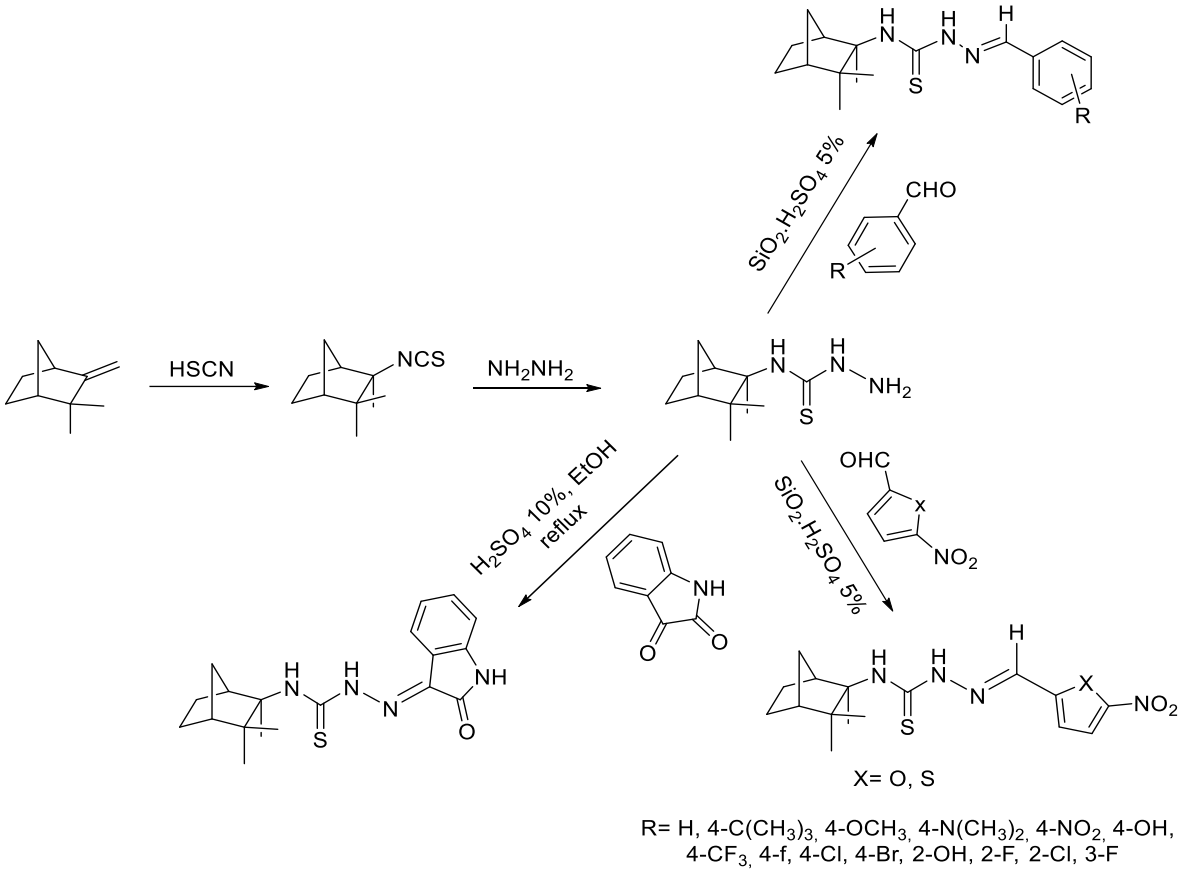


**Figure II.4. (-)**-camphene-thiosemicarbazones synthetic route [12]

Two indole-thiosemicarbazone derivatives novel series were developed and created by Bakherad et *al.*, who then assessed their cytotoxic effects on Hep-G2, MCF-7 and A-549 cell lines. The related aryl thiourea derivative was produced by hydrazine reacting with the aryl isothiocyanate derivatives in iso-propanol at room temperature for 30 minutes. And reacting thiourea with 2-aryl-1H-indole-3-carbaldehyde derivatives in the presence of a catalytic amount of acetic acid in EtOH at reflux to produce the corresponding indole-thiosemicarbazone derivatives [13].

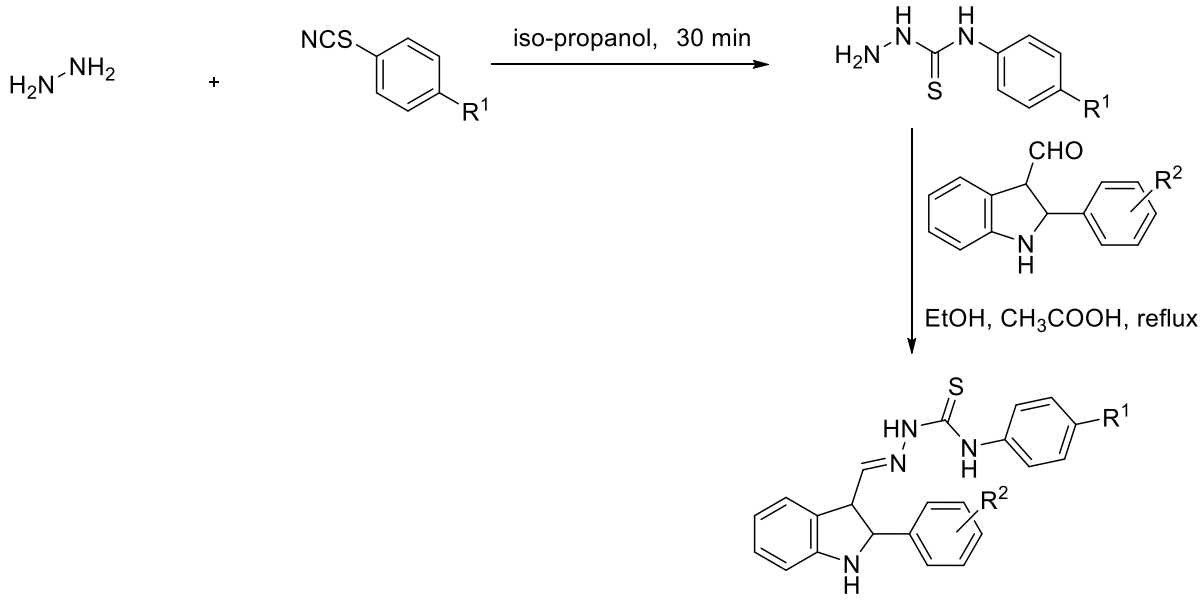


**Figure II.5**. Synthesis of indole-thiosemicarbazone derivatives [13]

4-benzoyl-5-methyl-2-phenyl-2,4-dihydro-3H-pyrazole-3-one was used to generate two novel N4-substituted-thiosemicarbazone derivatives ($H_2$ $L_1$, $H_2$ $L_2$) ,were synthesized and characterized by RUSNAC et *al.* They also reported these ligands chelating behavior with respect to copper (II) then examined the ligands and coordination compounds antiproliferative activity at three different doses on BxPC-3, RD, HEp-2, L20B cells and MDCK [14].

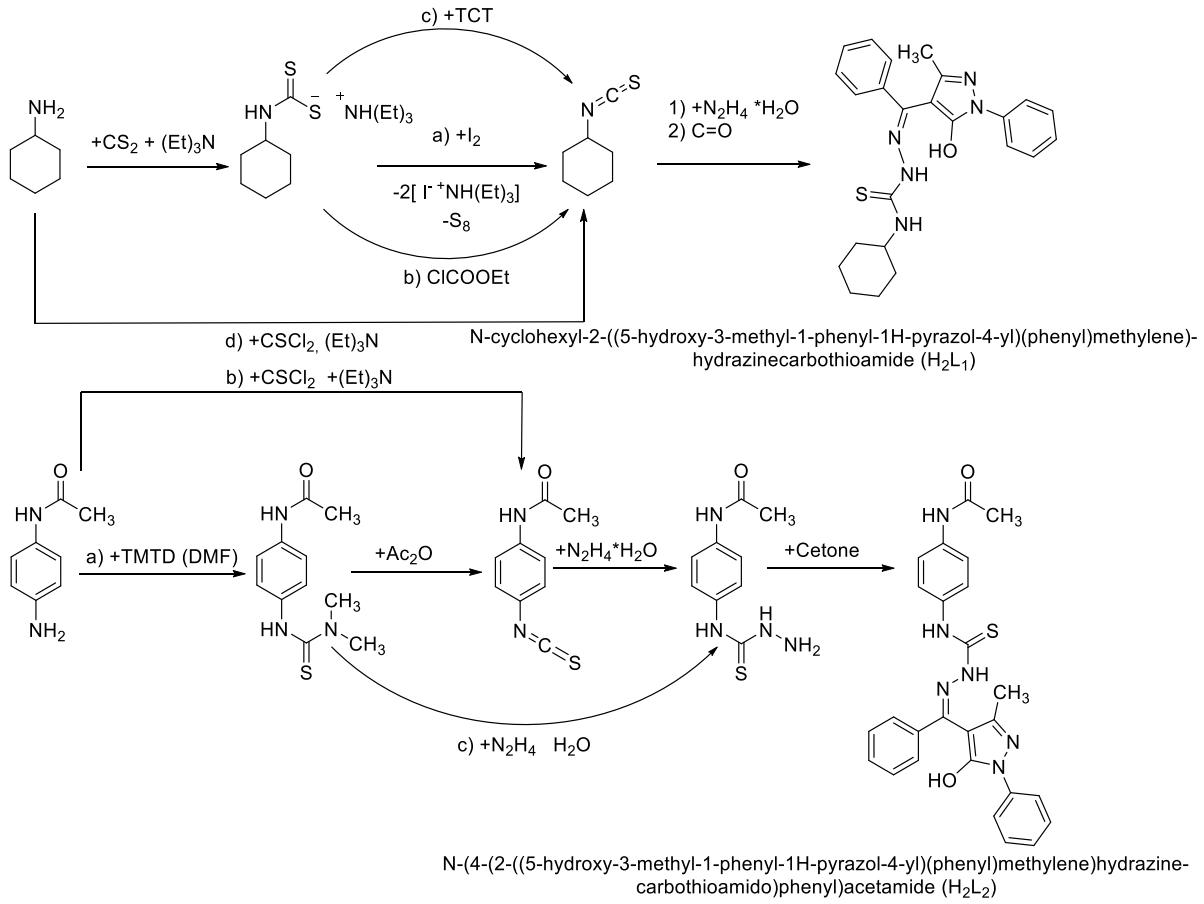


**Figure II.6.** N4-substituted-Thiosemicarbazone dérivatives [14]

Kumar et *al*. have developed a unique method for synthesizing thiosemicarbazones and have evaluated their anticancer efficacy *in vitro* using melanoma skin cancer cell lines [15].

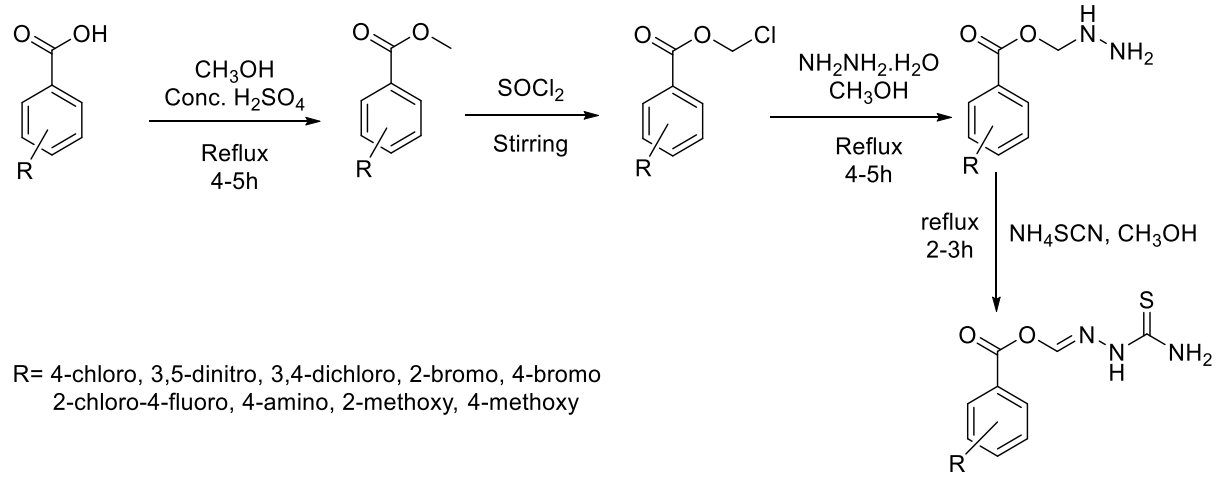


**Figure II.7.** TSC synthesis[15]

Ramkishore Matsa et *al*. used an easy and environmentally friendly synthetic process to produce a variety of thiosemicarbazone derivatives, which were then examined for their Drug-Like Molecular (DLM) characteristics [16].

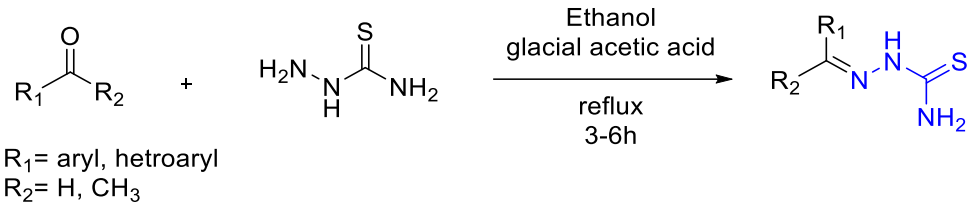


**Figure II.8.** TSCs synthesis using a green method [16]

Sibuh et *al*. described the production of 4-Nitrobenzaldehyde Thiosemicarbazone (4-NBTSc), and 3-Methoxybenzaldehyde Thiosemicarbazone (3-MBTSc) then assessed the anticancer properties of 4-NBTSc and 3-MBTSc in vitro against several cell lines [17].

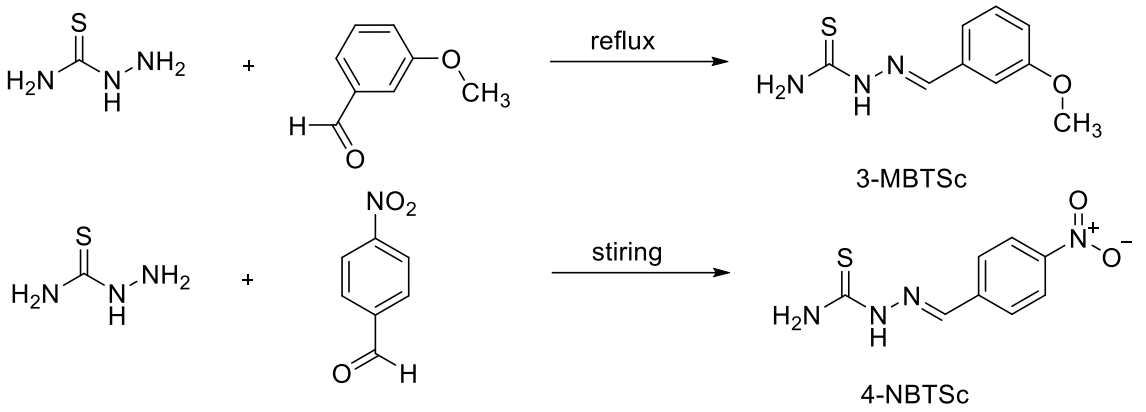


**Figure II.9.** TSCs derivatives [17]

The synthesis of several derivatives of semicarbazones and thiosemicarbazones was described by Oliveira et *al*. They were assessed for their toxicity to human peripheral blood mononuclear cells (PBMC) as well as their antiplasmodial activity [18].

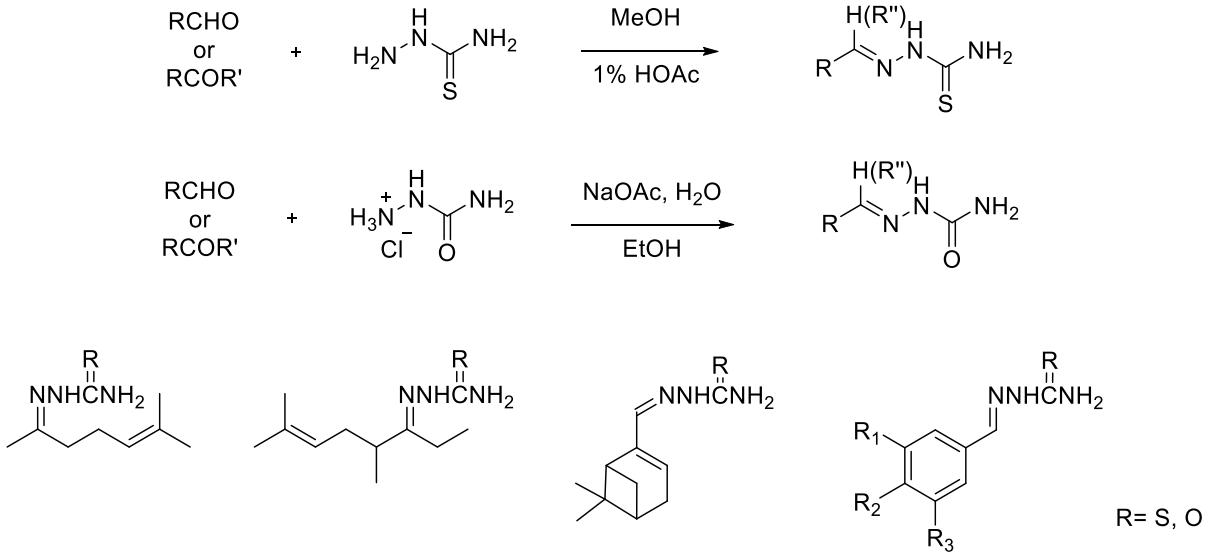


**Figure II.10.** Semicarbazones and thiosemicarbazones synthesis methods [18]

The synthesis of TSCs from substituted thiosemicarbazides ($NH_2NHC(S)NHR$) and 4-(propan-2-yl) benzaldehyde is described by Krishna et *al.* [19].

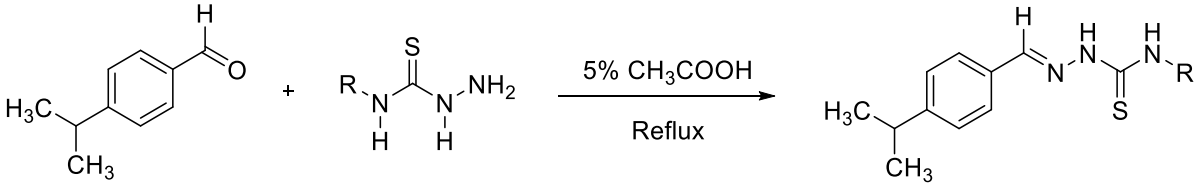


**Figure II.11.** 4-(propan-2-yl) benzaldehyde derivative[19]

Gavali et *al.* synthesized terephthalaldehyde bis(thiosemicarbazone) (TPTSC) by combining the ethanolic terephthalaldehyde solution with the ethanolic thiosemicarbazide solution and sonicating the mixture for 20 minutes [20].

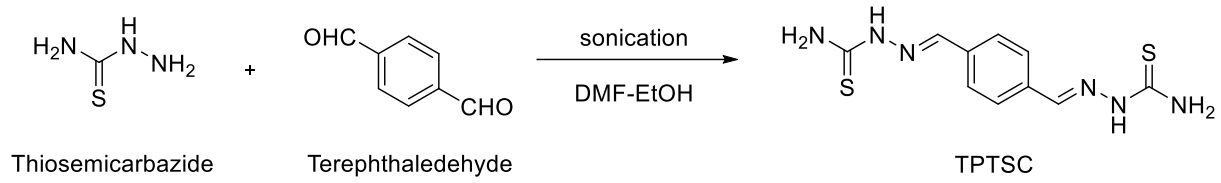


**Figure II.12.** Synthesis of TPTSC [20]

Ali et *al.* have synthesized dithiocarbazates and thiosemicarbazones in moderate to good yields using both the usual approach and ecologically friendly techniques (such as using lemon juice as a catlyst, solvent-free grinding, and using water as a solvent) [21].

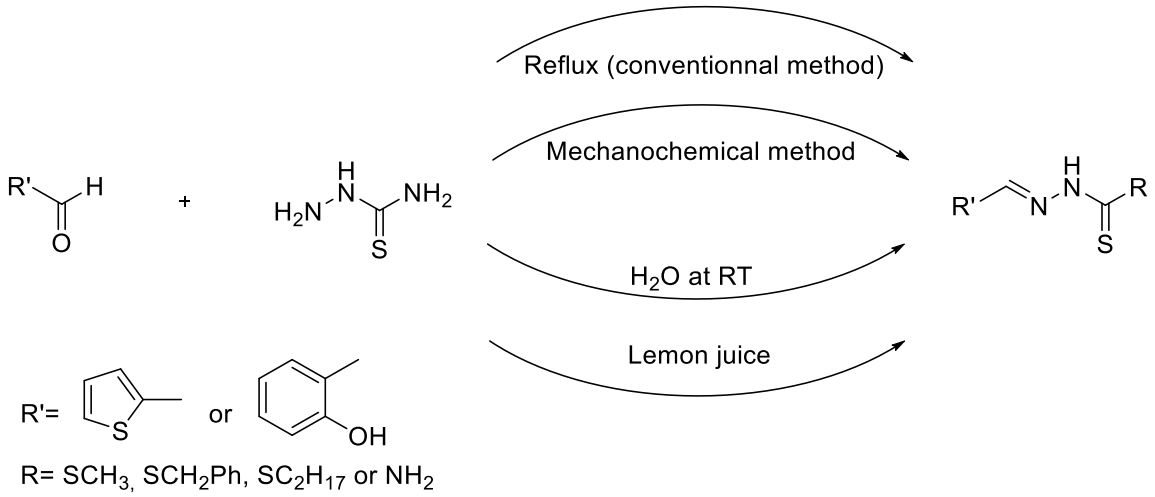


**Figure II.13.** Dithiocarbazates and thiosemicarbazones synthesis using ecofriendly techniques [21]

## II. Thiazole

### II.1. Introduction

In the realms of organic and medicinal chemistry featuring five-membered rings housing two heteroatoms, the thiazole ring stands out as one such example [22], a primary goal is the creation, synthesis, and enhancement of molecules holding promise as human therapeutics. Over the past decade, combinatorial chemistry has facilitated the generation of chemical libraries rooted in privileged structures [1], with particular emphasis on heterocyclic frameworks due to their

established significance in medicinal chemistry [2]. Among the various biologically active molecules.

The thiazole ring stands as a crucial framework within heterocyclic chemistry and the realm of drug design and exploration. Its significance is underscored by its extensive examination, rendering it one of the most thoroughly investigated heterocycles. This structural element have an important role in the efficacy of different drugs, including dasatinib (an anti-tumor medication), ritonavir (an anti-HIV agent), ravuconazole (an anti-fungal treatment), nitazoxanide (an anti-parasitic remedy), meloxicam (an anti-inflammatory drug), and thiamethoxam (an insecticide) [23].

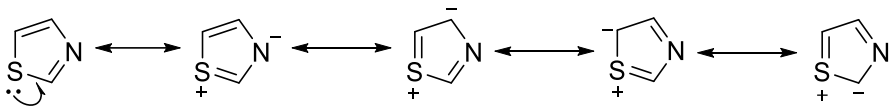

**Figure II.14.** The resonance structures of a thiazole compound [24]

Compounds featuring thiazole (TZ) groups have garnered considerable attention in chemistry of medicinal because of their prevalence in numerous molecules that are biologically active. These compounds exhibit a diverse array of pharmacological effects, including anti-inflammatory, antimicrobial, antineoplastic, antidiabetic, and anticonvulsant properties. Some drugs containing thiazole have shown potential antiviral activity, especially against COVID. Additionally, in drug discovery research thiazole ring is being recognized as a structural alert. Different drugs holding thiazole moieties have been implicated in toxicity, such as sudoxicam and thiabendazole. For example, epoxidation and a ring-opening reaction are the biotransformation processes for sudoxicam, resulting in the creation of covalent adducts by the synthesis of thioamides [25].

In recent decades, there has been significant advancement in the development of heterocyclic derivatives, resulting in the creation of numerous new agents sourced from both synthetic and natural origins. Within this category, thiazole stands out as a distinctive five-membered heterocyclic structure featuring nitrogen and sulfur atoms. It is widely utilized as a fundamental framework in various pharmaceutically significant compounds due to its broad spectrum of biological activities, including antibacterial, antivirus, and antifungal properties. Presently, Over ninety derivatives that contain thiazole are being investigated clinically, with several analogs already approved for the treatment of diverse diseases. Given their potential as privileged scaffolds, thiazole derivatives offer substantial promise for further exploration in the quest for novel drugs with enhanced therapeutic efficacy targeting similar biological pathways [26].

Heterocyclic frameworks hold a significant allure in medicinal chemistry due to their proven versatility . Among the different types of heterocyclic compounds, those featuring a five-membered ring have exhibited diverse biological properties. Notably, thiazole, identified by Hantzsch and Weber in 1887, has emerged as a focal point for industrial and pharmaceutical researchers in recent decades[26] .

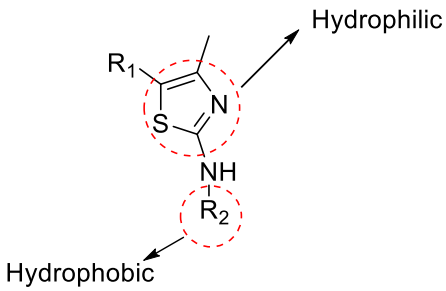


**Figure II.15.** Thiazole derivatives structure[24]

Thiazole, a prominent five-membered aromatic heterocycle distinguished by sulfur and nitrogen atoms, boasts distinct biological attributes. Studies have underscored the multifaceted biological potential of thiazole-containing compounds, spanning antioxidant , neuroprotective, hypnotic antifungal, diuretic, antipsychotic, antiallergic, antimalarial, antihypertensive, analgesic, antibacterial , anti-inflammatory , and anticancer activities among others[26].

Substantial progress has been achieved in recent decades in developing anticancer agents, including both natural and synthetic compounds. Thiazole, a unique heterocyclic 5-membered structure containing sulfur and nitrogen, functions as a vital foundational structure in numerous significant medicinal compounds. Thiazole is a key component in several clinically applied anticancer drugs like dasatinib and dabrafenib. Recent research has focused on thiazole-containing compounds as potential inhibitors of various biological targets implicated in cancer, showing promising effectiveness and reduced toxicity [27].

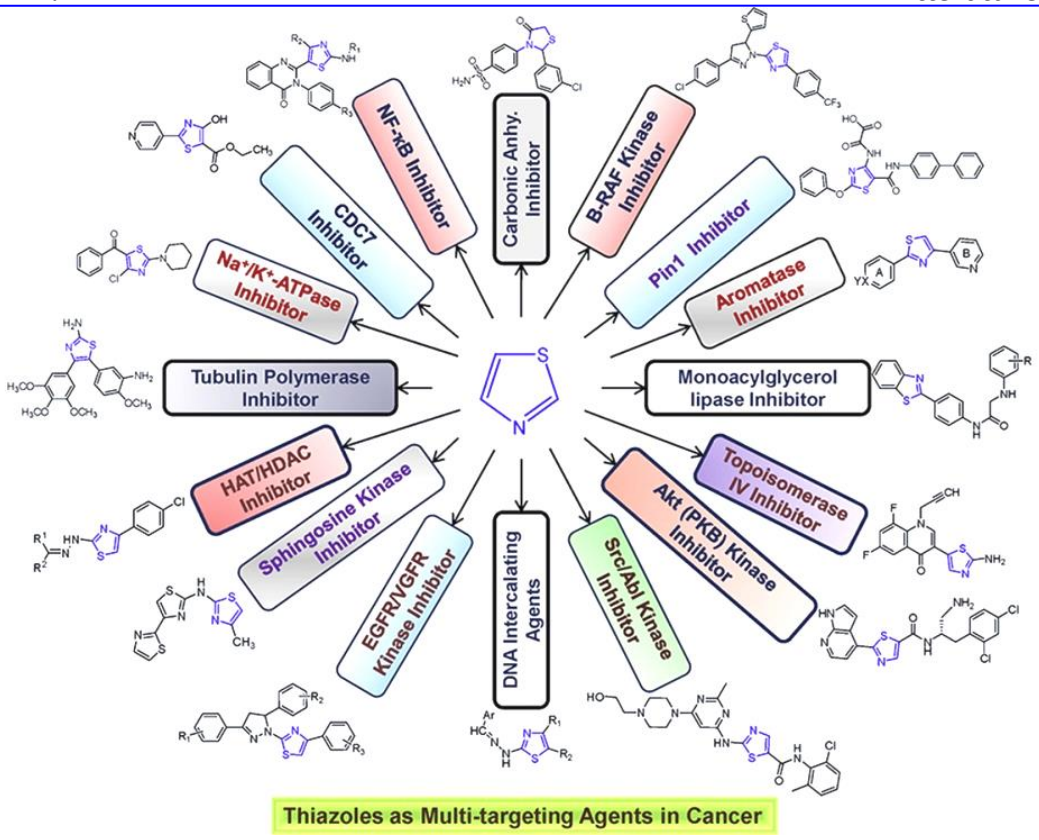


**Figure II.16.** Thiazole Compounds: Versatile Multi-Targeting Agents in Cancer Treatment [27]

## II.2. Thiazole synthesis methods

The synthetic methodology for producing thiazole derivatives has evolved significantly, driven by the distinct structural features and importance of thiazole compounds. This expansion has been facilitated through the application of diverse conditions, catalysts, and synthetic approaches. Several techniques, including the Gabriel, Cook-Heilbron, and Hantzsch synthesis are used to synthesize thiazoles [24].

### II.2.1. Hantzsch thiazole synthesis method (1887)

The Hantzsch synthesis is the earliest and most well-known technique for creating the ring of thiazole developed in 1887. The process involves cyclization reactions involving different reactants that contain the N-C-S fragment and alpha-halocarbonyl molecules. Thiourea, thioamides, thiosemicarbazides, and thiosemicarbazones are a few examples of these compounds.

Thioamides are frequently condensed with different alpha-halocarbonyl molecules. This reaction yields a large number of thiazoles having substituents at positions 2, 4, or 5 (aryl, heteroaryl, or alkyl). Mechanism of the reaction is as follows: an intermediate product is formed when the alpha carbon of the alpha-halocarbonyl is attacked by the thioamide sulfur atom nucleophilically. This intermediate compound is then dehydrated to yield the matching thiazole [28].

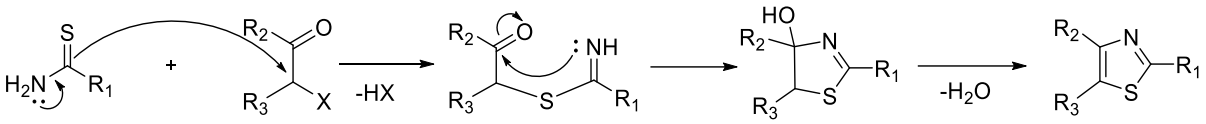


**Figure II.17.** Hantzsch reaction for the preparation of thiazole [28]

### II.2.2. Synthesis of Cook-Heilbron (1925)

The process known as the synthesis of Cook-Heilbron is used to create The thiazole ring using α-aminoamides or α-aminonitriles along with carbon disulfide. This method generates 5-amino thiazoles, where substitution happens at the second position , through the aminonitrile reaction with esters and salts of carbon disulfide, isothiocyanates, or thioacids under gentle conditions[29].

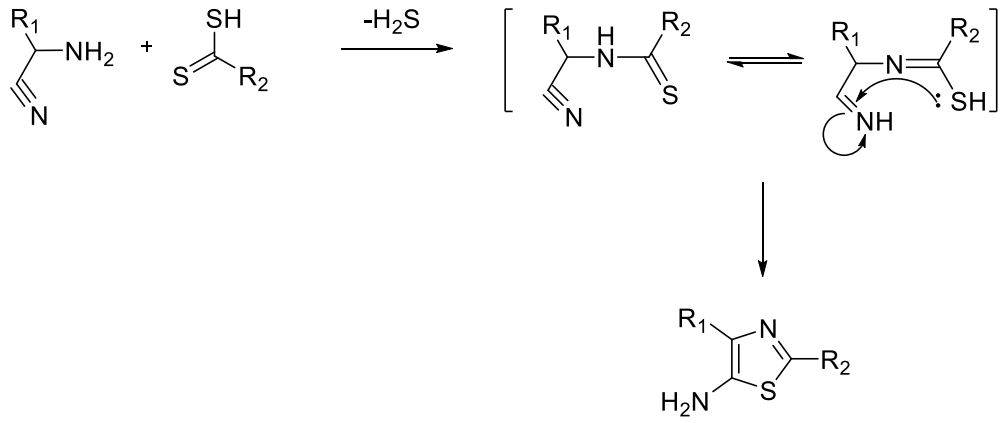


**Figure II.18.** Synthetic method of thiazole using Cook-Heilborn's reaction [30]

### II.2.3. Gabriel method

The Gabriel synthesis is an alternative method to synthesize thiazole derivatives , Gabriel created the original version of this reaction in 1910, which by reacting phosphorus pentasulfide with acylamino-ketone involves the closure of the thiazole ring, resulting in thiazole 2,5-disubstituted derivatives. This approach, advanced by Kotadiya, entails heating acylamino compounds such as phosphorus pentasulfide with N-(2-oxopropyl) acetamide to yield 2,5-dimethylthiazole [31].

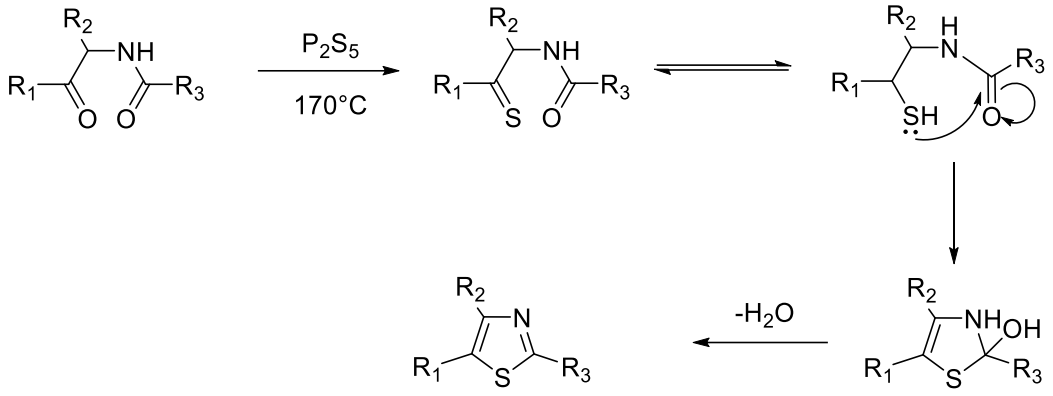


**Figure II.19.** Gabriel synthesis reaction mechanism [30]

### II.2.4. Condensation of thiourea with acetophenone

Using benzimidazole phenyl thiourea and 2-bromoacetophenone, Bangagde et *al.* created a unique and effective procedure to manufacture Benzimidazol-amino thiazoles under microwave irradiations. The manufactured products exhibit intriguing anticancer properties for lung cancer in humans [32].

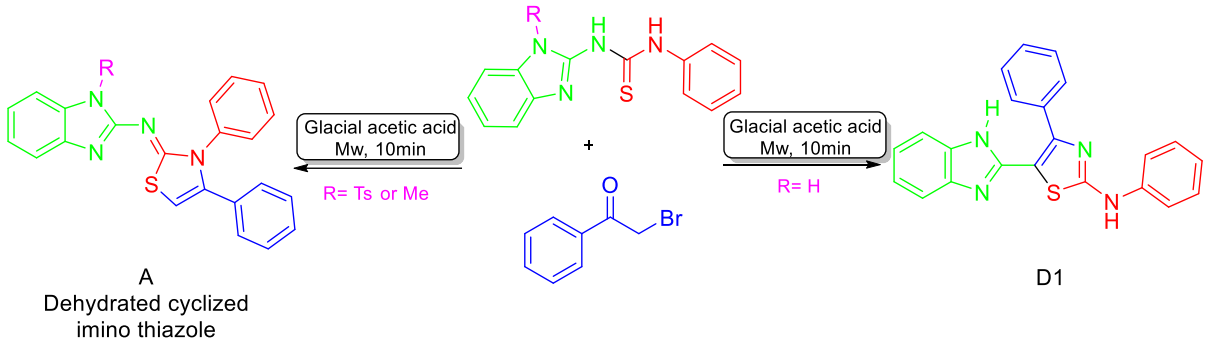


**Figure II.20.** Benzimidazol-Amino Thiazole synthesis [32]

### II.2.5. Synthesis of Thiazoles via intramolecular cyclization

In a modified Thorpe-Ziegler type cyclization, Avadhani revealed aryl/heteroaryl/alkyl dithioesters as thiocarbonyl coupling agents yielding an efficient one-pot process of 4-amino-2-(het)aryl/alkyl-5-functionalized thiazoles. the reaction demonstrated at positions 5 and 2 of thiazoles broad functional group compatibility , which proceeds in mild conditions and at room temperature with good yields [33].

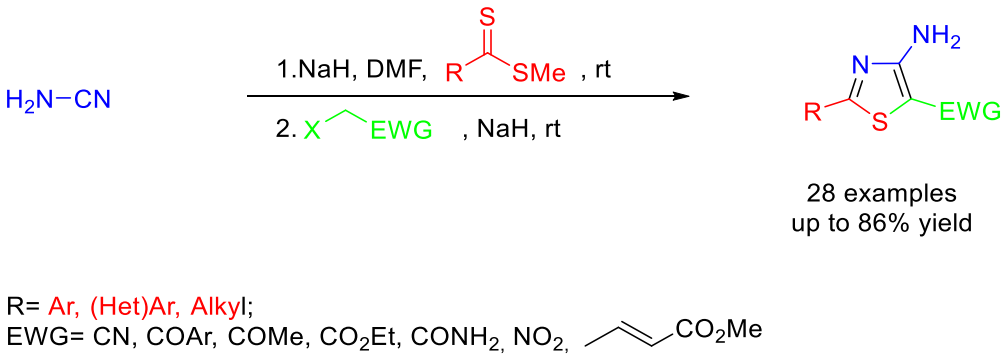


**Figure II.21** synthesis of thiazoles by intramolecular Thorpe–Ziegler Reaction [33]

### II.2.6. Condenstaion of alkyne with thioamides

Huang and colleagues synthesized 1,3-thiozoles in moderate to good yields via alkynes-thioamides cascade cyclization . They employed a photocatalyst in DCE (1,2-dichloroethane), stirred for 9 hours in an air atmosphere under the 9 W blue LEDs irradiation, achieving visible light-induced synthesis [34].


**Figure II.22.** The interaction of terminal alkynes with thioamides to create 1,3-thiazole derivatives [34].

### II.2.7. Condensation of thiosemicarbazones with halogeno-carbonyle

Gomha et *al*. synthesized using 1-(4-Methyl-2-(2-(1-(thiophen-2-yl) ethylidene) hydrazinyl) thiazol-5-yl) ethanone as a building block a new series of 5-(1-(2-(thiazol-2-yl)hydrazono) ethyl) thiazole derivatives. Using the MTT test, the synthesized compounds bioactivities were assessed of in relation to their anticancer effects against tumor cells (MCF-7) [35].

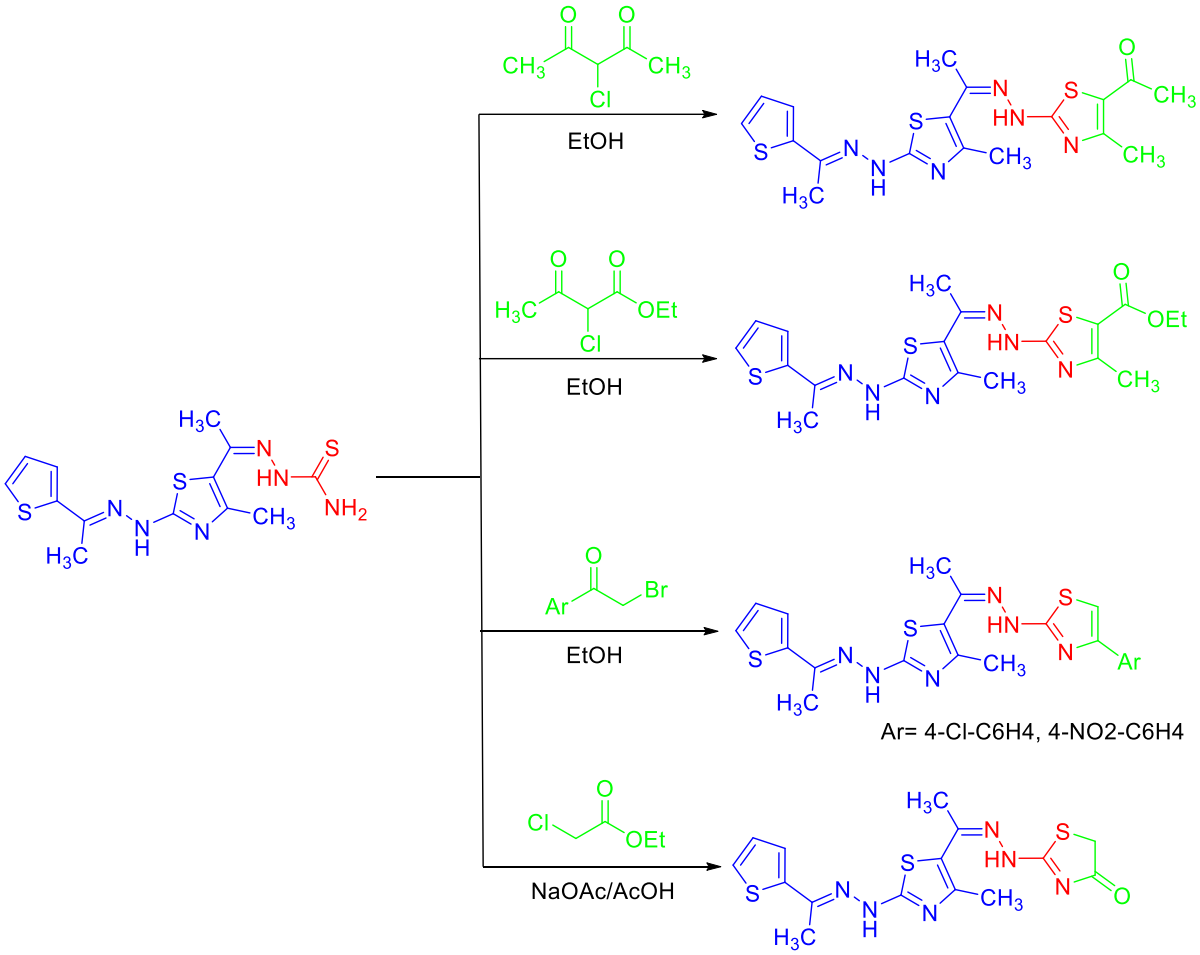


**Figure II.23.** Thiazole derivatives synthesized using thiosemicarbazone [35]

### II.3. Synthesis of TZ using ecofriendly methods

The use of different chemicals and polymers in production processes over the past few decades has been steadily increasing, with negative consequences for the human health and environment. To create products in the required number, synthetic chemists took into account the use of environmentally friendly synthetic processes such as "Green chemistry"[36].

### II.4. Using microwave-assisted synthesis

Mamidala et *al*. synthesized target thiazole analogues using a combination of thiocarbohydrazide, aldehyde, and phenacyl bromides using a microwave-assisted method, and assessed the analogues' efficacy as agents against breast cancer [37].

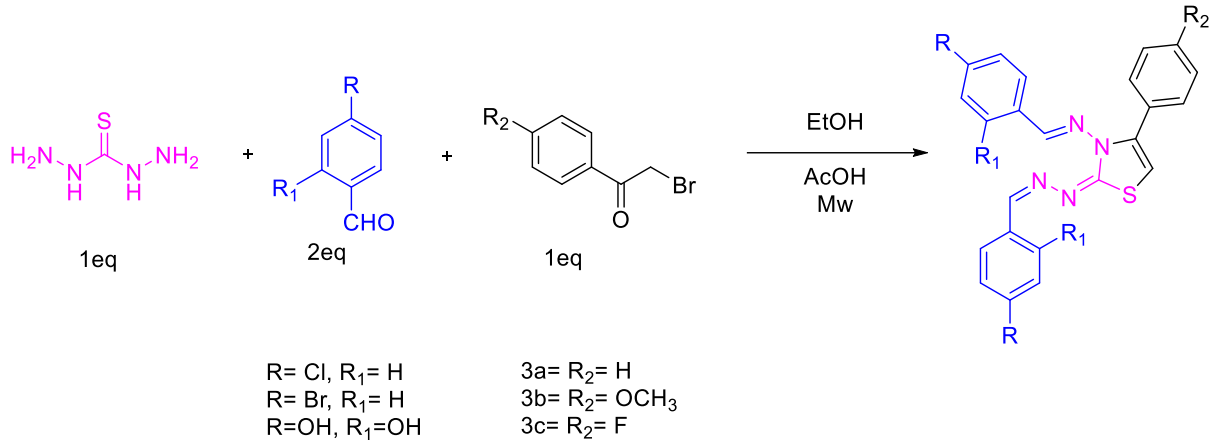


**Reaction Conditions:** EtOH, AcOH, microwave irradiation at 70°c and 210 W

**Figure II.24.** MW assisted method for the synthesis of thiazole analogues [37]

## II.5. One-pot multicomponent reactions in aqueous medium

An environmentally friendly one-pot multi-component method for producing biologically significant trisubstituted thiazoles was developed by Singh and colleagues. This method uses a reaction between easily accessible acetophenone, aryl thioamides, and barbituric acid in the presence of $O_2$ (air) and $FeCl_3 \cdot 6H_2O$ in DMF [38].

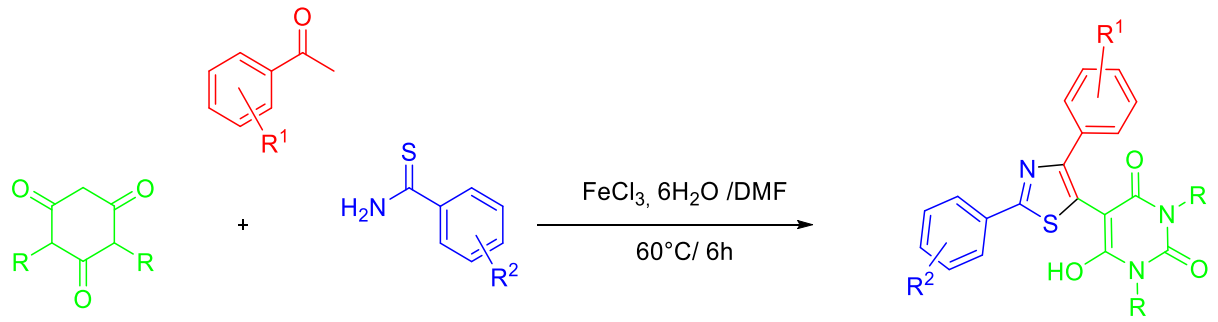


**Figure II.25.** Preparing substituted diphenyl 1, 3-thiazole with a one-pot multicomponent reaction [38]

## II.6. Using silica supported tungstisilisic acid

Using a reusable silica-supported tungstosilisic acid catalyst, Bouherrou et *al*. created an effective and environmentally friendly technique for synthesizing of novel thiazole derivatives in a very excellent yield. Then assessed the resulting compounds biological activity [39].

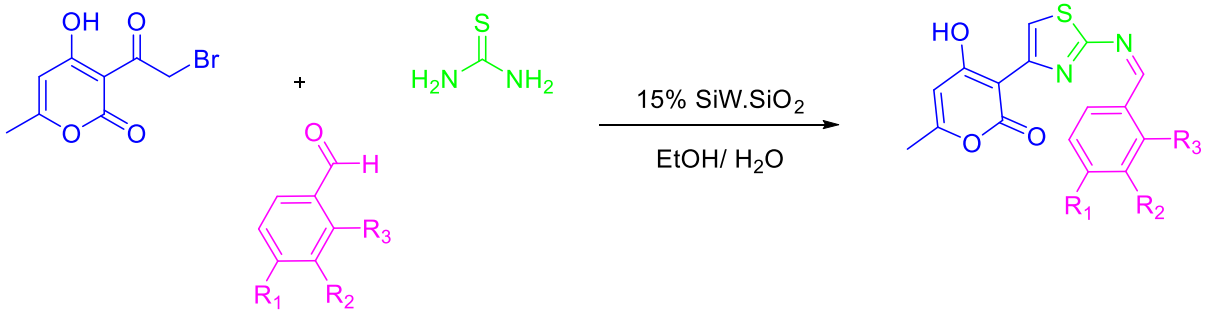


**Figure II.26.** One-pot synthesis using a friendly catalyst [39]

## II.7. Using Nanoparticles

Chitosan-ZnO (CS/ZnO) nanocomposite film was produced by Bashal et *al*. and has the potential to be a practical, efficient, recyclable, heterogeneous base catalyst for thiazole production[40].

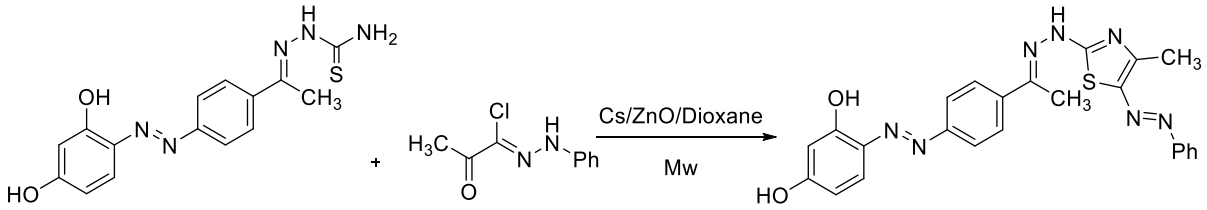


**Figure II.27.** Synthesis of TZ using a nanocatalyst [40]

## II.8. Biological Activities of Thiazole

Being one of the most often employed heterocyclic moieties, thiazole nuclei have great promise and are essential to many bioactive medications [41]. The literature indicates that there are more and more medications with this ring in their structures. The number of medications containing thiazole scaffold has increased significantly over the past ten years, reaching a peak of eight in 2019 [42].

Using a three-component one-pot synthesis, Sayed et *al*. prepared new derivatives of 5-(1-(2-(thiazol-2-yl)hydrazono)ethyl)thiazole. Three among these products were shown to have potential capabilities based on their growth inhibitory efficacy against three tumor cell lines (HepG2, HT-29, and HCT-116) *in vitro* [43].

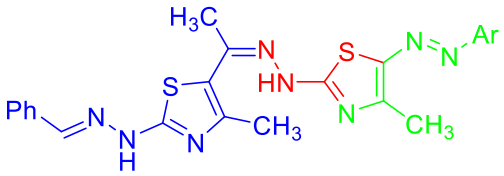

**4a-e**

Ar= **a**, $C_6H_5$; **b**, 4-$CH_3$-$C_6H_4$; **c**, 4-Cl-$C_6H_4$;
**d**, 2,4-Cl-$C_6H_3$; **e**, 4-$NO_2$-$C_6H_4$

**Figure II.28.** Derivatives of 5-(1-(2-(thiazol-2-yl)hydrazono)ethyl)thiazole [43]

A new HIV-1 RT class of inhibitors, , was developed and synthesized using the (Z)-3-(2-(4-arylthiazol-2-yl)hydrazono)indolino-2-one scaffold by Meleddu et *al*. These substances exhibit intriguing inhibitory effect on DP RT-associated HIV-1 processes as well as RNase H, potentially producing inhibitors that entirely block RT activities[44].

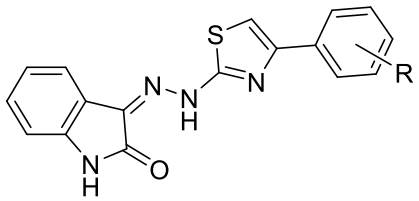

**EMAC2072-2082**

**R**= 4-Cl, 4-F, 4-Br, 4-$NO_2$, 4-$C_6H_5$, 2,4-F, 3-$NO_2$, 4-$CH_3$, 4-$OCH_3$, H, 2,4-Cl

**Figure II.29.** Indolinone derivatives [44]

Kemisetti and colleagues developed Schiff base derivatives by mixing 2-amino-benzothiazole-6-sulfonic acid amides with substituted aromatic aldehydes. PASS (Substances Spectra Activity Prediction) data were used to predict these compounds diuretic effects. The compounds diuretic action was evaluated, and the results showed they were more potent than the standard [45].

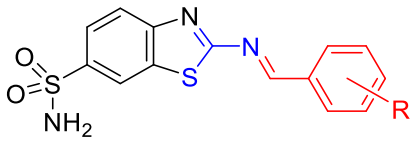

**Figure II.30.** Derivatives of Benzothiazoles [45]

A group of nine derivatives of thiazole featuring a system of cyclopropane created and evaluated their effectiveness against various Candida species by Biernasiuk et *al*. The MIC (mini mum inhibitory concentration) ranged in 7.81 - 0.008 μg/mL, demonstrating against all C. albicans isolates an extremely robust activity, which was comparable to or even higher than that of nystatin [46].

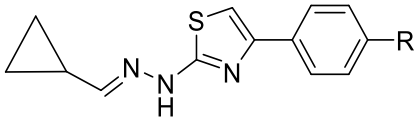

R= F, Br, Cl, $CH_{13}$, $OCH_3$, 2,4-diF, CN, $N_3$, $NO_2$

**Figure II.31.** Synthesized derivatives of TZ with potent activity against *Candida* spp [46]

Modrić et *al*. developed, produced, and assessed a library of 26 thiazole derivatives for their anti-inflammatory properties. The goal is to develop 1,3-thiazole derivatives into drug-like compounds with anti-inflammatory activity, acceptable ADME-Tox properties, and $IC_{50}$ values in the nM range, compound that showed the best activity is amide 7 with fused quinoxaline system [47].

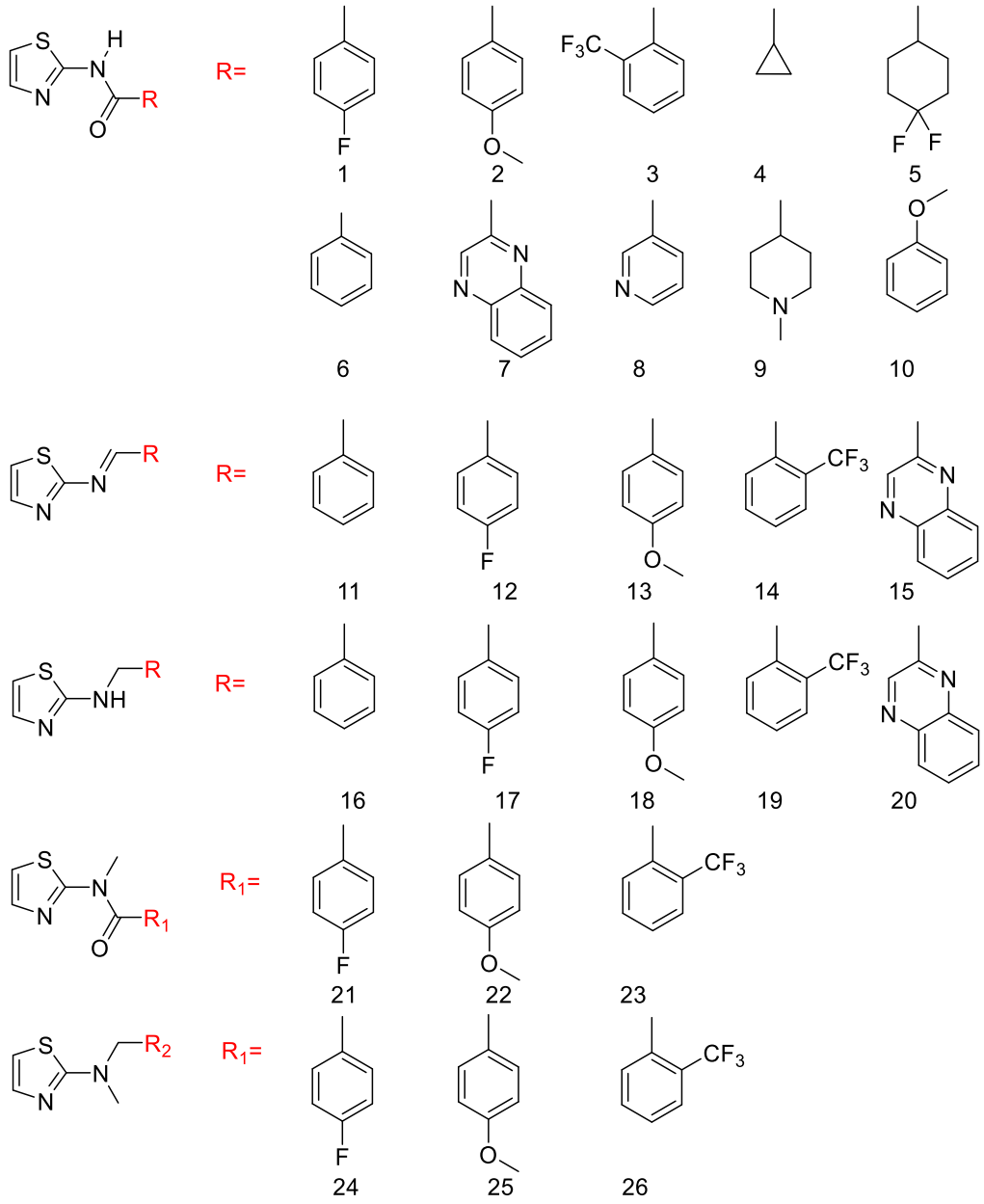


**Figure II.32.** Derivatives of thiazole with anti-inflammatory properties [47]

Al-Mathkuri et *al.* produced thiazole derivatives and assessed their antibacterial efficacy against Proteus vulgaris, Escherichia coli, Pseudomonas aeruginosa, and Staphylococcus aureus (Gram-positive). Against the investigated bacterial strains results showed lower potency. To obtain novel candidates with more significant antibacterial activity against various bacteria greater modification and optimization are needed [48].

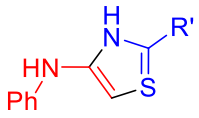

R'= $NH_2$, Me, $NH\text{-}NH_2$

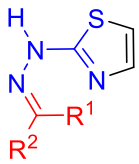

$R^1$=H, Me

$R^2$= Ph, 4-$NO_2$-Ph, 4-Cl-Ph, 4-OH-Ph, 4-$NH_2$-Ph

**Figure II.33.** Thiazole derivatives with antibacterial activity [48]

Hussein et *al.* created a number of novel derivatives of 2-[1-(1,3-diphenyl-1H-pyrazol-4-yl)ethylidene]hydrazinyl)-4-methyl-5-aryldiazinyl)-thiazole in an effective and practical manner. The studied compounds displayed strong antioxidant activity, as evidenced by the results from antioxidant activity assays (DPPH scavenging activity and the ABTS scavenging activity) [49].

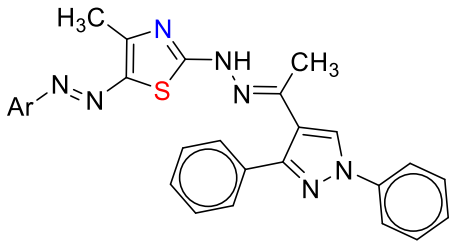

Ar=$C_6H_5$, 4-$CH_3C_6H_4$, 4-$ClC_6H_4$, 4-$NO_2C_6H_4$

**Figure II.34.** New derivatives of thiazole that have antioxydant activity [49]

### III. Thiazole 1,2,3-Triazole Hybrids

Notably in the past 20 years, for the creation of multi-target medications the molecular hybridization approach has been extensively thoroughly investigated as a valuable tool [50]. It is a potential technique for developing new generations of highly effective and safe medicinal candidates for various diseases, such as cancer, viral infections, and microbial infections[51]. To create hybrid conjugates of numerous medications that are clinically prescribed drug-drug combination techniques have been developed, aiming to tackle the intrinsic issues linked with these medications[51].

The hybrid drug design main goal is [51]:

*Increase efficacy by potentially interacting with multiple targets.

* Enhancing bioavailability by delivering the medication selectively to the site of action.

*Reducing toxicity.

*Avoiding medication resistance.

**Conclusion**

The notable biological significance of thiazoles and triazoles makes their hybridization a promising research area. This approach has the potential to create novel therapeutic agents with superior biological activities. The integration of thiazole and triazole heterocyclic rings has demonstrated the ability to produce compounds with enhanced solubility, bioavailability, and pharmacokinetic properties [52]. Furthermore, hybridization has been shown to boost the antimicrobial, antifungal, and anticancer properties of these compounds, positioning them as promising candidates for new therapeutic developments.

# Part II

# Findings and Discussion

## Introduction

In this section of the chapter, we will describe the synthesis pathway for derivatives of thiazoles starting from the 1,2,3-triazoles 1,4-disubstituted previously prepared. The reaction involves an initial reaction between the triazole derivatives and thiosemicarbazides to form thiosemicarbazones as intermediates. Subsequently, we employ an environmentally friendly, one-pot, multi-component method to synthesize biologically significant thiazole derivatives.

## I. Preparation of thiosemicarbazone derivatives

### I.1. Synthesis

In ethanol thiosemicarbazide (1.0 mmol) was reacted with several derivatives of 1,2,3-triazole (1.0 mmol), then few drops of acetic acid (AcOH) were added as a catalyst, to produce thiosemicarbazone derivatives as mentioned in [53]. At 90°C we refluxed the reaction mixture for three to four hours, and TLC (thin-layer chromatography) was used to monitor the progress of the reaction. Afterward, we placed the mixture in an ice bath in the refrigerator overnight to promote crystallization. The resulting precipitate was filtered then recrystallized from ethanol, achieving the final products in good yields. The resulting thiosemicarbazones were pure and did not require further purification.

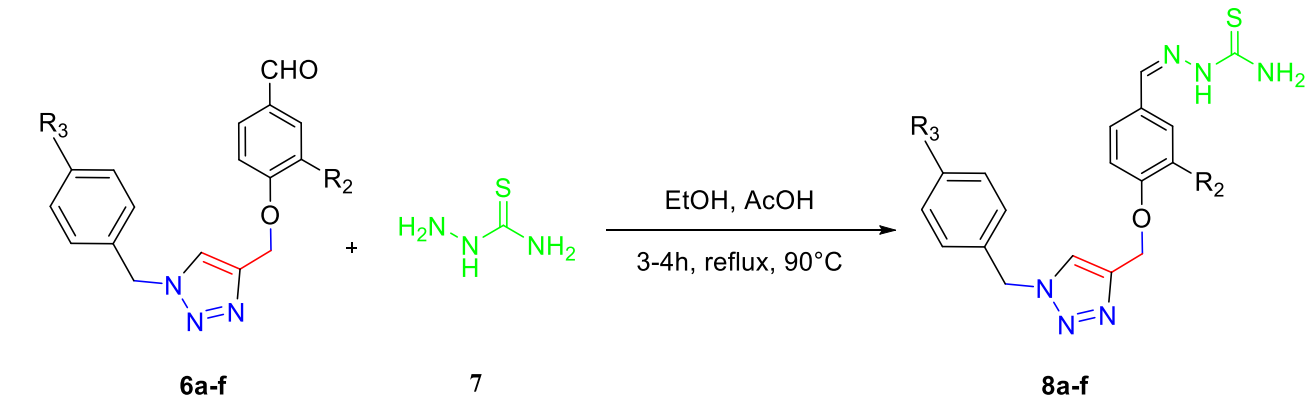


**6a-f** **7** **8a-f**

$R_2$: H, CHO, $OCH_3$
$R_3$: H,$CH_3$

**Figure II.35.** Synthesis of thiosemicarbazone derivatives using derivatives of 1,2,3-triazole as a starting material

**Table II.1.** Structural and physicochemical characteristics of thiosemicarbazone derivatives 8a-f

| **Ref** | Thiosemicarbazone derivatives | **Yield %** | **Melting points (°C)** | **FTIR ($cm^{-1}$)** | | | **$^1$H NMR (δ:ppm)** | |
|---|---|---|---|---|---|---|---|---|
| | | | | **C=N** | **C=S** | **N-H** | **N-H** | **CH=N** |
| **8a** | 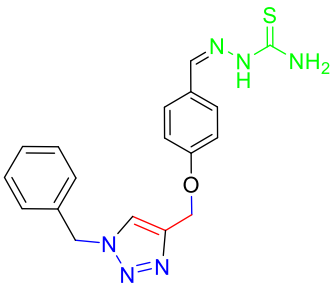 | 73 | 191-193 | 1594 | 1228 | 3160-3388 (NH stretching $NH_2$) **Primary and secondary amine groups** | 11.30 | 8.28 |
| **8b** | 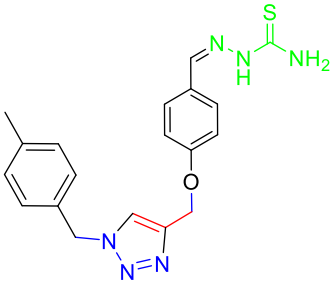 | 72 | 182-184 | 1589 | 1242 | 3160-3383 | 9.54 | 7.80 |
| **8c** | 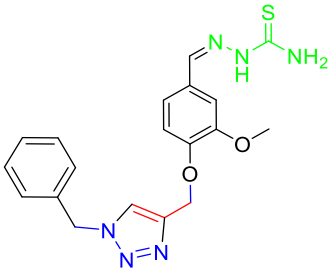 | 68 | 162-164 | 1598 | 1270 | 3146-3425 | 11.31 | 8.27 |
| **8d** | 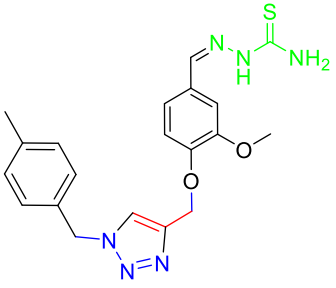 | 74 | 125-127 | 1580 | 1268 | 2996-3457 | 9.63 | 7.79 |

| | | | | | | | | |
|---|---|---|---|---|---|---|---|---|
| **8e** | 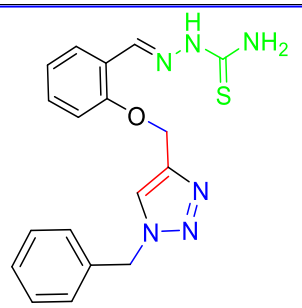 | 51 | 162-164 | 1589 | 1246 | 3028-3475 | 10.23 | 8.34 |
| **8f** | 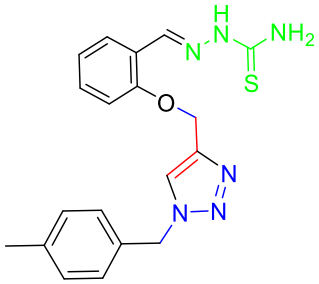 | 32 | 161-163 | 1591 | 1249 | 3018-3489 | 10.09 | 8.34 |

## I.2. Characterization

Using standard spectroscopic techniques (IR, $^{13}C$ NMR, and $^{1}H$ NMR), the structures of the thiosemicarbazone derivatives **8a-f** were determined. FT-IR spectra of thiosemicarbazone derivatives, shows broad peaks in the region **3388–3160 $cm^{-1}$** suggest the presence of NH stretching vibrations, typical for primary ($NH_2$) and secondary (NH) amine groups present in the thiosemicarbazone. The absorption bands of N-H bending, C=N stretching (from the triazole ring), and aromatic ring vibrations was observed around **1500–1700 $cm^{-1}$** . Peaks around **1251 and 1228 $cm^{-1}$** might correspond to C=S stretching in thiosemicarbazone, while an absorption band at approximately **1174 $cm^{-1}$** corresponding to the stretching vibration of C-O-C is observed**.**

Consequently, $^{1}H$ NMR spectroscopy was employed to elucidate the structures of products **8a–f**. The $^{1}H$ NMR spectrum of product **8e**, shown in Figure II.36. (a), reveals the following details: A singlet at 10.23 ppm corresponds to the CH=N proton, and its chemical shift indicates an electron-deficient environment. A singlet at 8.34 ppm likely represents CH proton in the triazole ring, likely corresponding to a proton with its downfield shift suggesting proximity to an electronegative group. The peaks between 7.81 and 7.19 ppm indicate a group of overlapping aromatic protons. A doublet at 6.98 ppm likely represents the $NH_2$ protons. A peak at 6.44 ppm is likely due to an NH proton in a thioamide environment. It appears as a singlet (s), indicating no coupling with neighboring protons and suggesting a strong downfield shift due to hydrogen bonding or an electron-withdrawing group. The singlet at 5.17 ppm may correspond to a $CH_2$-O group, with its downfield shift indicating proximity to an electronegative group. Another singlet at 5.60 ppm could represent protons in a similar environment to the 5.17 ppm peak, potentially another $CH_2$Ar group. Product **8f**'s $^{1}H$ NMR spectra displays a singlet at 2.35 ppm, which corresponds to

a typical non-aromatic methyl ($CH_3$) group. For compounds **8c** and **8d**, the methoxy groups (O-$CH_3$) are represented by signals at 3.79 and 3.87 ppm, respectively.

The $^{13}C$ NMR data indicate that compound **8e** has several key signals corresponding to its structural elements: The peak at 178.023 ppm is consistent with a carbon in a thioamide environment (**C=S**), confirming the presence of a thioamide group in the structure.

The peaks around 157.12 ppm likely correspond to carbon in aromatic ring attached to an oxygen ( **=C-O**) and the peak around 144.03 ppm likely correspond to carbons in an electron-deficient environment, such as **C=N**, which is also consistent with the proposed structure having such functional groups. Peak around 140.33 ppm suggest quaternary carbon and the peak around 122.93 ppm suggest carbon (**HC-N**) in a triazole ring. This chemical shifts match well with typical triazole carbons, which is affected by electron-donating or withdrawing groups, confirming this part of the structure.

An aromatic ring's quaternary carbon (**Cc**) is represented by the shift at 134.73 ppm, while two equivalent carbons (**Cb**) are represented by the shift at 129.18 ppm. Likewise, another pair of comparable carbons (**Ca**) in the aromatic ring is represented by the shift at 128.08 ppm. Furthermore, the signal at 126.36 ppm indicates that the aromatic ring contains a carbon (**Cd**).

Shift at 121.50 corresponds to the carbon in aromatic ring attached to the **C=N**. Shifts at 132.12, 128.81, 121.89 and 112.67 correspond to a carbons **$C_2$**, **$C_4$**, **$C_3$** and **$C_1$** respectively in the aromatic ring . The signal at 62.84 ppm is in the range for a methylene carbon attached to an electronegative atom, such as oxygen (**$CH_2$-O**). The peak at 54.29 ppm suggests another **$CH_2$** group, potentially a **$CH_2$Ar** group or a methylene adjacent to nitrogen or oxygen.

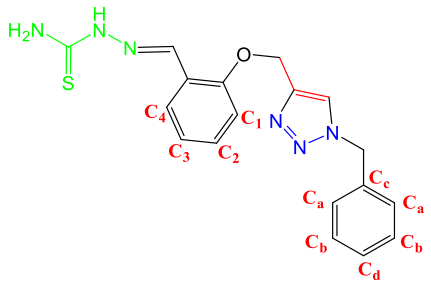


Overall, these chemical shifts correspond well to the expected carbon environments for compound **6e**, confirming its structure. Product **8f**'s $^{13}C$ NMR spectra reveals a peak at 21.17 ppm, which is most likely a signal for the methyl ($CH_3$) group. For compounds **8c** and **8d**, the methoxy groups (O-$CH_3$) are represented by signals at 56.14 and 56.02 ppm, respectively.

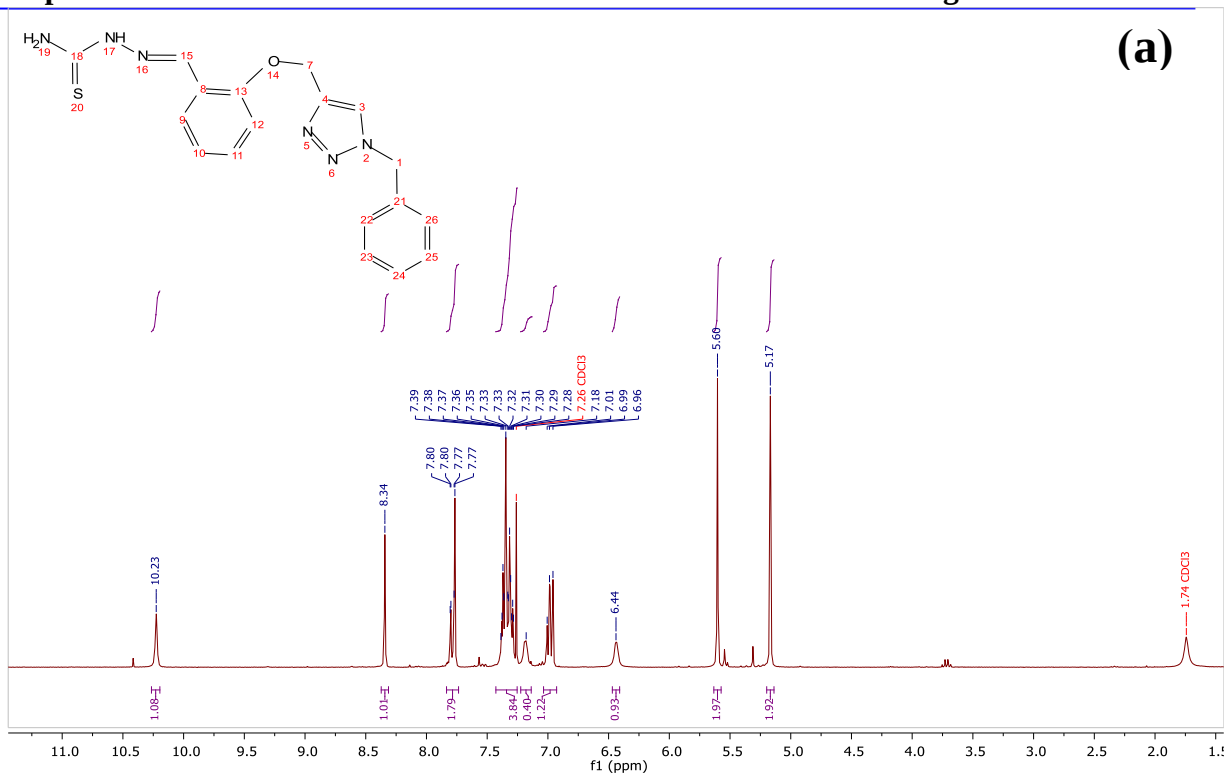


**1H NMR (300 MHz, Chloroform-*d*) δ 10.23 (s, 1H), 8.34 (s, 1H), 7.81 – 7.75 (m, 2H), 7.33 (dtt, 6H), 7.19 (d, 1H), 6.98 (dd, 2H), 6.44 (s, 1H), 5.60 (s, 2H), 5.17 (s, 2H).**

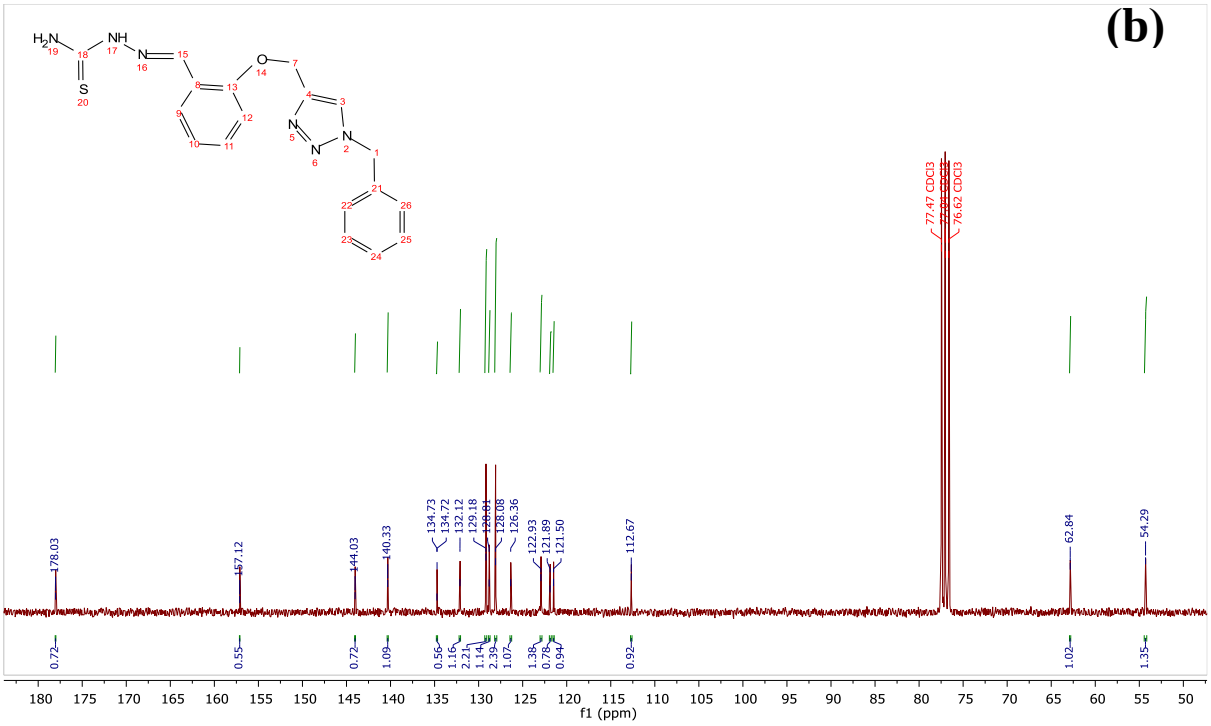


**13C NMR (75 MHz, $CDCl_3$) δ** 178.02, 157.12, 144.03, 140.33, 134.73, 132.12, 129.178, 128.801, 128.08, 126.36, 122.93, 121.89, 121.50, 112.67, 62.84, 54.291494.

**Figure II.36. (a)** $^{1}$H NMR spectra and **(b)** $^{13}$C NMR Spectra of compound **8e**

A proposed mechanism has been outlined to further elucidate the step-by-step transformation involved in the reaction. This mechanism highlights the key intermediates and transition states, offering a deeper understanding of the pathways leading to the formation of the final product.

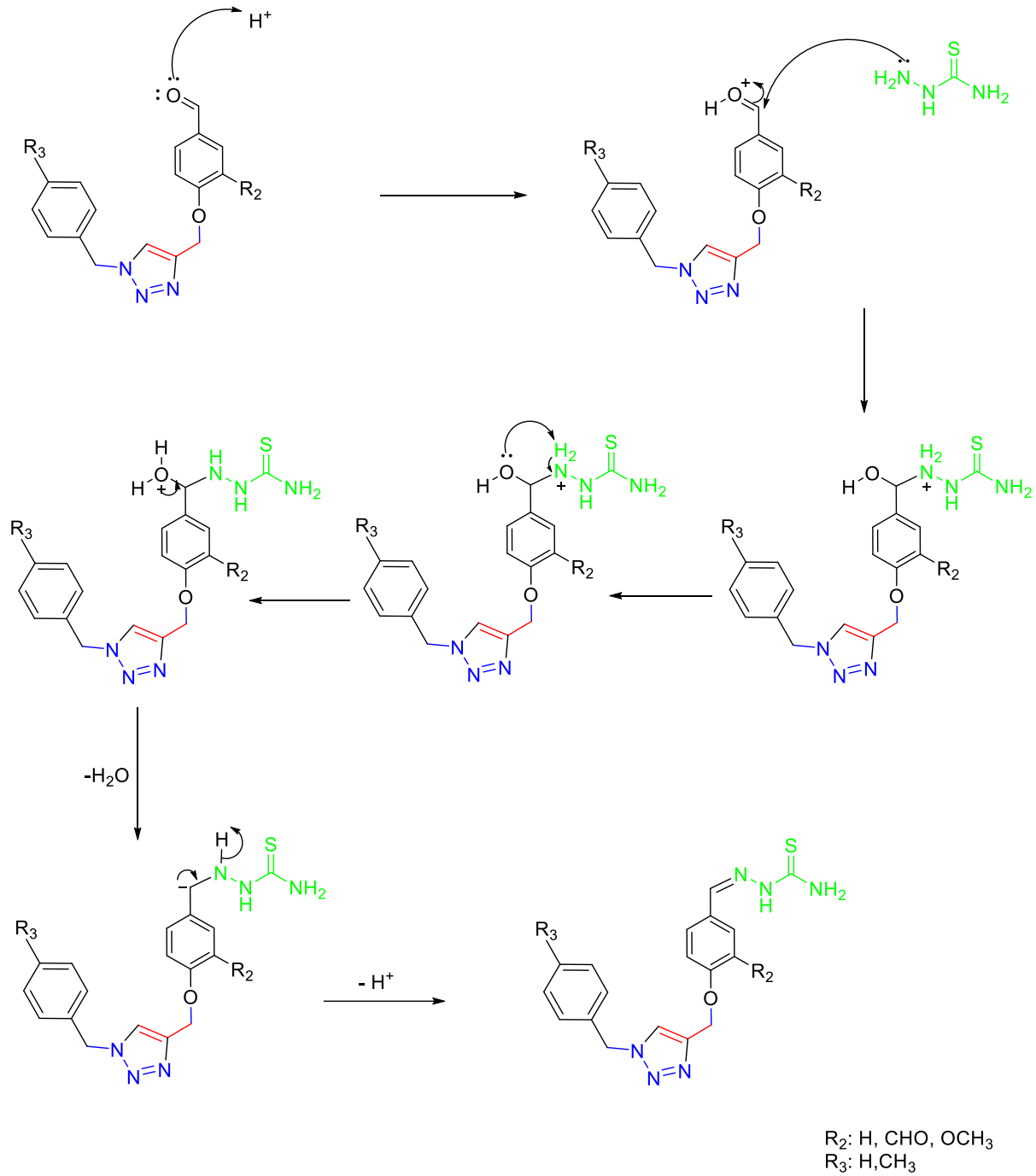


**Figure II.37.** Proposed mechanism for the reparation of thiosemicarbazones

## II. Preparation of thiazole derivatives

### II.1. Synthesis

Thiosemicarbazone derivative (1.0 mmol) was reacted with chloro acetone (1.0 mmol) in ethanol. For two to three hours at 80°C the reaction mixture was refluxed, TLC was utilized to monitor its progress. Filtration of the resulting precipitate and it was recrystallized from ethanol,

yielding the final products in good yields. The resulting thiozoles were pure and did not require further purification [54].

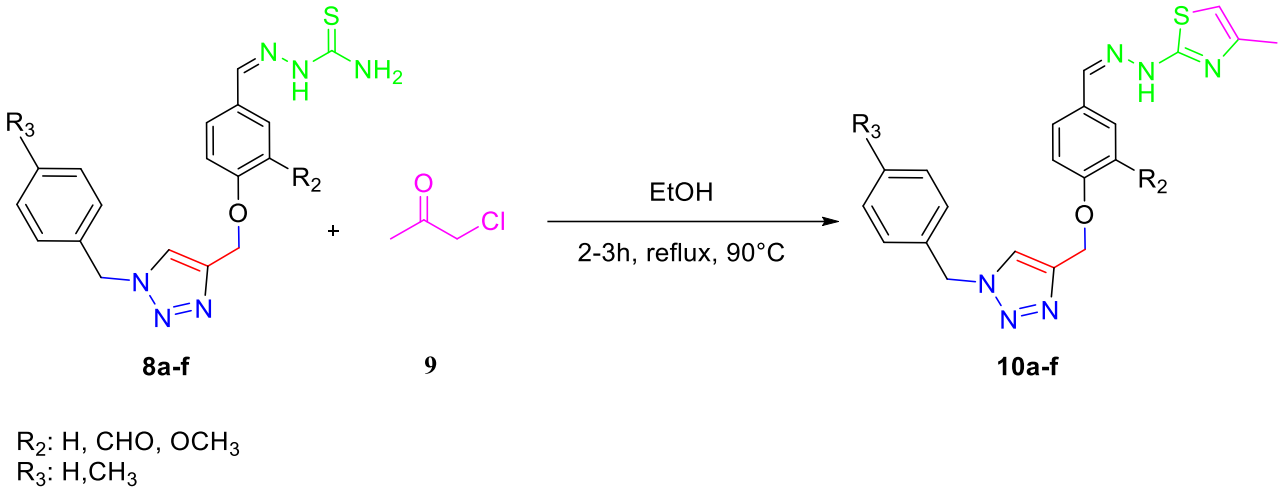


**Figure II.38.** Preparation of thiazoles

**Table II.2.** Structural and physicochemical characteristics of thiazole derivatives **10a-f**

| Ref | Thiazole derivatives | Yield % | Melting points (°C) | FTIR ($cm^{-1}$) | $^1H$ NMR (δ:ppm) | |
|---|---|---|---|---|---|---|
| | | | | N-H | CH(triazole) | CH(thiazole) |
| **10a** | 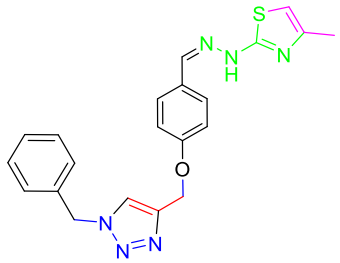 | 86 | 146-148 | 3142 | 7.23-7.25 | 5.67 |
| **10c** | 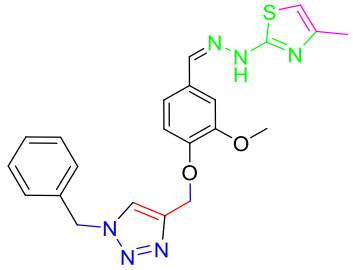 | 21 | 95-97 | 3373 | 7.38 | 6.35 |
| **10d** | 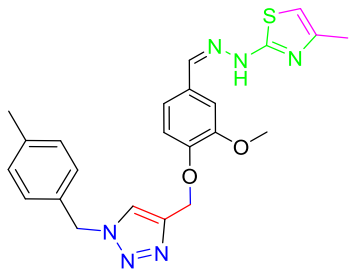 | 49 | 132-134 | 3383 | 7.37 | 6.59 |
| **10e** | 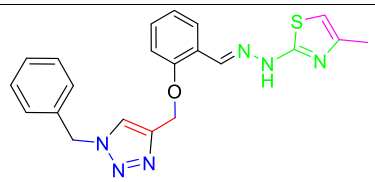 | 57 | 154-156 | 3343 | 7.38 | 6.36 |
| **10f** | 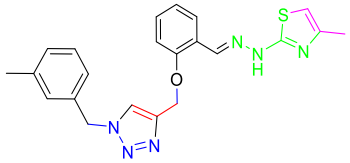 | 40 | 164-166 | 3338 | 7.90 | 6.98 |

## II.2. Characterization

The structures of the thiazole derivatives **10a-f** were determined using standard spectroscopic techniques (IR, $^{13}C$ NMR, and $^{1}H$ NMR). The thiazole derivatives' FT-IR spectra presents at 3380 $cm^{-1}$ a broad peak likely corresponds to N-H stretching, indicating the presence of the amine group (NH) in the structure. At 2922 $cm^{-1}$ the peak suggests stretching vibration of C-H, typically from aliphatic or aromatic C-H bonds. The C=N stretching from the imine (CH=N) group appears at 1603 $cm^{-1}$. At 1500 $cm^{-1}$, there is likely the aromatic rings C=C stretching. C-O stretching from the ether linkage ($CH_2$-O) in the molecule appears between 1100 to 1265 $cm^{-1}$ may corresponds to. These peaks align well with the expected functional groups in the synthesized compounds.

In the compound's **10c** $^{1}H$ NMR spectrum, the following signals are observed:

- The singlet at δ 8.27 ppm ,with 1H, assigned to the **CH=N** proton **He** (imine).
- The singlet at δ 7.93 ppm with 1 proton , corresponding to the **NH** proton
- δ 7.38 ppm (d, 1H), likely corresponding to the to the proton of the triazole ring **Hd** (**CH-N**).
- Aromatic protons, such as those from the phenyl ring, appear in the ranges δ 7.36-7.37 ppm (m,1H), δ7.34-7.35 (m, 1H), δ 7.32-7.33 (m,2H) and δ7.30-7.31 (m, 1H).
- δ 7.24-7.25 ppm (d, 1H) is assigned to the proton **Hb**.
- δ 7.16 ppm (s, 1H) is assigned to the proton **Ha**.
- δ 7.14 ppm (d, 1H) is assigned to the proton **Hc**.
- At δ 6.35 ppm singlet with 1H is assigned to the proton **Hf**, CH proton of the thiazole ring.
- Peaks at δ 5.61 (s, 2H) and δ 5.15 (s, 2H) are attributed to methylene protons, corresponding to **$CH_2$-Ar** and **$CH_2$-O**, respectively.
- A singlet at δ 3.77 ppm (s, 3H) is corresponds to a methoxy group **O-$CH_3$**, and methyl group **$CH_3$** on the thiazole ring appears at δ 2.16 ppm (s, 3H).

The obtained structure is:

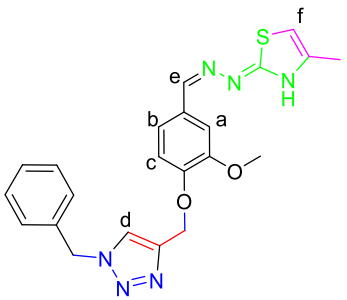

The $^{1}$H NMR spectra of compound **10c** shows that we initially had the suggested structure, but it seems there was a structural rearrangement because the spectrum shows the **NH** pic as a singlet at δ 7.93 ppm.

A singlet showed up at 2.24 ppm in the product's **10d** $^{1}$H NMR spectrum, corresponding to a typical non-aromatic methyl (**$CH_3$**) group.

In the $^{13}$C NMR spectrum of compound **10c**, the observed chemical shifts are as follows:

A peak at 149.80 ppm likely corresponds to the imine group **$C_3$** (**C=N**), while the peak at 149.05 ppm is likely assigned to the carbon **$C_2$** in the thiazole ring (**C=N**). Peak around 143.26 ppm suggest quaternary carbon in the triazole ring and the peak around 120.38 ppm suggest carbon (**HC-N**) in the triazole ring.

The signal at 136.48 ppm could be attributed to the aromatic quaternary carbon **$C_4$** of the aromatic ring (**C-C=N**). while two equivalent carbons (**Cb**) are represented by the shift at 129.25 ppm. Likewise, another pair of comparable carbons (**Ca**) in the aromatic ring is represented by the shift at 128.44 ppm. Furthermore, the signal at 125.36 ppm is attributed to the carbon **$C_1$** in thiazole ring (**HC-S**).

The peak at 62.22 ppm is consistent with the **$CH_2$-O** carbon. Additionally, the peak at 55.82 ppm likely represents the **$CH_2$-Ar** carbon and the signal at 53.31 ppm matches the methoxy group (**O-$CH_3$**).

Some of the peaks in the spectrum were not visible because of their small size, suggesting that the product has low solubility. Furthermore, the peaks are frequently weak in the $^{13}$C NMR spectrum because carbon-13 makes up just around 1% of the carbon in nature.

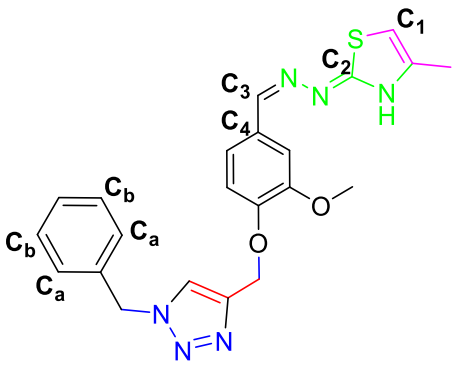


Product **10d**'s 13C NMR spectra reveals an extra peak at 21.16 ppm, corresponding to a $CH_3$ group attached to the phenyl ring.

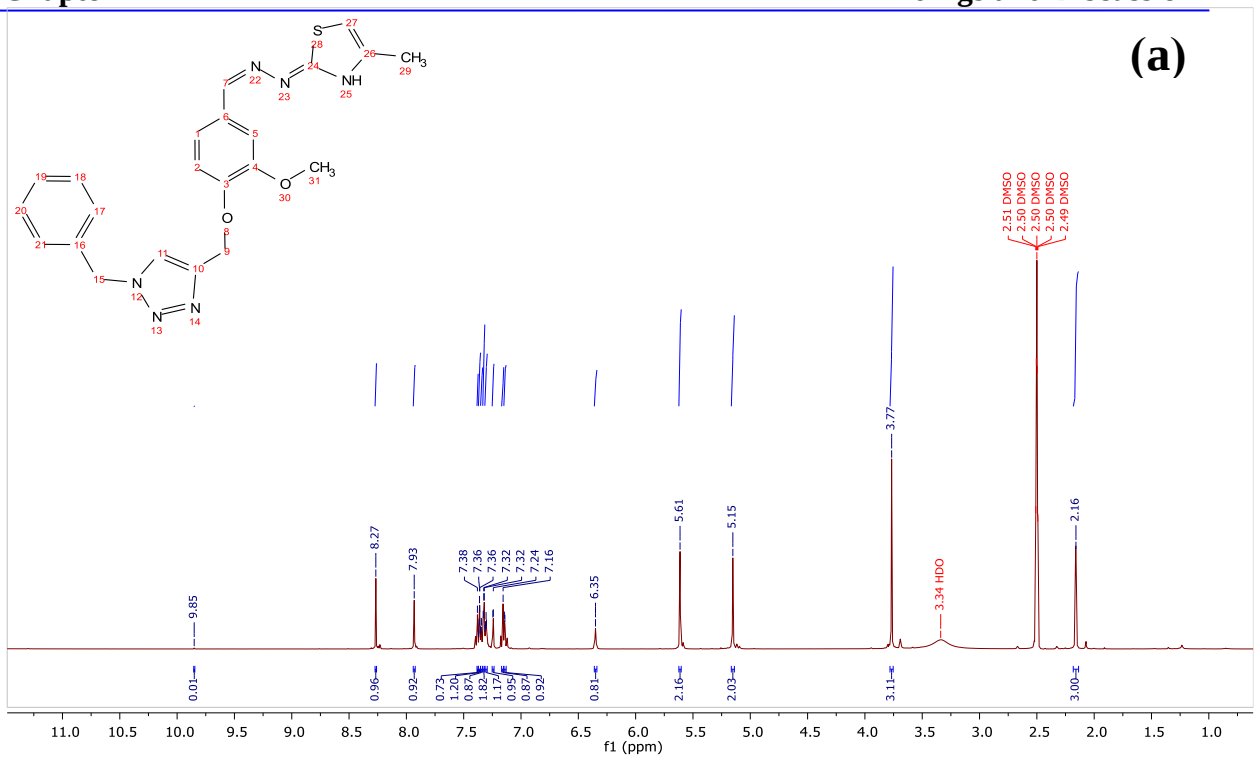


**1H NMR (400 MHz, DMSO-$d_6$) δ** 8.27 (s, 1H), 7.93 (s, 1H), 7.38 (s, 1H), 7.37 – 7.36 (m, 1H), 7.35 – 7.34 (m, 1H), 7.33 – 7.32 (m, 2H), 7. – 7.30 (m, 1H), 7.24-7.25 (d, 1H), 7.16 (s, 1H), 7.14 (d, 1H), 6.35 (s, 1H), 5.61 (s, 2H), 5.15 (s, 2H), 3.77 (s, 3H), 2.16 (s, 3H).

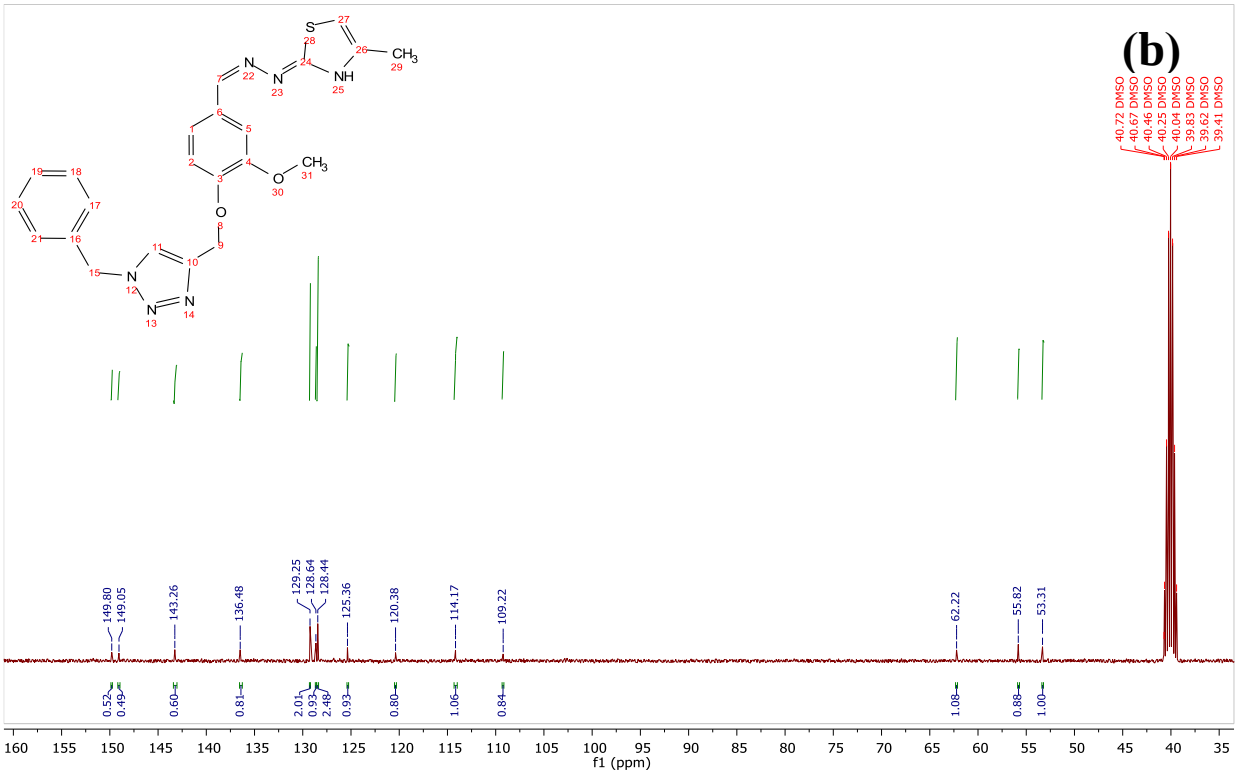


**13C NMR (101 MHz, DMSO) δ** 149.80, 149.05, 143.26, 136.48, 129.25, 128.64, 128.44, 125.36, 120.38, 114.17, 109.22, 62.22, 55.82, 53.31.

**Figure II.39.** Compound **10c**'s **(a)** 1H and **(b)** 13C NMR spectra.

A proposed mechanism has been outlined to further understand the final product's leading

pathways.

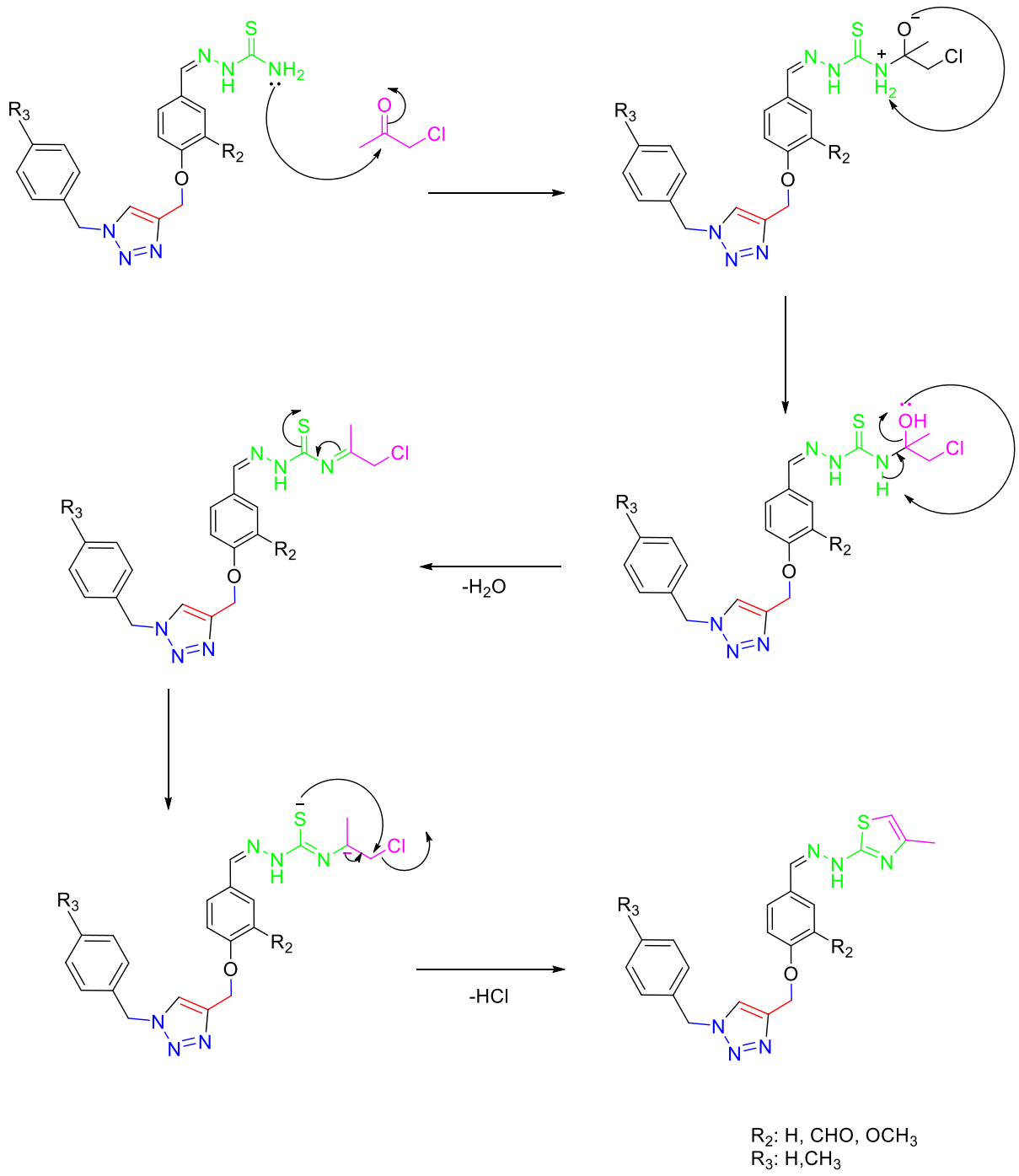


**Figure II.40.** Mechanism for the preparation of Thiazoles

## Conclusion

In this chapter, we successfully synthesized thiazole derivatives from thiosemicarbazone precursors achieving moderate to good yields, which, to our knowledge, had never been described before. The spectroscopic data strongly supported the formation of the thiazole ring and highlighted key functional groups and chemical shifts corresponding to the expected structure. These compounds were subjected to various *in vitro* antioxidant tests, the results of which will be presented in the third chapter.

**References**


[1] E. A. Nyawade, M. O. Onani, S. Meyer, and P. Dube, "Synthesis, characterization and antibacterial activity studies of new 2-pyrral-L-amino acid Schiff base palladium (II) complexes," *Chemical Papers,* vol. 74, pp. 3705-3715, 2020.

[2] M. Khalid *et al.*, "An efficient synthesis, spectroscopic characterization, and optical nonlinearity response of novel salicylaldehyde thiosemicarbazone derivatives," *ACS omega,* vol. 6, no. 24, pp. 16058-16065, 2021.

[3] B. Sever, G. Akalın Çiftçi, A. Özdemir, and M. Altıntop, "Design, synthesis and in vitro evaluation of new thiosemicarbazone derivatives as potential anticancer agents," *Journal of Research in Pharmacy,* vol. 23, no. 1, 2019.

[4] E. J. Siddiqui, I. Azad, A. R. Khan, and T. Khan, "Thiosemicarbazone complexes as versatile medicinal chemistry agents: a review," *Journal of drug delivery and therapeutics,* vol. 9, no. 3, pp. 689-703, 2019.

[5] M. Asif and S. Alghamdi, "Chemical and Biological potentials of semicarbazide and thiosemicarbazide derivatives and their metals complexes," *Advanced Journal of Chemistry, Section B,* vol. 3, no. 3, pp. 243-270, 2021.

[6] B. Shakya and P. N. Yadav, "Thiosemicarbazones as potent anticancer agents and their modes of action," *Mini Reviews in Medicinal Chemistry,* vol. 20, no. 8, pp. 638-661, 2020.

[7] R. H. Dhabale, S. Shah, N. Tiwari, and P. Patani, "Review of Semicarbazone, Thiosemicarbazone, and their transition metal complexes, and their biological activities," *Journal of Pharmaceutical Negative Results,* pp. 2416-2424, 2022.

[8] O. Aygun, A. M. Grześkiewicz, C. N. Banti, S. K. Hadjikakou, M. Kubicki, and I. I. Ozturk, "Monomeric octahedral bismuth (III) benzaldehyde-N1-alkyl thiosemicarbazones: Synthesis, characterization and biological properties," *Polyhedron,* vol. 215, p. 115683, 2022.

[9] F. Muleta, T. Alansi, and R. Eswaramoorthy, "A review on synthesis characterization methods and biological activities of semicarbazone thiosemi-carbazone and their transition metal complexes," *J Nat Sci Res,* vol. 9, pp. 33-46, 2019.

[10] S. Gupta, N. Singh, T. Khan, and S. Joshi, "Results in Chemistry."

[11] F. Kanso, A. Khalil, H. Noureddine, and Y. El-Makhour, "Therapeutic perspective of thiosemicarbazones derivatives in inflammatory pathologies: A summary of in vitro/in vivo studies," *International Immunopharmacology,* vol. 96, p. 107778, 2021.

[12] M. R. Souza *et al.*, "Synthesis of novel (-)-Camphene-based thiosemicarbazones and evaluation of anti-Mycobacterium tuberculosis activity," *Natural product research,* vol. 33, no. 23, pp. 3372-3377, 2019.

[13] Z. Bakherad *et al.*, "Design and Synthesis of Novel Cytotoxic Indole-Thiosemicarbazone Derivatives: Biological Evaluation and Docking Study," *Chemistry & Biodiversity,* vol. 16, no. 4, p. e1800470, 2019.

[14] R. Rusnac, A. Rusnac, O. Garbuz, and A. Gulea, "Synthesis and structure of copper (II) coordination compounds with 4-N-substitute-thiosemicarbazone of 4-benzoil-5-methyl-2-phenyl-2, 4-dihidro-3H-pyrazol-3-one. Antioxidant, antimicrobial and antitumor properties," *Economy Transdisciplinarity Cognition,* vol. 22, no. 2, pp. 5-14, 2019.

[15] A. Kumar, R. Mishra, R. Mazumder, and A. Mazumder, "Design, Synthesis, Characterization, and Anti-Cancer Activity Evaluation of Novel Thiosemicarbazide Analogs," *Indian Journal of Pharmaceutical Education & Research,* vol. 57, no. 1, 2023.

[16] R. Matsa, P. Makam, M. Kaushik, S. Hoti, and T. Kannan, "Thiosemicarbazone derivatives: Design, synthesis and in vitro antimalarial activity studies," *European Journal of Pharmaceutical Sciences,* vol. 137, p. 104986, 2019.

[17] B. Z. Sibuh *et al.*, "Synthesis, in silico study, and anti-cancer activity of thiosemicarbazone derivatives," *Biomedicines,* vol. 9, no. 10, p. 1375, 2021.

[18] R. B. de Oliveira, E. M. de Souza-Fagundes, R. P. Soares, A. A. Andrade, A. U. Krettli, and C. L. Zani, "Synthesis and antimalarial activity of semicarbazone and thiosemicarbazone derivatives," *European journal of medicinal chemistry,* vol. 43, no. 9, pp. 1983-1988, 2008.

[19] M. K. Panchangam, "Synthesis, structural characterization and DNA studies of trivalent cobalt complexes of (2E)-4N-substituted-2-[4-(propan-2-yl) benzylidene] hydrazinecarbothioamide," *Mediterranean Journal of Chemistry,* vol. 6, no. 3, pp. 88-97, 2017.

[20] L. V. Gavali *et al.*, "Novel terephthalaldehyde bis (thiosemicarbazone) Schiff base ligand and its transition metal complexes as antibacterial Agents: Synthesis, characterization and biological investigations," *Results in Chemistry,* vol. 7, p. 101316, 2024.

[21] N. H. S. O. Ali *et al.*, "Efficient eco-friendly syntheses of dithiocarbazates and thiosemicarbazones," *Green Chemistry Letters and Reviews,* vol. 13, no. 2, pp. 129-140, 2020.

[22] A. Petrou, M. Fesatidou, and A. Geronikaki, "Thiazole ring—A biologically active scaffold," *Molecules,* vol. 26, no. 11, p. 3166, 2021.

[23] X. Bai, D. Qin, and L. Yang, "Importance of substituents in ring opening: a DFT study on a model reaction of thiazole to thioamide," *Journal of Molecular Modeling,* vol. 27, pp. 1-10, 2021.

[24] I. H. A. Ripain and N. Ngah, "A brief review on the thiazole derivatives: Synthesis methods and biological activities," *Malays. J. Anal. Sci,* vol. 25, pp. 257-267, 2021.

[25] C. K. Jaladanki, S. Khatun, H. Gohlke, and P. V. Bharatam, "Reactive metabolites from thiazole-containing drugs: Quantum chemical insights into biotransformation and toxicity," *Chemical research in toxicology,* vol. 34, no. 6, pp. 1503-1517, 2021.

[26] Z.-X. Niu *et al.*, "Application and synthesis of thiazole ring in clinically approved drugs," *European Journal of Medicinal Chemistry,* vol. 250, p. 115172, 2023.

[27] P. C. Sharma, K. K. Bansal, A. Sharma, D. Sharma, and A. Deep, "Thiazole-containing compounds as therapeutic targets for cancer therapy," *European journal of medicinal chemistry,* vol. 188, p. 112016, 2020.

[28] A.-M. Borcea, I. Ionuț, O. Crișan, and O. Oniga, "An overview of the synthesis and antimicrobial, antiprotozoal, and antitumor activity of thiazole and bisthiazole derivatives," *Molecules,* vol. 26, no. 3, p. 624, 2021.

[29] S. J. Patil, S. Sadashiv, and B. Nandeshwarappa, "Promising Medicinal Chemistry of Thiazole, their Derivatives, Biological Significance," *Advances in Chemical Biology-An Insight to New Applications and Developments Volume–1,* p. 34, 2023.

[30] C. B. Mishra, S. Kumari, and M. Tiwari, "Thiazole: A promising heterocycle for the development of potent CNS active agents," *European journal of medicinal chemistry,* vol. 92, pp. 1-34, 2015.

[31] A. P. Shukla and V. Verma, "A Systematic Review On Thiazole Synthesis And Biological Activities," *Educational Administration: Theory and Practice,* vol. 30, no. 5, pp. 4444-4457, 2024.

[32] V. M. Bangade, P. R. Mali, and H. M. Meshram, "Synthesis of potent anticancer substituted 5-Benzimidazol-2-amino Thiazoles controlled by Bifunctional Hydrogen Bonding under Microwave irradiations," *The Journal of Organic Chemistry,* vol. 86, no. 9, pp. 6056-6065, 2021.

[33] A. Avadhani, P. Iniyavan, Y. Kumar, and H. Ila, "Single-pot preparation of 4-amino-2-(het) aryl-5-substituted thiazoles employing functionalized dithioesters as thiocarbonyl precursors," *The Journal of Organic Chemistry,* vol. 86, no. 12, pp. 8508-8515, 2021.

[34] X. Huang *et al.*, "Visible light-induced difunctionalization of alkynes: the synthesis of thiazoles and 1, 1-dibromo-1-en-3-ynes," *The Journal of Organic Chemistry,* vol. 84, no. 23, pp. 15283-15293, 2019.

[35] S. M. Gomha *et al.*, "Thiazole-based thiosemicarbazones: Synthesis, cytotoxicity evaluation and molecular docking study," *Drug design, development and therapy*, pp. 659-677, 2021.

[36] D. Sharma *et al.*, "Green chemistry approaches for thiazole containing compounds as a potential scaffold for cancer therapy," *Sustainable Chemistry and Pharmacy*, vol. 23, p. 100496, 2021.

[37] S. Mamidala, V. S. Mudigunda, S. R. Peddi, K. K. Bokara, V. Manga, and R. R. Vedula, "Design and synthesis of new thiazoles by microwave-assisted method: evaluation as an anti-breast cancer agents and molecular docking studies," *Synthetic Communications*, vol. 50, no. 16, pp. 2488-2501, 2020.

[38] M. Singh, V. B. Yadav, M. D. Ansari, M. Malviya, and I. Siddiqui, "Efficient one-pot synthesis of substituted diphenyl 1, 3-thiazole through multicomponent reaction by using green and efficient Iron-catalyst via Cross-Dehydrogenative Coupling (CDC)," *Molecular Diversity*, pp. 1-6, 2022.

[39] H. Bouherrou *et al.*, "Synthesis and biological evaluation of new substituted hantzsch thiazole derivatives from environmentally benign one-pot synthesis using silica supported tungstosilisic acid as reusable catalyst," *Molecules*, vol. 22, no. 5, p. 757, 2017.

[40] A. H. Bashal, S. M. Riyadh, W. Alharbi, K. H. Alharbi, T. A. Farghaly, and K. D. Khalil, "Bio-based (Chitosan-ZnO) nanocomposite: Synthesis, characterization, and its use as recyclable, ecofriendly biocatalyst for synthesis of thiazoles tethered Azo groups," *Polymers*, vol. 14, no. 3, p. 386, 2022.

[41] S. Khan *et al.*, "Synthesis, DFT Studies, molecular docking and biological activity evaluation of thiazole-sulfonamide derivatives as potent Alzheimer's inhibitors," *Molecules*, vol. 28, no. 2, p. 559, 2023.

[42] S. Hosseininezhad and A. Ramazani, "Thiazole Ring-The Antimicrobial, Anti-Inflammatory, and Anticancer Active Scaffold," *Arabian Journal of Chemistry*, p. 105234, 2023.

[43] A. R. Sayed *et al.*, "One-pot synthesis of novel thiazoles as potential anti-cancer agents," *Drug design, development and therapy*, pp. 1363-1375, 2020.

[44] R. Meleddu *et al.*, "(3Z)-3-(2-[4-(aryl)-1, 3-thiazol-2-yl] hydrazin-1-ylidene)-2, 3-dihydro-1H-indol-2-one derivatives as dual inhibitors of HIV-1 reverse transcriptase," *European journal of medicinal chemistry*, vol. 93, pp. 452-460, 2015.

[45] D. Kemisetti *et al.*, "Novel Benzothiazole Derivatives Synthesis and its Analysis as Diuretic Agents," *Evidence-Based Complementary and Alternative Medicine*, vol. 2023, 2023.

[46] A. Biernasiuk *et al.*, "The newly synthesized thiazole derivatives as potential antifungal compounds against Candida albicans," *Applied Microbiology and Biotechnology*, vol. 105, no. 16, pp. 6355-6367, 2021.

[47] M. Modrić, M. Božičević, I. Faraho, M. Bosnar, and I. Škorić, "Design, synthesis and biological evaluation of new 1, 3-thiazole derivatives as potential anti-inflammatory agents," *Journal of molecular structure*, vol. 1239, p. 130526, 2021.

[48] T. S. Fandi Al-Mathkuri, A. B. Sabti, and A. A. Raheem, "Synthesis, characterization, and antimicrobial activity of some thiazole derivatives," *Egyptian Journal of Chemistry*, vol. 65, no. 6, pp. 293-303, 2022.

[49] A. M. Hussein *et al.*, "Synthesis, in vitro antioxidant, anticancer activity and molecular docking of new thiazole derivatives," *Results in Chemistry*, vol. 7, p. 101508, 2024.

[50] P. de Sena Murteira Pinheiro, L. S. Franco, T. L. Montagnoli, and C. A. M. Fraga, "Molecular hybridization: a powerful tool for multitarget drug discovery," *Expert Opinion on Drug Discovery*, vol. 19, no. 4, pp. 451-470, 2024.

[51] H. M. S. Kumar, L. Herrmann, and S. B. Tsogoeva, "Structural hybridization as a facile approach to new drug candidates," *Bioorganic & Medicinal Chemistry Letters*, vol. 30, no. 23, p. 127514, 2020.

[52] M. A. Shareef *et al.*, "Synthesis of new triazole fused imidazo [2, 1-b] thiazole hybrids with emphasis on Staphylococcus aureus virulence factors," *Bioorganic & Medicinal Chemistry Letters*, vol. 29, no. 19, p. 126621, 2019.

[53] H. Abdelbaki, A. Djemoui, M.R. Ouahrani, M. Messaoudi, I.B. Amor, H. Alsaeedi, D. Croun, M. Bechelany, A. Barhoum, Synthesis of Bioactive 1, 4-Disubstituted 1, 2, 3-Triazole-Linked Thiosemicarbazone Derivatives using Cu2O Microbeads Catalysis for Enhanced Antibacterial and Antioxidant Activities, Journal of Molecular Structure, (2024) 140784.

[54] H. Abdelbaki, A. Djemoui, A. Benarfa, S. Lahcene, A. Souadia, M. Messaoudi, M.R. Ouahrani, Preparation of Bioactive Thiazole Derivatives using 1, 2, 3-triazole-linked Thiosemicarbazone Derivatives and their Antioxidant Activities, Tuijin Jishu/Journal of Propulsion Technology, 45 2024.

# Chapter III

# Exploring Antioxidant Properties

## Introduction

Identifying synthetic molecules with desired pharmacological qualities, such as antibacterial and antioxidant capabilities, is crucial for discovering novel therapeutic agents [1].Among these, the thiazole ring stands out due to its unique structural characteristics. The sulfur and nitrogen atoms within the thiazole ring are arranged such that the pi (π) electrons can freely transition between bonds, giving the ring its aromatic properties[2].

Another noteworthy scaffold in medicinal chemistry is the 1,2,3-triazole ring. This ring's distinctive structural features, synthetic adaptability, and pharmacological potential make it a valuable asset in the field. Click chemistry makes the 1,2,3-triazole ring easily accessible, allowing for the construction of chemical collections aimed at various ailments[3].

Given these promising attributes, this chapter focuses on evaluating the biological activities of our synthetic products, particularly their antibacterial and antioxidant properties.

## I. Antioxidant activity evaluation

### I.1.Oxidation

Oxidation occurs when an electron or atom of hydrogen is moved from a material to an oxidant. Oxidative processes produces free radicals that have the ability to start chain reactions, which, when they take place inside of cells, can cause damage or even death [4].

### I.2.Oxidative stress

In the last thirty years, in the medical sciences, the oxidative stress concept has garnered a lot of attention. It actively contributes to the physiology of numerous prevalent illnesses, (including diabetes, acute renal failure …etc). Potentially as a result of the cells' metabolism of oxygen hazardous reactive oxygen species (ROS) are produced. In typical conditions, the rate at which oxidants are removed balances the rate at which they are formed, both in terms of amplitude and rate. On the other hand, oxidative stress arises from an imbalance between antioxidants and pro-oxidants. Their functionality is significantly affected by elevated reactive oxygen species (ROS) levels in biological cells, resulting in impaired cell function, aging, or illness [5].

### I.3. Free radicals

Free radicals are described as molecules or their constituent parts that are able to exist on their own. Because one or more of their unpaired electrons reside in an outer atomic or

molecular orbital, they are referred to as "radical". A free radical is highly reactive, unstable, and has an odd number of electrons. It is a characteristic that causes chain reactions. In an effort to form a stable complex, free radicals try to form bonds with other atoms, single electrons, or even molecules, by either receiving or giving an electron from other molecules, they function as reducing or oxidizing agents [6].

Free radicals are Reactive oxygen species produced as byproducts of several bodily activities and are always present in the body. Antioxidant processes eliminate them from the body under normal circumstances. When these defense systems are compromised, radicals build up excessively and play a role in the onset of numerous illnesses [7].

### I.4. Antioxydant

Antioxidant is a molecule that inhibits, stops, or controls a substrate's oxidation (oxidizable substrate). It could be an inorganic or organic substance. But the definition of an antioxidant changed depending on its applications. The substrate from *in vitro* or *in vivo* systems need to be oxidized. Still, *in vitro* research was the first to explain the mechanisms and idea of antioxidants[8]. Antioxidants have the function of reducing free radicals within biological cells.

#### I.4.1. Mechanism of Action

##### I.4.1.1. Electron Donation

Antioxidants typically act as reducing agents because they undergo oxidation, allowing them to neutralize free radicals by donating electrons, thereby removing the unpaired state of free radicals and slowing down the oxidation process [9].

##### I.4.1.2. Metal Ion Chelation

Some antioxidants have the ability to chelate to copper and iron metal ions , which can catalyze redox processes that result in the creation of free radicals [10].

##### I.4.1.3. Radical Scavenging

The main way that antioxidants scavenge free radicals is by giving them electrons or hydrogen. According to this method, an antioxidant directly interacts with a free radical, giving them hydrogen in exchange for the free radical's free electron. Then, a complex between, let's say, the antioxidant radical (free radical acceptor) and the radical forms. Antioxidants oxidize as a result, and free radicals are neutralized [11].

#### I.4.2. Types of Antioxidants

To counteract the damaging effects of free radicals, cells utilize a variety of **Endogenous**

(enzymatic )and **Exogenous** (nonenzymatic) antioxidant defense mechanisms to preserve a pro-antioxidant equilibrium [12].

### I.4.2.1.Endogenous Antioxidants

Are vital antioxidants that the body produces, and they include enzymes like superoxide dismutase (SOD), catalase (CAT), and glutathione peroxidase (GPX) [13].

### I.4.2.2.Exogenous Antioxidants

These are derived from food diet and encompass vitamins. As part of non-enzymatic defenses, substances like vitamin E, carotenoids, polyphenols, glutathione (GSH), and vitamin C are included[13].

## I.5. Methods used to evaluate the antioxidant activity

The most commonly used assays to evaluate antioxidant activity include the free radical scavenging assay using 2,2′-azinobis(3-ethylbenzothiazoline-6-sulfonate) (ABTS) and the diphenylpicrylhydrazyl (DPPH) assay.

### I.5.1.DPPH assay

The DPPH antioxidant assay is suitable for evaluating the capacity of functional foods to counteract radicals, such as synthetic components, herbal extracts and or pure natural. This is due to the DPPH radical's stability, ease of use in experiments, and cost-effectiveness. In this method, antioxidants (AH) are added to a DPPH solution. During the reaction, an antioxidant molecule donates a hydrogen atom to the nitrogen atom of the DPPH radical, reducing it to form DPPH-H hydrazine. spectrophotometric measurements can quantify the extent of DPPH radical quenching , Typically, the absorbance decrease is measured between 515 and 520 nm.. The concentration needed to reduce the initial DPPH radical concentration by 50% is used to express a substance's antioxidant capacity [14].

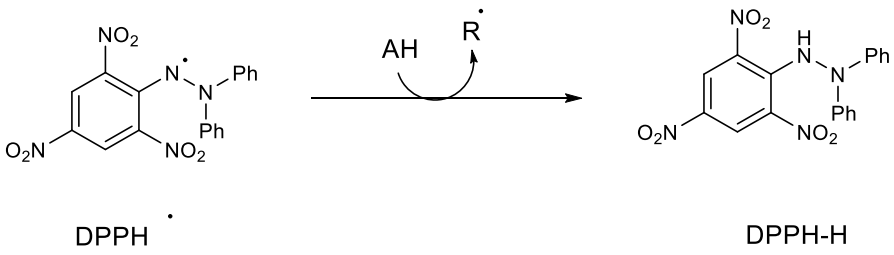


**Figure III.1.** DPPH structure getting reduced by an antioxidant (AH)

This commonly used test is easy to set up and can be modified for high-throughput assessments. The methodology established by Brand-Williams and his team (1995) was used to evaluate the DPPH radical scavenging. A 1 mL volume of different concentrations of the tested substances (1, 5, 10, 50, 100, 200, 300, 400 and 500 µg/mL) in methanol was combined with 2two milliliters of a DPPH solution in methanol at a concentration of 0.004% (w/v). For 30 minutes the mixture was incubated in the dark at room temperature, during which hydrogen transfer reaction from the antioxidant to DPPH• was tracked using UV-visible spectroscopy by measuring the reduction in absorption at 517 nm.

This formula was used to determine the free radical percentage of inhibition (I %) of production from DPPH:

$$\% \text{ DPPH scavenging} = \frac{\text{A control} - \text{A sample}}{\text{A control}} 100$$

Here, the control reaction's absorbance (just the DPPH solution) is $A_{control}$, while the absorbance of the tested compound is $A_{sample}$. Additionally, a calibration curve for vitamin C was created to correlate different concentrations with their I %.

### I.5.2.ABTS assay

The ABTS assay relies on a decolorization reaction where a stable radical of ABTS (2,2'-azino-bis(3-ethylbenzothiazoline-6-sulfonic acid)) is produced prior to interacting with an antioxidant . This method is advantageous because it provides reliable results for both fat-soluble and water-soluble antioxidants , as well as for pure compounds, mixtures, and plant extracts. Additionally, it maintains stability across a broad pH range and is characterized by its speed, cost-effectiveness, and sensitivity [15]. The compound's total antioxidant activity in the ABTS assay is determined by the spectrophotometric approach.

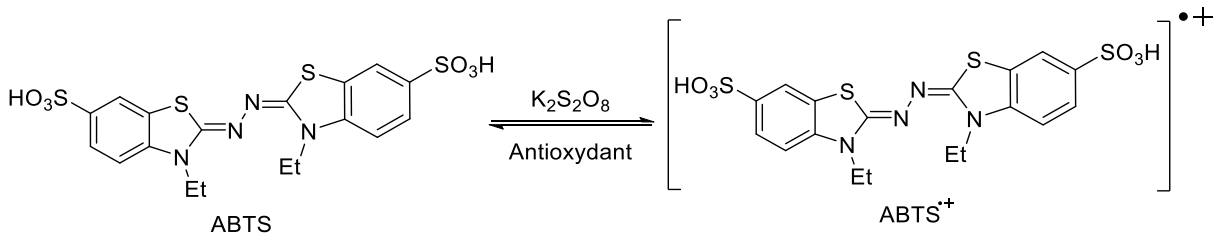


**Figure III.2.** $ABTS^{\bullet+}$ radical structure

A 2.4 mM solution of potassium persulfate is mixed with a 7 mM solution of ABTS in water. The two stock solutions are combined in proportionately and let it react in the dark at room temperature for 12 hours to generate the $ABTS^{\bullet+}$ radical cation. Before use, the solution is diluted to obtain an absorbance at 740 nm that equals 0.700 ± 0.005. For the evaluation, 10 μL of the solutions different concentrations of the compounds to be tested is mixed with 990 μL of the diluted $ABTS^{\bullet+}$ radical solution. After 7 minutes, using a spectrophotometer at 734 nm the absorbance is measured. The percentage reduction of the $ABTS^{\bullet+}$ radical is calculated using the following formula:

$$\% \text{ ABTS scavenging} = \frac{\text{A control} - \text{A sample}}{\text{A control}} 100$$

Where, the absorbance of the control reaction is $A_{control}$, while the absorbance of the tested compound is $A_{sample}$.

The $IC_{50}$ value, which translates to the antioxidant's amount needed to reduce 50% of the starting concentration of $ABTS^{\bullet+}$ radical cation, is used to express the results the assay of ABTS. The compounds' chemical structures, including the degree of esterification, their relative positions within the aromatic ring and the quantity of hydroxyl groups, has a significant impact on their antioxidant qualities [14].

## II. Findings and discussion

The products tested for their antioxidant activity are the synthesized 1,2,3-triazole, thiosemicarbazone and thiazole derivatives. The assays for DPPH and ABTS radical scavenging were systematically carried out at least twice for each compound. The collected results provided insights into the structure-activity relationship of our compounds in this tests.

### II.1. Antioxidant activity of 1,2,3-triazole derivatives

The 1,2,3-triazole derivatives were initially prepared as a stock solution with a concentration of 1 mg/mL. From there, a variety of dilutions were made. Each curve's linear regression equation is found, and the concentration that corresponds to 50% inhibition is computed to get the $IC_{50}$.

**Table III.1.** the *in vitro* antioxidant activity of the compounds **6a-f** using DPPH• free radical assay, with ascorbic acid as standard

| | **Compounds** | **Concentration ( µg/ml)** | | | | | | | | | | **$IC_{50}$ ( µg/ml)** |
|---|---|---|---|---|---|---|---|---|---|---|---|---|
| | | **0** | **1** | **5** | **10** | **50** | **100** | **200** | **300** | **400** | **500** | |
| **DPPH• free Radical Scavenging Activity (%)** | **6a** | **0** | 31.1 | 32.7 | 53.4 | 58.1 | 62.4 | 71.9 | 76.4 | 80.0 | 83.7 | **8.96** |
| | **6b** | **0** | 30.0 | 39.3 | 40.2 | 56.8 | 63.4 | 73.3 | 78.0 | 81.1 | 81.2 | **35.64** |
| | **6c** | **0** | 35.3 | 41.0 | 52.0 | 63.6 | 73.1 | 78.3 | 81.1 | 81.1 | 81.5 | **9.09** |
| | **6d** | **0** | 30.1 | 35.5 | 60.1 | 80.4 | 86.0 | 86.2 | 87.6 | 89.5 | 91.9 | **8.41** |
| | **6e** | **0** | 31.4 | 41.4 | 68.1 | 76.1 | 76.4 | 76.4 | 76.6 | 78.9 | 83.0 | **6.63** |
| | **6f** | **0** | 29.9 | 30.0 | 39.4 | 77.1 | 78.0 | 77.1 | 77.1 | 77.5 | 76.7 | **19.77** |
| | **AA** | **0** | 17.1 | 77.8 | 83.7 | 91.2 | 98.5 | 98.6 | 98.6 | 98.4 | 98.7 | **3.76** |

The table III.1 presents the scavenging activity percentages for different compounds (**6a-f**) and ascorbic acid at varying concentrations (0, 1, 5, 10, 50, 100, 200, 300, 400, and 500 µg/ml).

The standard antioxidant, ascorbic acid, shows a high scavenging activity starting from 17.09% and peaking at nearly 99% with an $IC_{50}$ of **3.76 µg/ml**. While some compounds (like **6d** and **6e**) have comparable or lower $IC_{50}$ values than ascorbic acid, they do not reach the same level of maximum scavenging activity.

Compound **6e** exhibited the strongest antioxidant activity, with an IC50 value of 6.63 µg/ml, among these compounds. Compounds **6d** (8.41 µg/ml), **6a** (8.96 µg/ml), and **6c** (9.09 µg/ml) also demonstrated strong antioxidant activities, comparable to ascorbic acid. Meanwhile, compounds **6f** (19.77 µg/ml) showed moderate activity, and compound **6b** had a significantly higher $IC_{50}$ of 35.64 µg/ml, indicating weak antioxidant activity, suggesting lower efficacy compared to other compounds.

The findings show that a number of compounds, most notably **6d** and **6e**, have low $IC_{50}$ values and significant DPPH free radical scavenging activity, indicating that they are potent antioxidants. Compound **6e** exhibits remarkable promise owing to its low $IC_{50}$ value and strong scavenging percentage. Comparatively speaking to the other compounds studied, compound **6b** seems to be less effective as an antioxidant. All things considered, these results point to compounds **6a**, **6c**, **6d**, and **6e** as possible subjects for additional study into their antioxidant qualities and possible uses in medical domains where oxidative stress is a problem.

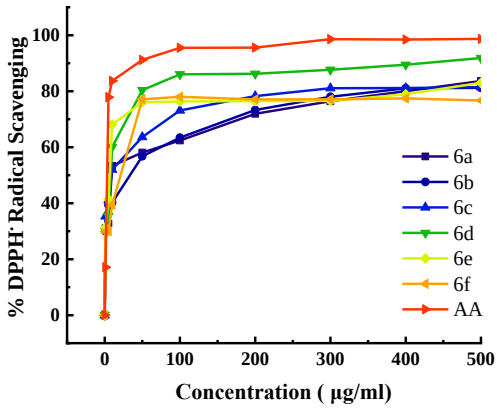


**Figure III.3**. Results of DPPH• free radical scavenging activity (%) of the 1,2,3-triazole derivatives **6a-f**

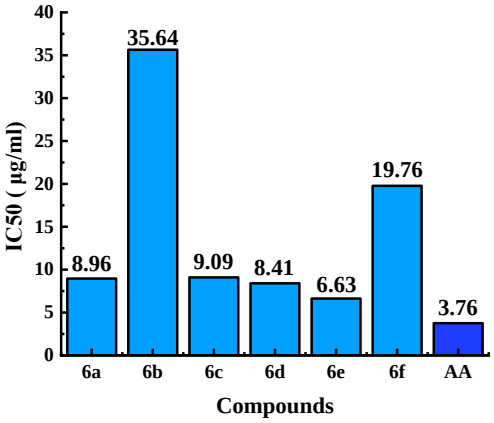


**Figure III.4.** $IC_{50}$ ( µg/ml) results of the DPPH• free radical assay of 1,2,3-triazole derivatives **6a-f** with ascorbic acid as standard

## II.2. Antioxidant activity of thiosemicarbazone derivatives

First we've prepared a stock solution of the thiosemicarbazone derivatives that has a 1 mg/mL concentration, then we prepared a range of dilutions from it. To calculate the IC50, the linear regression equation for each curve is determined, and the concentration corresponding to 50% inhibition is calculated.

**Table III.2.** the compounds **8a-f's** *in vitro* antioxidant activity with the DPPH• free radical assay, with ascorbic acid as standard.

| | Compounds | Concentration ( µg/ml) | | | | | | | | | | $IC_{50}$ ( µg/ml) |
|---|---|---|---|---|---|---|---|---|---|---|---|---|
| | | **0** | **1** | **5** | **10** | **50** | **100** | **200** | **300** | **400** | **500** | |
| **DPPH• free Radical Scavenging Activity (%)** | **8a** | **0** | 30.0 | 40.2 | 50.0 | 80.0 | 80.0 | 80.1 | 80.1 | 81.3 | 83.0 | **10.01** |
| | **8b** | **0** | 35.4 | 39.1 | 43.0 | 49.0 | 52.0 | 69.4 | 79.1 | 82.3 | 85.1 | **68.06** |
| | **8c** | **0** | 49.6 | 51.5 | 64.4 | 65.4 | 80.2 | 96.3 | 96.5 | 96.7 | 96.9 | **2.39** |
| | **8d** | **0** | 30.0 | 41.0 | 65.6 | 75.9 | 76.9 | 95.5 | 95.5 | 96.9 | 97.2 | **6.22** |
| | **8e** | **0** | 48.3 | 48.9 | 49.1 | 82.0 | 85.1 | 88.1 | 89.0 | 89.0 | 89.0 | **11.69** |
| | **8f** | **0** | 48.6 | 49.2 | 83.0 | 84.0 | 91.0 | 91.1 | 91.0 | 97.0 | 97.0 | **5.40** |
| | **AA** | **0** | 17.1 | 77.8 | 83.7 | 91.2 | 98.5 | 98.6 | 98.6 | 98.4 | 98.7 | **3.76** |

**Table III.3.** the compounds **8a-f's** *in vitro* antioxidant activity using ABTS assay , with **BHT** as standard.

| | Compounds | Concentration ( µg/ml) | | | | | | | | | | $IC_{50}$ ( µg/ml) |
|---|---|---|---|---|---|---|---|---|---|---|---|---|
| | | **0** | **1** | **5** | **10** | **50** | **100** | **200** | **300** | **400** | **500** | |
| **Percentage Inhibition of the $ABTS^{•+}$ (%)** | **8a** | 0 | 1.69 | 4.6 | 4.4 | 21.1 | 36.2 | 74.0 | 98.9 | 98.9 | 98.9 | **137.08** |
| | **8b** | 0 | 1.47 | 2.4 | 7.1 | 16.7 | 39.9 | 57.7 | 63.7 | 85.9 | 90.7 | **156.57** |
| | **8c** | 0 | 0.68 | 1.5 | 3.1 | 14.0 | 31.3 | 67.8 | 91.2 | 91.4 | 91.4 | **151.78** |
| | **8d** | 0 | 5.19 | 6.7 | 10.0 | 16.8 | 36.8 | 58.9 | 93.8 | 93.8 | 93.8 | **160.12** |
| | **8e** | 0 | 3.05 | 4.6 | 5.4 | 16.8 | 32.9 | 65.5 | 97.3 | 99.3 | 99.3 | **151.78** |
| | **8f** | 0 | 5.10 | 6.6 | 7.9 | 13.3 | 40.7 | 74.2 | 96.1 | 96.1 | 96.1 | **128.66** |
| | **BHT** | 0 | 4.33 | 12.2 | 29.4 | 34.1 | 65.0 | 68.0 | 72.1 | 91.0 | 92.3 | **75.17** |

The $IC_{50}$ values from the antioxidant activity assays are summarized in Tables III.2 and III.3 The scavenging activity of the thiosemicarbazone derivatives (**8a–f**) was compared to standard antioxidants, BHT ($IC_{50}$ = 75.17 µg/ml) for the ABTS assay and ascorbic acid (IC50 = 3.76 µg/ml) for the DPPH assay.

In the DPPH assay, compound **8c** with an $IC_{50}$ value of 2.39 µg/ml showed the strongest anti-oxidant activity, even higher than ascorbic acid. compared to ascorbic acid, compounds **8d** (6.22 µg/ml) and **8f** (5.40 µg/ml) also demonstrated strong antioxidant activities,. Meanwhile, com-pounds **8a** (10.01 µg/ml) and **8e** (11.69 µg/ml) showed moderate activity, and compound **8b** had a significantly higher $IC_{50}$ of 68.06 µg/ml, indicating weak antioxidant activity.

In the ABTS assay, all thiosemicarbazone derivatives (8a–f) displayed weak antioxidant activity compared to **BHT**, with $IC_{50}$ values above 100 µg/ml. Among these, compound **8f** had the lowest $IC_{50}$ value (128.66 µg/ml), reflecting moderate antioxidant activity, though still weaker than **BHT**. The remaining compounds (**8a, 8b, 8c, 8d, and 8e**) showed IC50 values above 130 µg/ml, indicating weak antioxidant potential.

While the DPPH assay revealed strong antioxidant properties for several compounds, in particular **8c**, which was better than ascorbic acid, the ABTS assay showed weaker activity overall. Notably, compounds **8e, 8a,** and **8f** demonstrated better scavenging abilities than **BHT** in this assay.

Overall, these findings suggest that the synthesized thiosemicarbazone derivatives (**8a–f**) have strong antioxidant potential, particularly in the DPPH assay, and require further investigation for their potential therapeutic applications in treating disorders related to oxidative stress.

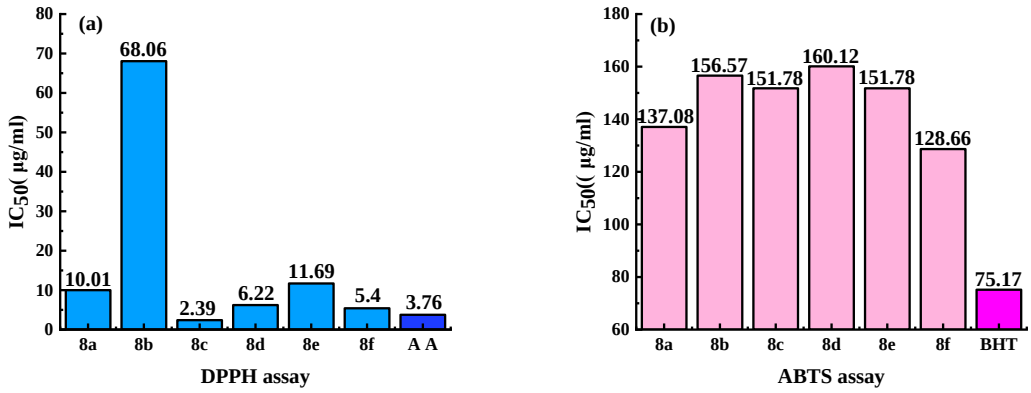


**Figure III.5.** $IC_{50}$ **( µg/ml)** of thiosemicarbazone derivatives **8a-f** (**a**) $DPPH^{\bullet}$ free radical assay with ascorbic acid as standard. (**b)** assay of $ABTS^{\bullet+}$, with the standard BHT

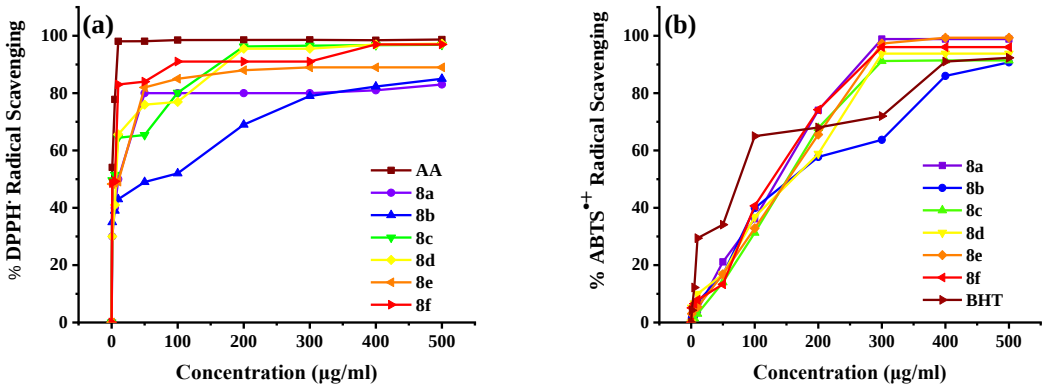


**Figure III.6.** Results of antioxidant assays of the thiosemicarbazone derivatives **8a-f (a) 8a-f %** $DPPH^{\bullet}$ free radical scavenging and **(b) 8a-f** $\%ABTS^{\bullet+}$ free radical scavenging .

The literature indicates that the thiazole cycle have good antioxidant activity. This study aims to confirm that the functional groups of thiazole play an essential role in increasing hydrogen supply as well as in the ability to donate and to accept electron. Furthermore, it is suggested that these groups may help to stabilize radical forms after electron donation or hydrogen addition. On this basis, thiazoles were synthesized and tested for their antioxidant activity.

### II.3. Antioxidant activity of thiazole derivatives

We've prepared a stock solution of the thiazole derivatives 10a-f that has a 1 mg/mL concentration, then we prepared from it a range of dilutions ( 1, 5, 10, 50, 100, 200, 300, 400 and 500 µg/ml). To calculate the IC50, the linear regression equation for each curve is determined, and the concentration corresponding to 50% inhibition is calculated.

**Table III.4.** the compounds **8a-f's** *in vitro* antioxidant activity utilizing DPPH˙ free radical assay, with ascorbic acid as standard

| | Compounds | Concentration ( µg/ml) | | | | | | | | | | $IC_{50}$ ( µg/ml) |
|---|---|---|---|---|---|---|---|---|---|---|---|---|
| | | **0** | **1** | **5** | **10** | **50** | **100** | **200** | **300** | **400** | **500** | |
| **DPPH˙ free Radical Scavenging Activity (%)** | **10a** | **0** | 47.6 | 64.33 | 73.59 | 74.08 | 92.76 | 93.86 | 94.26 | 94.39 | 95.36 | **2.39** |
| | **10b** | **0** | 58.7 | 65.74 | 66.45 | 92.27 | 92.89 | 94.75 | 96.78 | 97.84 | 98.37 | **0.62** |
| | **10c** | **0** | 31.4 | 61.1 | 73.99 | 95.94 | 97.48 | 98.85 | 98.85 | 97.97 | 97.48 | **3.49** |
| | **10d** | **0** | 47.5 | 54.04 | 54.08 | 58.59 | 65.08 | 80.04 | 90.07 | 95.58 | 96.16 | **2.12** |
| | **10e** | **0** | 50.8 | 58.85 | 67.68 | 95.89 | 96.51 | 96.51 | 97.88 | 98.32 | 96.38 | **0.34** |
| | **10f** | **0** | 51.2 | 60.88 | 76.42 | 93.07 | 94.57 | 94.83 | 95.54 | 95.63 | 95.67 | **0.07** |
| | **AA** | **0** | 17.1 | 77.84 | 83.70 | 91.20 | 98.51 | 98.56 | 98.58 | 98.44 | 98.69 | **3.76** |

**Table III.5.** the compounds **8a-f**'s *in vitro* antioxidant activity using ABTS assay , with BHT as standard

| | Compounds | Concentration ( µg/ml) | | | | | | | | | | $IC_{50}$ ( µg/ml) |
|---|---|---|---|---|---|---|---|---|---|---|---|---|
| | | **0** | **1** | **5** | **10** | **50** | **100** | **200** | **300** | **400** | **500** | |
| **Percentage Inhibition of the $ABTS^{\bullet+}$ (%)** | **10a** | 0 | 0.67 | 4.75 | 7.91 | 10.17 | 23.39 | 37.63 | 52.53 | 74.58 | 76.61 | **281.33** |
| | **10b** | 0 | 0.79 | 4.63 | 6.78 | 7.01 | 8.36 | 28.14 | 51.07 | 57.29 | 70.96 | **293.6** |
| | **10c** | 0 | 1.69 | 3.62 | 4.07 | 5.88 | 17.06 | 36.49 | 62.15 | 89.27 | 90.17 | **252.74** |
| | **10d** | 0 | 1.69 | 4.41 | 5.42 | 8.70 | 11.98 | 23.28 | 42.15 | 57.63 | 61.81 | **350.7** |
| | **10e** | 0 | 1.02 | 3.95 | 7.79 | 8.25 | 15.37 | 30.96 | 46.10 | 70.51 | 84.97 | **316.48** |
| | **10f** | 0 | 1.01 | 2.26 | 3.95 | 9.04 | 20.79 | 39.2 | 59.21 | 70.73 | 86.44 | **253.15** |
| | **BHT** | 0 | 4.33 | 12.21 | 29.40 | 34.10 | 65.01 | 68.01 | 72.05 | 91.03 | 92.33 | **75.17** |

The IC50 values from the antioxidant activity assays are summarized in Tables III.4 and III.5.

We used **BHT** (IC50 = 75.17 μg/ml) as standard for ABTS assay and ascorbic acid (IC50 = 3.76 μg/ml) for DPPH assay.

In the **DPPH** assay, the percentage of **DPPH** deletion increases while in the range for most compounds. This suggests that higher concentrations of these compounds result in greater antioxidant activity. The IC50 of all tested compounds was better than ascorbic acid value. For example, compound **10f** with low IC50 value has a peculiar IC50 value of 0.07 μg/mL, indicating very effective at very low concentration indicating more potency in scavenging DPPH particles Compound **10b** shows if very high activity is deleted, up to about 98% at 500 μg in /mL The most intense antioxidant activity revealed, with IC50 value of 0.62 μg/ml, even higher than ascorbic acid, compound **10e** with lower IC50 (0.34 μg/ml )value and higher percentage of radical scavenging ,is more potent than ascorbic acid IC50 value of compounds **10c** , **10a** and **10d** , which exhibited antagonizing effects bacterial consumption, currently 3.49, 2.39 and 2.12 μg/mL, respectively, indicating weaker antioxidant activity compared to others such as **10f**, **10b**, and **10e**.

The IC50 values from these results suggest that some compounds are more potent than others in neutralizing free radicals. When these results are compared with known antioxidants such as ascorbic acid about, it is clear that some tested compounds give the best results in terms of efficacy. Further research could investigate the mechanisms behind their antioxidant activities and potential applications in various industries.

In the ABTS assay, all thiazole derivatives (**10a–f**) showed weaker antioxidant activity compared to **BHT**, with IC50 values greater than 200 μg/ml Among these compounds, **10c** and **10f** were The lowest IC50 values were 252.74 and 253.15 μg/ml, respectively exhibited, respectively moderate antioxidant activity but still weaker than **BHT** The other compounds (**10a**, **10b**, **10d**, and **10e**) have IC50 values above 280 μg/ml, indicating low antioxidant activity.

In general, the percentage of ABTS deletion increased with increasing concentrations of all compounds; however, this percentage was relatively low compared to the DPPH test results. For example, compound **10a** showed the highest percentage of 76.61% at a maximum concentration of 500 μg/mL with an IC50 value of 281.33 μg/mL, indicating a lower antioxidant activity compared to others with compound **10b** tested with an IC50 value of 293.6 μg/mL The highest concentration (500 μg/mL) which showed a maximum scavenging percentage of 70.96%, indicating moderate antioxidant activity. In contrast, compound **10f** had a value of 253.15 μg/mL IC50, indicating a slight but still effectiveness is not as strong as many antibiotics . **BHT** achieved the maximum percentage of 92.33% at 500 μg/mL with IC50 value of 75.17 μg/mL only, which

exhibited significantly higher potency than the tested compounds.

Overall, the higher IC50 values of all tested compounds indicate that higher concentrations are required to achieve significant antioxidant activity against ABTS particles Notably, compared to DPPH test results for which some compounds had relatively low IC50 values (e.g., compound **10f** = 0.07 µg/mL) were present. Then the ABTS test indicates that these agents may not be effective in neutralizing ABTS particles. This difference highlights the importance of multiple tests with c.

Further studies could investigate the mechanisms behind these differences and evaluate possible modifications to enhance the antioxidant effects of these compounds for better use.

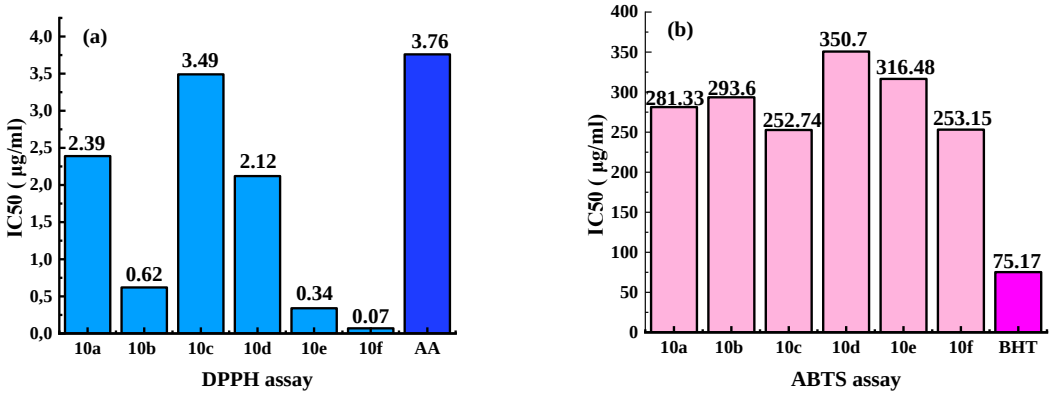


**Figure III.7.** IC50 **(** µg/ml**)** of thiazole derivatives **10a-f** (**a**) DPPH• free radical assay with ascorbic acid as standard. (**b)** $ABTS^{\bullet+}$ assay, with BHT as standard

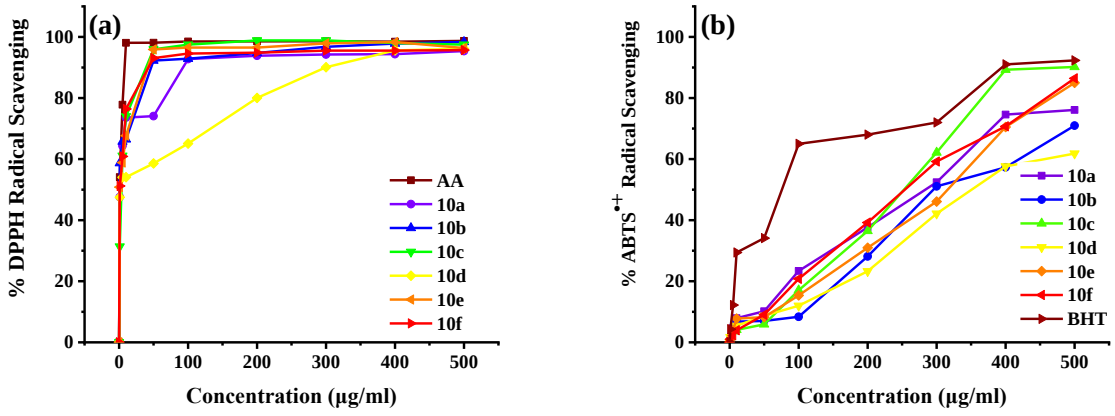


**Figure III.8.** antioxidant assays results of the thiazole derivatives **10a-f (a) 10a-f's %** DPPH• free radical scavenging and **(b)** % $ABTS^{\bullet+}$ free radical scavenging of **10a-f**.

## Conclusion

In this chapter, we explored the antioxidant effects of triazole, thiosemicarbazone and thiazole derivatives, employing both the DPPH and ABTS assays to evaluate their activity. Our findings revealed a significant correlation between the chemical structures of these derivatives and their antioxidant efficacy, underscoring the importance of structural features in determining biological activity. Notably, most synthesized derivatives exhibited substantial antioxidant activity, with variations observed across different testing methods. These results not only highlight the potential of thiosemicarbazone and thiazole derivatives as effective antioxidants but also suggest avenues for further research into optimizing their structures for enhanced efficacy. Future studies could focus on elucidating the mechanisms behind their antioxidant properties and exploring their applications in various fields, including pharmaceuticals and food preservation.

**References**


[1] G. K. Kiriiri, P. M. Njogu, and A. N. Mwangi, "Exploring different approaches to improve the success of drug discovery and development projects: a review," *Future Journal of Pharmaceutical Sciences,* vol. 6, pp. 1-12, 2020.

[2] M. F. Arshad *et al.*, "Thiazole: A versatile standalone moiety contributing to the development of various drugs and biologically active agents," *Molecules,* vol. 27, no. 13, p. 3994, 2022.

[3] D. Lengerli, K. Ibis, Y. Nural, and E. Banoglu, "The 1, 2, 3-triazole 'all-in-one'ring system in drug discovery: A good bioisostere, a good pharmacophore, a good linker, and a versatile synthetic tool," *Expert opinion on drug discovery,* vol. 17, no. 11, pp. 1209-1236, 2022.

[4] Y. R. Girish, K. S. Sharath Kumar, K. Prashantha, S. Rangappa, and M. S. Sudhanva, "Significance of antioxidants and methods to evaluate their potency," *Materials Chemistry Horizons,* vol. 2, no. 2, pp. 93-112, 2023.

[5] I. G. Munteanu and C. Apetrei, "Analytical methods used in determining antioxidant activity: A review," *International journal of molecular sciences,* vol. 22, no. 7, p. 3380, 2021.

[6] G. Martemucci, C. Costagliola, M. Mariano, L. D'andrea, P. Napolitano, and A. G. D'Alessandro, "Free radical properties, source and targets, antioxidant consumption and health," *Oxygen,* vol. 2, no. 2, pp. 48-78, 2022.

[7] P. Chaudhary *et al.*, "Oxidative stress, free radicals and antioxidants: Potential crosstalk in the pathophysiology of human diseases," *Frontiers in chemistry,* vol. 11, p. 1158198, 2023.

[8] A. Zeb, "Concept, mechanism, and applications of phenolic antioxidants in foods," *Journal of Food Biochemistry,* vol. 44, no. 9, p. e13394, 2020.

[9] M. S. Malik, M. Azam, and M. A. R. Basra, "Impact of natural antioxidants on biological systems," *Life Sci,* vol. 4, pp. 139-162, 2020.

[10] J. Shen, P. T. Griffiths, S. J. Campbell, B. Utinger, M. Kalberer, and S. E. Paulson, "Ascorbate oxidation by iron, copper and reactive oxygen species: Review, model development, and derivation of key rate constants," *Scientific reports,* vol. 11, no. 1, p. 7417, 2021.

[11] S. Sundaram Sanjay and A. K. Shukla, "Mechanism of antioxidant activity," in *Potential Therapeutic Applications of Nano-antioxidants*: Springer, 2021, pp. 83-99.

[12] E. O. Olufunmilayo, M. B. Gerke-Duncan, and R. D. Holsinger, "Oxidative stress and antioxidants in neurodegenerative disorders," *Antioxidants,* vol. 12, no. 2, p. 517, 2023.

[13] A. B. Jena, R. R. Samal, N. K. Bhol, and A. K. Duttaroy, "Cellular Red-Ox system in health and disease: The latest update," *Biomedicine & Pharmacotherapy*, vol. 162, p. 114606, 2023.

[14] M. Parcheta, R. Świsłocka, S. Orzechowska, M. Akimowicz, R. Choińska, and W. Lewandowski, "Recent developments in effective antioxidants: The structure and antioxidant properties," *Materials*, vol. 14, no. 8, p. 1984, 2021.

[15] F. B. da Cruz, D. H. N. Martins, J. de Freitas Ferreira, P. de Oliveira Magalhães, D. Silveira, and Y. M. Fonseca-Bazzo, "Antioxidant activity of apis mellifera bee propolis: a review," *Journal of Natural Products Discovery*, vol. 1, no. 1, 2022.

# GENERAL CONCLUSION

The main objective of the work presented in this thesis was to synthesize new nitro-filled heterocycles for therapeutic purposes and to study the antioxidant capacity. In this study, we were able to synthesize thiazole derivatives newly realized by classical synthetic methods based on single-stage and multi-stage reactions to obtain synthetic 1,2,3-triazoles. This was followed by condensation with thiosemicarbazide to give a thiosemicarbazone derivative, followed by condensation with chloroacetone to give the desired thiazole compounds.

In the first chapter, we investigated the synthesis of 1,2,3-triazole derivatives, which revealed their inestimable promise in different aspects of heterocycling, especially chemistry. We also emphasized the development of environmentally friendly methods, especially through the use of metal-based micro/nanoparticles. In the second part of this chapter we prepared alkyne derivatives by synthesizing aromatic aldehydes with propargyl bromide. Then, we prepared $Cu_2O$ microbeads using *Artemisia campestris L.* extract. Finally, the synthesis of 1,2,3-triazole derivatives using alkyne derivatives, benzyl chloride derivatives and sodium azide in the presence of $Cu_2O$ microbeads as catalyst was carried out under one-pot multi-component reaction conditions.

In the second part of our study, we used a small amount of acetic acid as a catalyst, through a condensation reaction in ethanol between the $NH_2$ function of thiosemicarbazide and the aldehyde function at 1,2,3-triazole formed and then extended this reaction to chloroacetone, which enabled the synthesis of new thiazole derivatives.

In chapter three, the synthesized molecules were analyzed for antioxidant activity by two widely accepted methods: DPPH and ABTS assays. The results showed that these compounds exhibit significant antioxidant properties, suggesting potential utility in a variety of applications where oxidative stress is a concern.

Overall, this work highlights the advantages of using nanocatalysts in the synthesis of 1,2,3-triazole derivatives and successfully generates new thiazole derivatives with good yields and in addition, shows promising biological applications of the resulting heterocyclic compounds. Future research should focus on further exploring the structure-activity relationship (SAR) of these compounds and their potential therapeutic application in the prevention of oxidative stress-related diseases.

# Chapter IV

# Experimental Section

## Apparatus and Materials

### Solvents and Products

The commercially available starting organic compounds are used as received without additional purification. All reactions are carried out under an argon atmosphere unless otherwise stated. The reaction solvents are pre-dried and distilled according to standard methods.

The progress of the reactions and the purity of the obtained products have been monitored by thin-layer chromatography (TLC) on silica on aluminum (TLC, Silica Gel F254 Merck, Germany , 0.2 mm) and revealed under UV radiation at 254 nm.

The separation of products has been performed by recrystallization at low temperature or precipitation.

### 1.UV-Vis Spectrophotometer

The UV-Vis spectrophotometer (UV-vis, SP-UV 500DB/VDB, Spectrum Instruments, Shanghai) was utilized to measure the light absorbance and bandgap energy of Cu2O microbeads across a wavelength range of 220–600 nm.

### 2. X-ray Diffraction

X-ray diffraction (XRD, Miniflex 600 Rigaku, Tokyo, Japan) was conducted to evaluate the crystallinity and crystal structure of Cu2O microbeads, employing CuKα radiation (40 kV and 30 mA) with a wavelength of 1.5418 Å and a scanning speed of 0.5°.

### 3. Fourier Transform Infrared Spectroscopy

The chemical bonding within the $Cu_2O$ microbeads was investigated using Fourier transform infrared spectroscopy (FTIR, Agilent Cary 630), which covered a spectral range from 4,000 to 500 $cm^{-1}$. Furthermore, the FTIR was used to confirm the structure of the synthesized products in the same spectral range. The wavenumber was expressed in $cm^{-1}$ .

### 4. Scanning Electron Microscopy

The particle size and morphology of $Cu_2O$ microbeads were analyzed through scanning electron microscopy (SEM, Thermo Scientific Quatro, Thermo Fisher Scientific, Germany), while energy-dispersive X-ray (EDX) analysis was employed to ascertain the elemental composition.

### 5.Nuclear Magnetic Resonance of Proton ($^1H$) and Carbon ($^{13}C$)

spectra were recorded at frequencies of 300 and 400 MHz for the $^1H$ NMR and 75 and 101 MHz

for $^{13}C$ NMR, respectively, using Bruker AV III spectrometer (France) at room temperature. The chemical shifts (δ) are reported in parts per million (ppm) relative to the $Me_4Si$ (TMS) signal taken as an internal standard. Deuterated chloroform and DMSO were employed as the solvent. The multiplicity of the signals is indicated by the following abbreviations:

- **s**: singlet
- **d**: doublet
- **dd**: doublet of doublets
- **t**: triplet
- **q**: quartet
- **m**: multiplet, etc.

The coupling constants J (absolute values) are expressed in Hertz (Hz). The software Mestrenova-12.0.1-20560 was used to process the obtained spectra.

**6. Melting point**

Melting points were determined using Kofler System, LEICA VMHB (Germany).

**7.Materials and Products for Antioxidant Testing**

- **Dilution Solvent:** Methanol
- **Free Radicals:** DPPH and ABTS
- **Standards:** Ascorbic Acid, BHT
- Micropipettes

## Experimental Protocols

### $Cu_2O$ microbeads Preparation

### First step: Plant extraction

Fresh leaves of *Artemisia campestris L.* collected from Messad-Djelfa, Algeria (Latitude: 34.1667, Longitude:3.5 34° 10′0″North, 3° 30′0″East). were thoroughly washed with tap water and then allowed to dry at room temperature for 15 days. Once desiccated, the leaves were ground into a superfine powder. The extraction process was carried out using the maceration method. In an erlenmeyer flask, 10 g of the powdered leaves were combined with 100 mL of hot deionized water at 100°C for one hour. After the extraction, the mixture was filtered, and the resulting product was stored at 4°C until required.

### Second step: synthesis of $Cu_2O$ microbeads

A 10 mL solution of 1M $CuSO_4 \cdot 5H_2O$ was prepared and then mixed in an appropriate ratio with 10 mL of the previously prepared aqueous plant extract. This mixture was agitated magnetically at 70 °C for 30 minutes. During this process, $Cu_2O$ microbeads formed and dispersed throughout the solution, resulting in a color change from blue that was initially associated with the presence of $Cu^{2+}$ ions to a reddish-brown color. The $Cu_2O$ microbeads were collected using centrifugation, and the resulting $Cu_2O$ powder sample was dried for two hours at 80 °C.

**Cuprous oxide microbeads**

**Chemical formula:** $Cu_2O$ microbeads

**XRD:** 34.21°(111), 36.50°(111), 43.28°(200), 51.40° (211) .

**FTIR ($\upsilon$ $cm^{-1}$):** 612 (Cu-O), 3,100 (O-H), 2,890 and 2,656 (C-H), 2,120 ($CO_2$), 1,608 (C=C), 1,512 (C=O).

**UV-Vis:** At 220 nm a significant absorption peak ($Cu_2O$ microbeads formation). $Cu_2O$ microbeads bandgap around 2.7 eV.

**SEM images**: spherical flower-like structures with the size of 6 - 3 μm.

**SEM-EDX analysis:** 54.91% (copper), 23.73% (oxygen), 21.72% (carbon) .

**1,2,3-triazole preparation**

**1.Alkyne derivatives preparation:**

Alkynes were initially created from 4- hydroxybenzaldehyde, vanillin and salicylaldehide with propargyl bromide in DMF with stirring conditions at 80°C while $K_2CO_3$ was present. The reaction was monitored with TLC (eluent: Ehtyl acetate/Petroleum ether, 2/8). This process allowed for the synthesis of the desired alkynes in the form of light hazel and light beige crystals in excellent yields. The target compound, upon workup and purification by crystallization in EtOH, giving yields from 74- 83% after two hours.

**2. 1,2,3-triazole preparation**

One-pot, three-component 1,3-dipolar cycloaddition reaction was performed between the prepared alkynes, sodium azide and benzyl chloride in DMF:$H_2O$ (2:1, v/v) under reflux conditions at 90°c for 3-4 hours. The 20mg/mL of $Cu_2O$ microbeads was added to the mixture (used as the catalyst system), producing the relevant 1,2,3-triazole 1,4-disubstituted compounds in moderate to exceptional yields (33-85%). The reaction was monitored with TLC (eluent: Ehtyl acetate/ Petroleum ether, 2/8).

**4-(prop-2-yn-1-yloxy)benzaldehyde (3a)**

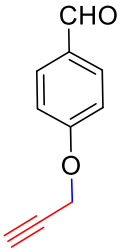


**Chemical Formula:** $C_{10}H_8O_2$, light hazel crystals.

**Melting point (mp):** 81-83°C.

**Yield:** 83%.

**FTIR (υ $cm^{-1}$):** 1000, 1250, 1160, 1580, 1600, 1680, 2110, 3200.

**3-methoxy-4-(prop-2-yn-1-yloxy)benzaldehyde (3b)**

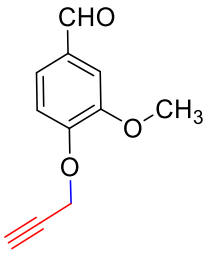


**Chemical Formula:** $C_{11}H_{10}O_3$, light beige crystals.

**Melting point (mp):** 84-86°C.

**Yield:** 75%.

**FTIR (υ $cm^{-1}$):** 1000, 1110, 1250, 1580, 1700, 1590, 2110, 2890, 3220.

**2-(prop-2-yn-1-yloxy)benzaldehyde (3c)**

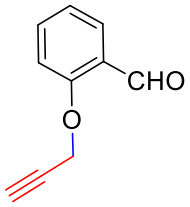


**Chemical Formula:** $C_{10}H_8O_2$, light beige crystals.

**Melting point (mp):** 66-68°C.

**Yield :**74%.

**FTIIR (υ $cm^{-1}$):** 1000, 1200, 1280, 1450, 1600, 1680, 2110, 2890, 3280.

**4-((1-benzyl-1H-1,2,3-triazol-4-yl)methoxy)benzaldehyde (6a)**

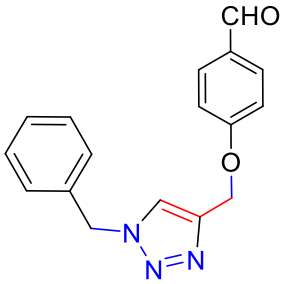


**Chemical Formula:** $C_{17}H_{15}N_3O_2$, light yellow crystals.

**Melting point (mp):** 140-143℃.

**Yield:** 70%.

**FTIR (υ $cm^{-1}$):** 1000, 1170, 1250, 1580, 1600, 1680, 2100.

**$^1$H NMR (300MHz, Chloroform-d) δ** 4.96 (d, 2H), 5.24 (s, 2H), 6.83–6.72 (m, 2H), 7.04–6.92 (m, 2H), 7.13–7.02 (m, 3H), 7.57–7.47 (m, 2H), 9.57 (s, 1H).

**$^{13}$C NMR (75MHz, Chloroform-d) δ** 54.35, 62.20, 115.11, 122.87, 128.18, 128.94, 129.23, 130.37, 132.01, 134.33, 143.64, 163.15, 190.82.

**4-((1-(4-methylbenzyl)-1H-1,2,3-triazol-4-yl)methoxy)benzaldehyde (6b)**

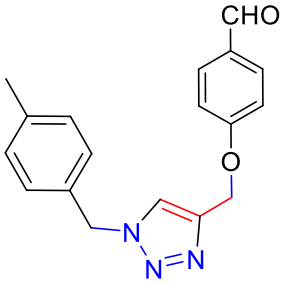


**Chemical Formula:**$C_{18}H_{17}N_3O_2$, Light yellow crystals.

**Melting point (mp):** 134-136℃.

**Yield:** 50%.

**FTIR (υ $cm^{-1}$):** 1000, 1170, 1250, 1580, 1,600, 1,680, 2100.

**$^1$H NMR (300 MHz, Chloroform-d) δ** 2.08 (s, 3H), 4.98 (d, 2H), 5.22 (s, 2H), 6.86–6.76 (m, 2H), 6.91 (s, 4H), 7.61–7.50 (m, 2H), 9.61 (s, 1H).

**$^{13}$C NMR (75 MHz, Chloroform-d) δ** 21.17, 54.16, 62.22, 115.11, 122.72, 128.24, 129.88, 130.37, 131.28, 132.00, 138.93, 143.56, 163.18, 190.79.

**4-((1-benzyl-1H-1,2,3-triazol-4-yl)methoxy)-3-methoxybenzaldehyde (6c)**

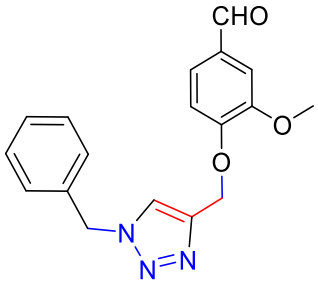


**Chemical Formula:** $C_{18}H_{17}N_3O_3$, yellow pale solid.

**Melting point (mp):** 124-126℃.

**Yield:** 85%.

**FTIR (υ $cm^{-1}$):** 990, 1130, 1250, 1500, 1580, 1680, 2100.

**$^1$H NMR (400MHz, Chloroform-d)δ** 3.95 (s,3H), 5.41 (s, 2H), 5.58 (s, 2H), 7.28 (s, 1H), 7.32 (dd, 2H), 7.51–7.39 (m, 5H), 7.64 (s, 1H), 9.90 (s, 1H).

**$^{13}$C NMR (75 MHz, Chloroform-d) δ** 54.32, 56.00, 63.01, 109.33, 112.74, 123.08, 126.66, 128.18, 128.89, 129.18, 130.68, 134.31, 143.65, 149.99, 153.06, 190.88.

**3-methoxy-4-((1-(4-methylbenzyl)-1H-1,2,3-triazol-4-yl)methoxy)benzaldehyde (6d)**

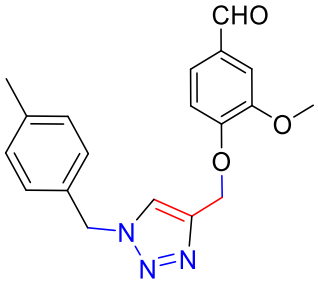


**Chemical Formula:** $C_{19}H_{19}N_3O_3$, yellow pale solid.

**Melting point (mp):** 109-111℃.

**Yield:** 33%.

**FTIR (υ $cm^{-1}$):** 1000, 1130, 1260, 1500, 1580, 1680, 2100.

**1H NMR (400 MHz, Chloroform-d)** δ 2.35 (s, 3H), 3.89 (s, 3H), 5.34 (s,2H), 5.47 (s, 2H), 7.17 (s, 4H), 7.21 (d, 1H), 7.45–7.37 (m, 2H), 7.55 (s, 1H), 9.84 (s, 1H).

**13C NMR (75 MHz, Chloroformd) δ** 21.14, 54.13, 56.01, 63.02, 109.30, 112.73, 122.97, 126.69, 128.24, 129.83, 130.66, 131.26, 138.88, 143.56, 149.99, 153.09, 190.89,

**2-((1-benzyl-1H-1,2,3-triazol-4-yl)methoxy)benzaldehyde (6e)**

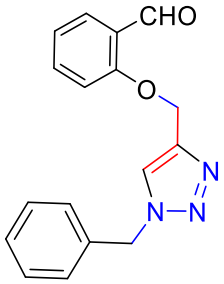


**Chemical Formula:** $C_{17}H_{15}N_3O_2$, white powder.

**Melting point (mp):** 138-140℃.

**Yield:** 70%.

**FTIR (υ $cm^{-1}$):** 1050 , 1260, 1450, 1600, 1680, 2100.

**1H NMR (300 MHz, Chloroform-d)δ** 2.34 (s, 3H), 5.29 (s, 2H), 5.49 (s, 2H), 7.04 (tt, 1H), 7.18 (s, 4H), 7.57–7.49 (m, 2H), 7.81 (dd, 1H), 10.41 (s, 1H).

**13C NMR (75MHz, Chloroform-d) δ** 54.36, 62.64, 113.08, 121.37, 122.78, 125.13, 128.14, 128.71, 128.95, 129.24, 134.35, 136.01, 143.82, 160.48, 189.61.

**2-((1-(4-methylbenzyl)-1H-1,2,3-triazol-4-yl)methoxy)benzaldehyde (6f)**

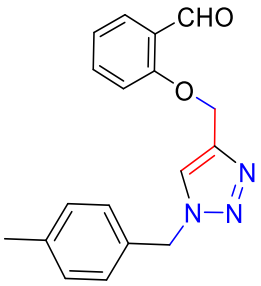


**Chemical Formula:**$C_{18}H_{17}N_3O_3$, white powder.

**Melting point (mp):** 141-143 °C.

**Yield:** 68 %.

**FTIR (υ $cm^{-1}$):** 1050, 1250, 1450, 1600, 1680, 2100.

**1HNMR (300MHz,Chloroform-d) δ** 2.34 (s, 3H), 5.29 (s, 2H), 5.49 (s, 2H), 7.04 (tt, 1H), 7.18 (s, 4H), 7.57–7.49 (m, 2H), 7.81 (dd, 1H), 10.41 (s, 1H).

**13C NMR (75MHz, Chloroform-d) δ** 21.18, 54.17, 62.65, 113.08, 121.33, 122.66, 125.12, 128.20, 128.65, 129.89, 131.30, 136.00, 138.91, 143.71, 160.51, 189.61.

**Preparation of thiosemicarbazone derivatives**

Thiosemicarbazide (1.0 mmol) was reacted with the prepared 1,2,3-triazole derivatives (1.0 mmol) in ethanol, with a few drops of acetic acid (AcOH) were added as a catalyst, to produce thiosemicarbazone derivatives. The reaction mixture was refluxed at 90°C for three to four hours, and the progress was monitored by thin-layer chromatography (TLC) (eluent: ethyl acetate/ petroleum ether, 2/8 ). Afterward, the mixture was placed in an ice bath in the refrigerator overnight to promote crystallization. The resulting precipitate was filtered and recrystallized from ethanol, yielding the final products in moderate to good yields. The resulting thiosemicarbazones were pure and did not require further purification.

**(Z)-2-(4-((1-benzyl-1H-1,2,3-triazol-4-yl)methoxy)benzylidene)hydrazine-1-carbothioamide (8a)**

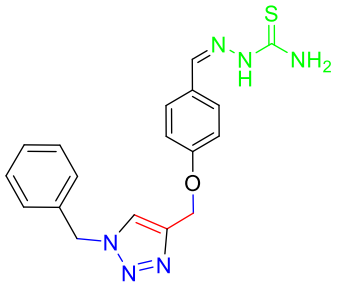

**Chemical Formula:** $C_{18}H_{18}N_6OS$, white powder.

**Melting point (mp):** 191-193°C.

**Yield:** 73%.

**FTIR (υ $cm^{-1}$ ):** 1116, 1228, 1295, 1561, 1595, 1917, 2109, 2113, 3157, 3250, 3321, 3378.

**The $^1$H NMR (400 MHz, DMSO-d6) δ** 5.19 (s, 2H), 5.61 (s, 2H), 7.06 (d, 2H), 7.28-7.43 (m, 5H), 7.74 (d, 1H), 7.90 (s, 1H), 8.01 (s, 1H), 8.09 (s, 1H), 8.28 (s, 1H), 11.30 (s, 1H).

**$^{13}$C NMR (101 MHz, DMSO) δ** 53.35, 61.71, 115.42, 115.65, 125.21, 127.58, 128.44, 128.65, 129.37, 129.26, 130.45, 136.47, 142.62, 143.27, 159.93, 178.19.

**(Z)-2-(4-((1-(4-methylbenzyl)-1H-1,2,3-triazol-4-yl)methoxy)benzylidene)hydrazine-1-carbothioamide (8b)**

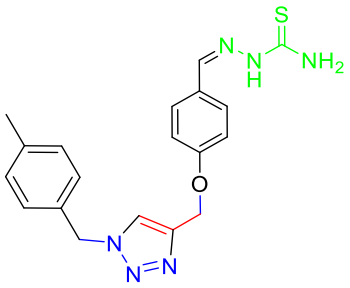

**Chemical Formula:** $C_{19}H_{20}N_6OS$, white powder.

**Melting point (mp):** 182-184°C.

**Yield:** 72%.

**FTIR (υ $cm^{-1}$):** 1178, 1246, 1292, 1562, 1594, 1918, 2078, 2114, 3160, 3256, 3324, 3383.

**$^1$H NMR (300 MHz, $CDCl_3$) δ** 1.20-1.33 (m, 1H), 2.36 (s, 3H), 5.22 (s, 2H), 5.50 (s, 2H), 6.35 (s, 1H), 6.94-7.05 (m, 2H), 7.19 (s, 4H), 7.52 (s, 1H), 7.54-7.63 (m, 2H), 7.81 (s, 1H), 9.54 (s, 1H).

**$^{13}$C NMR (75 MHz, $CDCl_3$) δ** 21.17, 54.15, 62.15, 115.24, 122.63, 128.24, 129.16, 129.86, 131.32, 143.55, 143.92, 160.41.

**(Z)-2-(4-((1-benzyl-1H-1,2,3-triazol-4-yl)methoxy)-3-methoxybenzylidene)hydrazine-1-carbothioamide (8c)**

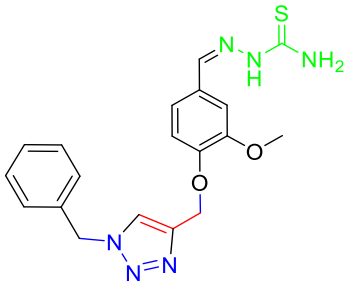


**Chemical Formula:** $C_{19}H_{20}N_6O_2S$, yellow powder.

**Melting point (mp):** 162-164℃.

**Yield:** 68%.

**FTIR (υ $cm^{-1}$):** 1060, 1200, 1267, 1582, 1595, 2063, 2111, 3151, 3235, 3371, 3417.

**$^1$H NMR (400 MHz, DMSO-d6) δ** 3.79 (s, 3H), 5.15 (s, 2H), 5.62 (s, 2H), 7.14 (s, 2H), 7.28-7.43 (m, 5H), 7.51 (s, 1H), 7.98 (s, 1H), 8.13 (s, 1H), 8.27 (s, 1H), 9.88 (s, 1H), 11.31 (s, 1H).

**$^{13}$C NMR (101 MHz, DMSO) δ** 18.00, 25.49, 53.32, 56.14, 62.14, 113.58, 109.38, 122.36, 125.37, 127.96, 128.46, 128.645, 129.25, 136.47, 142.90, 143.22, 149.68, 149.89, 152.11, 178178.12,.96.

**(Z)-2-(3-methoxy-4-((1-(4-methylbenzyl)-1H-1,2,3-triazol-4-yl)methoxy)benzylidene-1-carbothioqmide (8d)**

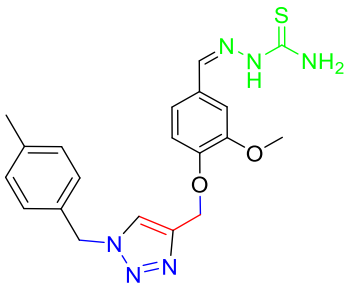

**Chemical Formula:** $C_{20}H_{22}N_6O_2S$, off-white powder.

**Melting point (mp):** 125-127℃.

**Yield:** 74%.

**FTIR (υ $cm^{-1}$):** 1140, 1222, 1261, 1544, 1578, 1710, 1997, 2050, 2115, 2994, 3147, 3308, 3450.

**$^1$H NMR (300 MHz, $CDCl_3$) δ** 2.34 (s, 3H), 3.87 (s, 3H), 5.28 (s, 2H), 5.47 (s, 2H), 6.41 (s, 1H), 7.09 (s, 1H), 7.16 (s, 5H), 7.26 (s, 2H), 7.54 (s, 1H), 7.79 (s, 1H), 9.63 (s, 1H).

**$^{13}$C NMR (75 MHz, $CDCl_3$) δ** 21.16, 54.13, 56.02, 63.02, 108.84, 113.56, 122.47, 122.94, 126.49, 128.25, 129.83, 131.28, 138.86, 143.91, 143.98, 149.89, 150.23, 178.34.

**(E)-2-(2-((1-benzyl-1H-1,2,3-triazol-4-yl)methoxy)benzylidene)hydrazine-1-carbothioamide (8e)**

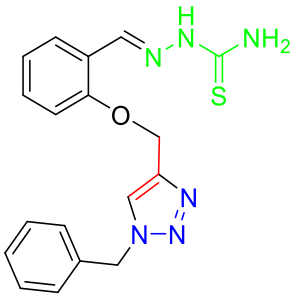

**Chemical formula:** $C_{18}H_{18}N_6OS$, light yellow powder.

**Melting point (mp):** 162-164℃.

**Yield:** 51%.

**FTIR (υ $cm^{-1}$):** 1092, 1218, 1246, 1576, 1584, 2186, 2970, 3019, 3151, 3345, 3468.

**$^1$H NMR (300 MHz, $CDCl_3$) δ** 5.17 (s, 2H), 5.60 (s, 2H), 6.44 (s, 1H), 6.98 (dd, 2H), 7.19 (d, 1H), 7.33 (dtt, 6H), 7.75-7.81 (m, 2H), 8.34 (s, 1H), 10.23 (s, 1H).

**$^{13}$C NMR (75 MHz, $CDCl_3$) δ** 54.29, 62.84, 112.67, 121.50, 122.93, 126.36, 128.08, 128.80, 129.18, 132.12, 134.73, 140.33, 144.03, 157.12, 178.03.

**(E)-2-(2-((1-(4-methylbenzyl)-1H-1,2,3-triazol-4-yl)methoxy)benzylidene)hydrazine-1-carbothioamide (8f)**

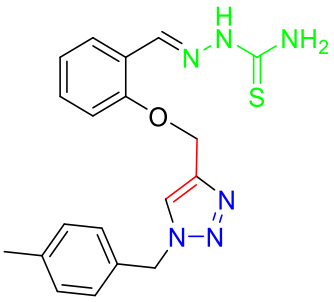


**Chemical formula:** $C_{19}H_{20}N_6OS$, yellow powder.

**Melting point (mp):** 161-163℃.

**Yield:** 32%.

**FTIR (υ $cm^{-1}$):** 1055, 1226, 1284, 1530, 1585, 1893, 2068, 2102, 3013, 3149, 3365, 3481.

**$^1$H NMR (300 MHz, $CDCl_3$) δ** 2.35 (s, 3H), 5.19 (s, 2H), 5.57 (s, 2H), 6.45 (s, 1H), 6.95-7.06 (m, 2H), 7.28–7.15 (m, 5H), 7.32-7.43 (m, 1H), 7.73 (s, 1H), 7.81 (dd, 1H), 8.34 (s, 1H), 10.09 (s, 1H).

**$^{13}$C NMR (75 MHz, $CDCl_3$) δ** 21.17, 54.12, 62.79, 112.69, 121.48, 121.87, 122.79, 126.42, 128.16, 129.84, 131.62, 132.12, 138.79, 140.33, 143.89, 157.15, 178.10.

**Preparation of thiazole derivatives**

### II.2.1. Synthesis

Thiosemicarbazone derivative (1.0 mmol) was reacted with chloro acetone (1.0 mmol) in ethanol. The reaction mixture was refluxed at 80°C for two to three hours, the progress was monitored by thin-layer chromatography (TLC) (eluent: ethyl acetate/ petroleum ether, 1/9 ). The resulting precipitate was filtered and recrystallized from ethanol, yielding the thiazole derivatives in moderate to good yields. These derivatives did not require any further purification.

**(Z)-2-(2-(4-((1-benzyl-1H-1,2,3-triazol-4-yl)methoxy)benzylidene)hydrazineyl)-4-methylthiazole (10a)**

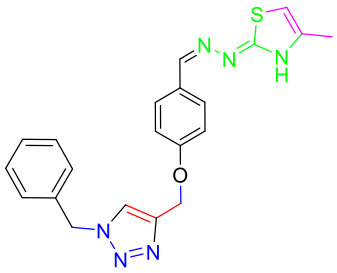

**Chemical formula:** $C_{21}H_{20}N_6OS$, light hazel powder .

**Melting point (mp):** 146-148℃.

**Yield:** 86 %.

**FTIR (υ $cm^{-1}$):** 1005, 1242, 1357, 1434, 1507, 1575, 2360, 2854, 2922, 3068, 3142.

**$^1$H NMR (400MHZ, DMSO-$d_6$) δ** 2.08 (s, 3H), 5.13-5.15 (d, 2H), 5.59-5.60 (d, 2H), 5.67 ( s, 1H), 7.04-7.06 (d, 2H), 7.23-7.25 (d, 1H), 7.30-7.32 (m, 3H), 7.34-7.36 ( m, 2H), 7.52-7.54 (d, 2H), 7.96 (s, 1H), 8.26-8.27 (d, 1H).

**$^{13}$C NMR (101 MHZ, DMSO-$d_6$)δ** 53.32, 61.65, 115.20, 115.62, 125.15, 125.23, 127.84, 128.32, 128.41, 128.62, 129.23, 129.26, 136.46, 136.49, 143.23, 143.49, 157.40, 159.41.

**(Z)-4-methyl-2-(2-(4-((1-(4-methylbenzyl)-1H-1,2,3-triazol-4-yl)methoxy)benzylidene) hydrazineyl)thiazole (10b)**

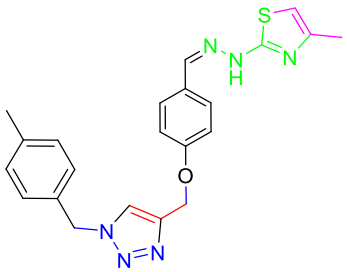

**Chemical formula:** $C_{22}H_{22}N_6OS$, beige powder.

**Melting point (mp):** 139-141℃.

**Yield:** 27%.

**FTIR (υ $cm^{-1}$):** 1005, 1169, 1246, 1310, 1379, 1511, 1603, 2626, 3119, 3365.

**(Z)-2-(2-(4-((1-benzyl-1H-1,2,3-triazol-4-yl)methoxy)-3-methoxybenzylidene) hydrazineyl)-4-methylthiazole (10c)**

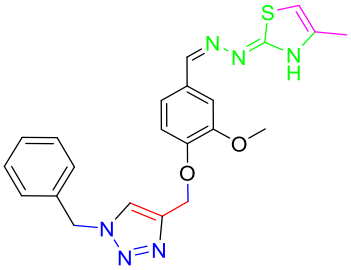

**Chemical formula:** $C_{22}H_{22}N_6O_2S$, light hazel powder.

**Melting point (mp):** 95-97°C.

**Yield:** 21%.

**FTIR (υ $cm^{-1}$):** 995, 1124, 1265, 1439, 1511, 1575, 1603, 2922, 3083, 3375.

**$^1$H NMR (400MHZ, DMSO-$d_6$) δ** 2.16 (s, 3H), 3.77 (s, 3H), 5.15 (s, 2H), 5.61 (s, 2H), 6.35 (s, 1H), 7.14 (s, 1H), 7.16 (s, 1H), 7.24-7.25 (d, 1H), 7.32-7.33 (m, 2H), 7.34-7.35 (m,1H), 7.36-7.37 (m,1H), 7.38 (s,1H), 7.93(s, 1H), 8.27(s, 1H).

**$^{13}$C NMR (101 MHZ, DMSO-$d_6$)δ** 53.31, 55.82, 62.22, 109.22, 114.17, 120.38, 125.36, 128.44, 128.64, 129.25, 136.48, 143.26, 149.05, 149.80.

**(Z)-2-(2-(3-methoxy-4-((1-(4-methylbenzyl)-1H-1,2,3-triazol-4-yl)methoxy)benzylidene) hydrazineyl)-4-methylthiazole (10d)**

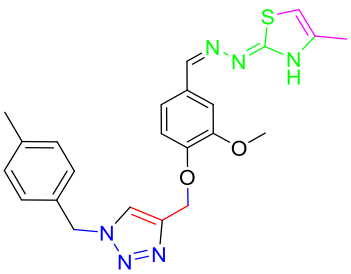

**Chemical formula:** $C_{22}H_{22}N_6O_2S$, light hazel powder.

**Melting point (mp):** 132-134°C.

**Yield:** 49%.

**FTIR (υ $cm^{-1}$):** 981, 1128, 1265, 1439, 1511, 1575, 2941, 3150, 3343, 3576.

**$^1$H NMR (400MHZ, DMSO-$d_6$) δ** 2.24 (d, 3H), 2.28 (s,3H), 3.79(s, 3H), 5.17 (s, 2H), 5.56 (s, 2H), 6.59 (s, 1H), 7.17-7.27 (m, 7H), 7.37 (s, 1H), 8.21(s, 1H), 8.25(s, 1H).

**$^{13}$C NMR (101 MHZ, DMSO-$d_6$) δ** 21.16, 53.13, 56.00, 62.18, 103.60, 113.93, 125.27, 128.51, 129.78, 133.46, 138.01, 143.09, 149.80.

**(E)-2-(2-(2-((1-benzyl-1H-1,2,3-triazol-4-yl)methoxy)benzylidene)hydrazineyl)-4-methylthiazole (10e)**

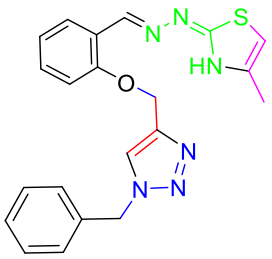

**Chemical formula:** $C_{21}H_{20}N_6OS$, beige powder.

**Melting point (mp):** 154-156℃

**Yield:** 57%.

**FTIR (υ cm$^{-1}$):** 1000, 1132, 1260, 1448, 1507, 1580, 1603, 2927, 3146, 3343, 3580

**$^1$H NMR (400MHZ, DMSO-$d_6$) δ** 2.15 (s, 3H), 5.23 (s, 2H), 5.63 (s, 2H), 6.36 (s, 1H), 7.00.7.03 (t, 1H), 7.25-7.27 (dd, 1H), 7.30-7.35 (m, 5H), 7.36-7.37 (m, 1H), 7.75-7.77 (dd, 1H), 8.27 (s, 1H), 8.31 (s, 1H), 11.71 (s, 1H).

**$^{13}$C NMR (101 MHZ, DMSO-$d_6$) δ** 17.54, 53.35, 62.24, 113.85, 121.70, 123.58, 125.27, 125.43, 128.36, 128.39, 128.65, 129.22, 129.27, 130.68, 136.45, 143.29, 156.29, 168.36.

**(E)-4-methyl-2-(2-(2-((1-(4-methylbenzyl)-1H-1,2,3-triazol-4-yl)methoxy)benzylidene) hydrazineyl)thiazole (10f)**

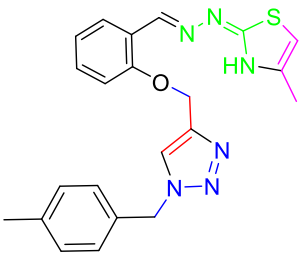

**Chemical formula:** $C_{22}H_{22}N_6OS$, yellow powder.

**Melting point (mp):** 164-167℃

**Yield:** 40%

**FTIR (υ $cm^{-1}$):** 1000, 1128, 1265, 1448, 1511, 1598, 2922, 3142, 3338, 3571.

**$^1$H NMR (400MHZ, DMSO-d6) δ** 2.28 (s, 3H), 5.22 (s, 2H), 5.57 (s, 2H), 6.96-7.00 (t, 1H), 7.13-7.30 (m, 6H), 7.35-7.40 (m, 1H), 7.90 (s, 1H), 8.08-8.10 (d, 2H), 8.27 (s,1H), 8.39 (s, 1H), 11.35 (s, 1H).

**$^{13}$C NMR (101 MHZ, DMSO-$d_6$) δ** 21.16, 53.18, 62.50, 113.78, 121.54, 123.21, 124.91, 126.68, 128.37, 128.44, 129.79, 131.64, 133.45, 137.99, 138.52, 143.25, 143.29, 157.11, 178.35.

# Annexe I

# NMR Spectra

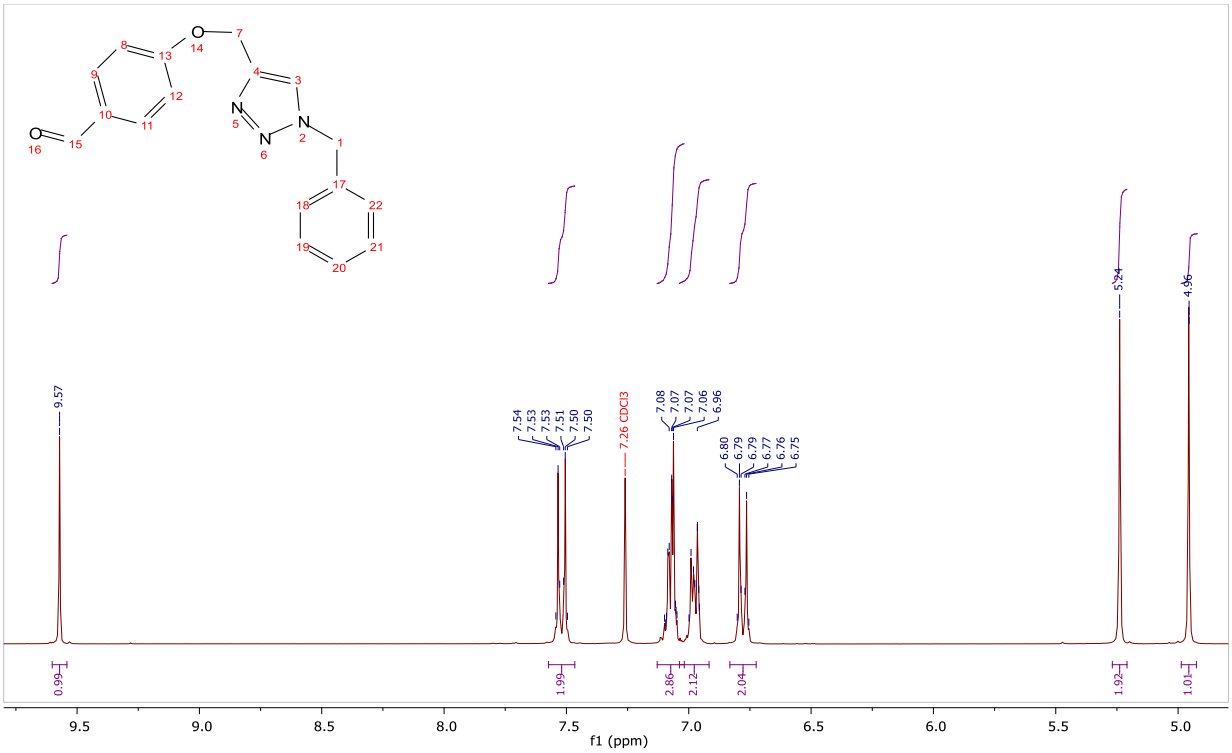


**1H NMR (300 MHz, Chloroform-*d*)** δ 9.57 (s, 1H), 7.57 – 7.47 (m, 2H), 7.13 – 7.02 (m, 3H), 7.04 – 6.92 (m, 2H), 6.83 – 6.72 (m, 2H), 5.24 (s, 2H), 4.96 (s, 2H).

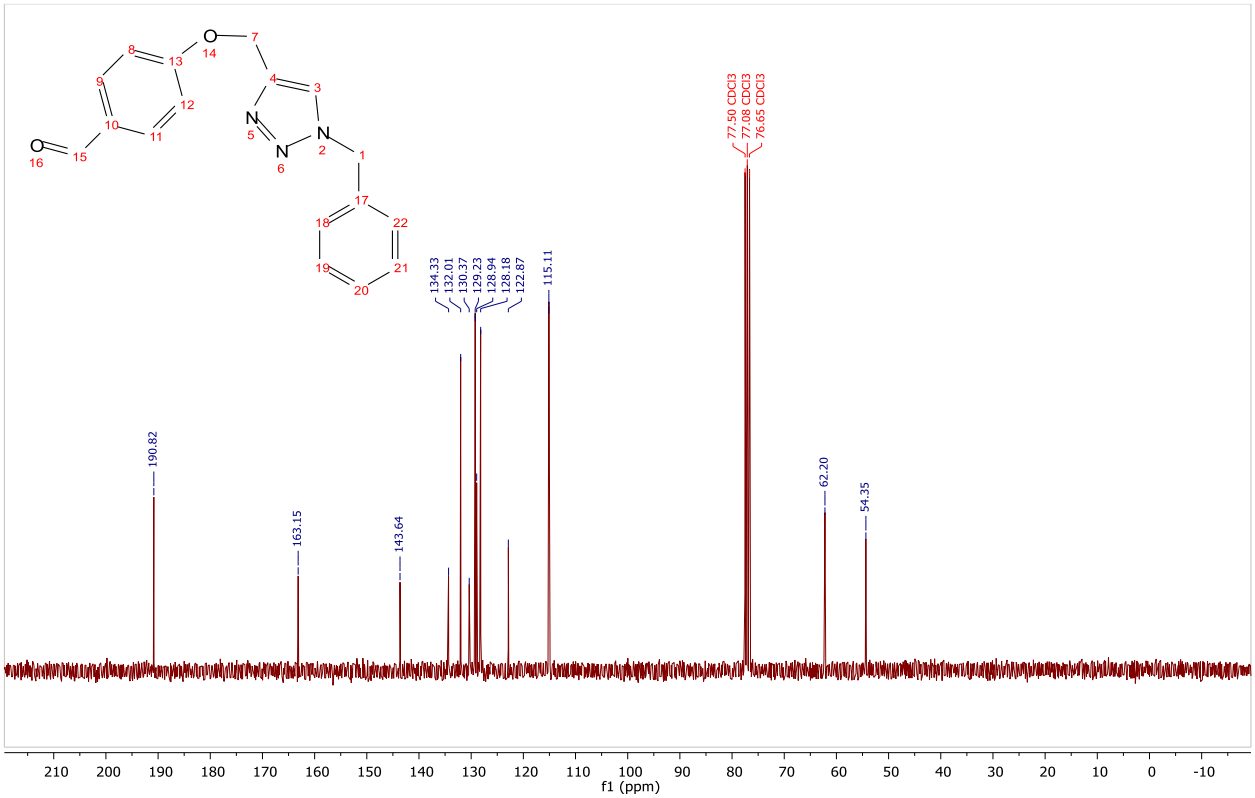


**13C NMR (75 MHz, CDCl3) δ** 190.817390, 163.154610, 143.635932, 134.332096, 132.014298, 130.371873, 129.227765, 128.944129, 128.179161, 122.871055, 115.106327, 77.502051, 77.078740, 76.653574, 62.199007, 54.353639

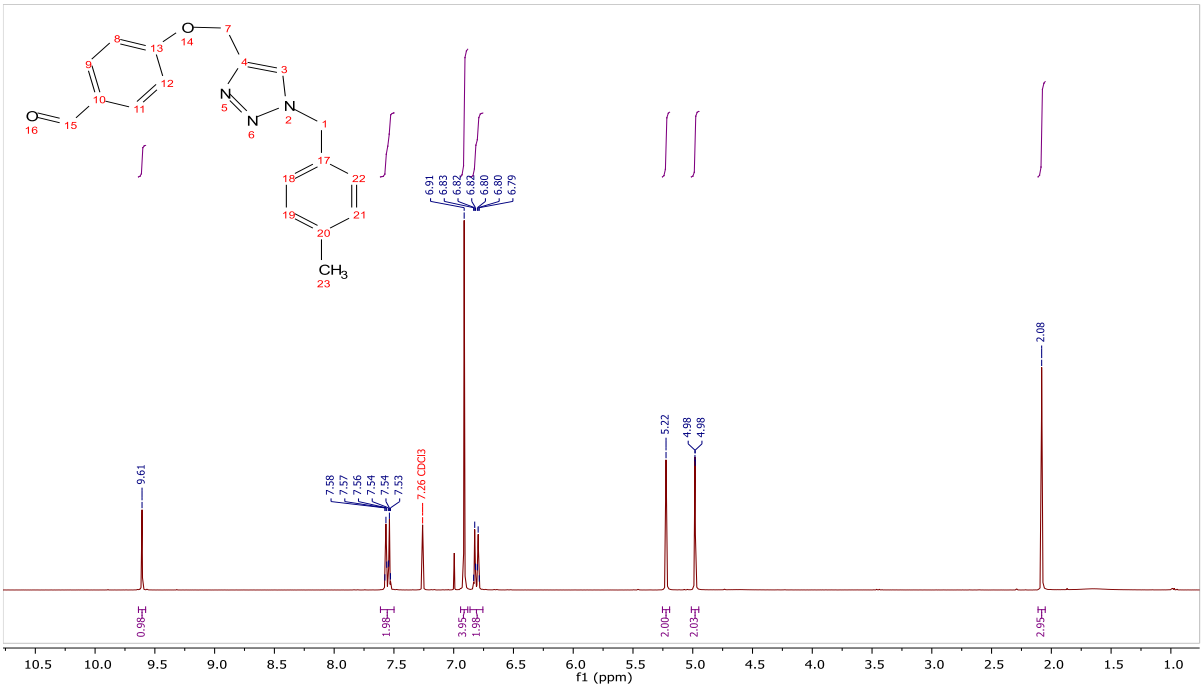


**$^{1}$H NMR (300 MHz, Chloroform-*d*) δ** 9.61 (s, 1H), 7.61 – 7.50 (m, 2H), 6.91 (s, 4H), 6.86 – 6.76 (m, 2H), 5.22 (s, 2H), 4.98 (d, 2H), 2.08 (s, 3H).

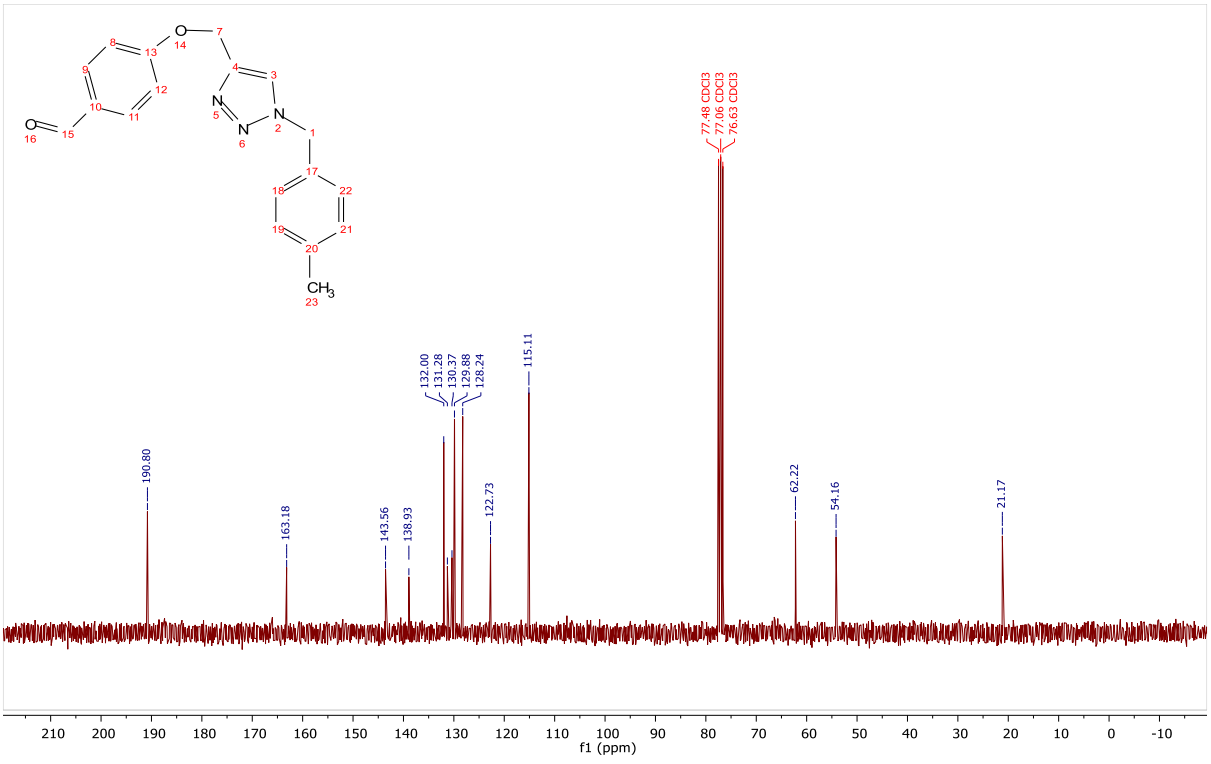


**$^{13}$C NMR (75 MHz, $CDCl_3$) δ** 190.795464, 163.176832, 143.555221, 138.925862, 132.002959, 131.284610, 130.373633, 129.875724, 128.242525, 122.725427, 115.112322, 77.481121, 77.058037, 76.633663, 62.222201, 54.164943, 21.172548

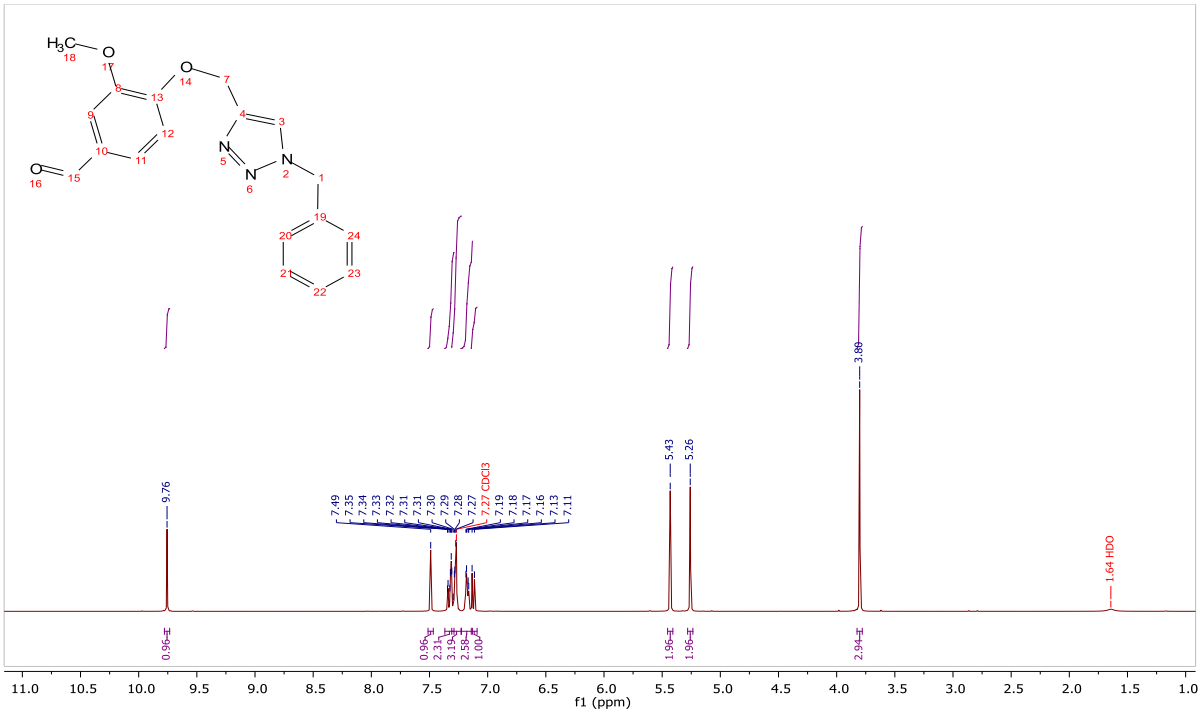


**$^1$H NMR (400 MHz, Chloroform*d*) δ** 9.76 (s, 1H), 7.49 (s, 1H), 7.37 – 7.29 (m, 2H), 7.31 – 7.23 (m, 3H), 7.17 (dd, 3H), 7.12 (d, 1H), 5.43 (s 2H), 5.26 (s, 2H), 3.80 (s, 3H).

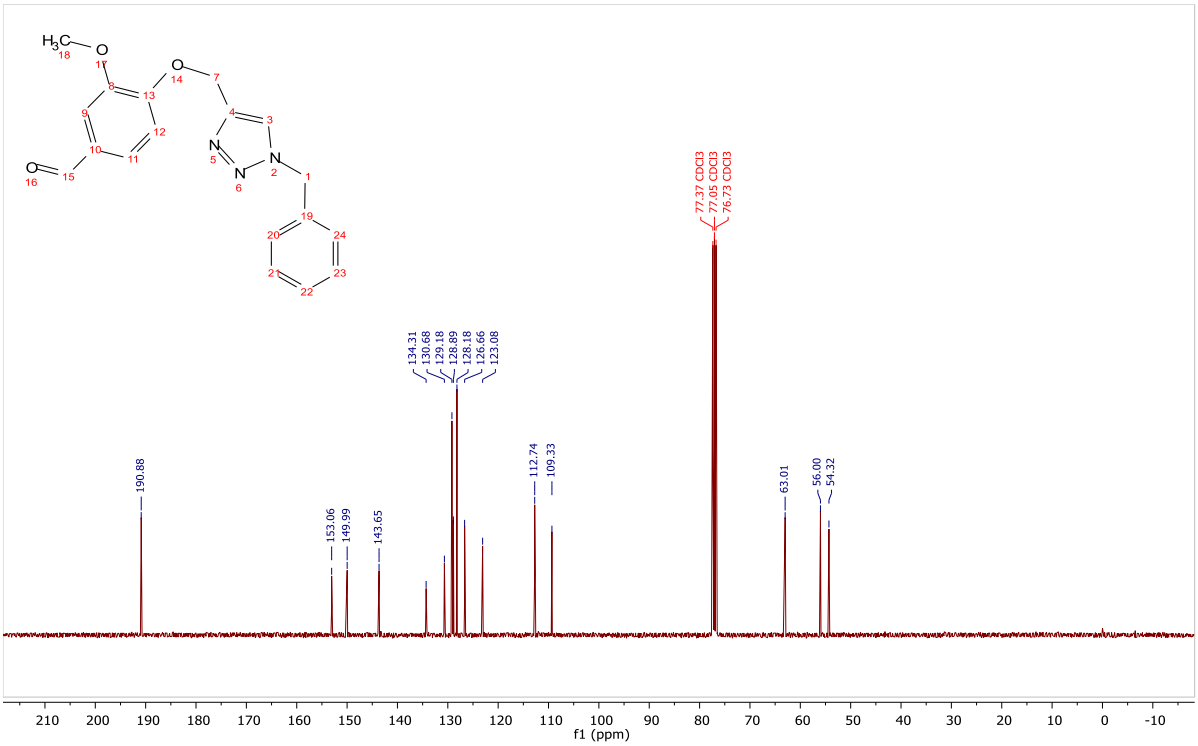


**$^{13}$C NMR (101 MHz, $CDCl_3$) δ** 190.881108, 153.064400, 149.987546, 143.653289, 134.305219, 130.675659, 129.180462, 128.893250, 128.184064, 126.660459, 123.082820, 112.742653, 109.325259, 63.011417, 55.998784, 54.315178.

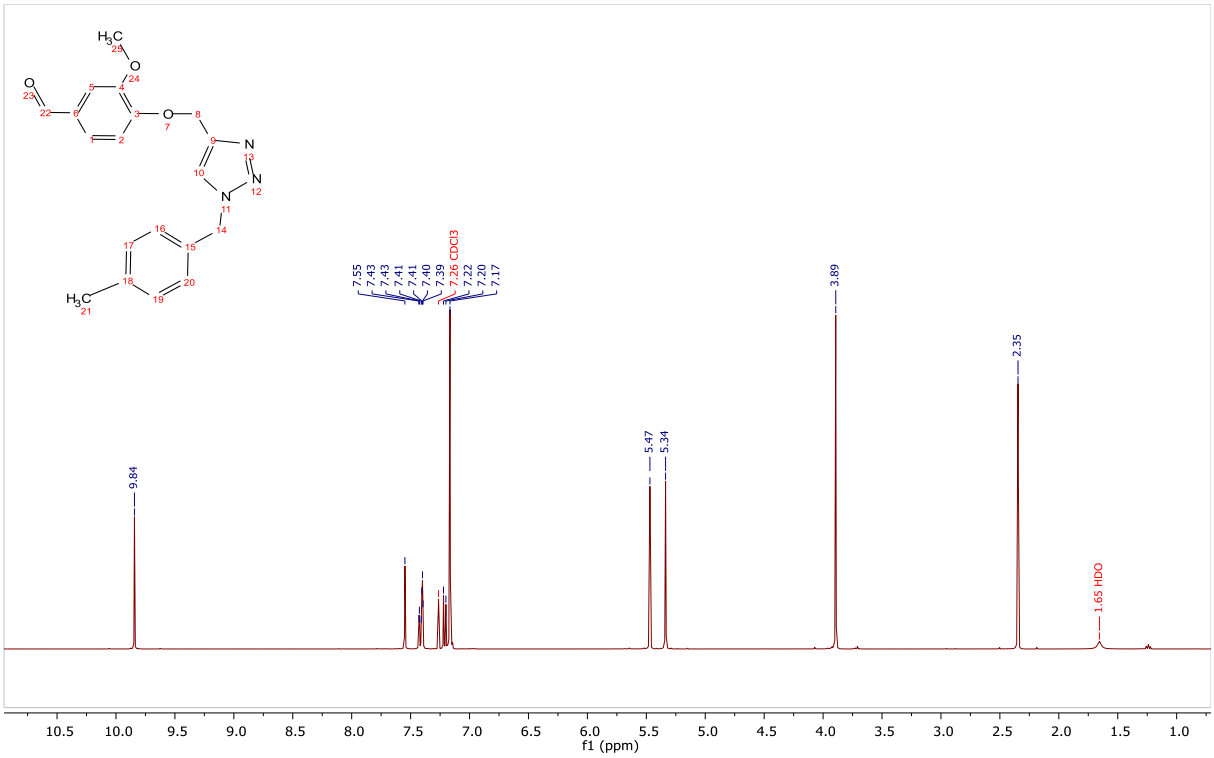


**$^{1}$H NMR (400 MHz, Chloroform-*d*) δ** 9.84 (s, 1H), 7.55 (s, 1H), 7.45 – 7.37 (m, 2H), 7.21 (d, 1H), 7.17 (s, 4H), 5.47 (s, 2H), 5.34 (s, 2H), 3.89 (s, 3H), 2.35 (s, 3H).

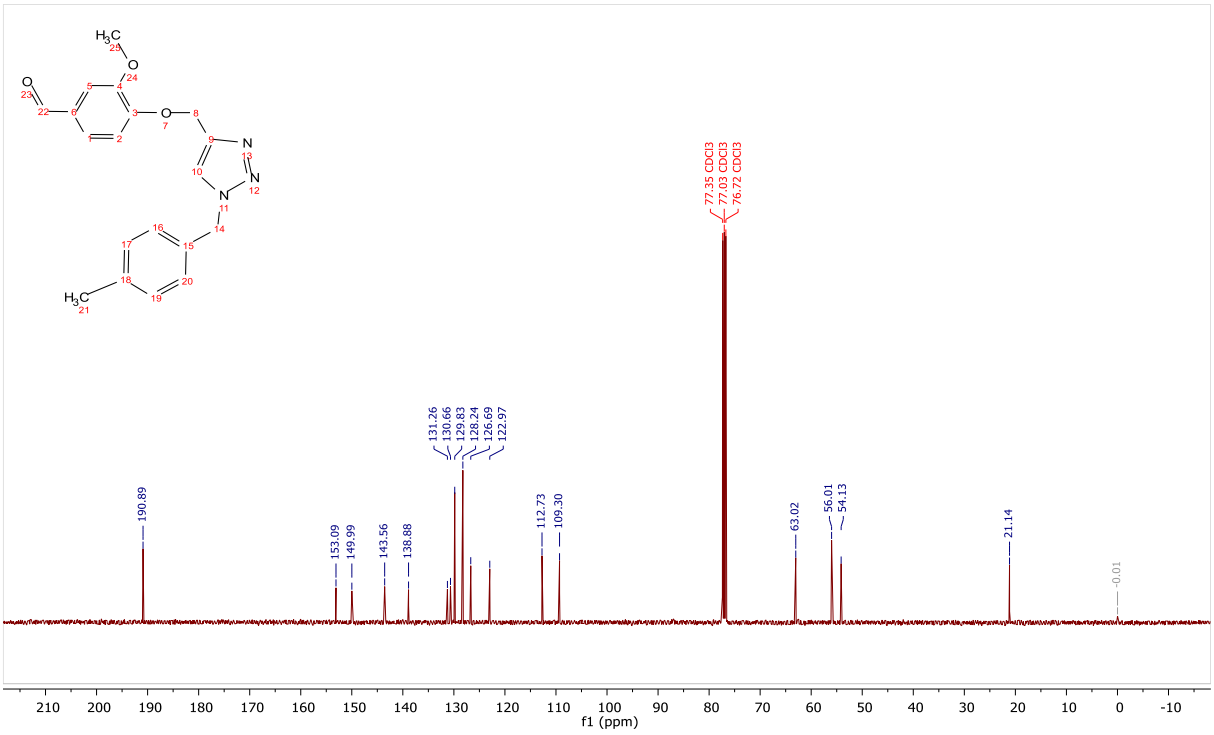


**$^{13}$C NMR (101 MHz, $CDCl_3$) δ** 190.89, 153.09, 149.99, 143.56, 138.88, 131.26, 130.66, 129.83, 128.24, 126.69, 122.97, 112.73, 109.30, 63.02, 56.01, 54.13, 21.14.

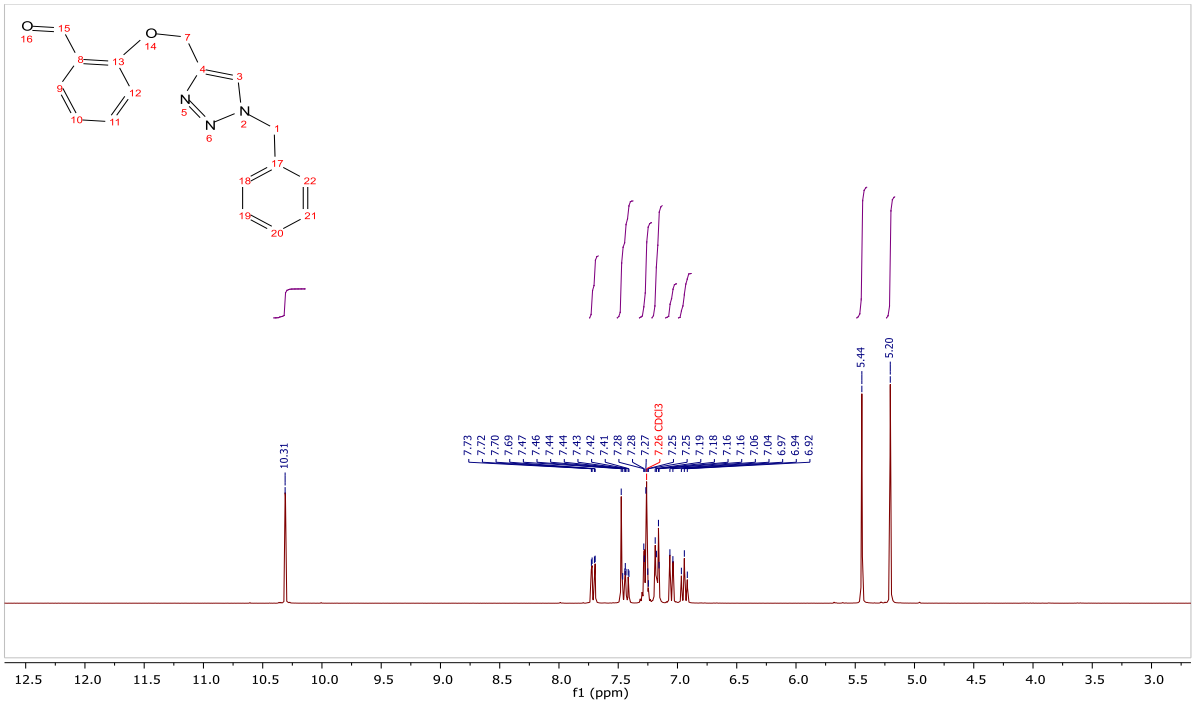


**$^1$H NMR (300 MHz, Chloroform*d*) δ** 10.31 (s, 1H), 7.71 (dd, 1H), 7.51 – 7.38 (m, 2H), 7.32 – 7.22 (m, 2H), 7.22 – 7.13 (m, 2H), 7.05 (d, 1H), 6.94 (t, 1H), 5.44 (s, 2H), 5.20 (s, 2H).

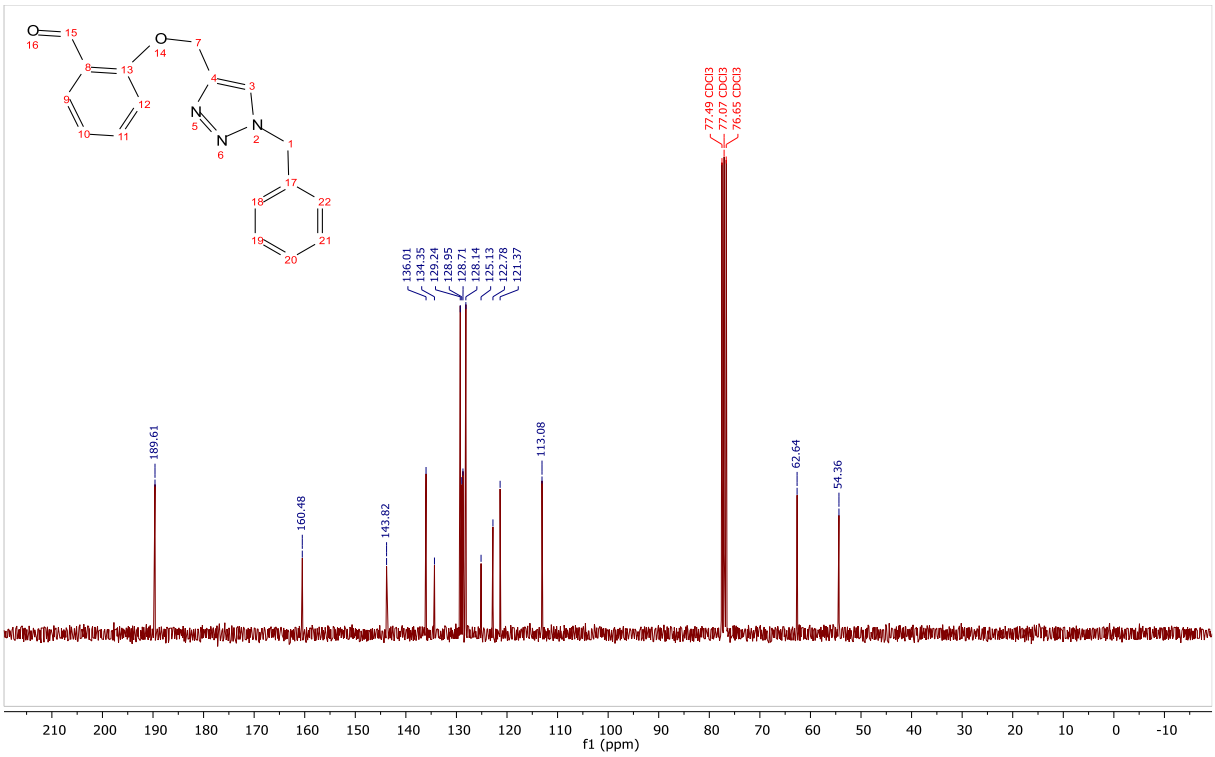


**$^{13}$C NMR (75 MHz, CDCl$_3$) δ** 189.608653, 160.479033, 143.817918, 136.009563, 134.346023, 129.242585, 128.950830, 128.711780, 128.135154, 125.130786, 122.783392, 121.367645, 113.079517, 62.638085, 54.363817.

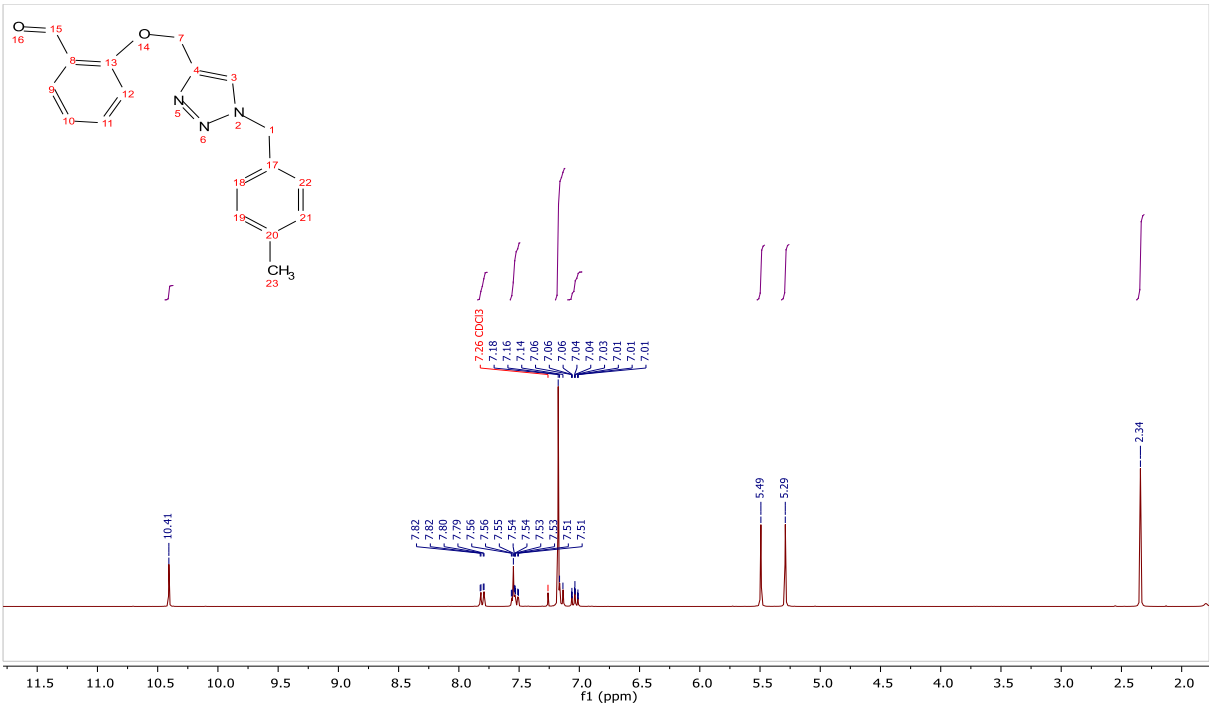


**1H NMR (300 MHz, Chloroform-d)**δ 10.41 (s, 1H), 7.81 (dd, 1H), 7.57 – 7.49 (m, 2H), 7.18 (s, 5H), 7.04 (tt, 1H), 5.49 (s, 2H), 5.29 (s, 2H) 2.34 (s, 3H).

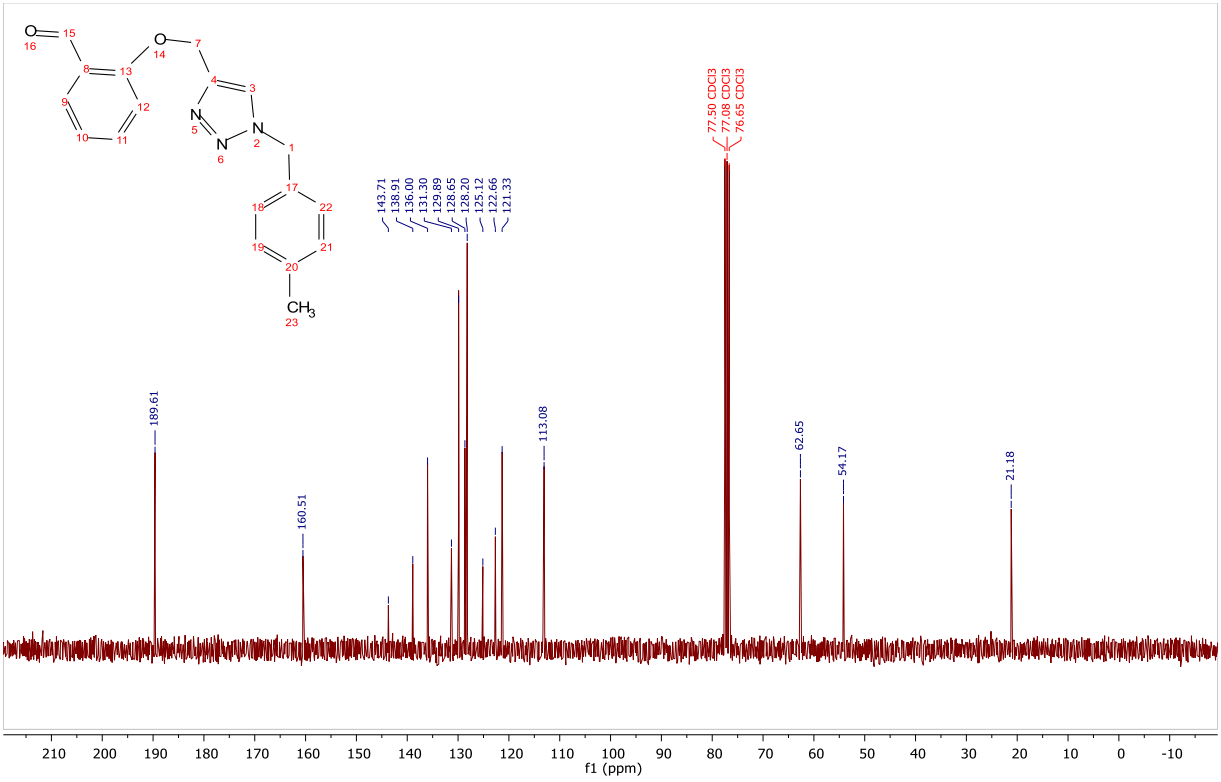


**13C NMR (75 MHz, CDCl3) δ** 189.614043, 160.514235, 143.710754, 138.911572, 136.001564, 131.299186, 129.894559, 128.652639, 128.200425, 125.123121, 122.659100, 121.331803, 113.077607, 62.645052, 54.172239, 21.179837.

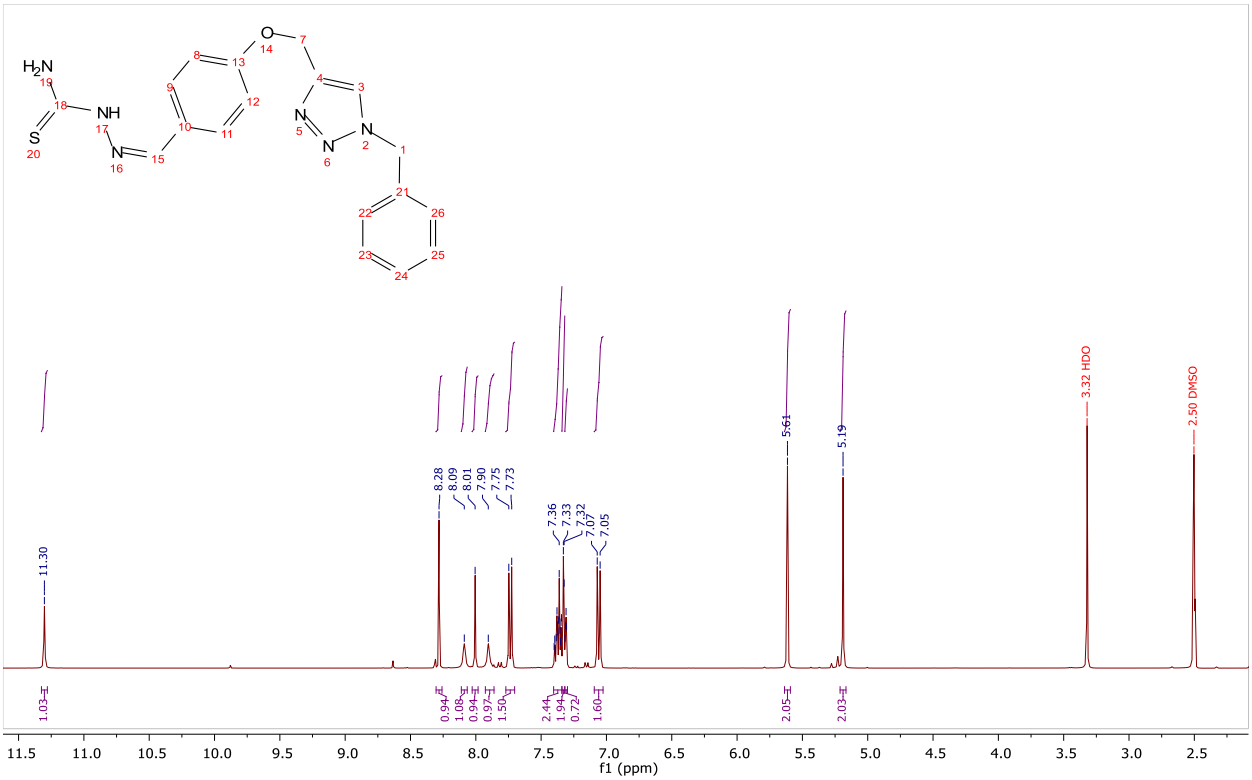


**1H NMR (400 MHz, DMSO-$d_6$) δ** 11.30 (s, 1H), 8.28 (s, 1H), 8.09 (s, 1H), 8.01 (s, 1H), 7.90 (s, 1H), 7.74 (d, 2H), 7.40 – 7.34 (m, 2H), 7.3 (d, 2H), 7.31 (s, 1H), 7.06 (d, 2H), 5.61 (s, 2H), 5.19 (s, 2H).

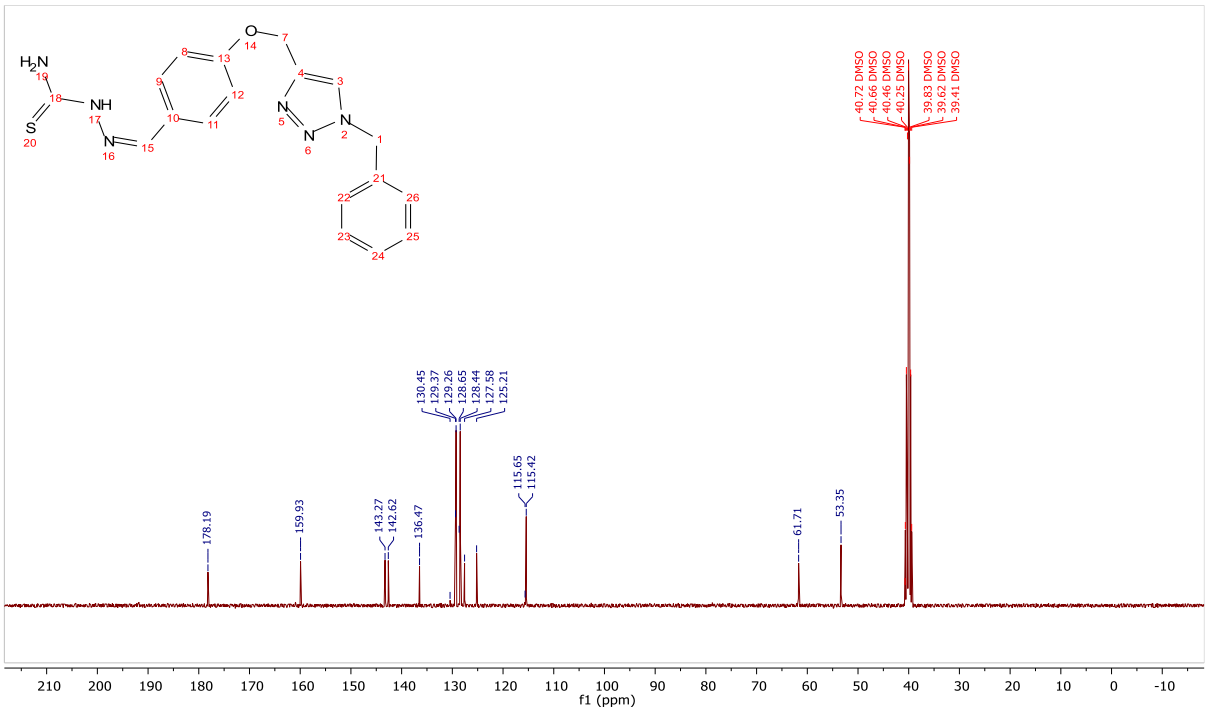


**13C NMR (101 MHz, DMSO) δ 178.19, 159.93, 143.27, 142.62, 136.47, 130.45, 129.37, 129.26, 128.65, 128.44, 127.58, 125.21, 115.65, 115.42, 61.71, 53.35.**

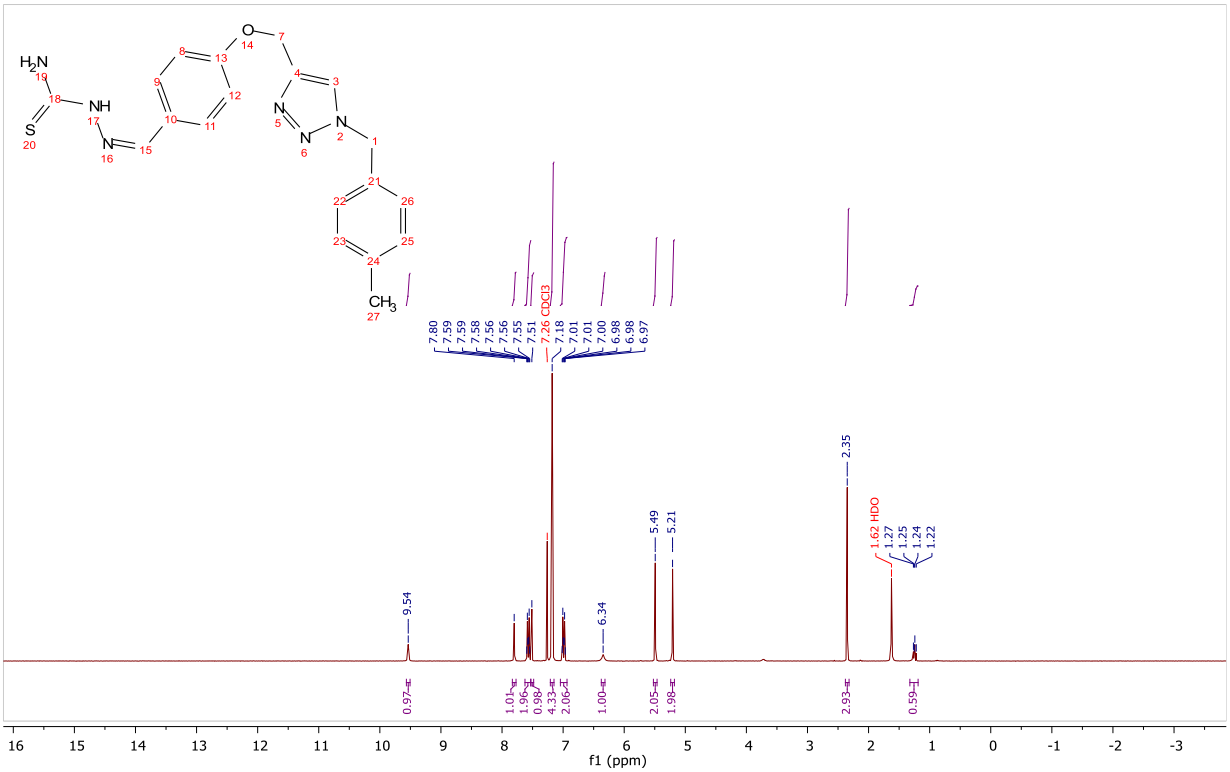


**1H NMR (300 MHz, Chloroform-*d*) δ 9.54 (s, 1H), 7.81 (s, 1H), 7.63 – 7.54 (m, 2H), 7.52 (s, 1H), 7.19 (s, 4H), 7.05 – 6.94 (m, 2H), 6.35 (s, 1H), 5.50 (s, 2H), 5.22 (s, 2H), 2.36 (s, 3H), 1.33 – 1.20 (m, 1H).**

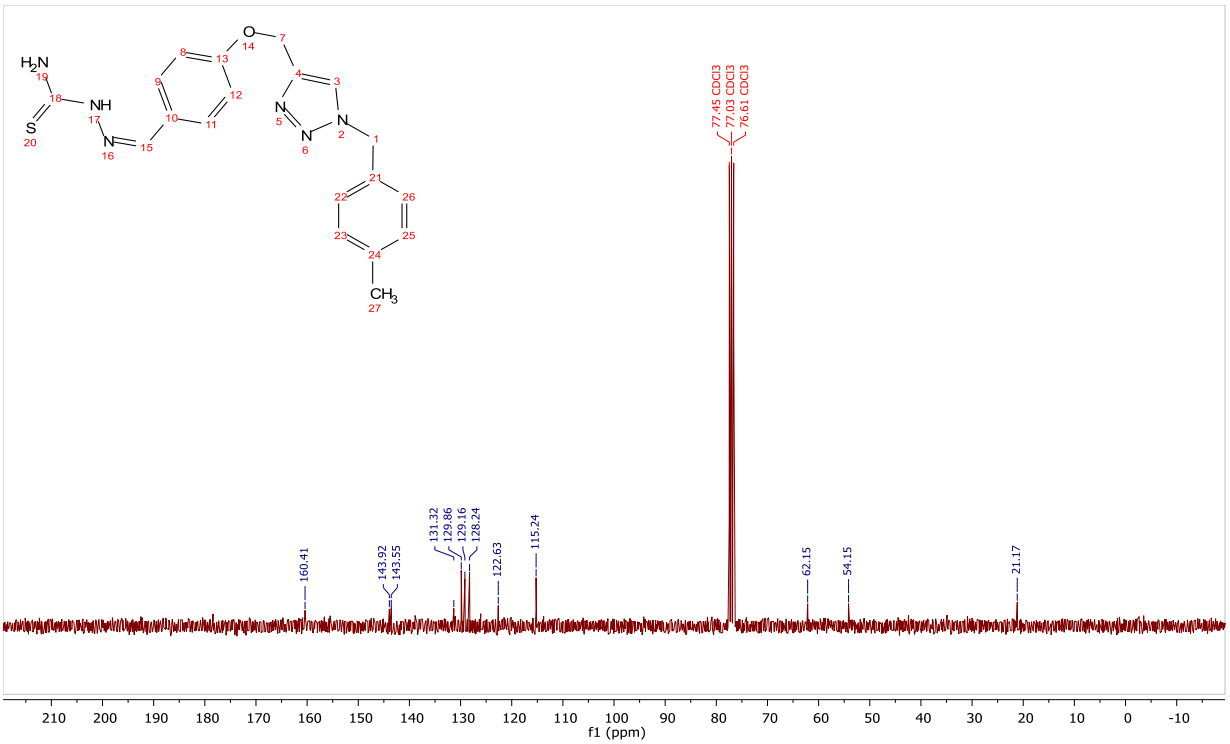


**13C NMR (75 MHz, $CDCl_3$) δ 160.41, 143.92, 143.55, 131.32, 129.86, 129.16, 128.24, 122.63, 115.24, 62.15, 54.15, 21.17.**

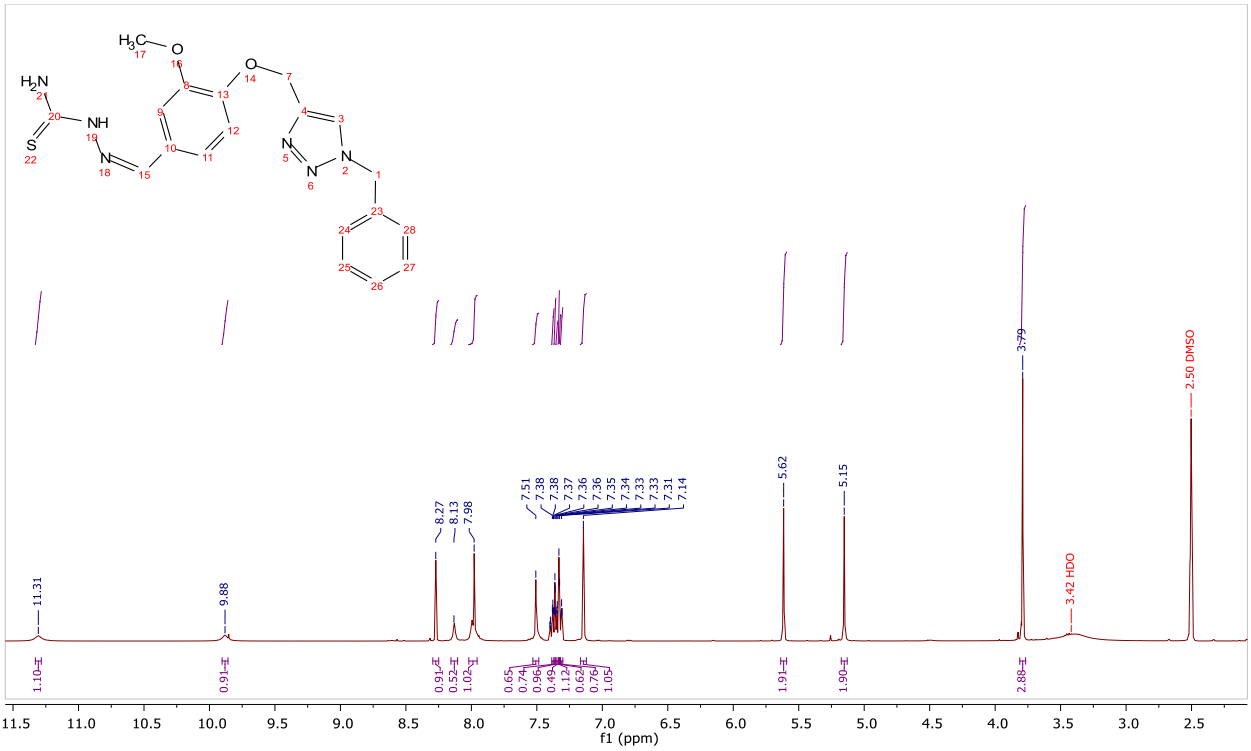


**$^1$H NMR (400 MHz, DMSO-$d_6$) δ** 11.31 (s, 1H), 9.88 (s, 1H), 8.27 (s, 1H), 8.13 (s, 1H), 7.98 (s, 1H), 7.51 (s, 1H), 7.38-7.37 (t, 1H), 7.37-7.36 (q,1H), 7.35-7.34 (d, 1H), 7.33 (s, 1H), 7.33 (s, 1H), 7.32 – 7.31 (t, 1H), 7.14 (s, 1H), 5.62 (s, 2H), 5.15 (s, 2H), 3.79 (s, 3H)**.**

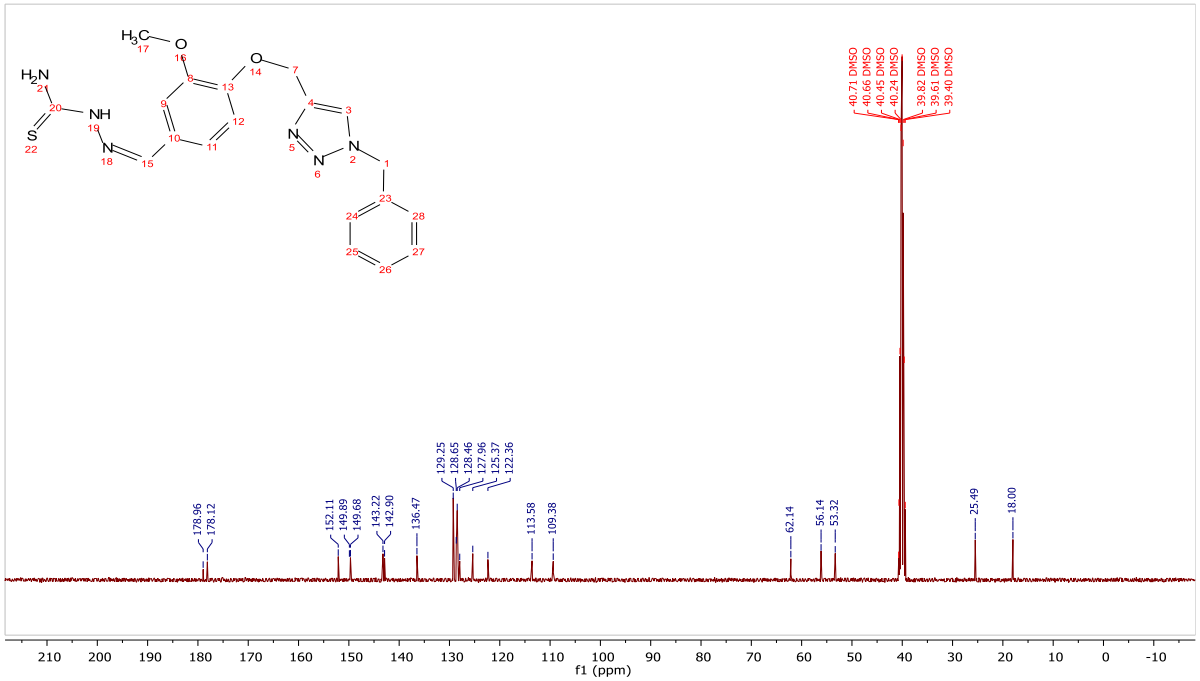


**$^{13}$C NMR (101 MHz, DMSO) δ 178.960, 178.12, 152.11, 149.89, 149.68, 143.22, 142.90, 136.47, 129.25, 128.645, 128.456, 127.96, 125.367, 122.36, 113.58, 109.38, 62.14, 56.14, 53.32, 25.49, 18.00.**

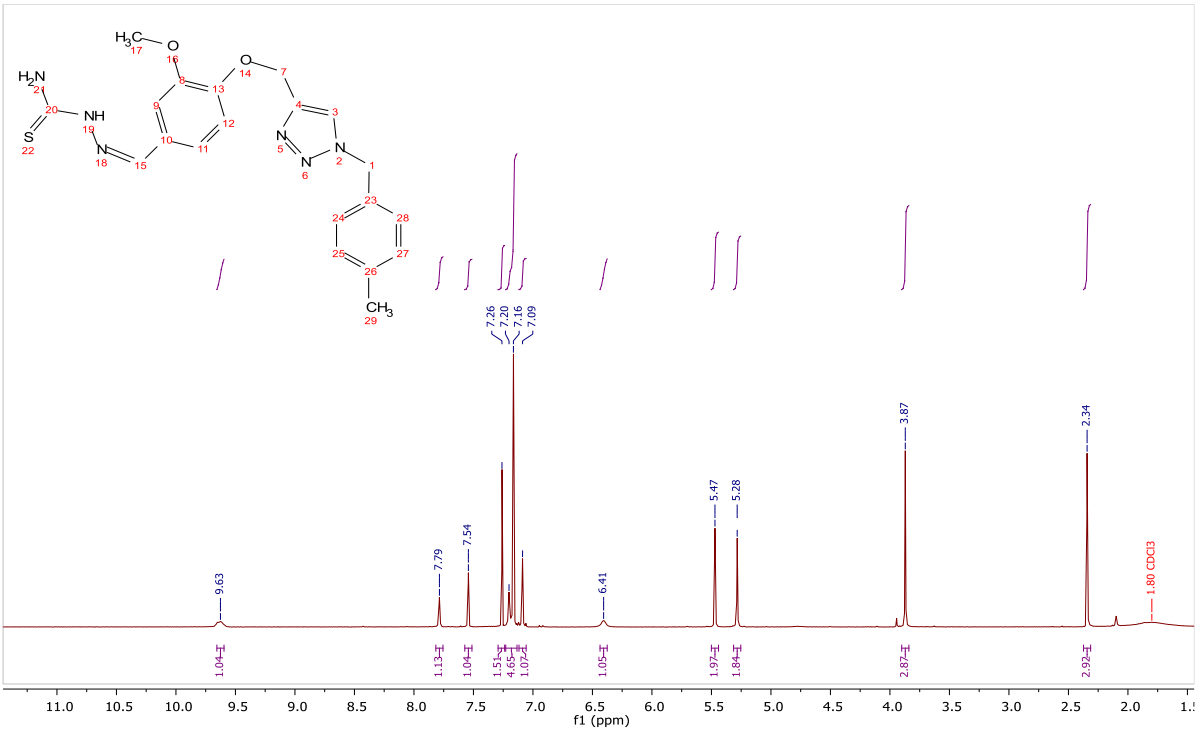


**1H NMR (300 MHz, Chloroform-*d*) δ 9.63 (s, 1H), 7.79 (s, 1H), 7.54 (s, 1H), 7.26 (s, 2H), 7.16 (s, 5H), 7.09 (s, 1H), 6.41 (s, 1H), 5.47 (s, 2H), 5.28 (s, 2H), 3.87 (s, 3H), 2.34 (s, 3H).**

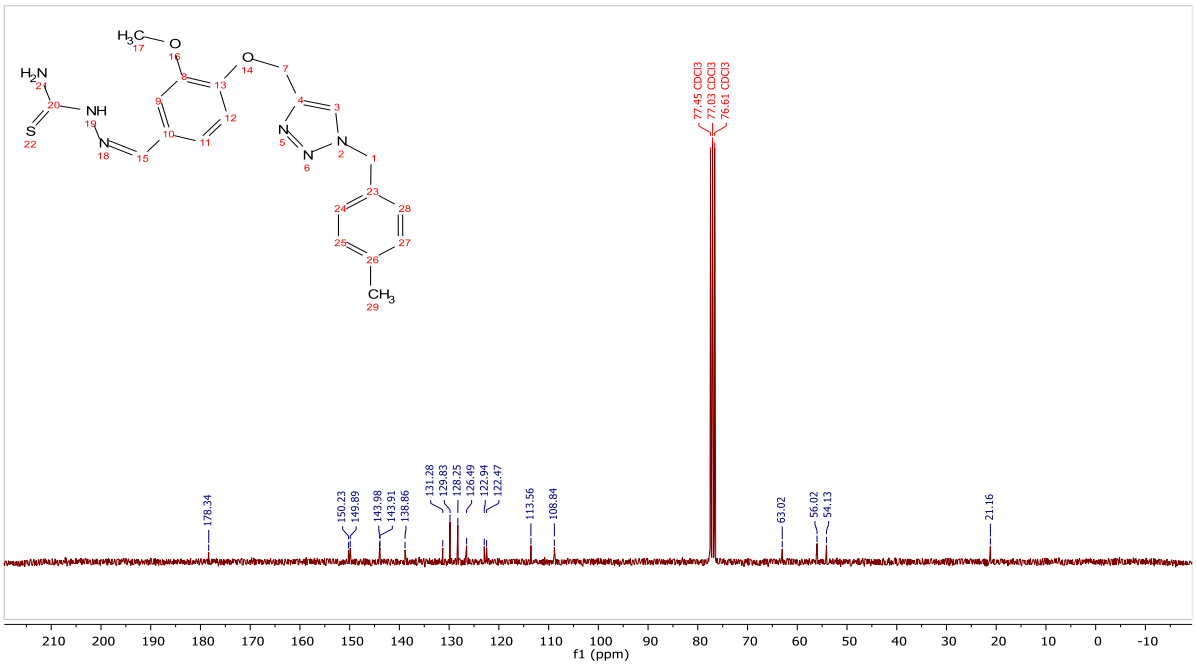


**13C NMR (75 MHz, $CDCl_3$) δ 178.34, 150.23, 149.89, 143.98, 143.91, 138.86, 131.28, 129.83, 128.25, 126.49, 122.94, 122.47, 113.56, 108.84, 63.02, 56.02, 54.13, 21.16.**

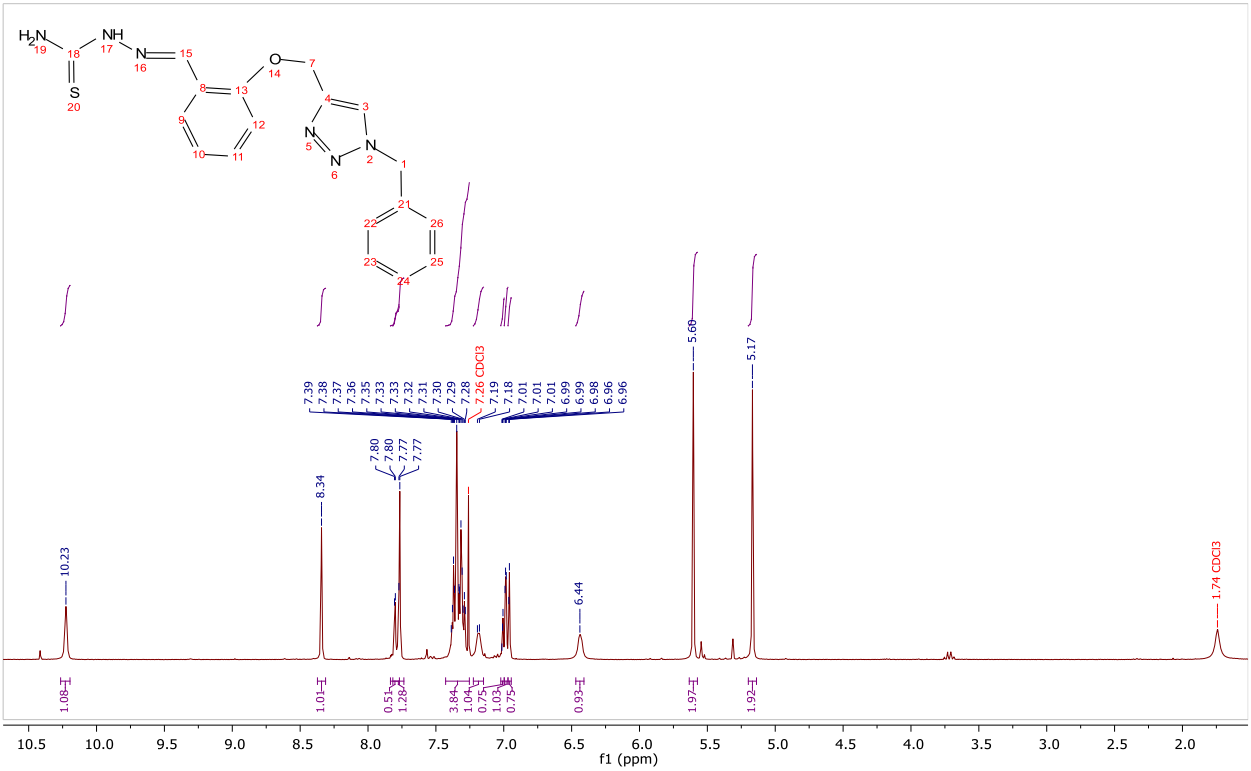


**$^1$H NMR (300 MHz, Chloroform*d*) δ** 10.23 (s, 1H), 8.34 (s, 1H), 7.80 (d,1H), 7.77 (s, 1H), 7.39 – 7.28 (m, 4H), 7.19-7.18 (s, 1H), 7.01 (s, 1H), 6.99 (s, 1H), 6.96 (s,1H), 6.44 (s, 1H), 5.60 (s, 2H), 5.17 (s, 2H).

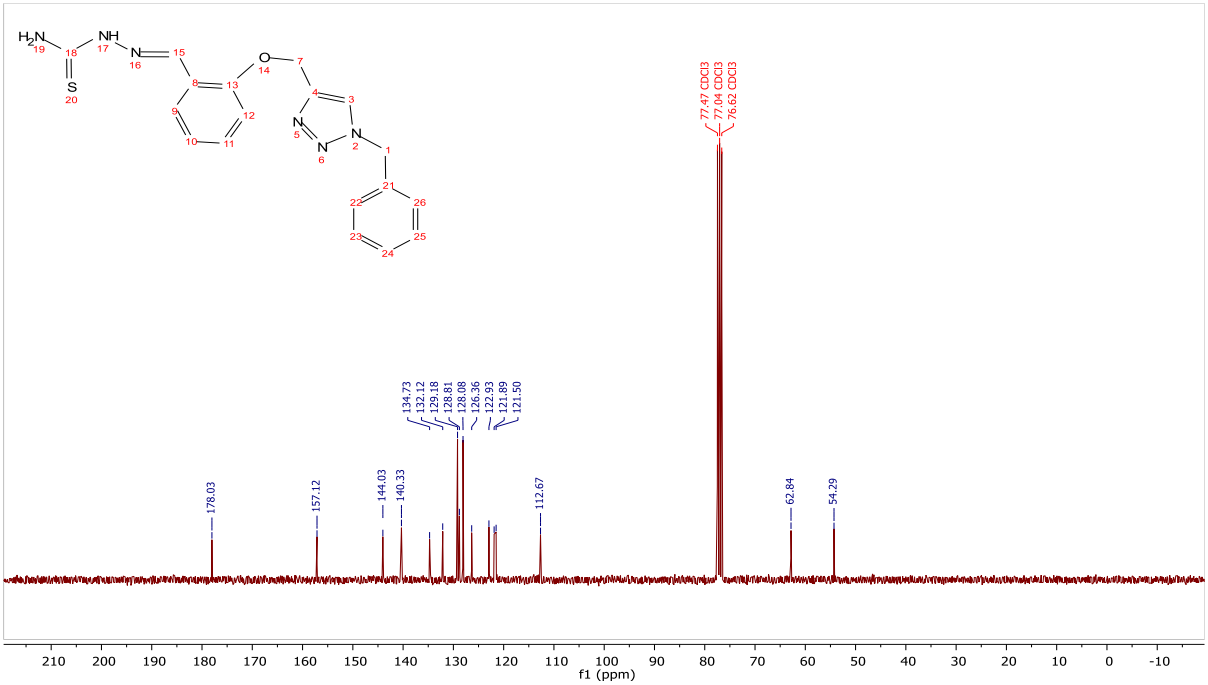


**$^{13}$C NMR (75 MHz, $CDCl_3$) δ 178.023, 157.12, 144.03, 140.33, 134.73, 132.12, 129.178, 128.801, 128.08, 126.36, 122.93, 121.89, 121.50, 112.67, 62.84, 54.291494.**

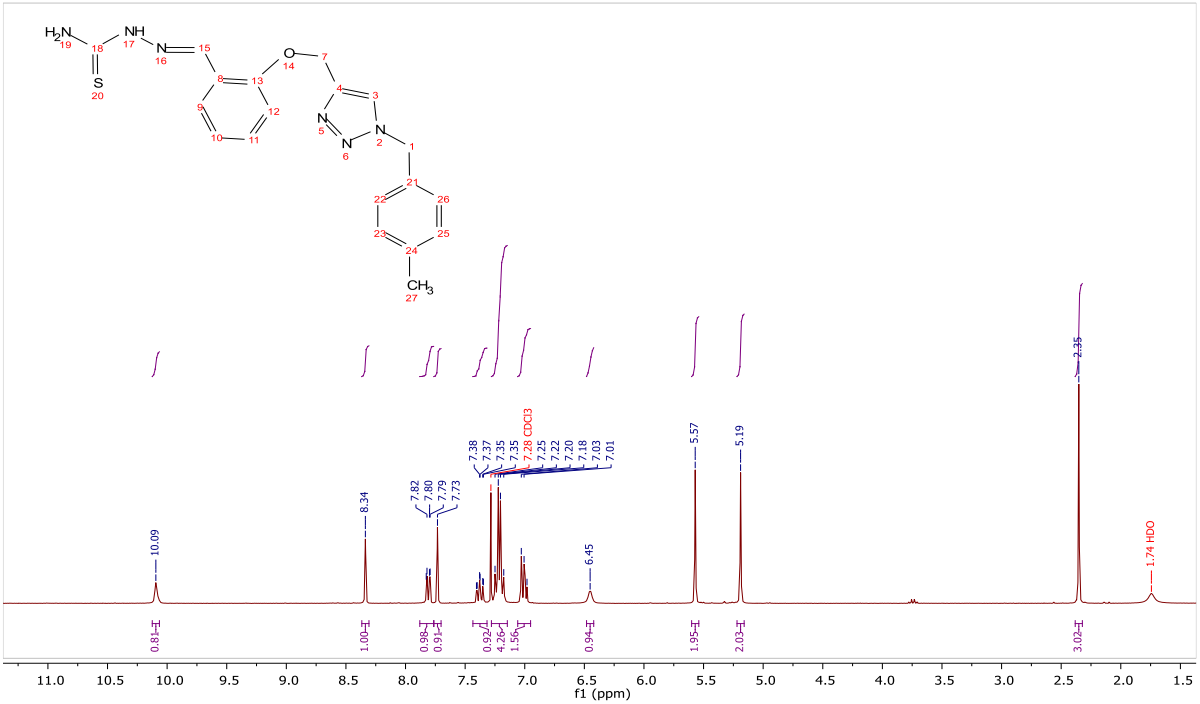


**$^1$H NMR (300 MHz, Chloroform-*d*) δ 10.09 (s, 1H), 8.34 (s, 1H), 7.81 (dd, 1H), 7.73 (s, 1H), 7.43 – 7.32 (m, 1H), 7.28 – 7.15 (m, 5H), 7.06 – 6.95 (m, 2H), 6.45 (s, 1H), 5.57 (s, 2H), 5.19 (s, 2H), 2.35 (s, 3H).**

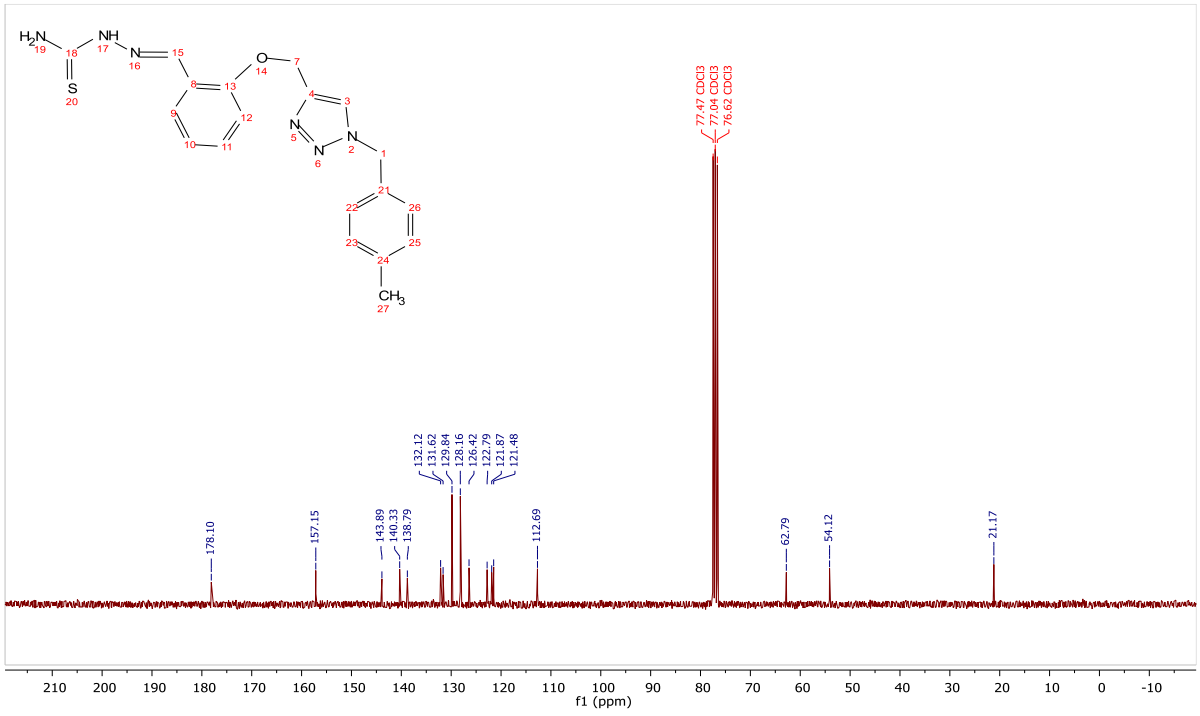


**$^{13}$C NMR (75 MHz, $CDCl_3$) δ 178.10, 157.15, 143.89, 140.33, 138.79, 132.12, 131.62, 129.84, 128.16, 126.42, 122.79, 121.87, 121.48, 112.69, 77.47, 77.04, 76.62, 62.79, 54.12, 21.17.**

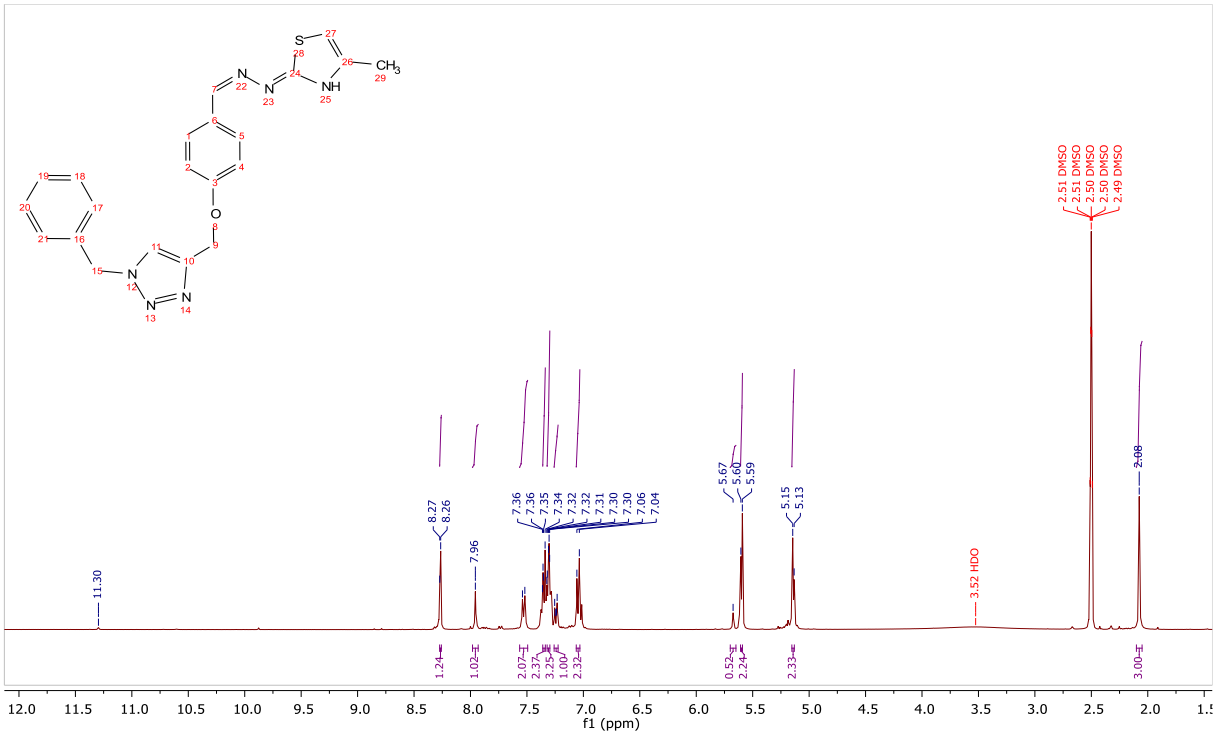


**$^1$H NMR (400 MHz, DMSO-$d_6$) δ** 8.27-8.26 (d, 1H), 7.96 (s, 1H), 7.54-7.52 (d, 2H), 7.36-7.34 (m, 2H), 7.32-7.30 (m, 3H), 7.25 – 7.23 (d, 1H), 7.04-7.06 (d, 2H), 5.67 (s, 1H) 5.60-5.59 (d, 2H), 5.15-5.13 (d, 2H), 2.08 (s, 3H).

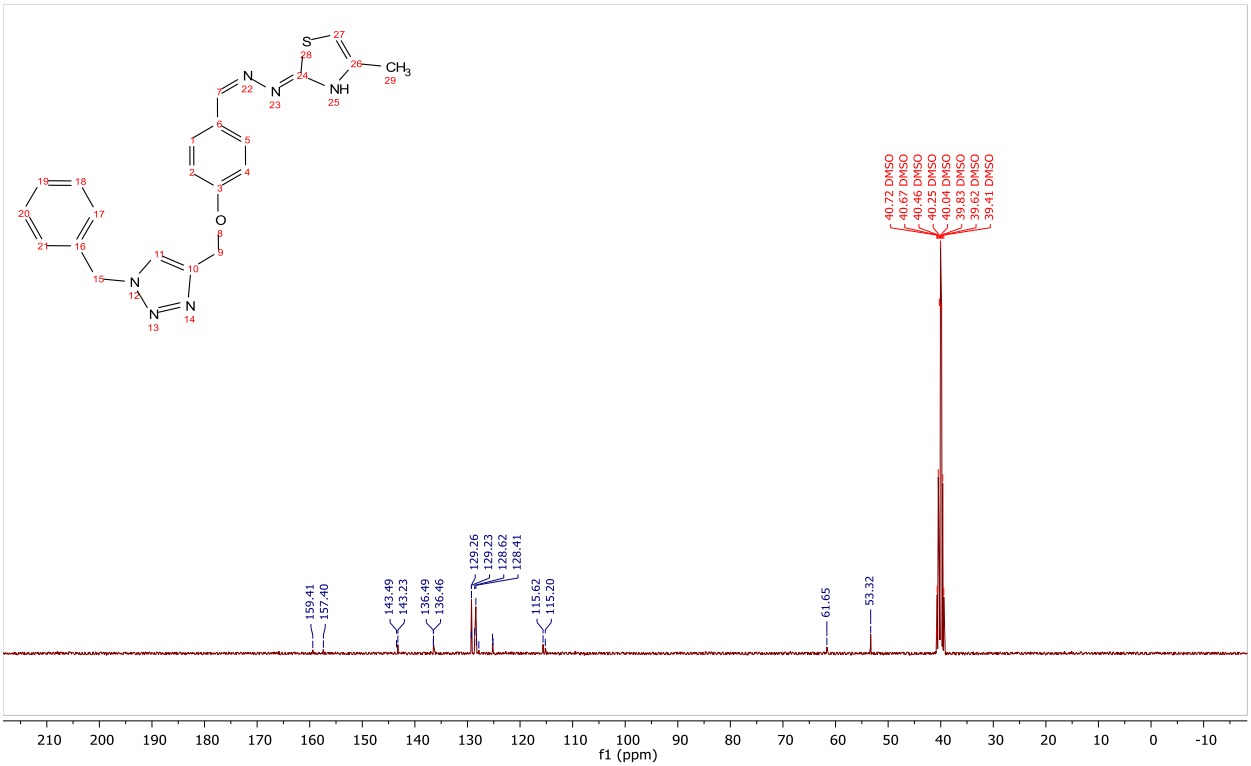


**$^{13}$C NMR (101 MHz, DMSO) δ** 159.41, 157.40, 143.49, 143.23, 136.49, 136.46, 129.26, 129.23, 128.62, 128.41, 128.32, 127.84, 125.23, 125.15, 115.62, 115.20, 61.65, 53.32.

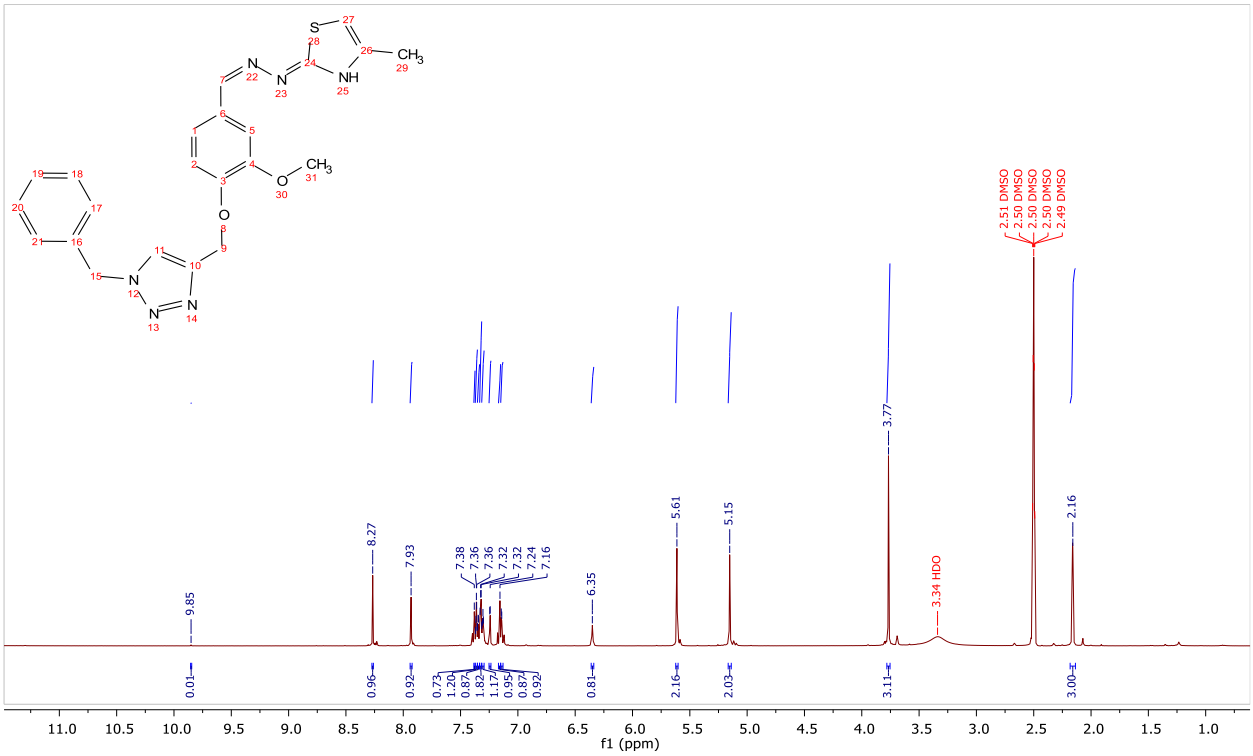


**$^{1}$H NMR (400 MHz, DMSO-$d_6$) δ** 8.27 (s, 1H), 7.93 (s, 1H), 7.38 (s, 1H), 7.37 – 7.36 (m, 1H), 7.35 – 7.34 (m, 1H), 7.33 – 7.32 (m, 2H), 7. – 7.30 (m, 1H), 7.24-7.25 (d, 1H), 7.16 (s, 1H), 7.14 (d, 1H), 6.35 (s, 1H), 5.61 (s, 2H), 5.15 (s, 2H), 3.77 (s, 3H), 2.16 (s, 3H).

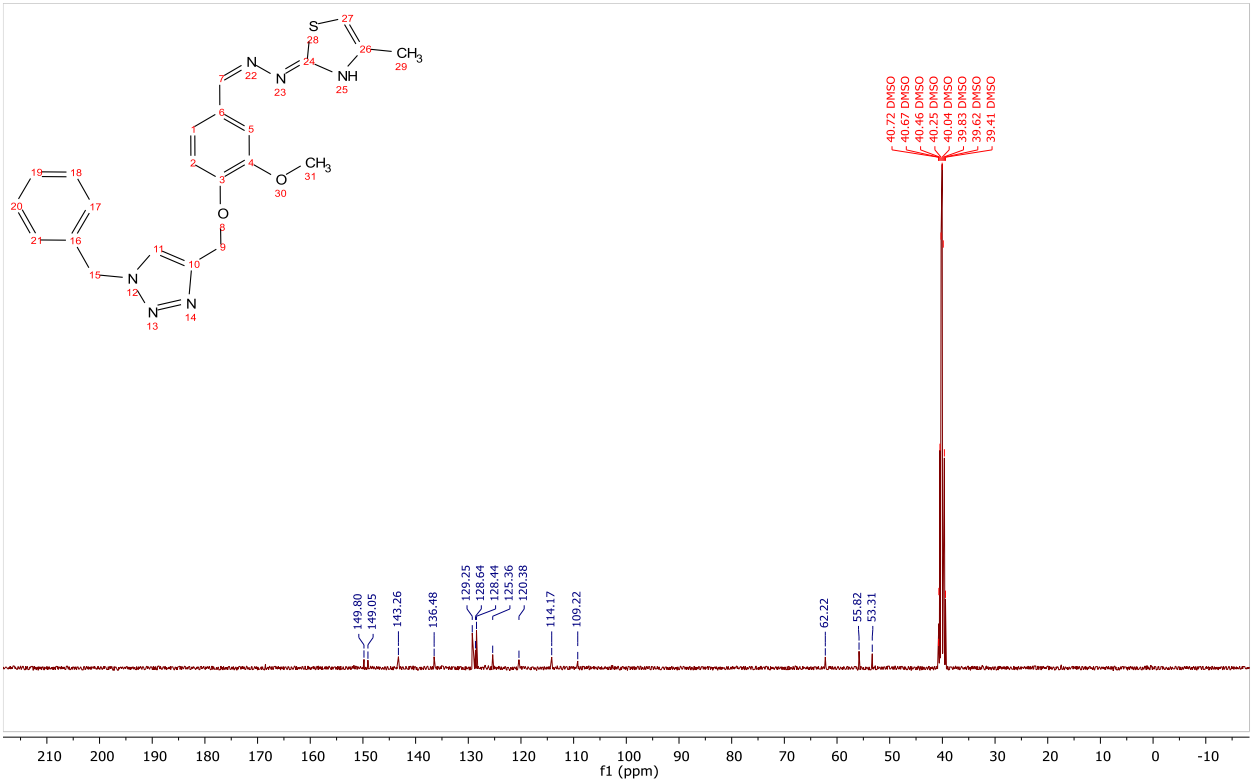


**$^{13}$C NMR (101 MHz, DMSO) δ** 149.80, 149.05, 143.26, 136.48, 129.25, 128.64, 128.44, 125.36, 120.38, 114.17, 109.22, 62.22, 55.82, 53.

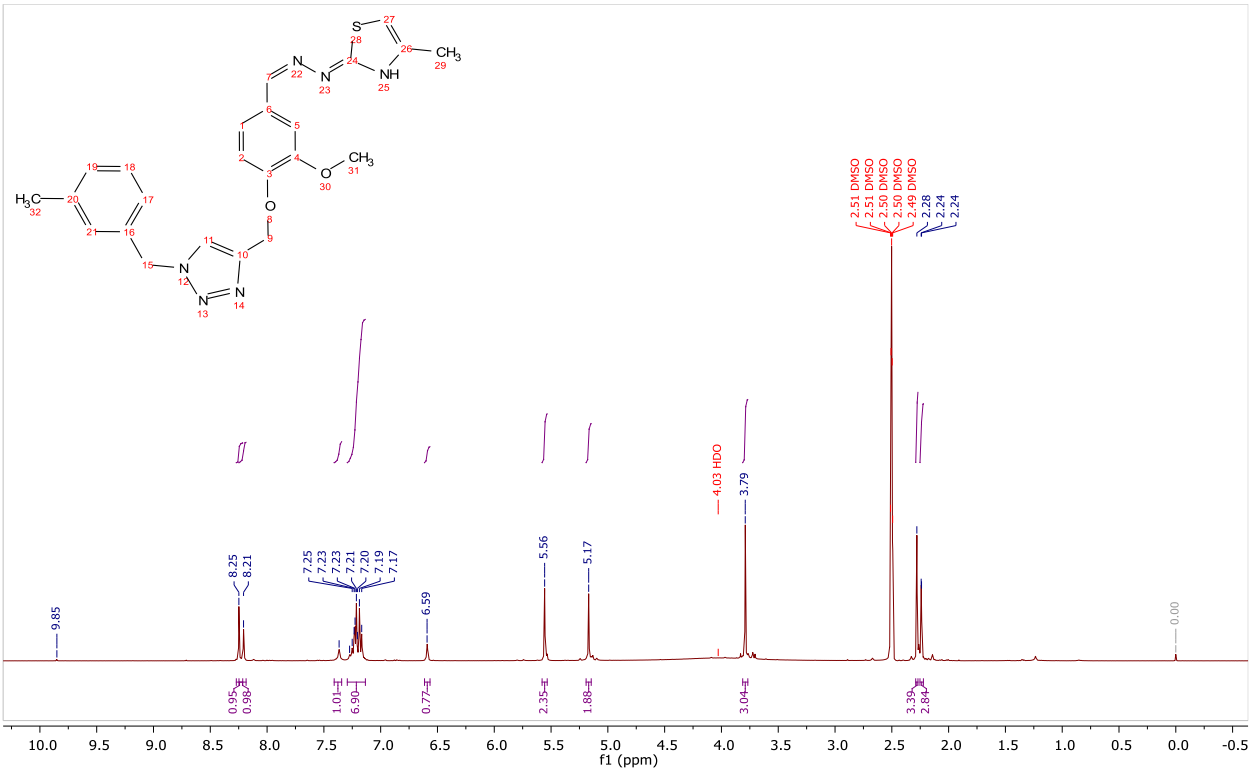


**$^{1}$H NMR (400 MHz, DMSO-$d_6$) δ** 8.25 (s, 1H), 8.21 (s, 1H), 7.37 (s, 1H), 7.27-7.17 (m, 7H), 6.59 (s, 1H), 5.56 (s, 2H), 5.17 (s, 2H), 3.79 (s, 3H), 2.28 (s, 3H), 2.24 (s, 3H).

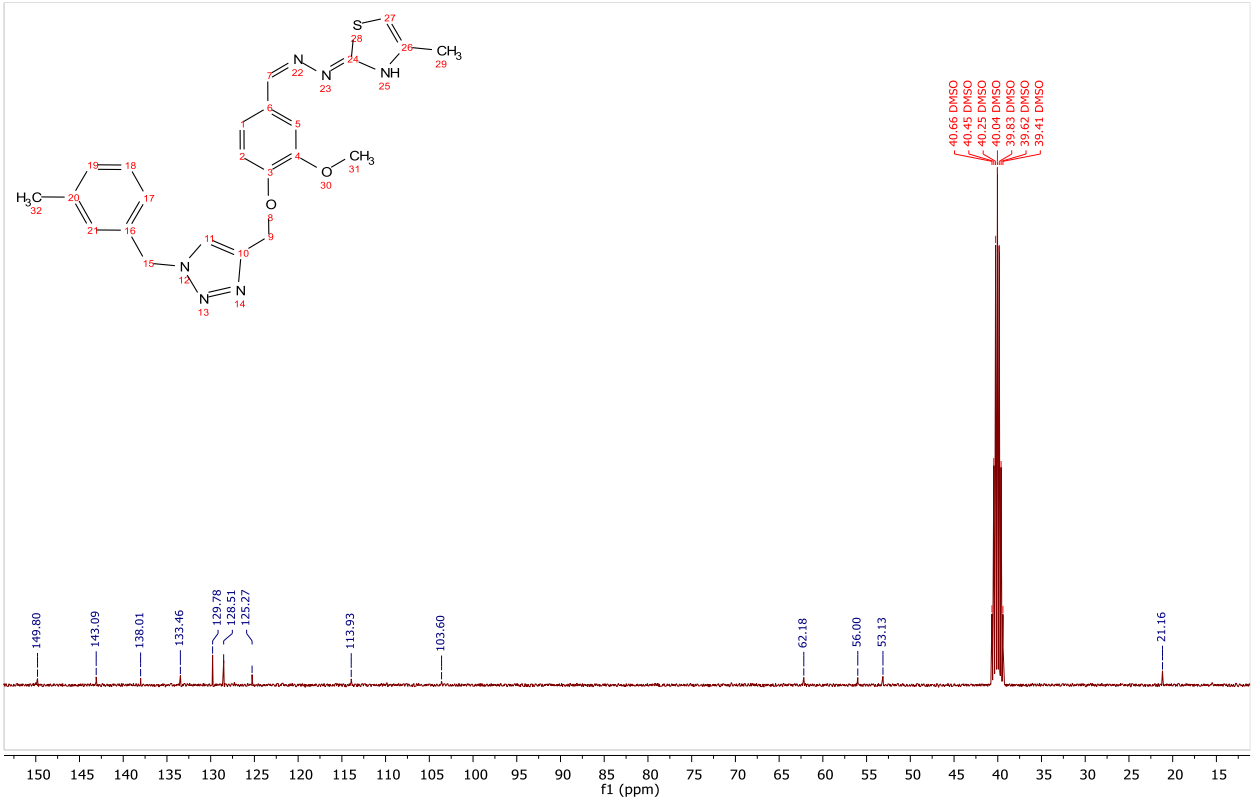


**$^{13}$C NMR (101 MHz, DMSO) δ** 149.80, 143.09, 138.01, 133.46, 129.78, 128.51, 125.27, 113.93, 103.60, 62.18, 56.00, 53.13, 21.16.

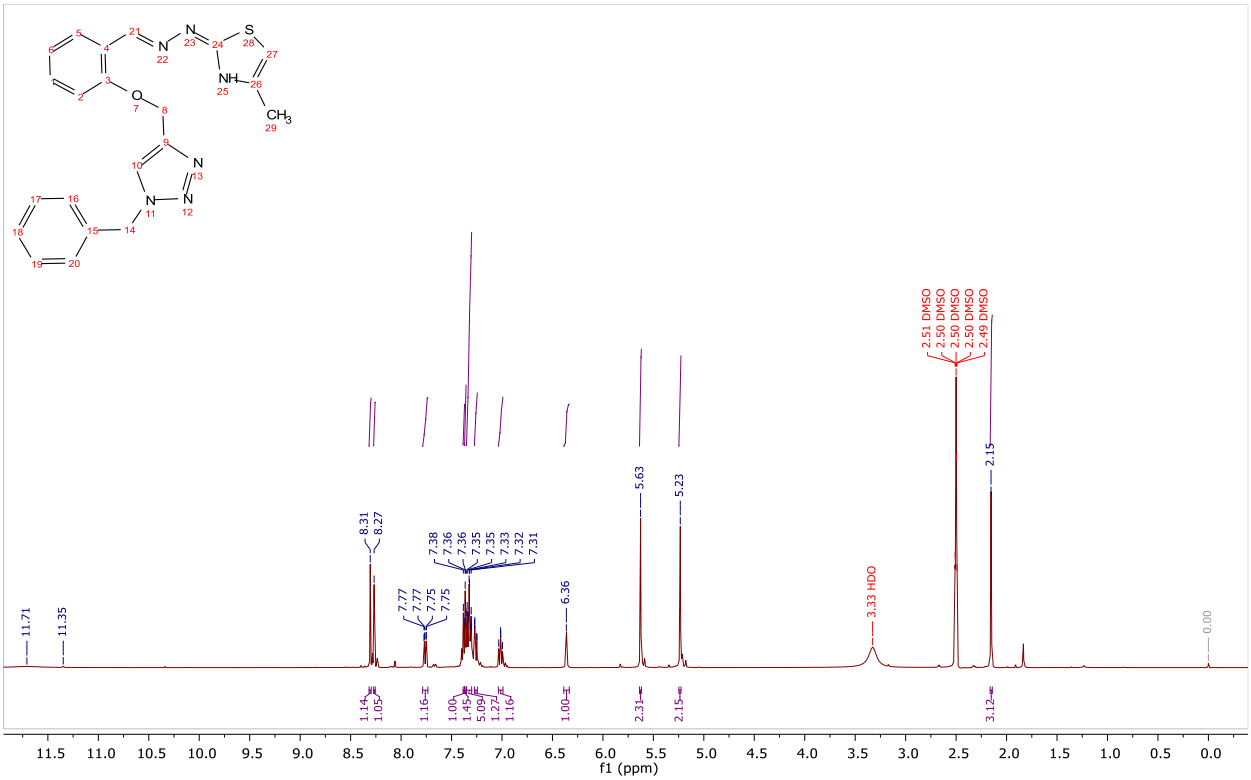


**$^{1}$H NMR (400 MHz, DMSO-$d_6$) δ** 8.31 (s, 1H), 8.27 (s, 1H), 7.77-7.75 (dd, 1H), 7.38 (s, 1H), 7.37-7.36 (m, 1H), 7.35-7.30 (m, 5H), 7.27-7.25 (dd, 1H), 7.03-7.00 (t, 1H), 6.36 (s, 1H), 5.63 (s, 2H), 5.23 (s, 2H), 2.15 (s, 3H).

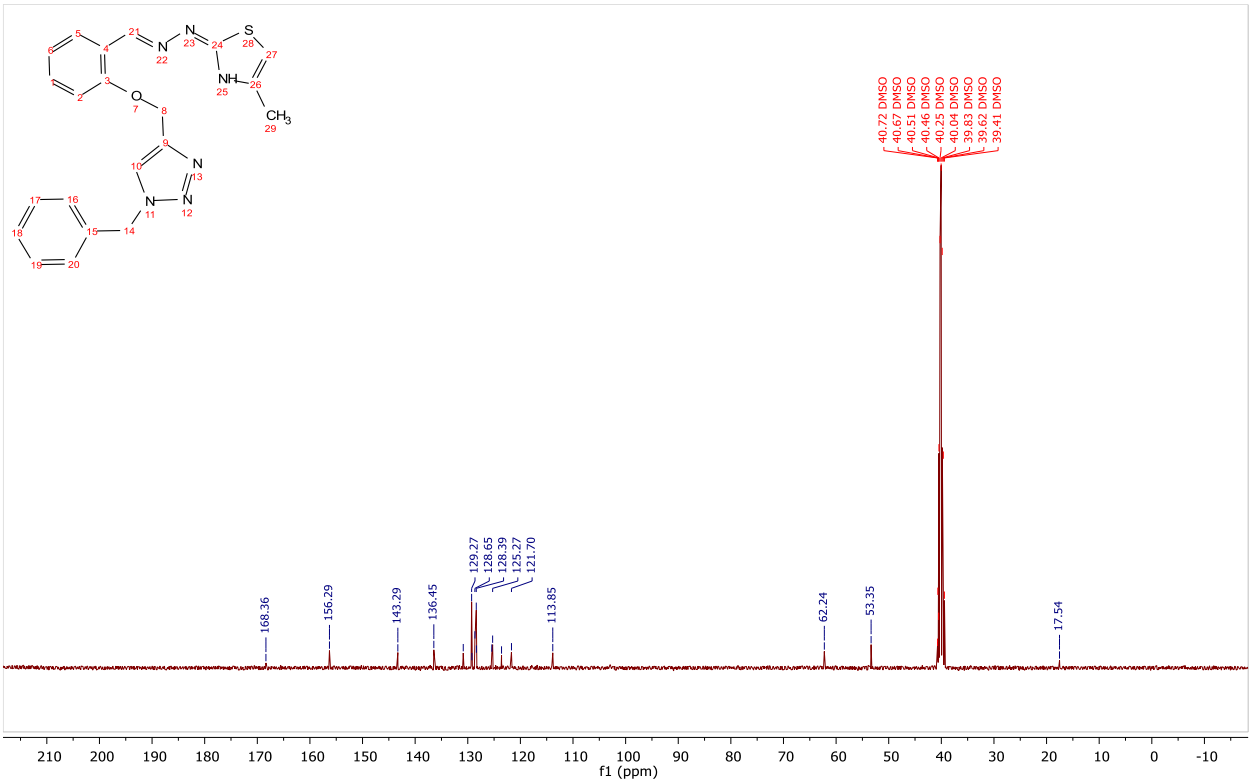


**$^{13}$C NMR (101 MHz, DMSO) δ** 168.36, 156.29, 143.29, 136.45, 130.86, 129.27, 129.22, 128.65, 128.39, 128.36, 125.43, 125.27, 123.58, 121.70, 113.851, 62.24, 53.35, 17.54.

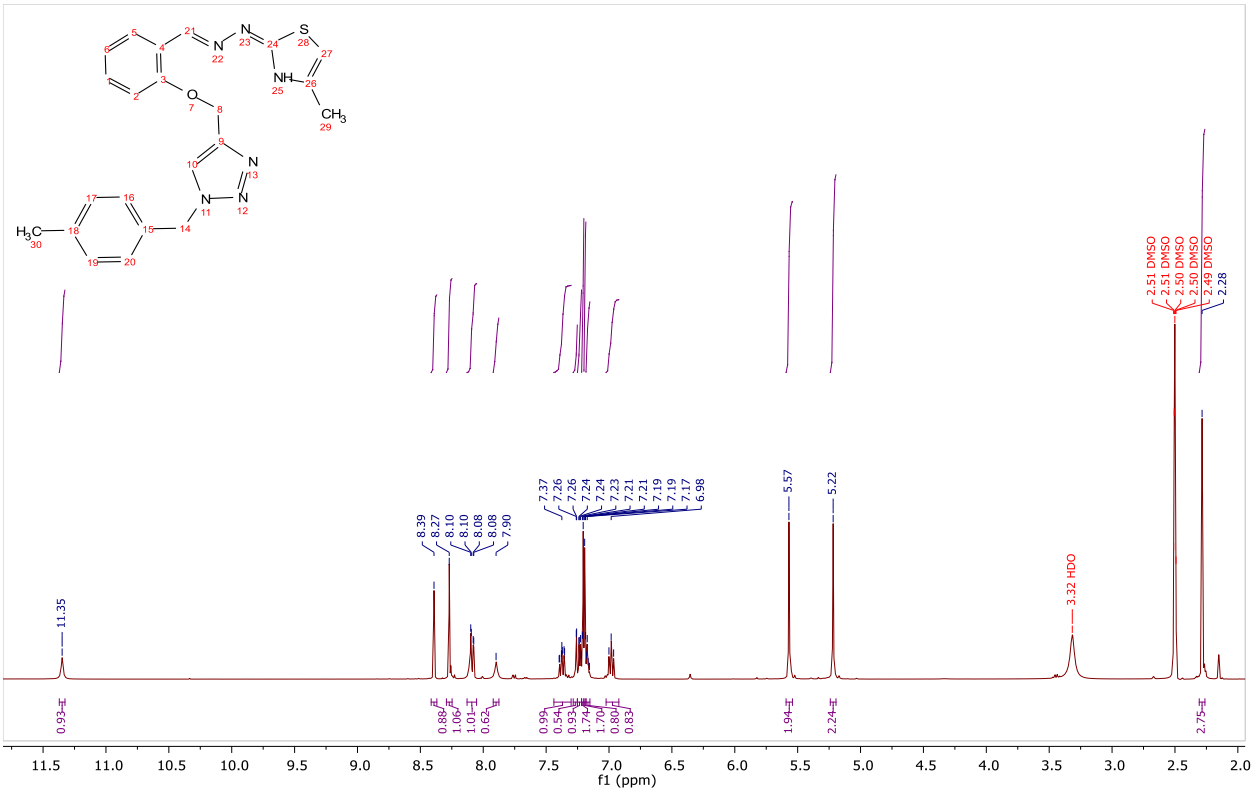


**$^1$H NMR (400 MHz, DMSO-$d_6$) δ** 11.35 (s, 1H), 8.39 (s, 1H), 8.27 (s, 1H), 8.10 – 8.08 (d, 2H), 7.90 (s, 1H), 7.40-7.35 (m, 1H), 7.30 – 7.13 6H), 7.00 – 6.96 (t, 1H), 5.57 (s, 2H), 5.22 (s, 2H), 2.28 (s, 3H).

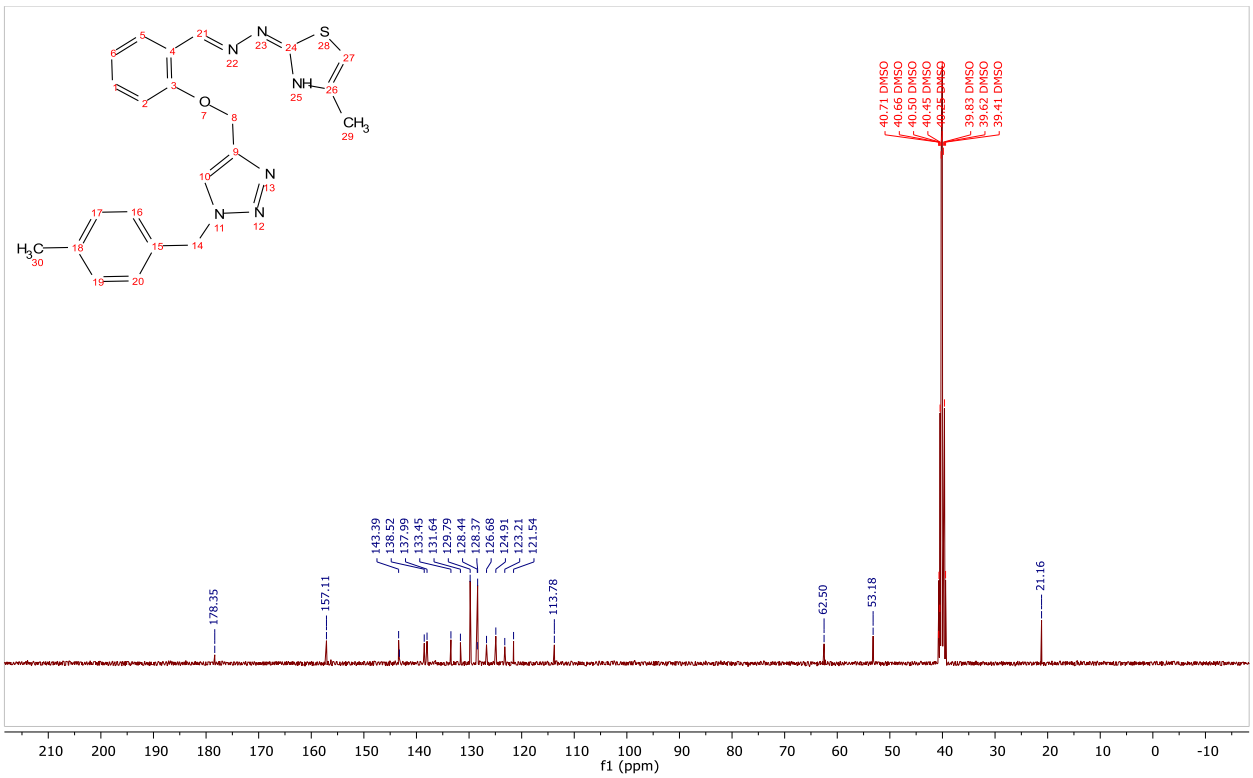


**$^{13}$C NMR (101 MHz, DMSO) δ** 178.35, 157.11, 143.393, 143.25, 138.52, 137.99, 133.45, 131.64, 129.79, 128.44, 128.37, 126.68, 124.91, 123.21, 121.54, 113.78, 62.50, 53.18, 21.16.

# Annexe II

# Scientific Achievements

**1.Scientific publication:**

This work has been the subject of 2 international publications and 1 national publication:

H. Abdelbaki *et al*., "Plant mediated synthesis of flower-like $Cu_2O$ microbeads from artimisia campestris L. Extract for the catalyzed synthesis of 1, 4-disubstituted 1, 2, 3-triazole derivatives," *Frontiers in Chemistry*, vol. 11, p. 1342988, 2024. https://doi.org/10.3389/fchem.2023.1342988


H. Abdelbaki, A. Djemoui, A. Benarfa, S. Lahcene, A. Souadia, M. Messaoudi, M.R. Ouahrani, Preparation of Bioactive Thiazole Derivatives using 1, 2, 3-triazole-linked Thiosemicarbazone Derivatives and their Antioxidant Activities, Tuijin Jishu/Journal of Propulsion Technology, 45 2024.

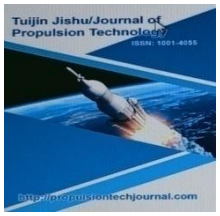


H. Abdelbaki, A. Djemoui, M.R. Ouahrani, M. Messaoudi, I.B. Amor, H. Alsaeedi, D. Croun, M. Bechelany, A. Barhoum, Synthesis of Bioactive 1, 4-Disubstituted 1, 2, 3-Triazole-Linked Thiosemicarbazone Derivatives using $Cu_2O$ Microbeads Catalysis for Enhanced Antibacterial and Antioxidant Activities, Journal of Molecular Structure, (2024) 140784. https://doi.org/10.1016/j.molstruc.2024.140784

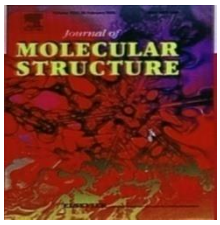


**2. Scientific conferences :**

**International scientific conference :**

Synthesis of ketimine and evaluation of its anticorrosion activity

**National scientific conferences :**

Biosyntesis of 1,2,3-triazole with an ecofriendly synthesized $Cu_2O$ nanoparticles as catalyst


Synthesis of naphtho[1,2-e][1,3]oxazine-3-one derivatives from 1,2,3-triazole under Solvent-free Condition and evaluation of their antioxydant activity

## Abstract:

In this study, we synthesized 1,2,3-triazoles via a one-pot, multi-component reaction using $Cu_2O$ microbeads as catalysts, enhancing reaction conditions and yields (33-85%). The $Cu_2O$ microbeads were synthesized in a green environment using an aqueous extract of *Artemisia campestris L.*, resulting in a flower-like morphology with a cubic close-packed crystal structure and a particle size of 3-6 µm.

Following triazole synthesis, we created thiosemicarbazone intermediates with moderate to good yields (32-74%) by condensing triazoles with thiosemicarbazide, allowing for thiazole derivatives formation in moderate to exceptional yields (21-86%), by their condensation with chloroacetone that expands their pharmacological applications.

Finally, we evaluated the antioxidant activity of the synthesized products (triazoles, thiosemicarbazones, and thiazoles) using standard radical scavenging assays (DPPH and ABTS) to assess their therapeutic potential against oxidative stress-related diseases. These compounds exhibit significant antioxidant properties.

The structures of the synthesized compounds were confirmed using $^{13}C$ NMR, $^{1}H$ NMR, and FTIR techniques.


**Key words :** 1,2,3-triazole, $Cu_2O$ microbeads, thiosemicarbazone, thiazole, antioxidant activity.


**الملخص :**

في هذه الدراسة، قمنا بتصنيع 1، 2، 3- تريازول من خلال تفاعل متعدد المكونات بخطوة واحدة باستخدام ميكروبيدات $Cu_2O$ كمحفز، لتحسين شروط التفاعل و المردود (33-85 %). ميكروبيدات $Cu_2O$ تم تصنيعها في بيئة خضراء باستخدام المستخلص المائي لنبات الدقفت *(Artimisia Campestris L.)* لينتج شكلا يشبه الزهرة مع بنية بلورية مكعبة ذات تعبئة كثيفة و حجم يبلغ 3-6 µm .

بعد تصنيع التريازول، صنعنا وسائط ثيوسيماكربازون بمردود من متوسط إلى جيد (32-74 %)عن طريق تكثيف التريازول مع ثيوسيماكربازيد، مما سمح بتكوين مشتقات الثيازول بمردود من متوسط إلى ممتاز (21-86 %) بعد تكثيفها مع الكلورو اسيتون لتوسيع تطبيقاتها الصيدلانية.

أخيرًا، قمنا بتقييم النشاط المضاد للأكسدة للمركبات المصنعة (التريازول، الثيوسيماكربازون والثيازول) باستخدام اختبارات قياسية لالتقاط الجذور الحرة (DPPH و ABTS ) لتقييم إمكانياتها العلاجية ضد الأمراض المرتبطة بالإجهاد التأكسدي. أظهرت هذه المركبات خصائص هامة مضادة للأكسدة.

تم تأكيد بنية المركبات المصنعة باستخدام تقنيات الأشعة تحت الحمراء و الرنين النووي المغناطيسي للبروتون و الكربون.

**الكلمات المفتاحية:** 1،2،3– تريازول، ميكروبيدات $Cu_2O$ ، ثيوسيميكاربازون، ثيازول، النشاط المضاد للاكسدة.

**Résumé**

Dans cette étude, nous avons synthétisé des 1,2,3-triazoles par une réaction multi-composants en une seule étape, utilisant des $Cu_2O$ microbilles comme catalyseurs, améliorant les conditions réactionnelles et les rendements (33-85%). Les microbilles de $Cu_2O$ ont été synthétisées dans un environnement écologique à partir d'un extrait aqueux d'*Artemisia campestris L.*, résultant une morphologie florale, une structure cristalline cubique à empilement compact et une taille de particule de 3-6 µm.

Après la synthèse des triazoles, nous avons crée des intermédiaires thiosemicarbazones avec des rendements modérés à bons (32-74%) en condensant les triazoles avec la thiosemicarbazide, permettant ainsi la formation de dérivés thiazoles avec des rendements modérés à exceptionnels (21-86 %) par leur condensation avec la chloroacétone, élargissent leurs applications pharmacologiques.

Enfin, nous avons évalué l'activité antioxydante des produits synthétisés (triazoles, thiosemicarbazones et thiazoles) en utilisant des tests standard de piégeage des radicaux (DPPH et ABTS) pour évaluer leur potentiel thérapeutique contre les maladies liées au stress oxydatif. Ces composés présentent des propriétés antioxydante significatives.

Les structures des composés synthétisés ont été confirmées à l'aide des techniques de RMN $^{13}C$, RMN $^{1}H$ et FTIR.

**Mots-clés :** 1,2,3-triazole, microbilles de $Cu_2O$, thiosemicarbazone, thiazole, activité antioxidante.